620.5
U58
B91
AUG 1 1931

U. S. DEPARTMENT OF COMMERCE

BUREAU OF STANDARDS JOURNAL OF RESEARCH

Vol. 7 JULY, 1931 No. 1

CONTENTS

RP. No.	TITLE AND AUTHOR	Page
329.	Soil-corrosion studies, 1930. Rates of corrosion and pitting of bare ferrous specimens. K. H. Logan and V. A. Grodsky	1
330.	Automatic volume control for aircraft radio receivers. W. S. Hinman, jr	37
331.	Apparent and partial molal heat capacities in aqueous solutions of 19 uni-univalent electrolytes. Frederick D. Rossini	47
332.	Measurement of Lenard rays. Lauriston S. Taylor	57
333.	A new test for predicting the durability of varnishes (the photo-chemical embrittling test). J. H. Wilson	73
334.	Interpolation of the O. S. A. "excitation" data by the fifth-difference osculatory formula. Deane B. Judd	85
335.	Experiments on metering of large volumes of air. Howard S. Bean, M. E. Benesh, and Edgar Buckingham	93
336.	A course indicator of pointer type for the visual radio range-beacon system. F. W. Dunmore	147
337.	The visible and ultra-violet absorption spectra of carotin and xanthophyll and the changes accompanying oxidation. H. J. McNicholas	171
338.	Theory of design and calibration of vibrating reed indicators for radio range beacons. G. L. Davies	195

BUREAU OF STANDARDS JOURNAL OF RESEARCH

CONTENTS OF RECENT NUMBERS

January, 1931 (Vol. 6, No. 1)

RP265. Determination of magnesium in Portland cement and similar materials by the use of 8-hydroxyquinoline. J. C. Redmond and H. A. Bright. Price 5 cents.

RP266. An improved apparatus and method for the analysis of gas mixtures by combustion and absorption. Martin Shepherd. Price 15 cents.

RP267. Determination of small quantities of volatile organic acids in sulphuric acid solutions. D. N. Craig. Price 5 cents.

February, 1931 (Vol. 6, No. 2)

RP268. Strain measurement in the reinforcement for the dome of the Natural History Building. W. C. Lyon, H. L. Whittemore, A. H. Stang, and L. R. Sweetman. Price 15 cents.

RP269. A radio method for synchronizing recording apparatus. T. Parkinson and T. R. Gilliland. Price 10 cents.

RP270. The tensile properties of alloy steels at elevated temperatures as determined by the "short-time" method. William Kahlbaum, R. L. Dowdell, and W. A. Tucker. Price 15 cents.

RP271. Further studies of the X-ray standard ionization chamber diaphragm system. L. S. Taylor and G. Singer. Price 10 cents.

RP272. An optical coincidence gage. I. C. Gardner and F. A. Case. Price 10 cents.

RP273. The band spectra of Scandium-, Yttrium-, and Lanthanum monides. W. F. Meggers and John A. Wheeler. Price 15 cents.

RP274. Probabilities of recombination into the state of cæsium. C. Boeckner. Price 10 cents.

RP275. Regularities in the second spectrum of Xenon. C. J. Humphreys, T. L. deBruin, and W. F. Meggers. Price 5 cents.

RP276. The resistance of chromium-plated gages to wear. Harry K. Hirschman. Price 10 cents.

RP277. Compressive tests of jointed H-section steel columns. James H. Edwards, H. L. Whittemore, and A. H. Stang. Price 15 cents.

RP278. Critical study of the bursting strength test for paper. F. T. Carson and F. V. Worthington. Price 10 cents.

March, 1931 (Vol. 6, No. 3)

RP279. A method for the standardization of permeameters at high magnetizing forces. R. L. Sanford. Price 5 cents.

RP280. Determination of the toluene content of a mid-continent petroleum. Johannes H. Bruun, R. T. Leslie, and Sylvester T. Schicktanz. Price 5 cents.

RP281. The mechanism of the atomization of liquids. R. A. Castleman, jr. Price 5 cents.

RP282. Separation of normal octane from petroleum by distillation and crystallization. R. T. Leslie and Sylvester T. Schicktanz. Price 10 cents.

RP283. Further measurements of propeller fan characteristics. Paul S. Ballif and H. L. Dryden. Price 10 cents.

RP284. A precision cryostat with automatic temperature regulation. R. B. Scott and F. G. Brickwedde. Price 5 cents.

RP285. The paper-making properties of phormium tenax (New Zealand flax). Merle B. Shaw, George W. Bicking, and Martin J. O'Leary. Price 10 cents.

RP286. A method for the separation and gravimetric determination of osmium. Raleigh Gilchrist. Price 10 cents.

RP287. Application of the fluorating process to fructose. D. H. Brauns and Harriet L. Frush. Price 5 cents.

RP288. Moisture expansion of glazes and other ceramic finishes. H. G. Schurecht and G. R. Pole. Price 5 cents.

RP289. Extension of the standard visibility function to intervals of 1 millimicron by third-difference osculatory interpolation. Deane B. Judd. Price 5 cents.

RP290. Durability and strength of bond between mortar and brick. L. A. Palmer and J. V. Hall, jr. Price 10 cents.

RP291. Heat transfer through building walls. M. S. Van Dusen and J. L. Finck. Price 15 cents.

Research papers are available as separates for purchase from the Superintendent of Documents United States Government Printing Office, Washington, D. C.

U. S. DEPARTMENT OF COMMERCE
R. P. LAMONT, Secretary
BUREAU OF STANDARDS
GEORGE K. BURGESS, Director

BUREAU OF STANDARDS JOURNAL OF RESEARCH

July, 1931
Vol. 7, No. 1

UNITED STATES
GOVERNMENT PRINTING OFFICE
WASHINGTON : 1931

For sale by the Superintendent of Documents, Washington, D. C. - - - - Price $2.75 Per Year on Subscription

For a partial list of previous research papers appearing in BUREAU OF STANDARDS JOURNAL OF RESEARCH, see pages 2 and 3 of the cover.

RP329

SOIL-CORROSION STUDIES, 1930

RATES OF CORROSION AND PITTING OF BARE FERROUS SPECIMENS

By K. H. Logan and V. A. Grodsky

ABSTRACT

During 1930 the National Bureau of Standards removed from 70 test locations approximately 1,300 specimens of ferrous pipe materials. This paper reports the results of the examinations of these specimens. The extent of the corrosion is found to depend largely on the character of the soil. Rates of corrosion appear to vary somewhat from year to year, but the general tendency is for the rate to decrease as the time of exposure increases. The data do not indicate that there is a one best pipe material regardless of soil conditions. The material which appears best in one soil may appear inferior in another soil. It is too early to state whether this will hold true at the close of long-time tests. Supplementary tests indicate that at least a number of soils have characteristic corrosive properties which can be expected wherever those soils are found.

CONTENTS

	Page
I. Introduction	1
1. Relation of this report to previous ones	1
2. Purpose of the investigation and the effects of the methods used on the precision of the results	2
II. Method of presenting the data	8
III. Precision of measurements	10
IV. Data obtained in 1930	11
V. Significance of data	27
VI. Data on miscellaneous ferrous materials	31
VII. Summary	34

I. INTRODUCTION

1. RELATION OF THIS REPORT TO PREVIOUS ONES

As a part of its investigation of stray-current electrolysis the National Bureau of Standards began in 1922 a study of the relation of soils to the deterioration of buried pipe. This study was planned to extend over 10 or more years and involved the cooperation of a large number of manufacturers and public-utility organizations. It seems wise to publish from time to time progress reports concerning the work in order that those cooperating may keep in touch with the results of their cooperation. The first report entitled "Bureau of Standards Soil-Corrosion Studies. I. Soils, Materials, and the Results of Early Observations" was published as Technologic Paper No. 368 in 1928. As the title indicates, it describes the soils and materials then under observation and records the rates of corrosion observed when specimens were removed in 1924 and 1926. This paper is neces-

sary for the complete understanding of the later reports. In August, 1929, the bureau published a second report known as Research Paper No. 95 entitled "Soil Corrosion Studies, 1927–28." That report gives the results of the examinations of ferrous specimens removed in 1928, together with a description of related field and laboratory studies.

The present report covers the results of the examinations of ferrous specimens removed in 1930 with such supplementary information as seems necessary for the interpretation of the data. The results of the examination of the nonferrous pipe specimens, the organic and metallic protective coatings, and the relation of soils to corrosion will be discussed in later papers. The investigation still has at least four years to run, and final conclusions can not be drawn until the data now available can be combined with those to be obtained later.

2. PURPOSE OF THE INVESTIGATION AND THE EFFECTS OF THE METHODS USED ON THE PRECISION OF THE RESULTS

The primary purpose of the investigation was to determine the extent to which soil conditions are responsible for the corrosion of underground pipes. This purpose determined the selection of the soils, the materials, and the method of testing. The results so far obtained indicate that the selections are quite satisfactory for the purpose for which they are intended but for some other purposes the data are not so well adapted, as will be pointed out.

The main objective in selecting the soils was to obtain soil representative of conditions encountered by underground pipes without regard to corrosiveness. For this reason the test locations are most numerous in those regions where underground pipe systems are extensive.

As is well known to all who have had extensive experience in the laying of gas or water mains, in most cities several varieties of soils are found, some of which are much more corrosive than others. For this reason it is necessary to avoid the association of the results of the tests with the cities in or near which they are conducted. This is illustrated by the fact that a rather corrosive soil, Susquehanna, is under test near Meridian, Miss. None of this soil is found within the boundaries of the city, and the rates of corrosion of buried pipes there are said to be much less than the rate found for Susquehanna clay. Likewise the rate of corrosion of specimens in Fairmount loam in Cincinnati, Ohio, is said to be considerably less than that experienced in one section of the city where a different soil is encountered. The data are indicative of corrosion under the described soil conditions, but not necessarily of the average corrosion of the pipes in the cities near the test locations.

In each test location an attempt was made to bury the specimens at approximately the depth at which pipes were laid in that locality. On this account, in the Southern States the specimens are at a depth of from 18 to 24 inches, while farther north their depth varies from 3 to 5 feet. Consequently, the specimens in the South frequently lie in the surface soil or upper subsoil, while those in the North may lie in the lower subsoil or parent material. Often in a given locality there is as much difference between the characteristics of the surface-soil and the subsoil as between two widely separated and different soils. While the method of burial adopted is quite satisfactory for indicating the soil corrosion in the locality of the test, it is not ade-

quate for correlating corrosion with soil types, because other things being equal the corrosion in any soil depends upon the soil horizon in which the pipe is buried. If a pipe is so laid that it passes from one soil horizon to another it may be expected to corrode at a different rate from that if laid wholly in either horizon.

The desire to make the tests in soils in which pipe systems are in service resulted in the selection of a number of soils which were found by the tests to be only slightly corrosive. Such soils are not suitable for the determination of the resistance of a material to corrosion.

An attempt was made to select typical representatives of the desired soil series, but in some instances the necessity of selecting an available site where assistance in burying specimens could be obtained resulted in placing the specimens in a trench, throughout

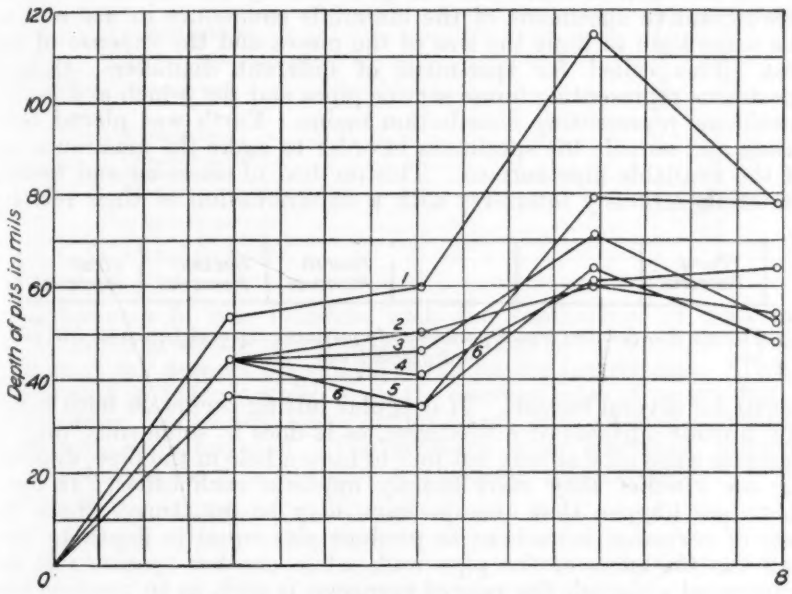

FIGURE 1.—*Variation in pitting soil No. 15*

the length of which the soil texture or moisture was not quite uniform. This lack of uniformity is responsible for some of the inconsistencies in rates of corrosion and pitting which are observed at some locations. This is illustrated by Figure 1 in which are plotted pitting data for a location where these variations are somewhat abnormal. The circles show the depth of the deepest pit on each of six materials at the end of four intervals of exposure. In order to compare equal amounts of exposed areas it is necessary to consider one 6-inch specimen of one material, two 3-inch specimens of another, and four 1½-inch specimens of a third material.

It will be noticed that the rates of pitting of all the materials are greatest for the first period. This is the case for most materials in most test locations and indicates that the initial rate of pitting is usually greater than subsequent rates. The specimens removed at the close of the 4-year period showed little or no greater depth of

pits over the specimens removed two years earlier. The specimens removed at the end of six years showed, with one exception, deeper pits than those removed two years later. Figure 2 shows the relative positions of the sets of specimens in the trench. The most logical way to account for the differences in depths of pitting is to conclude that the soil at one end of the trench where the third set was removed is not the same as at the other end of the trench. Several test locations give similar results for most specimens and a large number of the locations show erratic results for at least one material. Where the abnormal results apply to one material only, it is probable that irregularities in the material are responsible. Evidently, then, the results at the close of any one test period in a given soil can not safely be taken as a measure of the relative performance of materials in the soil or of the corrosiveness of the soil.

The selection of materials was governed by the desire to expose representative specimens of the materials commonly in use and at the same time to limit the size of the pieces and the expense of the test. This called for specimens of different diameters, 1½-inch specimens representing house service pipes and the 3-inch and 6-inch specimens representing distribution mains. Earth was placed both inside and outside the specimens in order to make the maximum use of the available pipe surface. This method of selecting and testing materials seriously interferes with a determination of their relative

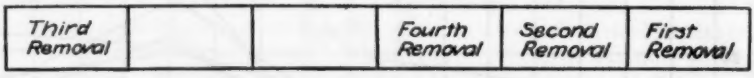

FIGURE 2.—*Relative trench positions of specimens removed from soil No. 15 at different times*

merits for several reasons. If irregular pitting occurs on both inside and outside surfaces of a specimen, as it does in some soils, pits on opposite sides may or may not join to form a hole in the pipe, depending on whether they start exactly opposite each other. It may, therefore, happen that one specimen may be punctured where the rate of corrosion is such as to produce pits equal in depth to one-half the thickness of the pipe wall, while another specimen is not penetrated although the rate of corrosion is such as to produce pits equal in depth to two-thirds of the wall thickness. Again, the 1½-inch specimens, because of their thinner walls, will be punctured before the thicker walled 3-inch specimens.

The puncture of a specimen creates a problem with respect to the computation of rates of penetration, for which there appears to be no entirely satisfactory solution. In the absence of a better method, the rate of penetration for a material in a given soil for periods subsequent to the one in which a puncture from the outside only has been observed has been taken as the thickness of the pipe wall divided by the age of the specimen when the puncture was first discovered. Since rates of pitting decrease with time for most soils, this method yields a somewhat higher final rate of penetration than would be found if the specimen were thicker. It has been necessary to apply this treatment in this report only to the data for soil No. 23.

Different rolling mills and foundries finish their products differently, some being smoother than others. This difference in roughness may

have no effect on the rate of corrosion, but it affects the precision with which the depth of the pits can be determined.

This is illustrated in Table 1, which indicates the original roughness of the specimens. Eight measurements on each of two uncorroded specimens of several materials were made with the depth gage used for determining pit depths. The table shows the arithmetical average deviation of the individual measurements from the average of all the measurements on one kind and size of material. It will be seen that for two materials the deviation is about 5 mils, while for another it is about 30, or six times as great.

TABLE 1.—*Finish of representative specimens as furnished*

Identification letter	Material	Diameter	Average roughness
		Inches	*Mils*
a	Open-hearth iron	1½	5.0
b	Wrought iron	1½	8.1
d	Wrought iron	1½	8.1
e	Bessemer steel	1½	4.9
y	Bessemer steel	1½	7.5
B	Wrought iron	3	11
D	Wrought iron	3	8
K	Open-hearth iron	3	8
M	Bessemer steel	3	11.6
Y	Open-hearth steel+copper	3	12.3
C	de Lavaud cast iron	6	10.4
L	Northern pit cast iron	6	20.6
Z	Southern pit cast iron	6	29.9

Differences in size interfere with the comparison of materials. When small areas are concerned, other things being equal, it is probable that the deepest pit will be found on the largest area. This is illustrated in Table 2 which gives the average rates of penetration of the deepest pits on two materials for which both 1½-inch and 3-inch specimens were included. The averages cover specimens removed at the close of the 2, 4, 6, and 8 year periods, respectively.

TABLE 2.—*Effect of size of specimen on maximum rate of pitting*

Material	Maximum rate of pitting (mils per year)							
	2-year period		4-year period		6-year period		8-year period	
	Size of specimen (inches)							
	1½	3	1½	3	1½	3	1½	3
I	22.2	26.9	12.0	13.8	8.3	10.4	6.7	7.5
II	22.4	24.4	12.0	13.1	9.3	9.5	6.8	7.1

It will be noticed that in each case the 3-inch specimens showed deeper pits than the corresponding 1½-inch specimens. A study of the rates of loss of weight of the same materials indicates that for each period the 3-inch specimens show the lower rates of corrosion. Possible explanations for the greater corrosion of the smaller specimens are that they may have been subjected to greater internal strains due to quicker cooling, or to the additional rolling, to which the material from which they are formed is subjected, or that the

corroding solution may act more freely on the more curved surface of the smaller specimens. Whatever the explanation for the differences, it is evident that the rates of corrosion and pitting depend to some extent upon the size of the specimen, and that specimens of different sizes are not strictly comparable.

The differences in rates of loss of weight and rates of penetration of pits are frequently as great for two specimens of the same material as for two specimens of different materials. This is illustrated by Table 4, which shows the rates of loss of weight and rates of penetration of the deepest pits for individual specimens removed from soil No. 1 in 1930.

In order to get the necessary data on a single page in this and later tables it has been found necessary to refer to specimens by their identification letters. The significance of these letters is given in Table 3. The names of the soils, the locations of the tests and the ages of specimens removed in 1930 are given in Table 5.

TABLE 3.—*Identification of materials*

Identification letters	Material
1¼-INCH SPECIMENS	
a	Pure open-hearth iron, lap-welded.
b, d	Hand-puddled wrought-iron, butt-welded.
e	Bessemer steel, butt-welded.
y	Scale-free Bessemer steel butt-welded.
3-INCH SPECIMENS, LAP-WELDED	
A [1]	Pure open-hearth iron.
B, D	Hand-puddled wrought iron.
K	Open-hearth steel.
M	Bessemer steel.
N [1]	Bessemer steel, scale-free, butt-welded.
Y	Open-hearth steel, 0.2 per cent copper.
6-INCH CAST-IRON SPECIMENS	
C	de Lavaud centrifugal process.
CC	de Lavaud centrifugal process, only outside exposed to soil.
I [1]	Monocast centrifugal process.
L	Vertically cast in sand molds, northern ore.
P [1]	"Pit" cast iron, southern ore.
Z	Vertically cast in sand molds, southern ore.

[1] Specimens buried in 1928 for special tests.

TABLE 4.—*Data on individual specimens removed from soil No. 1 in 1930*

Mark	Rate of loss	Rate of penetration	Mark	Rate of loss	Rate of penetration
	Ounces per square foot per year	*Mils per year*		*Ounces per square foot per year*	*Mils per year*
a	0.680	5.7	K	0.800	5.7
	.624	5.7		.665	8.5
b	.945	12.8	M	.970	8.7
d	.835	6.4		.948	7.4
e	.899	6.1	Y	.864	5.2
	.875	7.4		.862	6.5
y	.852	5.5	C	.708	7.2
	.855	7.8		.847	9.6
B	.882	7.0	L	.963	28.8
D	.848	6.8	Z	.942	27.2

TABLE 5.—*Ages of specimens buried in 1922*

Soil No.	Soil	Location	Age of specimens at close of period (years)—			
			First	Second	Third	Fourth
1	Allis silt loam	Cleveland, Ohio	0.98	3.58	5.50	7.68
2	Bell clay	Dallas, Tex	2.09	4.03	5.93	7.93
3	Cecil clay loam	Atlanta, Ga	2.01	4.09	6.04	7.98
4	Chester loam	Jenkintown, Pa	1.38	4.03	6.12	7.96
5	Dublin clay adobe	Oakland, Calif	1.93	4.13	6.16	8.06
6	Everett gravelly sandy loam	Seattle, Wash	1.93	4.13	6.17	8.05
7	Fairmount silt loam	Cincinnati, Ohio	1.04	3.50	-------	7.68
8	Fargo clay loam	Fargo, N. Dak	1.13	3.80	5.83	7.74
9	Genesee silt loam	Sidney, Ohio	1.03	3.48	5.47	7.67
10	Gloucester sandy loam	Middleboro, Mass	1.33	4.01	6.10	7.93
11	Hagerstown loam	Baltimore, Md	1.36	3.97	6.01	7.84
12	Hanford fine sandy loam	Los Angeles, Calif	1.94	4.14	6.17	8.05
13	Hanford very fine sandy loam	Bakersfield, Calif	1.93	4.22	5.89	-------
14	Hempstead silt loam	St. Paul, Minn	1.13	3.80	5.83	7.72
15	Houston black clay	San Antonio, Tex	1.96	4.04	5.93	7.95
16	Kalmia fine sandy loam	Mobile, Ala	1.97	4.04	5.97	7.94
17	Keyport loam	Alexandria, Va	1.21	3.83	5.89	7.71
18	Knox silt loam	Omaha, Nebr	1.19	3.74	5.78	7.67
19	Lindley silt loam	Des Moines, Iowa	1.12	3.66	5.70	7.58
20	Mahoning silt loam	Cleveland, Ohio	.98	3.57	5.50	7.68
21	Marshal silt loam	Kansas City, Mo	1.47	4.02	6.05	-------
22	Memphis silt loam	Memphis, Tenn	1.72	3.68	5.55	7.59
23	Merced silt loam	Buttonwillow, Calif	1.93	4.27	6.16	7.95
24	Merrimac gravelly sandy loam	Norwood, Mass	1.32	4.01	6.10	7.93
25	Miami clay loam	Milwaukee, Wis	1.03	3.71	5.74	7.62
26	Miami silt loam	Springfield, Ohio	1.04	3.49	5.48	7.67
27	Miller clay	Bunkie, La	1.95	4.05	5.96	7.95
28	Montezuma clay adobe	San Diego, Calif	1.64	-------	5.56	-------
29	Muck	New Orleans, La	1.96	4.07	5.99	7.96
30	Muscatine silt loam	Davenport, Iowa	1.11	3.65	5.69	7.58
31	Norfolk sand	Jacksonville, Fla	2.01	4.07	6.02	7.98
32	Ontario loam	Rochester, N. Y	.94	3.73	5.82	7.65
33	Peat	Milwaukee, Wis	1.03	3.71	5.75	7.63
34	Penn silt loam	Norristown, Pa	1.38	4.03	6.12	7.96
35	Ramona loam	Los Angeles, Calif	1.93	4.14	6.16	8.05
36	Ruston sandy loam	Meridian, Miss	1.99	4.07	5.97	8.00
37	St. Johns fine sand	Jacksonville, Fla	2.00	4.07	6.03	7.98
38	Sassafras gravelly sandy loam	Camden, N. J	1.40	4.04	6.13	7.97
39	Sassafras silt loam	Wilmington, Del	1.38	4.02	6.11	7.95
40	Sharkey clay	New Orleans, La	1.96	4.06	5.98	7.96
41	Summit silt loam	Kansas City, Mo	1.47	4.02	6.05	7.94
42	Susquehanna clay	Meridian, Miss	1.98	4.07	5.97	8.00
43	Tidal marsh	Elizabeth, N. J	1.29	4.06	6.16	8.02
44	Wabash silt loam	Omaha, Nebr	1.09	3.63	5.68	7.58
45	Unidentified alkali soil	Casper, Wyo	1.18	3.78	5.79	7.68
46	Unidentified sandy loam	Denver, Colo	1.46	4.05	6.07	7.96
47	Unidentified silt loam	Salt Lake City, Utah	1.48	4.08	6.09	7.99

Specimens b, d, B, and D are of the same material but specimens b and B were supplied by one mill and d and D furnished by another mill. No claim is made by either mill that one of these sets of material is superior to the other. It will be seen from Table 4 that in soil No. 1 the rates of loss of weight for the four specimens b, d, B, and D are quite similar, but that the maximum rate of pitting for specimen b is greater than for any of the other specimens except L and Z which are of quite different material.

Similar departures of a single specimen from the average behavior of its group will be found in the data for about one-third of the soils under observation. An abnormally low rate of pitting occurs about

as often as one that is abnormally high. Usually the variations in the apparent behavior of two similar specimens are not the result of errors in testing, but originate in abnormal conditions in the material, the soil, or the contact between the soil and the specimen. The variations are significant of what may be expected when pipe is placed underground, and indicate that the performance of one specimen or one section of working pipe line should not be taken as representative of the performance of the material from which the specimen or pipe is made.

Attention is called to these irregularities in corrosion data in order that those who attempt to compare data on different materials shall realize the character of the data with which they deal. There is a tendency among those unfamiliar with corrosion research in general, and especially with those unfamiliar with underground corrosion, to assume that for a given pipe material in a specified soil there is a definite rate of corrosion just as the material has a definite density. Such, however, is not the case. The most characteristic phenomenon of underground corrosion is its erratic nature. While a sufficient amount of data may indicate the average performance of the materials, it is to be expected that in any specific case the performance of a material may depart widely from the average. This appears to be true for all the commonly used ferrous pipe materials.

II. METHOD OF PRESENTING THE DATA

During 1930 approximately 1,300 specimens of ferrous pipe were removed from 70 locations. With a few exceptions two specimens of each material under observation were removed from each soil under investigation.

Determinations of the loss of weight and depth of the five deepest pits were made for each specimen and these data are available for those who have need for them. To reach any conclusion from these data requires a very considerable amount of time and effort, and an attempt has therefore been made to put their essential features in a form which can be more readily understood. The first step in this process was to combine the similar data for the two specimens of the same material and to determine the avarage rate of loss of weight per unit area for each pair of specimens.

When a study of the pitting of the specimens was made there was some doubt regarding the proper method of reporting the results. It has seemed desirable to continue in this report the form of table previously used in earlier reports on the soil-corrosion investigation. The rates of pitting in these tables have been derived from measurements of the deepest pit on each specimen. Thus for the six specimens of Bessemer steel removed from each soil, the rate of pitting is based on six pits, while for the two specimens of open-hearth steel, removed from a single soil the rate of pitting is computed from the depth of two pits.

It has been shown, however, that for a given material the depth of the deepest pit on a small specimen depends somewhat on the size of the specimen. In order to take account of this effect of the size of the specimen, other tables have been prepared in which the number of pits chosen for the determination of the rate of penetration is

proportional to the size of the specimen. As in former computations, the deepest pit on each 1½-inch specimen is used, but for the 3-inch specimens the two deepest pits on each specimen and for the 6-inch specimens the four deepest pits on each specimen have been made the bases for determining the rates of penetration.

It will be found that this method unduly favors one size of specimen or another, depending on the soil, but that for the average of all soils for all periods the weighted rates of pitting for the 1½-inch and 3-inch wrought-iron specimens are identical, as they should be since both sizes of specimens were furnished by the same mills at the same time. The weighted average results for the 1½-inch and 3-inch Bessemer steel specimens are nearly the same, the 3-inch material showing a somewhat higher rate of penetration. As all the specimens of gray cast iron were 6 inches in diameter, it is not possible to determine directly the fairness of the method with respect to these specimens. Since data are presented for both the maximum pit and the weighted maximum pit, the reader can use his discretion as to which he will accept.

It also appeared desirable to rearrange the data so as to show whether specimens of the same material from different sources behaved similarly, and to show the apparent relative performance of different sizes of the same material in each soil after the data had been adjusted to take account of the size of the specimen.

A further complication of some of the data originates from the fact that the outer surface of the de Lavaud specimens is quite different from the inner surface. This was not realized by those conducting the test at the time it was decided to fill the specimens with earth. An attempt was made later to take account of this difference by burying in 1924 additional specimens of de Lavaud cast iron which were coated on the inside. The ages of these specimens are consequently about two years less than those of the specimens first buried. Because fewer of these specimens were buried none were removed in 1928. In Table 6 the ages of these de Lavaud specimens are given. In Tables 11 to 16 these specimens are indicated by a footnote reference.

Whether the coating of the specimens will have the desired result is somewhat doubtful and it is probable that the decision as to the behavior of this material will have to be based largely on the rates of pitting. Since observation has indicated that the corrosion of the outer and inner surfaces of the other materials also differed on account of differences of the packing of the soil or for other reasons, and because pipe failures are usually caused by pit holes rather than by loss of material, rates of pitting may be the better criteria for corrosion of all materials.

TABLE 6.—*Age of De Lavaud specimens that were coated on the inside* [1]

Soil No.	Soil	Age of specimens removed—	
		In 1926	In 1930
		Years	*Years*
2	Bell clay	1.84	5.84
3	Cecil clay loam	2.07	5.97
5	Dublin clay adobe	2.20	6.13
6	Everett gravelly sandy loam	2.20	6.12
12	Hanford fine sandy loam	2.21	6.12
15	Houston black clay	2.08	5.99
16	Kalmia fine sandy loam	2.07	5.98
27	Miller clay	2.11	6.01
29	Muck	2.11	6.01
31	Norfolk sand	2.07	5.98
35	Ramona loam	2.20	6.12
36	Ruston sandy loam	2.08	6.02
37	St. Johns fine sand	2.07	5.98
40	Sharkey clay	2.10	6.01
42	Susquehanna clay	2.08	6.02

[1] Outer surface only exposed to soil. These specimens were buried in 1924. None were removed in 1928.

III. PRECISION OF MEASUREMENTS

The value of data depends upon the significance of the phenomena observed and upon the precision of the observations. The significance of the observed phenomena can be best understood after the data have been presented. The precision of the data depends on the care and thoroughness with which the corrosion products were removed and upon the errors in determining the losses and pit depths. The losses were determined by checking the weights of the 6-inch specimens to 0.2 g and the 3-inch and 1½-inch specimens to 0.02 g. The losses in weight are such as to make the maximum error due to weighing about 1 per cent for the heaviest specimens in the least corrosive soils, and 0.1 per cent for the specimens in the more corrosive soils.

It is not possible to determine exactly the maximum errors due to improper cleaning of the specimens. It is estimated that they are less than 1 per cent for the rolled materials. In most cases there is no sharp distinction between the corroded and uncorroded sections of the cast-iron specimens. Fortunately the difficulty in determining when all of the corrosion products have been removed is roughly proportional to the extent of the corrosion. It is doubtful whether the error caused by improper cleaning exceeds 1 per cent for the most difficult specimens.

The pit measurements for all specimens were checked to 3 mils, but the true depth of any one pit may differ from the measured depth by from two to five times this amount on account of the roughness of the finish of the specimens as shown in Table 1.

From the above statements it will be evident that the number of figures carried in the following tables indicate the precision of the measurements. It should not be understood, however, that the figures indicate the precision with which the performance of the soils and materials have been determined. The significance of the data will be discussed after their presentation.

IV. DATA OBTAINED IN 1930

Tables 7 to 10, inclusive, are given for the benefit of those who prefer the method of presenting data used in previous soil-corrosion reports. The data are comparable with similar data in Tables 4, 5, and 6 of Technologic Paper No. 368 and with Tables 5, 6, and 7 of Research Paper No. 95. The names of the soils and the approximate locations of the test plots are given in Table 5.

In these tables the Bessemer steel is represented by four 1½-inch and two 3-inch specimens, the wrought iron by two 1½-inch and two 3-inch specimens, the pure open-hearth iron by two 1½-inch specimens, the open-hearth and copper-bearing steels each by two 3-inch specimens, and the cast irons each by two 6-inch specimens.

In order to make the data for different sizes of materials more nearly comparable, the data presented in the earlier reports and those for the 1930 specimens have been recalculated and rearranged to form Tables 11 to 18. In these tables which show rates of penetration the rates have been weighted according to the size of the specimens by averaging the deepest pits on the 1½-inch specimens, the two deepest pits on the 3-inch specimens and the four deepest pits on the 6-inch specimens. There were two specimens of each material except materials *L* and *Z* (see Table 3), of which there was but one specimen removed at a time from each soil.

TABLE 7.—*Rates of loss of weight of 8-year-old specimens*

[In ounces per square foot per year]

Soil No.[1]	Time buried	Bessemer steel	Wrought iron	Pure open-hearth iron	Open-hearth steel	Copper-bearing steel	Sand-mold cast iron	De Lavaud cast iron
		Number of specimens considered						
		6	4	2	2	2	2	2
	Years							
1	7.68	0.90	0.88	0.65	0.73	0.86	0.95	0.78
2	7.93	.47	.47	.48	.39	.29	.37	[2]
3	7.98	.53	.51	.46	.51	.48	.54	[2]
4	7.96	.67	.68	.65	.69	.73	.62	.71
5	8.06	.67	.75	.73	.70	.67	.82	[2]
6	8.05	.11	.11	.10	.10	.12	.10	[2]
7	7.68	.54	.55	.52	.51	.55	.57	.61
8	7.74	.46	.48	.43	.46	.55	.81	.73
9	7.67	.41	.45	.42	.44	.40	.48	.52
10	7.93	.57	.57	.55	.58	.58	.50	.54
11	7.84	.21	.24	.13	.17	.18	.17	.19
12	8.05	.11	.14	.12	.10	.14	15	[2]
13	[3]	[3]	[3]	[3]	[3]	[3]	[3]	[4]
14	7.72	.35	.37	.26	.22	.30	.38	.35
15	7.95	.67	.66	.63	.71	.63	.55	[2]
16	7.94	.57	.61	.64	.58	.64	.60	[2]
17	7.71	.88	.94	.84	.90	.96	.82	.94
18	7.67	.31	.35	.23	.25	.27	.39	.27
19	7.58	.38	.36	.33	.32	.33	.39	.34
20	7.68	.38	.43	.36	.38	.37	.48	.46
21	[4]	[4]	[4]	[4]	[4]	[4]	[4]	[4]
22	7.59	.93	.83	.76	.82	.99	.69	.84
23	7.95	2.24	2.46	2.28	2.65	3.00	4.98	2.65
24	7.93	.12	.12	.12	.11	.10	.07	.09
25	7.62	.25	.27	.23	.23	.23	.31	.28

[1] See Table 5 for names and locations of soils.
[2] De Lavaud specimens buried late.
[3] No regular specimens.
[4] No specimens removed.

TABLE 7.—*Rates of loss of weight of 8-year-old specimens*—Continued

[In ounces per square foot per year]

Soil No.	Time buried	Bessemer steel	Wrought iron	Pure open-hearth iron	Open-hearth steel	Copper-bearing steel	Sand-mold cast iron	De Lavaud cast iron
		Number of specimens considered						
		6	4	2	2	2	2	2
	Years							
26	7.67	0.22	0.23	0.17	0.19	0.22	0.27	0.23
27	7.95	.56	.54	.57	.62	.55	.53	[2]
28	5.56	1.84	1.63	1.86	1.92	1.92	1.68	.77
29	7.96	1.61	1.50	1.80	2.07	2.01	1.72	[2]
30	8.17	.52	.57	.50	.49	.47	.62	.59
31	7.98	.31	.27	.23	.28	.28	.22	[2]
32	7.65	.32	.35	.26	.33	.35	.45	.34
33	7.63	1.18	1.16	1.10	1.16	1.03	1.11	1.18
34	7.96	.43	.43	.37	.40	.40	.50	.58
35	8.05	.23	.26	.30	.26	.29	.25	[2]
36	8.00	.29	.30	.25	.26	.26	.13	[2]
37	7.98	.67	.78	.73	.77	.81	.81	[2]
38	7.97	.26	.25	.25	.24	.26	.16	.17
39	7.95	.55	.59	.52	.61	.64	.67	.75
40	7.96	.85	.85	.80	.89	.96	1.15	[2]
41	7.94	.60	.60	.61	.53	.55	.47	.32
42	8.00	1.01	.88	.74	.86	.70	1.40	[2]
43	7.98	1.28	1.65	1.14	1.36	1.81	.92	1.32
44	7.58	.30	.28	.22	.28	.28	.26	.21
45	7.68	.51	.60	.45	.50	.55	.77	.51
46	7.96	.70	.71	.71	.75	.84	.74	.71
47	7.99	.23	.26	.27	.26	.20	.30	.38

[2] De Lavaud specimens buried late.

TABLE 8.—*Rates of maximum penetration of 8-year-old specimens*

[In mils per year]

Soil No.	Time buried	Bessemer steel	Wrought iron	Pure open-hearth iron	Open-hearth steel	Copper-bearing steel	Sand-mold cast iron	De Lavaud cast iron
		Number of specimens considered						
		6	4	2	2	2	2	2
	Years							
1	7.68	7	8	6	7	6	28	8
2	7.93	6	5	6	6	6	12	[1]
3	7.98	9	8	8	8	9	21	[1]
4	7.96	5	5	7	7	10	9	6
5	8.06	6	6	5	6	6	9	[1]
6	8.05	2	2	2	2	2	1	[1]
7	7.68	4	5	3	6	3	4	7
8	7.74	8	7	8	11	12	11	14
9	7.67	5	6	5	6	5	5	7
10	7.93	5	5	6	7	5	5	5
11	7.84	7	8	8	7	8	8	[2] 3
12	8.05	[2] 2	[2] 2	[2] 2	2	3	[2] 1	[1]
13	[3]	[3]	[3]	[3]	[3]	[3]	[3]	[3]
14	7.72	15	11	11	10	21	8	10
15	7.95	6	8	7	6	7	11	[1]
16	7.94	9	10	7	11	9	19	[1]
17	7.71	4	5	4	5	5	4	6
18	7.67	5	6	7	7	7	[2] 1	[2] 1
19	7.58	6	6	6	8	9	22	10
20	7.68	5	5	4	5	8	9	7

[1] De Lavaud specimens buried late.
[2] Pit depths assumed to be 10 mils for calculating purposes.
[3] No regular specimens.

TABLE 8.—*Rates of maximum penetration of 8-year-old specimens*—Continued

[In mils per year]

Soil No.	Time buried	Bessemer steel	Wrought iron	Pure open-hearth iron	Open-hearth steel	Copper-bearing steel	Sand-mold cast iron	De Lavaud cast iron
		Number of specimens considered						
		6	4	2	2	2	2	2
	Years							
21	(4)	(4)	(4)	(4)	(4)	(4)	(4)	(4)
22	7.59	8	7	7	8	9	17	15
23	7.95	17	19	27	20	27	51	22
24	7.93	2	2	3	3	4	[2] 1	[2] 1
25	7.62	5	6	6	5	5	13	[2] 1
26	7.67	6	6	5	6	8	10	5
27	7.95	5	5	4	9	5	18	(1)
28	5.56	10	10	9	14	13	31	8
29	7.96	13	10	13	11	22	27	(1)
30	8.17	5	6	6	4	4	8	9
31	7.98	5	5	5	6	5	7	(1)
32	7.65	5	5	4	6	6	22	7
33	7.63	11	10	17	15	12	21	17
34	7.96	6	6	5	8	9	7	7
35	8.05	[2] 2	3	4	3	7	4	(1)
36	8.00	5	6	6	[2] 7	[2] 6	[2] 22	(1)
37	7.98	7	7	7	8	12	6	(1)
38	7.97	3	4	7	3	3	[2] 1	[2] 1
39	7.95	6	7	5	10	10	6	7
40	7.96	10	11	11	12	12	11	(1)
41	7.94	7	8	8	7	7	6	6
42	8.00	13	11	10	12	11	19	(1)
43	7.98	9	14	11	17	11	6	13
44	7.58	8	7	9	7	12	6	5
45	7.68	7	7	7	8	9	11	9
46	7.96	15	9	8	8	17	11	6
47	7.99	[2] 1	[2] 1	[2] 1	[2] 1	[2] 1	[2] 1	[2] 4

[1] De Lavaud specimens buried late.
[2] Pit depths assumed to be 10 mils for calculating purposes.
[4] No specimens removed.

TABLE 9.—*Pitting factors of 8-year-old specimens*

Soil No.	Time buried	Bessemer steel	Wrought iron	Pure open-hearth iron	Open-hearth steel	Copper-bearing steel	Sand mold cast iron	De Lavaud cast iron
		Number of specimens considered						
		6	4	2	2	2	2	2
	Years							
1	7.68	5.2	6.0	5.9	6.5	4.4	17.2	6.3
2	7.93	8.2	7.1	8.3	9.5	13.5	19.8	(1)
3	7.98	10.9	9.7	11.0	10.8	11.7	23.6	(1)
4	7.96	5.3	4.3	7.7	6.7	8.6	8.6	4.7
5	8.06	5.6	4.8	4.1	5.9	5.3	6.6	(1)
6	8.05	11.5	11.0	14.4	13.1	9.9	7.1	(1)
7	7.68	4.8	5.3	3.9	7.4	3.5	3.3	6.4
8	7.74	11.9	9.8	12.2	16.1	14.4	8.0	11.2
9	7.67	8.1	8.3	7.5	9.1	8.5	6.3	8.1
10	7.93	5.5	5.6	7.3	7.9	6.0	6.3	5.0
11	7.84	23.9	23.6	41.0	27.8	29.6	26.9	[2] 8.5
12	8.[illegible]	[2] 10.5	[2] 11.2	[2] 11.8	15.1	14.8	[2] 6.5	(2)
13	(3)	(3)	(3)	(3)	(3)	(3)	(3)	(3)
14	7.72	28.4	22.3	27.0	30.0	45.6	15.3	16.5
15	7.95	5.9	8.2	7.9	5.2	6.8	11.4	(1)

[1] De Lavaud specimens buried late.
[2] Pit depths assumed to be 10 mils for calculating purposes.
[3] No regular specimens.

TABLE 9.—*Pitting factors of 8-year-old specimens*—Continued

Soil No.	Time buried	Bessemer steel	Wrought iron	Pure open-hearth iron	Open-hearth steel	Copper-bearing steel	Sand mold cast iron	De Lavaud cast iron
		Number of specimens considered						
		6	4	2	2	2	2	2
	Years							
16	7.94	9.7	10.2	7.6	11.9	10.0	19.1	[1]
17	7.71	3.3	3.4	3.3	3.7	3.4	3.0	3.8
18	7.67	11.9	12.0	20.7	19.3	17.3	[2] 2.0	[2] 2.8
19	7.58	10.7	11.9	12.5	15.6	17.6	33.8	17.0
20	7.68	9.5	6.8	7.3	7.8	14.8	10.9	9.4
21	[4]	[4]	[4]	[4]	[4]	[4]	[4]	[4]
22	7.59	5.6	5.7	6.1	6.1	6.1	14.7	10.5
23	7.95	5.0	5.0	[5]	5.0	6.0	[5]	4.9
24	7.93	9.9	12.5	15.3	18.6	25.5	[2] 11.9	[2] 8.4
25	7.62	13.3	13.8	15.8	14.5	16.6	27.2	[2] 2.8
26	7.67	17.2	17.2	20.1	21.0	22.1	21.3	13.7
27	7.95	5.4	5.6	4.5	9.7	6.2	20.5	[1]
28	5.56	3.7	4.1	3.2	4.7	4.6	10.8	6.2
29	7.96	5.6	4.7	4.9	3.6	7.3	9.3	[1]
30	8.17	5.9	6.7	7.5	5.8	5.4	7.3	9.3
31	7.98	9.6	12.8	13.3	13.2	10.6	20.7	[1]
32	7.65	11.4	9.6	11.0	12.4	11.2	28.7	13.8
33	7.63	6.3	6.0	10.5	8.7	7.9	11.1	8.4
34	7.96	8.7	8.3	9.4	14.2	13.9	7.6	6.9
35	8.05	[2] 7.0	6.7	9.1	[2] 6.9	[2] 12.9	[2] 9.3	[1]
36	8.00	11.7	14.3	16.2	18.6	15.8	110.1	[1]
37	7.98	7.0	5.8	6.4	7.2	9.9	4.4	[1]
38	7.97	7.8	10.1	18.2	8.6	7.6	[3] 4.6	[3] 4.4
39	7.95	7.1	7.8	7.4	10.3	10.1	5.6	5.8
40	7.96	7.6	8.2	8.9	9.1	7.9	5.7	[1]
41	7.94	8.1	8.3	8.4	8.9	8.4	7.4	10.3
42	8.00	8.4	7.8	8.8	8.8	10.6	7.8	[1]
43	7.98	4.8	5.7	6.0	8.2	4.2	3.8	5.4
44	7.58	18.7	16.3	27.9	15.9	27.0	15.2	13.1
45	7.68	9.2	7.9	9.7	10.3	10.3	9.4	10.9
46	7.96	14.2	8.7	7.8	7.4	13.0	8.2	5.3
47	7.99	[2] 3.6	[2] 3.1	[2] 3.2	[2] 3.1	[2] 4.1	[2] 2.6	[2] 6.6

[1] De Lavaud specimens buried late.
[2] Pit depths assumed to be 10 mils for calculating purposes.
[4] Not taken up.
[5] Specimen penetrated in 1928.

TABLE 10.—*Rates of loss of weight, maximum penetration, and pitting factors for De Lavaud specimens buried in 1924 and removed in 1930*

Soil No.	Time buried	Rates of loss of weight	Maximum rates of penetration	Pitting factor [1]
	Years	*Ounces per square foot per year*	*Mils per year*	
2	5.84	0.33	8	14.1
3	5.97	.22	[2] 2	[2] 4.4
5	6.13	1.58	[2] 12	[2] 4.3
6	6.12	.23	2	4.1
12	6.12	.39	[2] 4	[2] 5.4
15	5.99	.89	10	6.3
16	5.98	.62	15	14.4
27	6.01	1.18	16	7.9
29	6.01	1.39	15	6.4
31	5.98	.68	13	11.4
35	6.12	.22	[2] 2	[2] 4.7
36	6.02	.07	10	83.7
37	5.98	1.01	[2] 2	[2] 1.0
40	6.01	.98	14	8.1
42	6.02	.96	19	13.1

[1] The pitting factor is the ratio of the depth of the deepest pit to the average depth of corrosion.
[2] Pit depths assumed to be 10 mils for calculating purposes.

Comparisons of the data for the different years discloses the fact that the rates of corrosion differ from year to year. Part of this difference can be accounted for by variations in weather conditions, soil, and specimens. While there is a tendency for the rates to decrease, the most nearly representative values are probably those representing the average performance of all the specimens removed. Tables 19 and 20 give these average values as derived from Tables 11 to 18. In Research Paper No. 95 a table (Table 8) was given for the relative corrosiveness of soils. This table was derived by weighting the data according to the ages of the specimens. If changes in weather conditions were the controlling cause of the variations in the data for different periods, this weighting according to the ages of the specimens might be justified. A further study of the data discloses instances in which some other causes must control, and as the weighting referred to takes no account of these factors it seems best to abandon this method of weighting, at least until its value is better understood.

Table 21 goes one step further in averaging by combining all the similar data for all materials for any one soil. The purpose of the table is to furnish the best available data on soil corrosiveness. The rates of loss of weight for each soil for each period in Table 21 are based on exposed areas of approximately 14.4 square feet of pipe surface, and the average for all periods upon a total area of exposure of about 58 square feet. The pitting data for each soil for any one period are the results of measurements of 40 pits distributed over an area of approximately 7.5 square feet, while the data for the average of the four periods are derived from measurements of 160 pits distributed approximately uniformly over a total area of almost 30 square feet of pipe surface. The length of trench involved in the data for each soil is approximately 70 feet. These figures justify a very considerable degree of confidence that the data are representative of conditions under investigation. The authors know of very few sets of corrosion data representing so many determinations and none covering so wide a territory or in which individual determinations have been made with the same degree of precision.

60869—31——2

TABLE 11.—*Rates of loss of weight of 2-year-old specimens* [1]

[In ounces per square foot per year]

Soil No.	1¼-inch specimens				3-inch specimens				6-inch specimens		
	a [2]	b	e	y	B	K	M	Y	C	L	Z
1	1.080	1.250	1.150	1.125	1.205	1.395	1.290	1.170	0.805	1.090	1.810
2	.900	.940	.860	1.170	.920	1.045	1.045	.875	[3].430	.760	1.100
3	.730	.910	.865	1.005	.785	.980	1.055	.860	[3].580	1.220	.740
4	1.055	.860	1.065	1.035	.980	1.015	1.010	1.120	.915	.880	1.100
5	.570	.470	.660	.700	.505	.515	.475	.495	[3] 1.175	.390	.540
6	.075	.080	.070	.110	.060	.075	.105	.080	[3].121	.050	.080
7	.460	.665	.605	.580	.585	.510	.645	.595	.605	1.100	1.400
8	.640	.580	.645	.670	.590	.540	.700	.635	.695	.640	1.830
9	.540	1.175	.705	.880	.545	.610	.610	.525	.700	.610	.780
10	1.015	.930	.930	1.005	.860	.785	1.015	.880	.755	.590	.840
11	.200	.345	.280	.400	.265	.295	.325	.265	.075	.180	.170
12	.130	.130	.200	.165	.080	.110	.160	.130	[3].035	.040	.220
13	1.285	1.550	1.900	2.735	2.015	2.335	1.715	2.110	1.410	1.980	1.820
14	.235	.325	.385	.480	.315	.415	.385	.400	.240	.120	.410
15	1.250	1.050	1.155	1.090	1.145	1.155	1.385	1.385	[3] 1.155	.670	1.270
16	.955	1.265	1.350	1.065	1.085	1.145	1.340	1.060	[3].765	1.420	1.080
17	1.220	1.210	1.130	1.200	1.340	1.245	1.350	1.215	1.155	1.150	2.740
18	.355	.595	.375	.470	.340	.270	.400	.400	.210		
19	.555	.755	.590	.605	.545	.565	.705	.750	.340	.500	.490
20	.950	.885	1.145	1.040	.920	1.050	.965	.950	.755	.900	1.320
21	1.370	1.410	1.440	1.445	1.500	1.355	1.395	1.440	1.090	1.670	1.400
22	.820	.920	1.170	1.100	.835	.890	.820	1.030	.625	.350	1.470
23	2.805	3.935	3.985	4.060	3.025	3.380	3.495	4.065	2.960	3.720	10.500
24	.150	.195	.200	.220	.155	.200	.215	.150	.135	.030	.190
25	.430	.580	.420	.430	.320	.355	.395	.400	.475	.580	.380
26	.765	.890	.800	.760	.790	.735	.865	.870	.765	.990	1.090
27	.205	.315	.250	.245	.305	.285	.300	.245	[3] 1.105	.220	.270
28	2.040	1.660	2.190	1.800	1.870	1.945	1.770	2.155	2.760	2.870	2.850
29	2.030	1.700	1.940	2.240	1.785	2.165	2.090	2.135	[3] 2.850	1.700	2.280
30	.810	.835	1.035	.805	.780	.965	.975	.915	1.040	1.070	1.180
31	.340	.625	.615	.755	.400	.620	.660	.525	[3] 1.090	.170	.580
32	.270	.510	.390	.395	.325	.420	.420	.340	.520	.650	.160
33	.420	.350	.400	.445	.430	.435	.390	.350	.420	.210	.490
34	.945	.925	.850	.780	.995	.985	1.055	.860	.910	.970	.940
35	.420	.450	.375	.370	.410	.470	.580	.485	[3].515	.300	.900
36	.585	.615	.680	.575	.415	.420	.485	.475	[3].360	.410	.540
37	1.155	1.130	1.190	1.175	1.210	1.200	1.265	1.215	[3] 1.955	.700	.950
38	.115	.135	.175	.170	.125	.185	.215	.200	.035	.040	.090
39	.755	.855	.840	.945	.845	.990	.850	.900	.865	.920	1.130
40	1.095	1.080	1.050	1.040	1.160	1.275	1.110	1.445	[3] 1.120	.990	1.350
41	.510	.370	.365	.675	.435	.430	.280	.270	.265	.840	.800
42	1.510	1.805	1.690	1.560	1.480	1.205	1.450	.970	[3] 1.145	3.120	1.780
43	1.050	1.345	1.455	2.200	1.580	1.705	1.760	1.870	.785	1.070	.760
44	.300	.595	.335	.475	.340	.320	.330	.385	.155	.250	.940
45	1.005	1.170	1.180	1.070	.930	.815	1.420	1.160	1.140	1.720	1.010
46	.535	.905	.830	.645	.695	.765	.820	.790	.355	1.730	1.220
47	.350	.250	.325	.255	.300	.395	.330	.255	.400	.310	.450

[1] See Table 4 for exact ages of specimens.
[2] See Table 3 for identification of specimens.
[3] C specimens exposed to soil on outside only. See Table 6 for ages of these specimens.

TABLE 12.—*Weighted maximum rates of pitting of 2-year-old specimens* [1]

[In mils per year]

Soil No.	1½-inch specimens				3-inch specimens				6-inch specimens		
	a [2]	b	e	y	B	K	M	Y	C	L	Z
1	5.1	5.1	5.1	5.1	5.1	5.1	5.1	5.1	13.1	37.2	43.9
2	2.4	2.4	2.4	2.4	2.4	2.4	2.4	2.4	[2] 3.9	16.3	19.0
3	31.0	23.0	22.0	28.0	25.4	25.9	23.7	26.9	[3] 4.8	31.8	30.0
4	3.6	3.6	3.6	3.6	3.6	3.6	3.6	3.6	3.6	7.6	13.9
5	2.6	2.6	2.6	2.6	2.6	2.6	2.6	2.6	[3] 17.7	2.6	2.6
6	2.6	2.6	2.6	2.6	2.6	2.6	2.6	2.6	[3] 4.5	2.6	2.6
7	4.8	4.8	4.8	4.8	4.8	4.8	4.8	4.8	4.8	4.8	4.8
8	39.0	27.0	34.0	27.0	25.6	38.7	41.1	50.7	4.4	49.1	58.2
9	44.0	30.0	24.0	22.0	31.1	30.6	26.7	32.0	4.9	17.0	18.2
10	19.0	11.0	14.0	12.0	17.9	16.0	15.6	17.1	11.4	3.8	3.8
11	36.0	28.0	24.0	21.0	27.2	23.5	27.6	27.0	21.1	3.7	23.0
12	2.6	2.6	2.6	2.6	2.6	2.6	2.6	2.6	[3] 4.5	2.6	2.6
13	18.5	16.5	25.0	19.0	23.1	31.6	27.7	32.5	13.2	2.6	31.0
14	30.0	33.0	23.0	24.0	26.3	27.2	32.1	51.8	4.4	10.4	18.6
15	16.0	17.0	20.0	18.0	19.5	17.2	20.5	19.9	[3] 6.1	24.5	33.2
16	22.0	18.0	19.0	21.0	20.7	17.9	19.4	22.5	[3] 13.8	20.9	19.5
17	4.1	4.1	4.1	4.1	4.1	4.1	4.1	4.1	4.1	41.7	23.8
18	23.0	17.0	16.0	12.0	17.0	20.2	12.2	21.2	4.2	42.6	4.2
19	30.0	21.0	23.0	21.0	23.4	21.7	25.7	29.9	12.7	23.2	4.5
20	5.1	5.1	5.1	5.1	5.1	5.1	5.1	5.1	5.1	5.1	5.1
21	3.4	3.4	3.4	3.4	3.4	3.4	3.4	3.4	3.4	3.4	3.4
22	26.0	20.0	25.0	25.0	21.5	21.9	27.8	26.5	2.9	31.8	26.0
23	27.0	25.0	25.0	26.0	23.4	40.8	26.6	32.1	16.4	28.4	82.0
24	3.8	3.8	3.8	3.8	3.8	3.8	3.8	3.8	3.8	3.8	3.8
25	23.5	19.0	18.0	25.0	20.4	24.0	26.9	24.5	11.4	4.9	36.7
26	4.8	4.8	4.8	4.8	4.8	4.8	4.8	4.8	4.8	17.5	4.8
27	2.6	2.6	2.6	2.6	2.6	2.6	2.6	2.6	[3] 10.8	2.6	2.6
28	12.5	15.6	20.0	16.0	16.5	23.3	20.0	21.3	18.0	16.9	28.8
29	25.0	19.0	28.0	29.0	20.8	30.2	19.9	16.7	[3] 15.7	19.3	18.5
30	21.0	9.0	11.0	11.0	9.2	14.4	13.1	13.7	4.5	4.5	4.5
31	15.0	16.0	33.0	19.0	17.5	22.0	22.9	24.6	[3] 8.6	2.5	11.7
32	43.0	27.0	22.0	23.0	30.3	22.3	27.1	27.9	5.3	27.4	35.9
33	4.9	4.9	4.9	4.9	4.9	4.9	4.9	4.9	4.9	4.9	4.9
34	14.0	15.0	14.0	13.0	15.2	17.8	16.3	20.5	3.6	3.6	24.3
35	2.6	6.5	2.6	2.6	2.6	2.6	8.5	9.3	[3] 4.5	2.6	20.2
36	14.0	19.0	17.0	19.0	17.7	22.9	20.4	18.1	[3] 14.4	19.0	20.4
37	19.0	17.0	24.0	24.0	20.5	21.3	25.0	40.8	[3] 4.8	2.5	2.5
38	3.6	3.6	3.6	3.6	3.6	3.6	3.6	3.6	3.6	3.6	3.6
39	3.6	3.6	3.6	3.6	3.6	3.6	3.6	3.6	3.6	3.6	3.6
40	23.0	15.0	19.0	16.0	14.4	19.1	15.7	20.5	[3] 15.5	12.0	17.6
41	13.0	27.0	22.0	27.0	29.8	19.4	27.9	20.9	7.1	4.9	22.3
42	27.0	29.0	30.0	25.0	26.5	28.9	34.2	27.5	[3] 21.5	46.7	46.2
43	14.0	28.0	18.0	22.0	32.0	33.1	50.6	26.6	20.3	3.9	3.9
44	34.0	34.0	26.0	29.0	23.9	34.4	29.1	34.6	4.6	4.6	26.8
45	7.3	17.0	13.0	11.4	4.2	6.6	19.9	20.8	4.2	39.2	23.5
46	39.0	37.0	38.0	37.0	30.6	25.0	37.7	51.4	5.1	18.8	20.2
47	3.4	3.4	3.4	3.4	3.4	3.4	3.4	3.4	3.4	3.4	3.4

[1] See Table 4 for exact age of specimens.
[2] See Table 3 for identification of specimens.
[3] See Table 6 for ages of these de Lavaud specimens.

TABLE 13.—*Rates of loss of weight of 4-year-old specimens* [1]

[In ounces per square foot per year]

Soil No.	1¼-inch specimens				3-inch specimens				6-inch specimens		
	a [2]	b	e	y	B	K	M	Y	C	L	Z
1	0.925	1.125	1.075	1.080	1.190	1.170	1.200	0.960	0.965	1.070	1.040
2	.710	.735	.750	.745	.860	.680	.770	.625	[3]	.640	1.310
3	.705	.775	.805	.850	.885	.815	.875	.895	[3]	.840	1.220
4	.915	.875	.880	.865	.920	.915	.855	.925	.905	1.060	.970
5	.350	.520	.600	.595	.540	.510	.525	.500	[3]	.420	.420
6	.175	.170	.210	.190	.135	.175	.130	.130	[3]	.070	.090
7	.700	.700	690	680	765	.835	.725	.725	.765	.840	
8	.505	.500	.535	.515	.445	.450	.495	.485	.495	.710	1.420
9	.495	.665	.665	.580	.630	.350	.535	.495	410	.700	.630
10	340	.520	.420	.290	.415	.305	.660	.390	.435	.600	.480
11	.230	.280	.265	.300	.245	.235	.255	.240	.165	.090	.350
12	.345	.470	.390	.475	.355	.370	.310	.390	[3]	.280	.480
13	.640	1.660	.930	.785	.710	.555	1.050	1.110	.685	1.430	2.550
14	.520	.650	.690	.645	.600	.590	.570	.515	.305	.500	.700
15	.895	.740	.745	.790	.770	.830	.955	.760	[3]	.660	1.000
16	.710	.955	.870	.760	.710	.745	.815	.855	[3]	.390	.780
17	.860	.840	.895	.850	.970	.900	.945	.950	.940	.850	1.080
18	.325	.495	.505	.435	.350	.305	.325	.445	.165	.290	.250
19	.540	.405	.600	.605	.625	.620	.495	.555	.375	.470	.230
20	.605	.660	.500	.645	.620	.605	.595	.565	.515	.660	.680
21	.630	.645	.730	.605	.695	.730	.710	.625	.620	.790	.800
22	.870	1.050	.940	1.000	.980	1.000	.955	.940	.675	1.170	1.060
23	2.620	3.105	3.205	2.465	2.800	2.790	2.805	2.260	2.890	5.250	8.240
24	.110	.160	.130	.085	.085	.090	.105	.080	.055	.060	.120
25	.190	.370	.290	.300	.195	.230	.255	.280	.305	.420	.480
26	.455	.640	.530	.530	.555	.550	.615	.540	.565	.780	1.120
27	.800	.775	.965	.885	.870	.865	.810	.665	[3]	.660	.800
28	[4]	[4]	[4]	[4]	[4]	[4]	[4]	[4]	[4]	[4]	[4]
29	1.785	1.900	1.800	1.670	1.775	1.790	1.710	1.940	[3]	1.910	2.190
30	.300	.325	.340	.315	.390	.355	.385	.340	.450	.460	.550
31	.500	.420	.525	.555	.510	.620	.510	.565	[3]	.360	.540
32	.310	.465	.435	.390	.380	.350	.360	.380	.425	.530	.530
33	.940	.890	.920	.935	1.005	.930	.975	1.020	.920	.880	.880
34	.400	.440	.440	.470	.465	.465	.455	.445	.435	.480	.420
35	.415	.490	.435	.340	.500	.475	.460	.435	[3]	.540	.870
36	.350	.500	.540	.515	.410	.420	.405	.365	[3]	.310	.330
37	1.035	1.075	1.080	1.045	1.100	1.090	1.115	1.215	[3]	1.000	1.010
38	.110	.185	.180	.145	.120	.105	.135	.135	.075	.070	.120
39	.780	.810	.730	.670	.795	.760	.790	.730	.710	.830	.660
40	.975	1.055	.960	.920	1.025	1.050	1.130	1.025	[3]	1.350	1.500
41	.685	.885	.750	.755	.665	.730	.610	.625	.460	.630	.670
42	1.095	1.800	1.395	1.440	1.190	.830	1.255	.840	[3]	1.850	2.720
43	.900	1.785	1.125	1.195	1.170	1.285	1.695	1.580	.775	1.170	.700
44	.380	.505	.560	.505	.395	.380	.345	.350	.275	.400	.250
45	.965	.790	.760	.880	.765	.855	.730	.865	2.065	1.200	1.030
46	.680	.790	.715	.640	.595	.635	.660	.795	.555	1.000	1.350
47	.315	.460	.540	.310	.315	.325	.385	.500	.460	.530	.650

[1] See Table 4 for exact age of specimens.
[2] See Table 3 for identification of specimens.
[3] C specimens not removed in 1928.
[4] No specimens.

TABLE 14.—*Weighted maximum rates of pitting of 4-year-old specimens* [1]

[In mils per year]

Soil No.	1¼-inch specimens				3-inch specimens				6-inch specimens		
	a [2]	b	e	y	B	K	M	Y	C	L	Z
1	13.0	9.0	11.0	11.0	11.1	10.1	12.3	12.6	14.2	16.8	22.1
2	14.0	10.0	9.0	12.0	10.7	10.8	10.5	11.0	(3)	7.3	10.6
3	18.0	16.0	19.0	16.0	14.9	12.3	16.9	18.8	(3)	11.2	19.7
4	8.0	7.0	7.0	6.0	5.7	7.3	7.1	9.8	7.3	8.6	13.9
5	7.0	5.0	9.0	8.0	6.6	7.2	6.7	7.4	(3)	6.9	6.2
6	4.2	2.4	3.7	2.4	3.0	3.3	2.4	2.4	(3)	2.4	2.4
7	8.0	2.8	6.4	4.6	4.9	8.3	5.4	4.1	6.2	2.9	9.6
8	12.0	9.0	11.0	10.0	10.0	13.1	11.8	14.0	2.6	11.8	15.3
9	13.0	14.0	15.0	15.0	14.9	15.0	18.8	18.2	8.3	9.5	11.1
10	2.5	8.0	2.5	5.0	3.9	2.5	3.8	2.5	2.5	2.5	2.5
11	16.0	17.0	13.0	15.0	15.6	13.0	18.6	14.4	4.9	5.4	11.0
12	11.0	10.0	11.0	10.0	10.4	9.5	10.4	12.8	(3)	4.0	11.1
13	6.0	13.0	11.0	9.0	8.6	12.6	12.9	12.2	12.2	20.6	24.6
14	14.0	16.0	14.0	14.0	15.6	13.9	16.1	18.6	2.6	2.6	7.8
15	11.0	7.0	9.0	7.0	7.2	8.1	10.2	11.2	(3)	11.0	8.0
16	11.0	11.0	13.0	12.0	11.3	11.3	15.5	15.0	(3)	10.1	12.6
17	6.0	4.3	6.0	5.0	5.8	5.8	7.2	5.0	3.3	5.5	3.4
18	11.0	11.0	13.0	9.0	8.9	13.0	10.9	9.4	9.0	20.3	19.7
19	10.0	12.0	14.0	10.0	9.8	12.4	15.8	13.7	8.0	16.7	8.1
20	2.8	2.8	2.8	2.8	2.8	2.8	2.8	2.8	2.8	2.8	2.8
21	15.0	10.0	12.0	16.0	14.7	9.5	11.8	10.1	9.2	11.7	11.6
22	12.0	12.0	14.0	12.0	14.6	15.5	13.5	13.7	11.5	23.9	23.9
23	22.0	24.0	27.0	19.0	22.3	29.1	24.5	21.2	30.4	42.5	67.8
24	2.5	2.5	2.5	2.5	2.5	2.5	2.5	2.5	2.5	2.5	2.5
25	9.0	8.0	7.0	8.0	8.1	7.4	9.6	9.3	8.1	4.0	11.5
26	11.0	13.0	12.0	13.0	10.1	12.0	15.9	12.8	8.7	8.8	12.2
27	5.0	5.0	8.0	8.0	7.8	8.9	6.6	8.6	(3)	11.0	12.4
28	(4)	(4)	(4)	(4)	(4)	(4)	(4)	(4)	(4)	(4)	(4)
29	16.0	12.0	15.0	17.0	16.0	18.7	14.1	20.6	(3)	10.0	10.7
30	2.7	2.7	2.7	2.7	4.5	4.1	3.4	4.9	2.7	2.7	2.7
31	6.0	6.0	6.0	6.0	7.2	11.0	6.4	8.4	(3)	7.9	8.3
32	12.0	11.0	8.0	7.0	10.5	9.1	9.6	10.6	10.2	8.6	9.1
33	10.0	2.7	4.8	7.0	8.2	7.8	10.0	10.1	11.3	7.7	5.3
34	5.7	5.2	2.5	4.5	3.8	4.2	3.5	5.5	6.7	4.0	4.7
35	3.9	7.0	2.4	2.4	4.7	4.0	5.1	5.0	(3)	4.2	7.6
36	9.0	9.0	7.0	8.0	9.0	11.6	10.6	10.0	(3)	9.7	13.8
37	11.0	10.0	15.0	16.0	13.9	14.0	13.1	22.3	(3)	2.5	2.5
38	2.5	7.0	2.5	2.5	2.5	2.5	2.5	2.5	2.5	2.5	2.5
39	11.0	6.1	9.0	6.0	3.3	4.2	7.2	10.5	8.1	8.5	7.2
40	15.0	13.0	10.0	9.0	9.9	11.1	10.2	10.3	(3)	9.6	15.5
41	8.0	9.0	10.0	11.0	10.2	9.0	10.3	8.6	2.5	6.3	4.5
42	16.0	18.0	18.0	19.0	19.2	19.8	19.3	17.7	(3)	38.5	26.7
43	10.0	11.0	9.0	11.0	20.6	17.9	18.5	13.6	8.9	3.8	33.3
44	21.0	12.0	15.0	15.0	12.3	11.5	12.1	13.4	11.2	15.4	15.0
45	9.0	7.0	6.0	6.0	7.5	8.7	7.7	12.4	11.5	14.6	10.6
46	20.0	16.0	19.0	20.0	15.7	13.4	25.3	26.7	2.5	11.7	11.6
47	2.5	2.5	2.5	2.5	2.5	2.5	2.5	2.5	7.0	2.5	3.5

[1] See Table 4 for exact age of specimens.
[2] See Table 3 for identification of specimens.
[3] C specimens not removed in 1928.
[4] No specimens.

TABLE 15.—*Rates of loss of weight of 6-year-old specimens* [1]

[In ounces per square foot per year]

Soil No.	1½-inch specimens				3-inch specimens				6-inch specimens		
	a [2]	b	e	y	B	K	M	Y	C	L	Z
1	0.810	1.000	1.010	0.855	0.985	0.975	0.930	0.845	0.855	0.950	1.160
2	.640	.705	.655	.575	.695	.680	.710	.715	[3] .335	.840	.940
3	.525	.695	.620	.580	.625	.585	.605	.695	[3] .221	.790	.600
4	.735	.715	.725	.755	.770	.755	.715	.800	.730	.710	.760
5	.790	.815	.735	.775	.805	.640	.785	.720	[3] 1.575	.680	.880
6	.105	.100	.135	.115	.100	.130	.155	.120	[3] .232	.070	.100
7	(4)	(4)	(4)	(4)	(4)	(4)	(4)	(4)	(4)	(4)	(4)
8	.540	.545	.500	.450	.505	.530	.575	.570	.585	.860	.980
9	.400	.420	.445	.425	.480	.490	.485	.470	.525	.460	.680
10	.560	.560	.570	.560	.560	.600	.560	.565	.500	.390	.520
11	.175	.235	.235	.210	.220	.230	.205	.260	.100	.160	.220
12	.520	.365	.550	.495	.540	.445	.440	.460	[3] .395	.350	.370
13	1.110	1.405	1.130	1.253	.935	1.037	1.330	1.453	1.120	2.163	2.163
14	.420	.635	.620	.530	.590	.550	.540	.505	.370	.740	.860
15	1.045	1.030	.950	.915	1.045	.955	.870	1.085	[3] .889	1.010	1.430
16	.880	.820	.735	.725	.930	.750	.840	.830	[3] .621	1.050	.920
17	.885	1.010	.955	.890	1.040	1.040	1.035	1.060	.830	1.140	.970
18	.390	.700	.560	.455	.500	.475	.545	.445	.395	.570	.880
19	.385	.520	.390	.410	.400	.405	.360	.370	.375	.400	.270
20	.445	.490	.445	.375	.420	.410	.515	.410	.575	.660	.710
21	.700	.735	.820	.775	.790	.840	.750	.765	.730	.830	1.040
22	.950	.975	.830	.975	.825	.830	.715	.645	.675	.710	.920
23	2.220	2.545	1.980	2.545	2.090	2.355	2.245	2.835	2.885	5.830	5.670
24	.145	.200	.220	.130	.185	.185	.180	.160	.140	.070	.190
25	.290	.290	.325	.330	.310	.290	.300	.260	.225	.310	.380
26	.265	.380	.305	.270	.225	.210	.245	.245	.335	.480	.340
27	.505	.635	.690	.505	.525	.515	.505	.530	[3] 1.177	.550	.760
28	1.855	1.667	1.711	1.911	1.602	1.921	1.894	1.917	.767	1.684	-------
29	1.670	1.485	1.580	1.645	1.545	1.610	1.485	1.560	[3] 1.393	1.810	1.800
30	.325	.400	.455	.350	.435	.470	.445	.410	.520	.360	.630
31	.255	.295	.305	.320	.245	.315	.380	.390	[3] .679	.310	.290
32	.300	.355	.395	.305	.390	.380	.445	.430	.400	.440	.530
33	.815	.795	.805	.975	.755	.975	.840	.525	.585	.250	.520
34	.500	.450	.450	.450	.455	.510	.465	.480	.460	.480	.460
35	.185	.190	.255	.165	.145	.110	.165	.220	[3] .220	.150	.260
36	.220	.285	.290	.295	.230	.310	.235	.265	[3] .071	.240	.310
37	.695	.760	.600	.765	.635	.690	.685	.625	[3] 1.011	.830	.940
38	.145	.135	.195	.135	.175	.215	.200	.200	.175	.120	.190
39	.390	.525	.430	.440	.530	.505	.520	.530	.585	.720	.810
40	.895	.920	.830	.880	1.015	1.105	1.040	.940	[3] .977	1.560	1.520
41	.760	.780	.750	.690	.540	.595	.685	.640	.355	.460	.630
42	1.180	1.330	1.290	1.225	.955	1.155	1.035	1.100	[3] .957	2.450	1.730
43	.935	1.290	1.570	1.205	1.160	1.005	1.245	1.350	.925	1.050	1.160
44	.395	.385	.395	.435	.370	.385	.360	.345	.175	.200	.390
45	.505	.545	.560	.540	.570	.535	.550	.520	.400	.420	.460
46	.475	.465	.510	.490	.465	.490	.425	.525	.365	.380	.600
47	.195	.240	.255	.190	.305	.265	.370	.240	.440	.440	.480

[1] See Table 4 for exact age of specimens.
[2] See Table 3 for identification of specimens.
[3] C specimens exposed to soil on outside only. See Table 6 for ages of these de Lavaud specimens.
[4] No specimens.

TABLE 16.—*Weighted maximum rates of pitting of 6-year-old specimens* [1]

[In mils per year]

Soil No.	1½-inch specimens				3-inch specimens				6-inch specimens		
	a [2]	b	e	y	B	K	M	Y	C	L	Z
1	10.0	8.0	7.0	10.0	13.6	9.4	9.0	8.7	11.4	12.5	17.8
2	7.0	7.0	8.0	7.0	6.1	6.8	8.6	9.7	[3] 6.0	8.9	7.4
3	11.0	10.0	11.0	12.0	10.5	12.4	9.6	10.1	[3] 1.7	15.3	22.3
4	13.0	8.0	7.0	8.0	7.7	8.9	7.4	14.2	8.1	6.6	6.9
5	7.0	6.0	8.0	5.0	6.5	9.9	9.3	6.0	[3] 8.9	8.8	11.9
6	4.0	1.6	1.6	1.6	2.1	2.3	3.0	2.9	[3] 1.6	1.6	1.6
7	(4)	(4)	(4)	(4)	(4)	(4)	(4)	(4)	(4)	(4)	(4)
8	11.0	9.0	9.0	9.0	11.1	12.0	9.6	12.0	10.3	13.3	11.6
9	3.3	6.0	5.0	5.0	5.6	7.5	6.4	5.6	6.4	1.8	6.3
10	7.0	6.0	6.0	7.0	7.5	6.1	6.4	8.2	5.8	5.3	7.5
11	11.0	12.0	10.0	12.0	10.2	9.4	13.3	11.4	3.4	2.6	7.6
12	9.0	10.0	11.0	9.0	10.4	8.7	9.8	9.6	[3] 1.6	3.5	9.3
13	8.0	16.0	11.0	14.0	9.6	13.4	12.0	8.4	2.2	30.0	30.0
14	15.0	14.0	14.0	14.0	16.6	13.4	15.7	25.2	3.2	6.3	6.3
15	11.0	10.0	9.0	9.0	10.1	10.7	9.9	9.4	[3] 6.7	13.5	15.8
16	15.0	14.0	16.0	20.0	13.3	9.9	15.7	14.6	[3] 12.9	21.4	10.0
17	5.0	4.0	4.0	5.0	5.2	5.5	5.0	5.6	6.8	10.5	7.7
18	12.0	12.0	12.0	12.0	10.3	10.8	10.3	13.1	12.2	15.2	15.2
19	8.0	9.0	8.0	8.0	9.7	10.2	9.5	8.6	6.4	16.6	15.4
20	2.9	5.0	3.9	6.0	4.5	3.8	5.8	4.1	10.3	9.0	6.3
21	12.0	9.0	10.0	10.0	9.9	9.0	10.1	9.3	8.5	14.1	8.6
22	12.0	10.0	10.0	10.0	10.5	10.9	10.9	10.5	11.0	24.2	24.2
23	27.0	20.0	15.0	16.0	14.4	17.0	15.8	20.3	23.3	31.7	41.8
24	1.6	1.8	1.6	2.6	3.1	2.8	2.3	3.6	1.6	1.6	1.6
25	8.0	7.0	7.0	6.0	7.8	7.9	9.5	8.6	6.1	7.6	10.7
26	13.0	12.0	12.0	12.0	12.6	11.7	14.0	13.6	4.9	7.5	8.7
27	3.5	5.0	5.0	7.0	4.6	8.3	5.3	7.3	[3] 15.4	9.4	10.8
28	9.0	10.6	10.7	9.9	9.8	12.7	9.9	12.7	7.0	30.0	
29	17.0	13.0	15.0	14.0	9.0	13.1	13.1	12.8	[3] 8.2	12.4	20.8
30	2.7	1.8	4.0	2.7	4.6	4.7	4.7	5.1	5.5	2.4	4.8
31	5.0	4.0	5.0	5.0	3.2	8.5	5.9	7.3	[3] 11.0	5.1	12.4
32	6.0	5.0	5.0	6.0	6.4	6.4	6.3	6.6	5.6	5.0	8.2
33	8.0	6.0	1.7	9.0	6.1	9.0	5.7	4.1	7.1	6.4	10.4
34	8.0	5.0	2.6	5.0	5.1	5.2	4.6	7.1	7.0	3.6	4.7
35	1.6	1.6	6.6	1.6	3.3	1.6	2.9	3.2	[3] 1.6	1.6	2.5
36	8.0	8.0	6.0	7.0	6.5	8.5	7.3	6.7	[3] 6.0	11.1	21.8
37	8.0	8.0	6.0	12.0	6.0	7.6	8.5	9.6	[3] 1.7	5.2	8.5
38	6.0	4.0	3.0	3.0	5.5	2.6	3.8	5.1	1.6	1.6	2.2
39	5.0	7.0	6.0	8.0	7.3	6.1	7.2	8.1	6.0	5.5	9.1
40	10.0	12.0	12.0	10.0	10.0	13.2	11.5	13.4	[3] 15.3	13.1	13.8
41	9.0	8.0	8.0	10.0	9.3	8.0	11.0	8.5	5.1	4.5	5.5
42	13.0	16.0	14.0	12.0	12.1	13.9	15.1	13.4	[3] 15.1	21.9	36.6
43	14.0	13.0	11.0	12.0	14.9	18.0	16.5	8.4	6.8	4.5	11.9
44	12.0	9.0	9.0	12.0	10.3	9.1	10.7	13.4	8.2	9.1	10.5
45	8.0	7.0	7.0	6.0	7.7	5.9	7.9	8.6	5.8	8.7	2.8
46	11.0	11.0	11.0	9.0	10.9	7.5	14.4	15.9	3.5	4.4	9.3
47	1.6	1.6	1.6	1.6	1.6	1.6	1.6	1.6	2.6	1.6	1.6

[1] See Table 4 for exact age of specimens.
[2] See Table 3 for identification of specimens.
[3] See Table 6 for ages of these de Lavaud specimens.
[4] No specimens.

TABLE 17.—*Rates of loss of weight of 8-year-old specimens* [1]

[In ounces per square foot per year]

Soil No.	1½-inch specimens				3-inch specimens				6-inch specimens		
	a [2]	b	e	y	B	K	M	Y	C	L	Z
1	0.652	0.890	0.887	0.853	0.865	0.732	0.959	0.863	0.777	0.963	0.942
2	.482	.464	.464	.455	.472	.390	.486	.284	(3)	.307	.425
3	.463	.546	.532	.494	.466	.514	.562	.477	(3)	.486	.601
4	.647	.674	.677	.662	.694	.693	.683	.729	.709	.613	.623
5	.730	.858	.625	.649	.649	.703	.726	.670	(3)	.822	.811
6	.097	.109	.125	.099	.113	.098	.113	.116	(3)	.090	.118
7	.516	.554	.571	.484	.541	.512	.542	.548	.613	.570	------
8	.431	.432	.409	.417	.531	.457	.542	.551	.730	.649	.963
9	.417	.444	.414	.388	.451	.439	.412	.399	.516	.426	.535
10	.549	.547	.566	.570	.595	.577	.580	.583	.536	.496	.509
11	.132	.279	.243	.188	.196	.174	.203	.176	.191	.170	.162
12	.121	.171	.112	.126	.115	.103	.107	.138	(3)	.074	.231
13	(4)	(4)	(4)	(4)	(4)	(4)	(4)	(4)	(4)	(4)	(4)
14	.258	.482	.320	.285	.248	.218	.433	.299	.349	.491	.265
15	.628	.591	.685	.686	.733	.712	.641	.631	(3)	.605	.499
16	.644	.633	.585	.566	.576	.583	.566	.642	(3)	.526	.673
17	.835	.917	.833	.853	.964	.901	.962	.962	.936	.858	.771
18	.230	.424	.374	.255	.284	.248	.295	.271	.267	.418	.357
19	.326	.400	.358	.371	.313	.320	.401	.327	.337	.396	.374
20	.356	.440	.356	.326	.414	.382	.461	.371	.456	.475	.483
21	(4)	(4)	(4)	(4)	(4)	(4)	(4)	(4)	(4)	(4)	(4)
22	.757	.817	.970	.791	.840	.817	1.024	.987	.838	.694	.682
23	2.283	2.574	1.952	2.343	2.340	2.649	2.413	3.000	2.647	4.223	5.737
24	.118	.122	.131	.107	.123	.112	.124	.100	.088	.049	.086
25	.232	.296	.261	.262	.250	.233	.238	.226	.275	.213	.402
26	.167	.268	.256	.203	.199	.192	.205	.222	.231	.241	2.96
27	.572	.535	.530	.676	.545	.616	.487	.548	(3)	.596	.454
28	(3)	(3)	(3)	(3)	(3)	(3)	(3)	(3)	(3)	(3)	(3)
29	1.800	1.633	1.726	1.760	1.368	2.065	1.395	2.008	(3)	1.617	1.821
30	.498	.571	.507	.517	.577	.487	.532	.467	.590	.573	.674
31	.232	.277	.298	.349	.267	.278	.287	.283	(3)	.225	.204
32	.255	.367	.351	.293	.327	.333	.302	.353	.336	.420	.484
33	1.098	1.204	1.209	1.148	1.116	1.156	1.167	1.025	1.184	1.220	.997
34	.370	.418	.432	.438	.442	.397	.418	.401	.582	.459	.535
35	.296	.260	.215	.209	.267	.261	.258	.286	(3)	.258	.237
36	.250	.369	.316	.293	.230	.255	.263	.257	(3)	.158	.102
37	.725	.767	.652	.646	.788	.766	.723	.813	(3)	.766	.853
38	.246	.244	.273	.231	.248	.244	.272	.263	.169	.157	.165
39	.520	.571	.583	.454	.616	.609	.620	.639	.753	.581	.762
40	.802	.817	.813	.691	.873	.893	1.033	.963	(3)	1.106	1.202
41	.605	.674	.631	.593	.533	.532	.583	.548	.320	.456	.477
42	.741	.962	1.029	1.161	.794	.856	.841	.698	(3)	1.409	1.397
43	1.137	2.041	1.290	1.426	1.265	1.359	1.123	1.806	1.317	.901	.943
44	.223	.305	.385	.267	.250	.278	.257	.281	.213	.191	.329
45	.449	.725	.541	.492	.533	.501	.494	.551	.513	.574	.968
46	.706	.785	.659	.717	.637	.746	.730	.838	.708	.663	.826
47	.269	.259	.213	.224	.266	.258	.252	.204	.383	.229	.370
Average	.542	.630	.576	.569	.566	.583	.584	.609	.606	.623	.706

[1] See Table 8 for exact age of specimens.
[2] See Table 4 for identification of specimens.
[3] Late.
[4] No specimens.

TABLE 18.—*Weighted maximum rates of pitting of 8-year-old specimens* [1]

[In mils per year]

Soil No.	1½-inch specimens				3-inch specimens				6-inch specimens		
	a [2]	b	c	y	B	K	M	Y	C	L	Z
1	5.7	9.6	6.8	6.6	6.8	6.7	7.5	5.4	7.0	27.3	24.9
2	6.1	4.6	5.2	6.3	5.4	4.9	5.7	5.4	-------	11.8	8.2
3	7.7	7.3	8.8	9.2	7.7	8.1	8.3	7.1	-------	14.4	15.3
4	7.5	4.5	5.6	5.5	4.5	6.4	5.0	8.4	5.4	4.6	9.6
5	4.5	6.7	5.4	4.7	4.3	5.8	6.5	5.0	-------	5.7	8.3
6	2.2	2.5	1.4	2.1	1.2	1.9	1.7	1.8	-------	1.2	1.2
7	3.0	4.4	3.3	3.3	4.5	5.2	4.8	2.8	5.3	2.9	3.1
8	7.9	6.8	8.5	6.7	7.8	10.7	9.0	10.9	13.1	9.2	9.2
9	4.7	6.0	4.9	4.2	5.5	5.6	5.6	4.9	6.1	3.0	5.1
10	6.2	4.0	4.8	4.7	5.7	6.0	4.8	5.0	4.1	3.8	5.8
11	8.2	8.2	7.2	5.9	8.2	7.0	8.9	7.5	2.3	3.7	9.9
12	2.2	1.7	2.2	1.2	2.4	2.1	1.7	3.0	-------	1.2	1.2
13	[3]	[3]	[3]	[3]	[3]	[3]	[3]	[3]	[3]	[3]	[3]
14	10.6	11.2	13.9	13.3	11.2	9.4	16.7	20.0	6.5	5.9	-------
15	7.4	8.3	7.7	4.8	6.9	5.6	5.3	6.3	-------	8.8	8.9
16	7.4	10.6	8.5	8.4	8.6	10.1	8.3	9.3	-------	14.4	16.1
17	4.1	4.7	4.7	3.8	4.7	4.8	4.4	4.6	5.1	2.8	4.3
18	7.2	4.8	5.3	5.5	9.1	9.5	8.2	8.6	1.3	1.3	1.3
19	5.7	5.3	6.0	5.2	6.5	7.5	6.9	8.0	6.6	18.0	20.8
20	5.6	4.6	4.7	4.5	4.0	4.6	5.4	6.6	6.5	5.8	7.8
21	[3]	[3]	[3]	[3]	[3]	[3]	[3]	[3]	[3]	[3]	[3]
22	7.0	7.3	8.3	6.9	7.4	7.4	8.3	8.9	11.3	14.7	14.7
23	2.4	18.2	18.2	16.0	19.6	19.7	16.8	27.2	20.5	27.1	41.8
24	2.7	2.3	1.1	2.3	2.3	2.4	1.9	3.3	1.3	1.3	1.3
25	5.6	4.6	4.7	4.5	6.8	4.9	5.9	5.0	1.3	7.9	11.7
26	5.1	6.1	5.0	5.8	5.5	5.1	6.2	7.2	3.8	7.0	9.7
27	3.9	4.3	3.3	4.5	4.8	7.5	5.6	4.7	-------	14.9	12.5
28	Late.	Late.	Late.	Late.	Late.	Late.	Late.	Late.	Late.	Late.	Late.
29	13.1	8.5	11.3	11.4	10.2	11.1	12.5	22.3	-------	22.3	26.4
30	5.6	4.5	4.0	4.2	7.3	4.1	5.5	3.8	8.7	5.1	8.7
31	4.6	5.6	4.6	4.8	4.7	5.3	3.9	4.2	-------	4.0	7.4
32	4.2	5.4	5.4	5.1	4.8	6.0	5.5	5.7	6.5	17.3	20.0
33	17.0	7.9	8.7	12.7	12.7	14.9	12.4	12.0	15.0	20.4	16.8
34	5.3	5.8	5.7	6.5	5.3	7.7	4.7	8.0	5.8	3.9	7.0
35	4.0	3.0	2.9	1.2	2.1	3.0	3.1	6.7	-------	6.1	1.2
36	6.1	6.7	4.4	4.7	5.8	6.5	6.1	5.8	-------	15.8	20.2
37	7.2	6.1	6.5	6.8	7.6	7.9	7.5	12.1	-------	4.6	5.9
38	6.6	3.5	2.5	3.1	3.9	2.9	3.1	2.9	1.3	1.3	1.3
39	6.0	6.2	5.8	5.2	7.3	8.3	6.3	8.6	6.8	4.1	6.9
40	10.9	12.7	8.0	9.3	11.1	14.9	14.4	13.3	-------	12.7	13.6
41	7.7	8.2	6.9	7.5	7.2	7.1	7.6	6.7	4.4	4.1	6.0
42	9.5	11.1	14.1	13.8	10.0	10.7	10.8	10.8	-------	13.6	20.0
43	10.6	12.8	9.6	8.7	13.8	15.8	9.2	9.7	10.3	5.6	1.3
44	9.4	6.5	8.2	6.5	7.2	6.1	7.7	10.4	4.3	4.5	6.5
45	6.6	6.0	7.9	5.9	6.8	7.5	7.3	8.4	7.1	11.6	8.3
46	7.5	10.0	13.6	14.8	8.5	7.9	15.0	13.0	5.4	6.3	9.2
47	1.3	1.3	1.3	1.3	1.3	1.3	1.3	1.3	2.9	1.3	1.3
Average	6.8	6.6	6.5	6.3	6.8	7.2	7.2	8.0	6.4	8.7	10.2

[1] See Table 8 for exact age of specimens. [2] See Table 4 for identification of specimens. [3] No specimens.

TABLE 19.—*Average rates of loss of weight of all specimens of one kind removed from 1924 to 1930*

[In ounces per square foot per year]

Soil No.	1½-inch specimens				3-inch specimens				6-inch specimens		
	a	b	e	y	B	K	M	Y	C	L	Z
1	0.867	1.066	1.030	0.978	1.061	1.068	1.095	0.959	0.850	1.018	1.238
2	.683	.711	.682	.736	.737	.699	.753	.625	.382	.637	.944
3	.606	.731	.705	.732	.690	.723	.774	.732	.400	.834	.790
4	.838	.781	.837	.829	.841	.844	.816	.893	.815	.816	.863
5	.610	.666	.655	.680	.625	.592	.628	.596	1.375	.578	.663
6	.113	.115	.135	.128	.102	.119	.126	.111	.176	.070	.097
7	.559	.640	.622	.581	.630	.619	.637	.623	.661	.837	1.400
8	.529	.514	.522	.513	.518	.494	.578	.560	.626	.715	1.298
9	.463	.676	.557	.568	.526	.472	.510	.472	.538	.549	.656
10	.616	.639	.621	.606	.607	.567	.704	.604	.556	.519	.587
11	.184	.285	.256	.274	.231	.233	.247	.235	.133	.150	.225
12	.279	.284	.313	.315	.272	.257	.254	.279	.214	.186	.325
13	1.012	1.538	1.320	1.591	1.220	1.309	1.365	1.558	1.072	1.858	2.178
14	.358	.523	.454	.485	.438	.443	.482	.430	.316	.463	.559
15	.954	.853	.884	.870	.923	.913	.963	.965	1.022	.736	1.050
16	.797	.918	.885	.779	.825	.806	.890	.847	.693	.846	.863
17	.950	.994	.953	.948	1.078	1.021	1.073	1.047	.965	.999	1.390
18	.325	.553	.453	.404	.368	.324	.391	.390	.259	.426	.496
19	.451	.520	.484	.498	.471	.477	.490	.500	.357	.441	.341
20	.589	.619	.611	.596	.593	.612	.634	.574	.575	.674	.798
21	.900	.930	.997	.942	.995	.975	.952	.943	.813	1.097	1.080
22	.849	.940	.977	.966	.870	.884	.878	.900	.703	.731	1.033
23	2.482	3.040	2.780	2.853	2.564	2.793	2.739	3.040	2.845	4.756	7.537
24	.131	.169	.170	.135	.137	.147	.156	.122	.104	.052	.146
25	.285	.384	.324	.330	.269	.277	.297	.291	.320	.381	.410
26	.413	.544	.473	.441	.442	.422	.482	.469	.474	.623	.711
27	.520	.565	.609	.578	.561	.570	.525	.497	1.141	.506	.571
28	1.947	1.663	1.950	1.855	1.736	1.933	1.832	2.036	1.763	2.277	2.850
29	1.821	1.679	1.761	1.829	1.618	1.907	1.670	1.911	2.121	1.759	2.023
30	.483	.533	.584	.497	.545	.569	.584	.533	.650	.616	.758
31	.332	.404	.436	.495	.355	.458	.459	.441	.884	.266	.403
32	.284	.424	.393	.346	.355	.371	.382	.376	.420	.510	.426
33	.818	.810	.833	.876	.828	.874	.843	.730	.777	.640	.722
34	.554	.558	.543	.534	.589	.589	.598	.546	.597	.597	.589
35	.329	.347	.320	.271	.330	.329	.366	.356	.367	.312	.567
36	.351	.442	.456	.419	.321	.351	.347	.340	.215	.279	.320
37	.902	.933	.880	.908	.933	.936	.947	.967	1.483	.824	.938
38	.154	.175	.206	.170	.167	.187	.205	.199	.113	.097	.141
39	.611	.690	.646	.627	.696	.716	.695	.700	.728	.763	.840
40	.942	.968	.913	.885	1.018	1.081	1.078	1.093	1.048	1.251	1.393
41	.640	.677	.624	.678	.543	.572	.539	.521	.350	.596	.644
42	1.131	1.474	1.351	1.346	1.105	1.011	1.145	.902	1.051	2.207	1.907
43	1.005	1.615	1.360	1.506	1.294	1.338	1.456	1.651	.950	1.048	.891
44	.324	.447	.419	.420	.339	.341	.323	.340	.204	.260	.477
45	.731	.807	.760	.745	.699	.676	.798	.774	1.029	.978	.867
46	.599	.736	.678	.623	.598	.659	.659	.737	.496	.943	.999
47	.282	.302	.333	.245	.296	.311	.334	.300	.421	.377	.487
Average	.673	.763	.739	.737	.701	.721	.738	.738	.724	.811	.991

TABLE 20.—*Average weighted maximum rates of pitting—all specimens removed from 1924 to 1930*

[In mils per year]

Soil No.	1½-inch specimens				3-inch specimens				6-inch specimens		
	a	b	e	y	B	K	M	Y	C	L	Z
1	8.4	8.0	7.5	8.2	8.3	7.8	8.5	7.9	11.4	23.3	27.2
2	7.3	6.0	6.2	6.8	6.2	6.2	6.8	7.1	5.0	11.1	11.3
3	17.0	14.1	15.4	16.1	14.6	14.7	14.6	15.7	3.3	18.2	21.8
4	8.2	5.6	5.8	5.7	5.4	6.5	5.8	9.0	6.1	6.8	11.1
5	5.3	5.1	6.2	5.1	5.0	6.4	6.3	5.2	13.3	6.0	7.2
6	3.1	2.3	2.3	2.2	2.2	2.5	2.4	2.4	3.0	1.9	1.9
7	5.4	4.0	4.8	4.2	4.7	6.1	5.0	3.9	5.4	3.5	5.8
8	17.3	12.9	15.6	13.1	13.6	18.6	17.9	21.9	7.6	20.9	23.6
9	16.2	13.9	12.2	11.5	14.3	14.7	14.4	15.2	6.4	7.8	10.2
10	8.8	6.6	6.9	6.6	8.7	7.6	7.6	8.2	5.9	3.8	4.9
11	17.8	16.2	13.4	13.5	15.3	13.2	17.1	15.1	7.9	3.9	12.9
12	6.0	6.1	6.5	5.8	6.4	5.7	6.1	7.0	3.0	2.8	6.0
13	11.0	15.4	15.7	14.0	13.8	19.2	17.5	17.7	9.2	11.6	28.5
14	17.3	18.5	16.2	16.2	17.4	16.0	20.1	28.9	4.2	6.3	10.9
15	11.3	10.5	11.4	9.6	10.9	10.4	11.5	11.7	6.4	14.5	16.5
16	14.0	13.6	14.2	15.1	13.5	12.3	14.7	15.4	13.4	16.7	14.6
17	4.8	4.4	4.8	4.6	4.9	5.0	5.2	4.8	4.8	15.1	9.8
18	13.2	11.3	11.6	9.5	11.3	13.4	10.4	13.1	6.7	21.4	10.1
19	13.5	11.9	12.6	11.2	12.3	12.9	14.5	15.0	8.4	18.6	12.2
20	4.1	4.3	4.1	4.5	4.1	4.1	4.8	4.7	6.2	5.7	5.5
21	10.1	7.3	8.5	9.5	9.3	7.3	8.4	7.6	7.1	9.8	7.9
22	14.3	12.5	14.5	13.6	13.3	13.9	15.1	14.9	9.2	23.3	24.7
23	23.6	21.8	21.2	19.3	19.9	26.7	20.9	25.2	22.7	32.4	57.3
24	2.6	2.5	2.2	2.8	2.9	2.9	2.6	3.3	2.3	2.3	2.3
25	11.6	9.5	9.1	10.8	10.8	11.1	13.0	11.9	6.7	6.1	17.7
26	8.4	8.9	8.5	8.9	8.2	8.4	10.2	9.6	5.5	10.2	8.8
27	3.7	4.2	4.7	5.4	5.0	6.8	5.0	5.8	13.1	9.5	9.6
28	10.7	13.0	15.5	12.9	13.2	18.0	15.0	17.0	12.5	23.5	28.8
29	17.8	13.0	17.2	17.6	14.0	18.3	14.9	18.1	12.0	16.0	19.1
30	8.0	3.4	5.4	4.5	6.4	6.8	6.7	6.9	5.3	3.7	5.2
31	7.5	8.2	12.2	8.9	8.2	11.7	9.8	11.1	9.8	4.9	10.0
32	16.2	12.2	10.2	10.3	13.0	10.9	12.1	12.7	6.9	14.6	18.3
33	10.0	5.4	5.0	8.3	8.0	9.2	8.3	7.8	9.6	9.9	9.4
34	8.2	7.7	6.2	7.3	7.3	8.7	7.3	10.3	5.8	3.8	10.2
35	3.0	5.2	3.6	2.0	3.2	2.8	4.9	6.1	3.1	3.6	7.9
36	9.3	10.7	8.7	9.5	9.8	12.4	11.1	10.2	10.2	13.9	19.1
37	11.2	10.6	13.0	14.7	12.0	12.7	13.5	21.2	3.3	3.7	4.9
38	4.8	4.6	3.0	3.1	3.9	2.9	3.2	3.5	2.2	2.2	2.4
39	6.3	5.8	6.2	5.8	5.4	5.5	6.1	7.7	6.1	5.4	6.7
40	14.9	12.9	12.3	10.9	11.4	14.6	13.0	14.4	15.3	11.9	15.1
41	9.5	12.9	11.8	13.8	14.1	10.9	14.2	11.2	4.8	5.0	9.6
42	16.2	18.4	18.9	17.5	17.0	18.3	19.9	17.4	18.3	30.2	32.4
43	12.1	16.2	11.8	13.4	20.3	21.2	23.7	14.6	11.6	4.4	12.6
44	19.4	15.2	14.5	15.6	13.4	15.3	14.9	18.0	7.1	8.4	14.7
45	7.8	9.5	8.4	7.4	6.6	7.2	10.7	12.6	7.5	18.5	11.3
46	19.4	18.4	20.4	20.3	16.4	13.5	23.1	26.8	4.1	10.3	12.6
47	2.2	2.2	2.2	2.2	2.2	2.2	2.2	2.2	4.0	2.2	2.5
Average	10.6	9.9	10.0	9.8	9.9	10.7	11.1	11.9	7.6	10.8	13.5

TABLE 21.—*Weighted average rates of loss of weight and penetration of deepest pits for each test period for all materials*

Soil No.	Rates of loss of weight (ounces per square foot per year)					Rates of penetration (in mils per year)				
	2 years	4 years	6 years	8 years	Average	2 years	4 years	6 years	8 years	Average
1	1.187	1,066	0.939	0.852	1.011	12.3	13.0	10.7	10.4	11.5
2	.901	.794	.689	.412	.687	5.3	10.6	7.4	6.4	7.3
3	.886	.887	.592	.515	.703	24.8	16.3	11.5	9.4	15.0
4	.994	.922	.743	.678	.835	4.9	7.9	8.7	6.1	6.9
5	.588	.493	.849	.727	.707	4.0	7.0	8.0	5.7	6.5
6	.082	.138	.126	.108	.116	2.8	2.9	2.1	1.7	2.4
7	.720	.756	------	.556	.727	4.8	5.8	------	3.9	4.8
8	.759	.602	.621	.600	.645	35.8	11.0	10.7	9.1	16.6
9	.673	.536	.496	.452	.539	25.3	14.0	5.3	5.1	12.4
10	.842	.450	.532	.553	.594	12.9	3.0	6.7	5.0	6.9
11	.226	.228	.192	.188	.209	23.8	13.1	9.3	7.0	13.3
12	.121	.378	.440	.129	.265	2.8	10.0	8.3	1.9	5.6
13	1.853	1.078	1.377	------	1.436	21.9	13.0	14.2	------	15.8
14	.324	.534	.563	.332	.436	25.5	12.2	13.0	11.9	15.6
15	1.160	.820	1.028	.639	.928	19.2	8.9	10.4	7.0	11.3
16	1.135	.743	.836	.597	.829	19.5	12.4	14.8	10.2	14.3
17	1.373	.930	.981	.901	1.046	9.3	5.2	6.0	4.4	6.2
18	.341	.317	.526	.305	.378	17.2	12.2	12.4	5.6	12.0
19	.549	.482	.381	.353	.441	21.5	11.9	10.0	8.8	12.0
20	.963	.596	.515	.424	.624	5.1	2.8	5.6	5.5	4.7
21	1.377	.689	.799	------	.955	3.4	12.0	9.9	------	8.4
22	.865	.938	.786	.839	.857	23.2	15.2	13.1	9.3	15.4
23	4.150	3.562	3.144	3.023	3.470	32.1	30.0	22.0	21.7	26.5
24	.159	.089	.160	.101	.127	3.8	2.5	2.2	2.0	2.6
25	.433	.304	.292	.264	.323	21.1	8.3	7.9	5.7	10.8
26	.848	.637	.302	.226	.503	6.0	11.8	11.1	6.0	8.7
27	.360	.798	.637	.550	.612	3.3	8.1	7.4	6.6	6.6
28	2.282	------	1.569	------	1.990	19.0	------	12.2	------	16.4
29	2.107	1.862	1.599	1.717	1.839	21.9	14.9	13.5	14.9	16.2
30	.971	.402	.455	.554	.595	9.9	3.3	3.9	5.6	5.7
31	.579	.513	.355	.265	.456	17.6	7.4	6.6	4.9	9.3
32	.414	.418	.409	.352	.398	26.5	9.6	6.2	7.8	12.5
33	.395	.937	.673	1.138	.786	4.9	7.7	6.7	13.7	8.3
34	.937	.447	.469	.465	.580	14.3	4.6	5.2	6.0	7.5
35	.496	.515	.185	.257	.362	6.1	4.7	2.6	3.3	4.1
36	.481	.399	.245	.235	.334	18.3	9.8	8.8	8.2	11.4
37	1.202	1.081	.758	.763	.982	18.3	12.1	7.4	7.2	11.0
38	.122	.114	.175	.218	.157	3.6	2.9	3.6	2.9	3.3
39	.906	.748	.568	.640	.715	3.6	7.4	6.9	6.5	6.1
40	1.176	1.129	1.102	.954	1.091	17.1	11.3	12.2	12.1	13.3
41	.454	.639	.575	.502	.542	20.1	8.2	7.9	6.7	10.7
42	1.604	1.444	1.322	.993	1.331	31.1	21.2	16.6	12.4	20.4
43	1.334	1.165	1.132	1.298	1.232	23.0	14.2	12.0	9.8	14.7
44	.373	.364	.320	.260	.329	25.5	14.3	10.3	7.0	14.2
45	1.155	1.127	.493	.575	.837	15.2	9.3	6.9	7.6	9.8
46	.819	.756	.458	.729	.690	30.9	16.6	9.8	10.1	16.8
47	.343	.444	.342	.283	.353	3.4	3.0	1.7	1.4	2.4
Average	.895	.745	.690	.603	.726	15.4	10.1	8.9	7.4	10.5

Statistical studies indicate that for a given soil there may be significant differences between the performance of different materials, but until this is more definitely established it may be well to use data representing the average corrosiveness of the soils with respect to all the ferrous pipe materials. In Table 21 the average rates of loss of weight have been weighted in accordance with the exposed areas of the specimens; that is, the data on the two 6-inch "C" specimens have been given a weight of 4, the 6-inch "L" and "Z" specimens (of which there was but one of each removed from each soil for each test period) and the 3-inch specimens (of which two of each kind were removed each time) a weight of 2 and the data for the 1½-inch specimens a weight of 1. This gives equal weights to equal exposed areas, but it does not give equal weights to all materials; pure open-hearth iron being given less weight than the other materials.

V. SIGNIFICANCE OF THE DATA

The precision of the determination of the rates of loss of weight and penetration by pitting has already been discussed. There remain for consideration two questions—the precision with which the data represent the corrosion phenomena, and the extent to which the observed phenomena are indicative of the relation of soils to the behavior of pipe materials throughout the life of those materials.

While the rates of loss in weight and penetration for individual specimens have been determined with degrees of precision that may justify the number of significant figures carried in the tables, it should not be understood that the corrosive properties of the soils or the behavior of the materials in any soil can be so accurately expressed. Several students of corrosion have made statistical studies of the soil-corrosion data and have arrived at widely different conclusions because of the use of different methods of treating the data. If the precision of the data is computed from the data for a single material in a single soil a figure indicating a very low degree of precision will be obtained. If, however, all materials in one soil are considered or if one material in all soils is made the basis for computations, the results indicate a much higher degree of precision. Thus Dr. V. H. Gottschalk, a member of the underground corrosion section of the National Bureau of Standards has determined (by a statistical study of the data) that the average value of the 8-year data for the average rate of loss of weight of any one material in all soils as given at the bottom of Table 17 is correct to about 7.5 per cent and that the corresponding value for the average rate of penetration is correct to about 6 per cent. The standard error[1] for the average values at the bottom of Table 19 is about 10 per cent and that of the averages at the bottom of Table 20 about 7 per cent. The standard errors for the data in Table 21 are of similar magnitude. The precisions of the data for each period have not been calculated, but preliminary calculations indicate that they will not depart widely from the values for the 1930 data.

Having obtained a rough idea of the precision of the data, the reader is in a position to examine them for their significance. On account of the differences in materials and in soil conditions this is a rather difficult task and the character of some of the conclusions reached

[1] See R. A. Fisher, Statistical Methods for Research Workers, Oliver & Boyd, London, for a discussion of standard error.

will be tentative and will depend somewhat on the experience and purpose of the examiner. Perhaps the most positive conclusion that can be reached is that the rate of corrosion differs widely for different soils. This is illustrated by Figure 3 which shows the rates of loss and pitting for the average of all materials in the most corrosive and least corrosive soil under investigation. Table 20 indicates quite

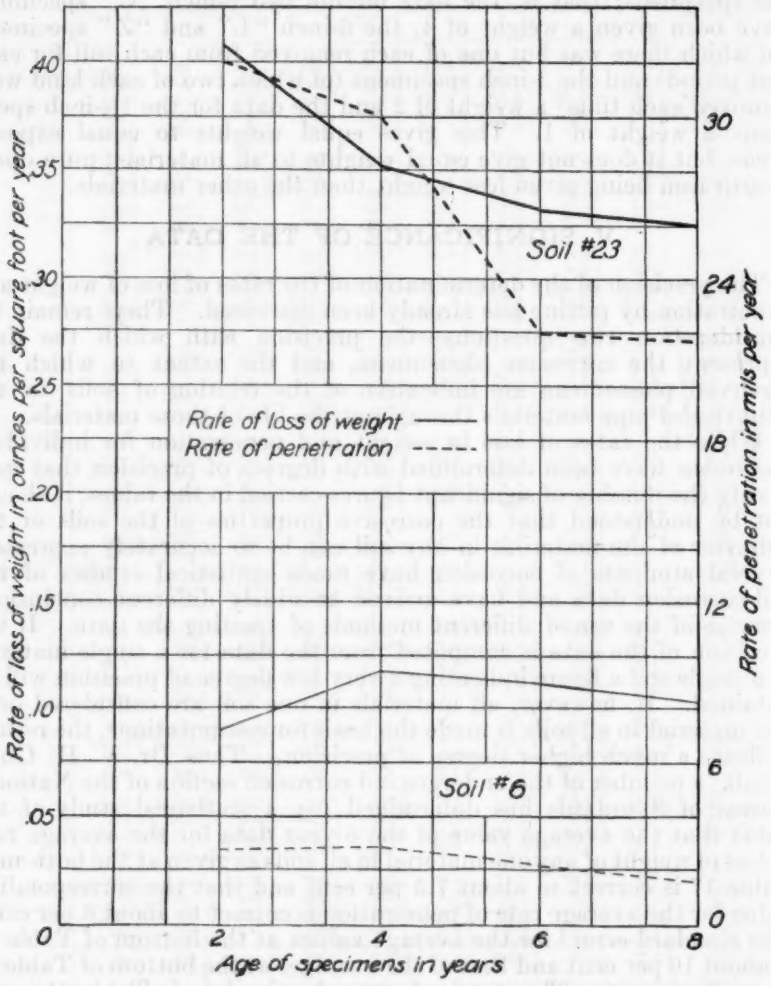

FIGURE 3.—*Rates of corrosion of all materials in worst and best soils*

definitely that if a soil is corrosive with respect to one ferrous material it is corrosive with respect to the others also.

It will be observed that both the weighted average rate of loss of weight, and the weighted average rate of penetration, for all materials in all soils (Table 21) decrease with the age of the specimens. This is shown graphically by the lines (— . —) in Figure 4, which shows also the average performance of three commonly used materials. It will be noticed that the average decrease in rate of pitting over the

8-year period is about 50 per cent, half of this decrease occurring prior to the removal of the 4-year-old specimens. The average rate of loss of weight has also decreased, but to a smaller extent. Comparing the average performances of materials 1, 2, and 3, it will be noted that though they behave nearly alike, their apparent relative merits depend upon the period of observation and upon whether rates of loss of weight or rates of penetration are the bases for comparison.

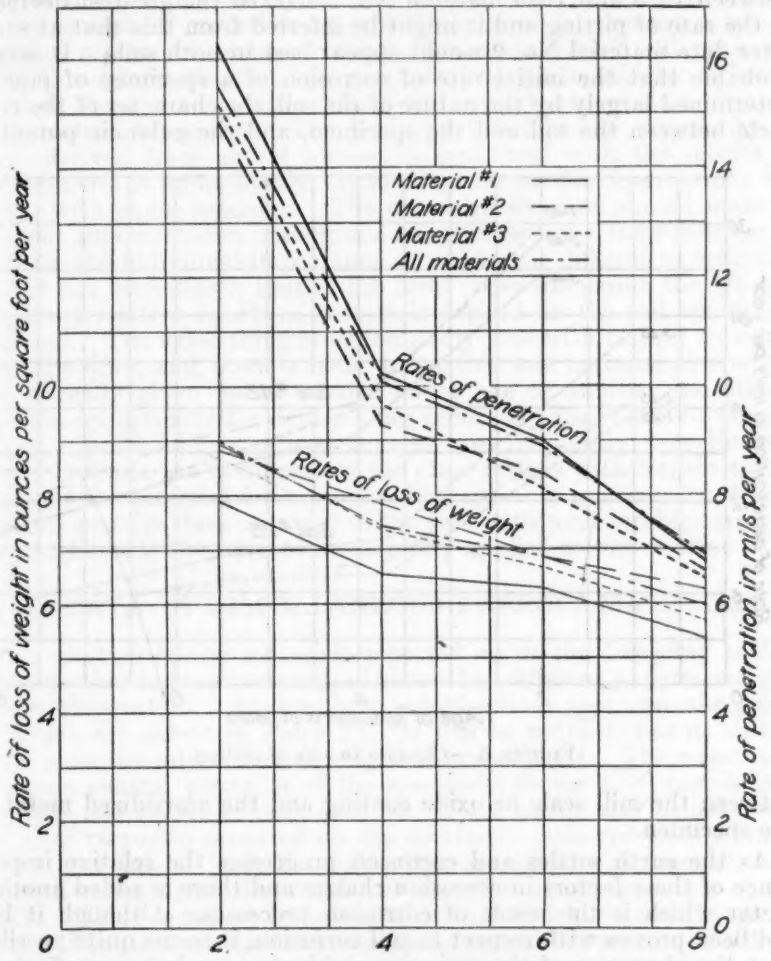

FIGURE 4.—*Change in rates of loss in weight and pitting*

Whether the differences indicated by the data are real or merely the result of lack of precision of the data will be more apparent at the close of the investigation. It is evident, however, that since the rate of corrosion decreases with time, other things being equal, the thicker the specimen the lower will be its rate of deterioration if the test is continued until the puncture of the specimen occurs. This observation has a very practical application to the selection of the wall thickness of pipes which are exposed without protection to corrosive soils.

When the behaviors of materials in a given soil are compared, it will be noticed that for most soils the differences between the ferrous materials is not large and their relative merits depend on the bases of comparison and on the soil chosen. This is illustrated in Figure 5, which shows the rates of penetration for three commonly used ferrous pipe materials in two quite different soils. Material No. 3, which is the worst of the three in soil No. 25, is the best in soil No. 42, but between 1928 and 1930 material No. 2 showed the greatest decrease in the rate of pitting and it might be inferred from this that at some later date material No. 2 would appear best in both soils. It seems probable that the initial rate of corrosion of a specimen of pipe is determined largely by the nature of the soil, the character of the contacts between the soil and the specimen, and the galvanic potential

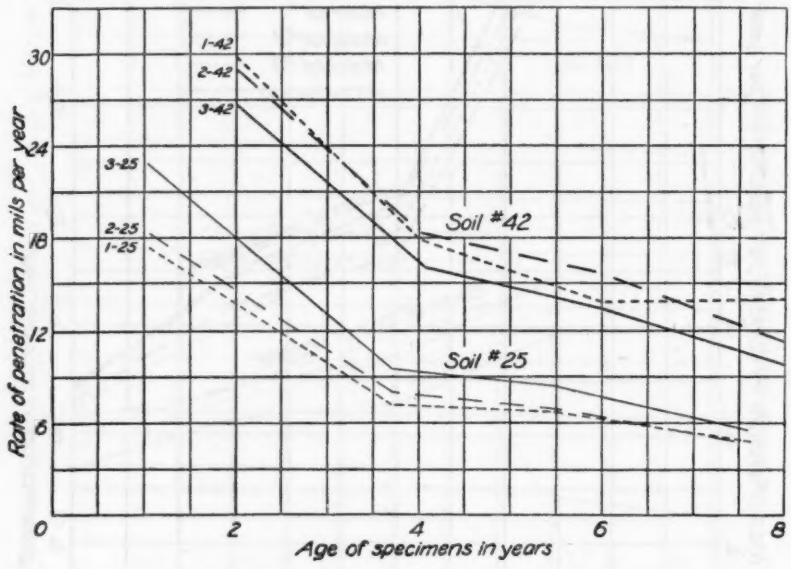

FIGURE 5.—*Changes in rate of pitting*

between the mill scale or oxide coating and the unoxidized metal of the specimen.

As the earth settles and corrosion progresses the relative importance of these factors in corrosion change and there is added another factor which is the result of corrosion processes. Although it has not been proven with respect to soil corrosion, it seems quite possible that the character of the corrosion products may have an effect on the sustained rate of corrosion and, hence, on the life of the material.

It is also possible that slight differences in the composition of the metal will result in marked differences in the character of the corrosion product and in the rate of corrosion. The American Society for Testing Materials has shown this to be the case with respect to the presence of small amounts of copper in sheet steel exposed to atmospheric corrosion.

At present the precision of the soil-corrosion data for individual materials in each soil has not been determined. Inspection of the

data on each specimen indicates that for a number of soils the standard error must be large and that significant differences in materials may be obscured because of the lack of precision of the data. Because of the uncertainties as to the significance of the data now available and because of possible changes in the apparent relative merits of materials which may appear in later data the authors believe that they should not attempt to compare materials at this time.[2]

The amount and variety of the data, while perhaps not justifying a comparison of materials at this time, serve to present a rather definite picture of some corrosion phenomena which will probably hold throughout the test. A great deal has been said by different authors from time to time about the importance of data derived from actual experience. The basis for belief in the superiority of data derived from actual service as compared with the results of experiments is undoubtedly sound in so far as the observations are made with equal precision. The data already cited should make it evident that corrosion underground is affected by a large number of factors, the individual importance of which it is difficult to estimate, and it has been shown that in the tests under discussion the life and apparent relative merits of materials depend on the soil conditions selected. The same thing is undoubtedly true with respect to working pipe lines, and there is little doubt that one material or another has actually given better service under one or another conditions, but the opportunity for determining accurately the conditions under which a material has proved superior are frequently very limited, and this limits the usefulness of the observations with respect to the value of the material for a proposed service. It is necessary, therefore, to examine data obtained in the field with considerable care and thoroughness if they are to be correctly applied to new work.

VI. DATA ON MISCELLANEOUS FERROUS MATERIALS

In addition to the materials reported on in the foregoing tables, several other ferrous materials of somewhat different natures are also under observation. Among these is high-silicon cast iron, the losses of which are shown in Table 22. It will be noticed that in all but three soils the rate of loss of weight is insignificant. There seems to be some general corrosion of the specimens in the tidal marsh (soil No. 43) and in Miller clay (soil No. 27), a heavy clay usually wet. Peculiar corrosion occurred on the specimens removed from Montezuma clay adobe (soil No. 28). One specimen was cracked, and marked softening of the metal was observed along the edges of the crack. There is reason to believe that the crack preceded the corrosion. The other specimen had on it one spot about the size of a dime at one edge where the material had softened much as in the case of the so-called graphitic corrosion of cast iron, although the corrosion product was even softer, being easily cut by the finger nail. With the exception of this specimen none of the specimens of high-silicon cast iron have shown definite evidence of pitting.

[2] At the advisory conference held on Jan. 30, 1931, for the purpose of criticizing the manuscript of this paper, the following resolution was adopted by the pipe manufacturers and users by a revised vote of 6 to 5 (several members of the conference not voting): "That the Bureau of Standards include in the next report the statement that it is the sense of this meeting that conclusions as to the relative merits of materials, based on these data by individuals, should not be published or used for sales purposes until the completion of the test."

In 1924 specimens of malleable iron, high-tensile cast iron, and cast steel were added to the tests. These specimens were buried in only six or seven locations selected because of the wide differences in their characteristics. The soils are described in Technologic Paper No. 368.[3]

TABLE 22.—*Average rates of loss of weight of high-silicon cast-iron specimens*

Soil No.	Buried	Rate of loss of weight	Soil No.	Buried	Rate of loss of weight
	Years	*Ounces per square foot per year*		*Years*	*Ounces per square foot per year*
1	7.68	0.019	25	7.62	0.002
2	5.84	.002	26	7.67	.000
3	5.97	.004	27	7.95	.148
4	7.96	.007	28	5.56	[2] .211
5	8.06	.042	29	7.96	.068
6	8.05	.004	30	8.17	.091
7	7.68	.022	31	5.98	.004
8	7.74	.004	32	7.65	.006
9	7.67	.019	33	7.63	.041
10	7.93	.002	34	7.96	.034
11	7.84	.000	35	6.12	.041
12	[1]	[1]	36	8.00	.003
13	[1]	[1]	37	5.98	.007
14	7.72	.024	38	7.97	.001
15	5.99	.021	39	7.95	.022
16	5.98	.023	40	7.96	.007
17	7.71	.013	41	7.94	.004
18	7.67	.004	42	8.00	.007
19	7.58	.002	43	7.98	.545
20	7.68	.073	44	7.58	.003
21	[1]	[1]	45	7.68	.011
22	7.59	.004	46	7.96	.001
23	7.95	[2] .001	47	7.99	.086
24	7.93	[3] .005			

[1] Lost.
[2] One specimen only.
[3] Both specimens softened where chipped or cracked.

Table 23 gives the rates of loss of weight of these specimens. The malleable cast-iron and the cast-steel specimens were in the form of elbows, and on account of this, satisfactory measurement of pit depths could not be made with the apparatus at hand. Table 23 also indicates in a general way the condition of the specimens with respect to pitting. Generally speaking, the worst corrosion of the malleable iron and cast steel occurred near the ends of the specimens.

Chromium-iron-alloy specimens were buried in seven locations in 1926. The manufacturer supplying these specimens stated that they were tubes made by the Mannesman process from material containing approximately 26 to 28 per cent chromium, silicon and manganese about 0.5 per cent, and carbon about 0.2 per cent. Table 24 shows the rates of corrosion of these specimens. The behavior of the specimens was peculiar in that nearly all of the corrosion was in the form of pits which in most cases were confined to points under or adjacent to the asphalt used to protect the identification numbers on the ends of the specimens.

[3] B. S. Tech. Paper No. 368, Bureau of Standards Soil Corrosion Studies. I. Soils, Materials, and Results of Early Observations, p. 462.

TABLE 23.—*Corrosion of special cast specimens*

RATES OF LOSS OF WEIGHT

(Ounces per square foot per year)

Soil No.	Age, years	Specimens							
		P	CC	I	MD	MC	V	E	S
13	6.13	0.947	0.698	[1] 0.470	1.025	1.845	0.989	1.136	1.406
24	6.62	.173	.292	.269	.209	.224	.139	.146	.140
28	5.56	[1] 2.886	-------	[1] 1.045	-------	-------	-------	1.691	.976
29	6.01	1.144	[2] .875	.645	.915	.882	1.073	1.149	1.032
42	6.02	1.257	-------	.591	1.196	1.876	1.202	1.068	1.419
43	6.70	.738	1.830	.597	1.610	.991	.944	.790	1.076
45	6.50	2.105	2.545	1.137	2.176	2.204	1.489	[2] 1.176	.876

MAXIMUM RATES OF PITTING

(Mils per year)

13	6.13	26.5	13.4	[1] 18.9	6.7	24.5	24.6	S, a	S, w
24	6.62	U	U	U	2.4	U	U	U, a	U, a
28	5.56	[1] 34.2	-------	[1] 20.0	-------	-------	-------	P, w	S, a
29	6.01	10.6	8.8	7.1	13.1	16.8	14.6	P, b	P, b
42	6.02	32.4	-------	22.4	23.9	22.8	19.7	S, a	S, a
43	6.70	12.5	27.0	23.4	14.9	17.2	13.3	P, b	S, b
45	6.50	23.5	18.2	15.7	20.3	19.4	21.8	P*, w	P, a

[1] One specimen missing.
[2] No coating inside specimen.

P, 6-inch southern cast iron, 2 specimens.
CC, 6-inch de Lavaud cast iron coated inside, 2 specimens.
I, 6-inch monocast cast iron, 2 specimens.
MD, 6-inch de Lavaud cast iron, 1 specimen, both surfaces machined.
MC, 4-inch cast iron, 1 specimen, both surfaces machined.
V, High tensile cast iron, 2 specimens.
S, 2-inch malleable elbow.
E, 2-inch cast steel elbow.
U, no pitting.
S, slight pitting.
P, general pitting.
a, specimens about the same as others in the same soil.
b, specimens better than others in the same soil.
w, specimens worse than others in the same soil.

TABLE 24.—*Average* [1] *rates of loss of weight and maximum pitting for chromium iron alloy tubes*

Soil No.	Buried	Rate of loss	Average maximum rate of pitting	
			Under asphalt	Exposed
	Years	*Ounces per square foot per year*	*Mils per year*	*Mils per year*
23	3.90	0.029	9.3	N
24	3.92	.004	N	N
28	3.92	.193	28.2	VS
29	3.90	.049	3.4	VS
42	3.94	.051	10.7	N
43	3.92	.573	28.7	16.0(H)
45	3.91	.024	N	VS

[1] Average of 3 specimens in each soil.

N, no pitting.
VS, very slight pitting.
H, one hole through each of two specimens just outside asphalt protection.

On some specimens the rate of penetration of these pits was much greater than for ordinary steel pipe in the same soil. An explanation offered for this pitting is that the limitation or exclusion of oxygen under the asphalt prevented the formation of the film which usually protects this alloy from corrosion.

In cases where only one test was conducted in a given soil it is somewhat doubtful whether the data obtained are indicative of the corrosivity of that type of soil since they may be results of some accidental condition. It was deemed advisable, therefore, to start check tests in at least part of the soils under investigation, and specimens of pipe were buried in 25 additional locations in 1928.

Results of this test, as indicated by the examination of two specimens of each material removed from each of these locations in 1930 are given in Tables 25 and 26. The data are comparable with those in Tables 11 and 12 rather than with data on specimens buried for longer periods. In general, the indications are that soils have typical corrosion characteristics which are modified to some extent by local conditions. The discussion of the relation of soil characteristics to corrosion is reserved for a later paper to be prepared when more data on soil characteristics have been secured.

VI. SUMMARY

The data on the specimens removed in 1930 are, for the most part, in good agreement with those on specimens removed earlier, and confirm the tentative conclusions reached in previous reports. These may be summarized as follows:

The corrosion of ferrous materials buried in soils depends largely on the characteristics of the soils.

TABLE 25.—*Action of soils in special tests—average of all specimens removed*

Soil No.	Soil	Location	Age of specimens	Rate of loss of weight	Penetration of pits
			Years	*Ounces per square foot per year*	*Mils per year*
101	Billings silt loam [1]	Grand Junction, Colo.	1.90	2.83	31
102	do.[2]	do	1.90	2.46	21
103	do.[3]	do	1.90	3.96	31
104	Cecil clay	Charlotte, N. C.	1.93	1.33	32
105	Cecil clay loam	Macon, Ga.	1.95	1.91	31
106	do	Salisbury, N. C.	1.93	1.76	31
107	Cecil fine sandy loam	Raleigh, N. C.	1.92	1.09	30
108	Cecil gravelly loam	Atlanta, Ga.	1.94	1.68	29
109	Fresno fine sandy loam [1]	Fresno, Calif.	1.90	3.22	38
110	do.[2]	do	1.90	2.31	38
111	do.[3]	Kernell, Calif.	1.57	2.88	27
112	Imperial clay [2]	Niland, Calif.	1.88	4.21	48
113	do.[3]	do	1.88	4.98	49
114	Lake Charles clay	El Vista, Tex.	.93	1.60	17
115	Memphis silt loam	Vicksburg, Miss.	2.02	.89	21
116	Merced clay	Los Banos, Colo.	1.93	3.70	30
117	Merced clay loam adobe	Tranquility, Calif.	1.92	3.91	49
118	Niland gravelly sand	Niland, Calif.	1.88	3.58	43
119	Norfolk sandy loam	Macon, Ga.	1.95	1.38	34
120	do	Pensacola, Fla.	1.95	.42	8
121	Norfolk sand	Tampa, Fla.	1.97	.27	5
122	Panoche clay loam	Mendota, Calif.	1.92	1.01	12
123	Susquehanna clay	Shreveport, La.	2.02	1.99	19
124	Susquehanna silt loam	Troop, Tex.	.86	3.44	45
125	Susquehanna fine sandy loam	Shreveport, La.	2.02	1.63	15

[1] Low alkali. [2] Moderate alkali. [3] High alkali.

TABLE 26.—*Rates of loss of weight and pitting for specimens in special test*

Soil No.	Buried	Rate of loss of weight (ounces per square foot per year)					Weighted maximum rate of penetration (mils per year)				
		A	B	N	P	C	A	B	N	P	C
	Years										
101	1.90	2.060	2.714	2.031	3.621	2.895	35.8	33.8	30.4	19.5	33.8
102	1.90	2.074	2.686	2.248	2.655	2.454	21.7	19.2	13.8	19.4	29.9
103	1.90	1.937	2.625	1.891	7.322	3.327	31.3	22.4	18.6	48.6	34.5
104	1.93	1.507	1.562	1.287	1.421	1.056	34.3	35.6	44.2	22.8	22.4
105	1.95	1.658	1.834	1.731	2.283	1.774	24.7	23.1	26.4	40.8	40.1
106	1.93	1.343	1.315	1.053	2.143	2.147	30.2	23.2	24.6	41.6	36.8
107	1.92	1.069	1.221	1.263	1,123	.912	28.0	30.7	32.8	28.6	29.5
108	1.94	1.427	1.720	1.766	1.960	1.446	32.7	19.6	27.2	34.0	33.3
109	1.90	2.484	3.088	2.731	3.893	3.209	35.5	34.5	37.6	53.3	30.8
110	1.90	2.073	2.358	2.163	2.683	2.097	37.5	30.0	21.3	55.5	43.8
111	1.57	2.761	2.851	3.318	2.876	2.738	33.3	27.9	20.2	31.1	23.2
112	1.88	3.792	3.858	3.868	4.522	4.452	39.8	29.3	35.2	79.7	53.6
113	1.88	4.377	4.307	4.395	5.331	5.572	47.9	28.5	28.1	72.8	67.8
114	.93	1.603	1.367	1.407	1.678	1.728	31.7	16.4	14.8	10.8	10.8
115	2.02	.906	.918	.850	1.040	.730	15.0	15.3	15.3	31.3	29.9
116	1.93	3.151	3.445	2.996	4.163	4.002	23.6	25.5	18.1	46.7	38.1
117	1.92	3.950	4.130	4.160	4.098	3.468	59.8	47.4	41.1	50.4	44.5
118	1.88	2.870	2.665	2.909	4.629	3.678	48.9	36.4	28.1	60.3	40.3
119	1.95	1.207	1.328	1.326	1.536	1.364	36.4	22.6	23.7	46.3	40.9
120	1.97	.564	.480	.411	.335	.413	10.2	9.9	9.5	5.1	5.1
121	1.95	.361	.290	.243	.211	.277	5.1	5.1	5.1	5.1	5.1
122	1.92	.998	1.169	1.000	1.011	.923	23.0	14.6	12.4	5.2	5.2
123	2.02	1.688	1.937	1.786	2.365	1.879	21.0	21.2	19.9	15.8	15.0
124	.86	2.779	3.033	3.131	4.533	3.038	51.2	51.5	54.4	32.8	32.6
125	2.02	1.484	1.564	1.560	1.981	1.423	13.7	13.9	14.0	17.5	15.5

A, open-hearth iron.
B, wrought iron.
C, sand-mold centrifugally-cast iron.
N, Bessemer steel.
P, pit-cast iron.

The data so far obtained do not indicate that any one of the commonly used pipe materials is markedly superior to the others for general use underground. In some locations one material or another appears slightly superior, but the precision of the data are insufficient to justify a comparison of materials. There is a possibility that subsequent results will indicate that over longer periods some material is better than others. This can only be determined at the close of the tests.

The corrosiveness of a soil can never be precisely expressed because of the variations in the soil, differences in the methods of back filling the trenches, the depth of burial of the pipes and the variations in moisture and temperature from year to year.

In most soils the rate of corrosion of buried pipe decreases with time. Several causes appear to be responsible for the corrosiveness of soils, and it is improbable that a single satisfactory method for determining soil corrosiveness can be developed.

The data on the materials examined are presented in tabular form in Tables 5 to 26.

WASHINGTON, January, 1931.

AUTOMATIC VOLUME CONTROL FOR AIRCRAFT RADIO RECEIVERS

By W. S. Hinman, jr.

ABSTRACT

An automatic volume-control device is described for use primarily in the reception of visual type radio range-beacon signals, the device being easily applied to existing aircraft radio receiving sets. This device operates on the output voltage of the radio receiver, and is provided with a filter unit to prevent operation of the automatic volume control by signals other than those from the range beacon. The controlling voltage is derived from the output of the radio receiver, part of which is rectified and then applied as negative bias to the radio-frequency amplifier. The automatic volume control maintains a substantially constant output voltage for input voltage variations of the order of 5,000 to 1. A distance indicator, operating in conjunction with the automatic volume-control device, is provided to serve as a gage of distance from the transmitting station.

A variation of the automatic volume-control device is given which is intermediate between completely automatic and manual volume control. This semiautomatic volume-control arrangement serves the purpose of simplifying the use of the range beacon on the part of the pilot, and at the same time permits the retention of sense of approach to the beacon station without requiring the addition of a distance indicator.

CONTENTS

	Page
I. Introduction	37
II. The filter unit	38
III. The automatic volume-control device	40
1. General description	40
2. Control grid method	40
3. Semiautomatic control using control-grid method	44
4. Semiautomatic control using screen-grid method	45
IV. Acknowledgment	46

I. INTRODUCTION

One of the advantages of the visual type radio range beacon [1] is that automatic volume control may be used in its reception. In the course of a flight on an air route equipped with a radio range beacon, the changes in the input voltage to the receiving set are of the order of 5,000 to 1. This has hitherto necessitated frequent adjustment of receiving set sensitivity by the pilot, so that the output voltage to the indicator might remain fairly constant. These adjustments are increasingly frequent as the airplane approaches the beacon station, since the beacon field intensity then varies most rapidly. The elimination of this need of frequent manual adjustment was the object of this development of automatic volume control.

The development was particularly necessary for the operation of a range-beacon arrangement as part of a system of aids to the blind

[1] J. H. Dellinger, H. Diamond, and F. W. Dunmore, Development of the Visual Type Airway Radio Beacon System, B. S. Jour. Research, 4, p. 425; March, 1930. Proc. Inst. Radio Engrs., 18, p. 796; May, 1930.

landing [2] of aircraft. In the course of the landing maneuvers, the range of input voltage variations is as great as those encountered during a flight on a radio range beacon. The pilot has no time to adjust volume, since the instruments and the controls of the airplane require his full attention.

The automatic volume control described in this paper was developed to meet a number of practical conditions. One is that it be light in weight. Another is that it be easily applied to existing types of aircraft radio receivers; this points to an automatic volume control operated by the output voltage of the radio receiver, for any other means for automatically controlling the voltage would necessitate difficult alterations in the radio receiver. Another condition is that when automatic volume control is used on the visual radio

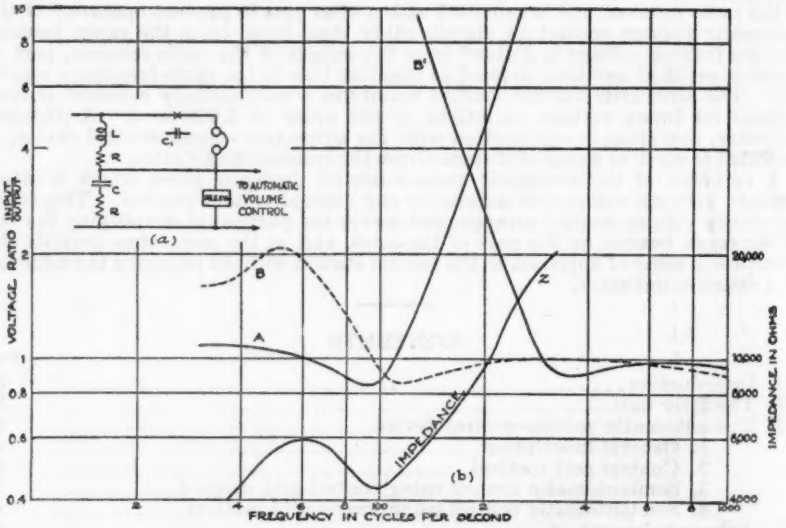

FIGURE 1.—*Performance graphs of filter unit*

range beacon, it must be operated by the signal of the beacon station only, in order that the ability of the course indicator (which may be either a reed indicator or a reed converter [3]) to distinguish between that signal and any interfering signal be preserved. Here, again, an automatic volume control operating on the output of the radio receiver offers a simple means of attaining this end. A filter unit may be used in the output of the radio receiver so that the signals of the radio range beacon only are applied to the automatic volume control.

II. THE FILTER UNIT

Since the frequencies of the visual radio range beacon are between 65 and 108 cycles, a low pass filter unit may be used to separate these signals from any other signals. However, the radio receiver must

[2] H. Diamond and F. W. Dunmore, A Radiobeacon and Receiving System for Blind Landing of Aircraft, B. S. Jour. Research, 5, pp. 897–931; October, 1930.
[3] F. W. Dunmore, A Course Indicator of Pointer Type for the Visual Radio Range-Beacon System, B. S. Jour. Research, 7, p. 147.

also be used for speech reception, and sometimes for simultaneous reception of both speech and radio range-beacon transmissions.[4]

In order that speech may be received, a high pass filter unit also is necessary. The use of two such filter units makes weight and size important in the filter unit design.

For this reason the filter circuit arrangement shown in Figure 1 (*a*) was developed. Condenser *C* forms a parallel resonant circuit with the reed indicator, and is adjusted to resonate at about 60 cycles. Inductor *L* forms a series resonant circuit with the parallel circuit formed by condenser *C* and the reed indicator, and is adjusted

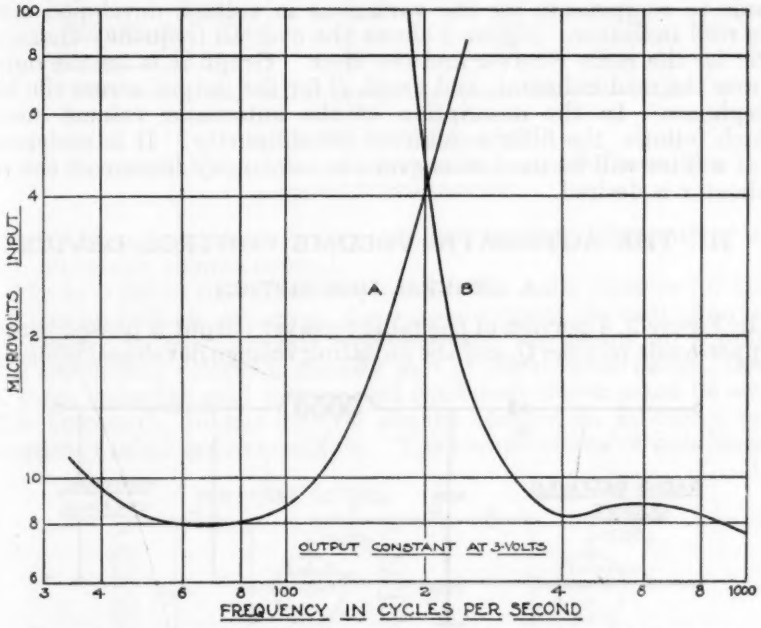

FIGURE 2.—*Over-all performance graph of radio receiver and filter unit*

to resonate at about 90 cycles. These two resonance points are shown in graph *Z* of Figure 1 (*b*), which shows the input impedance of the filter. The impedance of inductor *L* is low at frequencies lower than the point of series resonance, but is increasingly high at higher frequencies. The impedance of the parallel resonance circuit is, of course, high at frequencies near its point of resonance, but increasingly low at higher frequencies. The lower frequencies develop highest voltage across condenser *C* and the reed indicator, while the higher frequencies develop highest voltage across inductor *L*. The head telephones are connected across inductor *L*, but have little effect on the filter characteristics because of their high impedance. Resistors *R* reduce the resonance effects of the filter so that the voltage developed across the reed indicator is uniform over the required frequency range. The graphs of Figure 1 (*b*) show the ratio of the voltage applied to the filter, to the voltage applied to the reed

[4] F. G. Kear and G. H. Wintermute, A Simultaneous Radiophone and Visual Range Beacon for the Airways. Will appear in B. S. Jour. Research for August.

indicator and the head telephones at various frequencies. Referring to graph A, it will be noted that practically no voltage of frequencies higher than 250 cycles is developed across the reed indicator. However, low frequency cut-off for the head telephones (see graph B) is very poorly defined. Small condenser C_1 is placed in series with the head telephones at X of Figure 1 (a). This sharpens the low-frequency cut-off for the head telephones as shown by graph B'. Since speech depends largely on the higher frequencies for intelligibility, the performance indicated in B' is satisfactory. Graph Z of Figure 1 (b) shows the impedance presented by the filter to the plate of the output tube. The variation in impedance at reed frequencies tends to compensate for the variations in voltage developed across the reed indicator. Figure 2 shows the over-all frequency characteristic for the radio receiver and the filter. Graph A is for the output across the reed indicator, and graph B for the output across the head telephones. In the description of the automatic volume control which follows, the filter is omitted for simplicity. It is understood that a filter will be used whenever the selectivity feature of the reed indicator is desired.

III. THE AUTOMATIC VOLUME CONTROL DEVICE

1. GENERAL DESCRIPTION

In Figure 3, a portion of the radio receiver output is passed through copper-oxide rectifier Q, and the pulsating voltage developed is changed

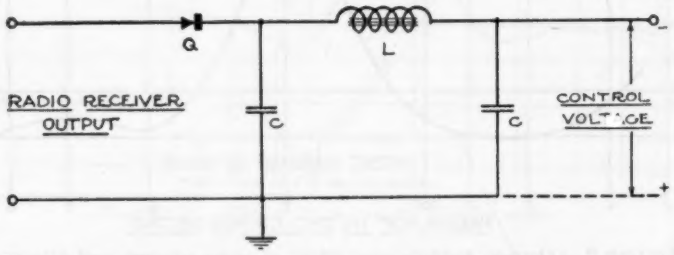

FIGURE 3.—*Electrical circuit arrangement of automatic control unit*

to nearly steady direct voltage by condensers C and inductor L. This voltage is applied to the radio-frequency amplifier in such a way that it decreases the sensitivity of the radio receiver. Since this control voltage is directly proportional to the receiving set output voltage, any increase in input voltage to the radio receiver automatically increases the controlling voltage, thereby tending to oppose the normal increase in output voltage. Thus the output voltage of the radio receiver is held substantially constant for varying input voltages.

Three methods have been developed for applying automatic volume control to aircraft radio receivers. The advantages of each are shown.

2. CONTROL-GRID METHOD

In Figure 4, the output voltage of the radio receiver is applied to a voltage divider P which applies part, or all, of this output voltage to rectifier Q. The output of Q is filtered and applied as a direct voltage of negative polarity to the control grids of the radio-frequency am-

plifier. Voltage divider P is used for controlling the output voltage. Its setting determines the degree of automatic control to be used. Rectifier Q is a high resistance, half-wave, copper-oxide rectifier, with low-current capacity. In the filter, resistor r is used in place of the usual inductor to save weight and space. Since the control grids of the radio-frequency tubes in the receiving set draw no power from the rectifier, resistance is as effective as inductance. Switch S is

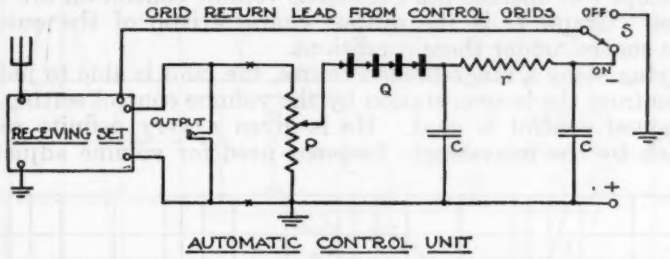

FIGURE 4.—*Electrical circuit arrangement of automatic control unit applied to radio receiver*

provided to allow the receiving set to be operated either with or without automatic volume control.

Figure 5 shows the means employed in the radio receiver for applying the controlling voltage to the control grids of the radio-frequency amplifier. In most aircraft receiving sets, the means for supplying this controlling voltage is already part of the receiver design, though in some cases the grid resistor and condenser shown must be added. The automatic volume control should operate on as many radio-frequency tubes as are available. The control characteristic becomes

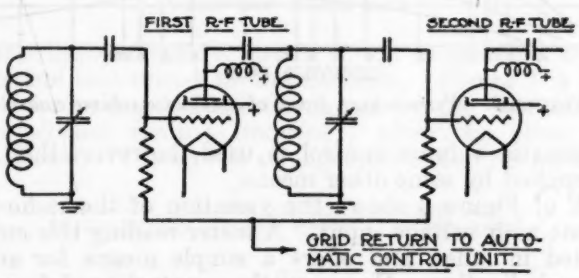

FIGURE 5.—*Method of applying control voltage to radio-frequency control grids*

flatter as more controlling tubes are used. It is necessary that care be taken in the design of the filter for the automatic volume control. At high input voltages a flutter is apt to be produced in the output of the radio receiver. This flutter is a reaction phenomenon produced by remodulation of the radio-frequency carrier by the small a. c. component of the controlling voltage.

Figure 6 gives graphs showing the characteristics of the automatic volume control when applied to a radio receiver consisting of two stages of radio-frequency, a detector, and two stages of audio-frequency. A is the normal overload graph without automatic volume control. B is a graph showing output voltage for varying input volt-

ages when automatic volume control is used and corresponds to maximum setting of voltage divider P of Figure 4. C is a graph taken with voltage divider P set at less than its maximum position so that the output voltage of the receiver is greater than the controlling voltage of the automatic volume control. Where it is desired that the receiving set be controlled at lower output voltages, a step-up transformer must be inserted at XX (fig. 4) so that sufficient controlling voltage may be developed to operate the automatic volume control on low output voltages. Graph D is the output characteristic of the automatic volume control under these conditions.

In flying along a range-beacon course, the pilot is able to judge the distance from the beacon station by the volume control setting, when full manual control is used. He is given a very definite sense of approach by the increasingly frequent need for volume adjustment.

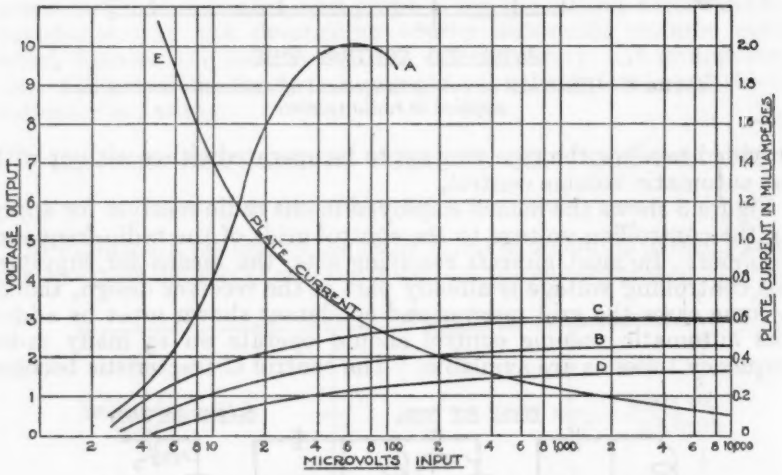

FIGURE 6.—*Performance graph of automatic volume control*

When automatic volume control is used, however, this indication must be supplied by some other means.

Graph E of Figure 6 shows the variation of the radio-frequency plate current with voltage input. A meter reading this current may be calibrated in miles, and offers a simple means for accomplishing distance indication. However, the greatest need for a distance indicator occurs at high input voltages, when the pilot is nearing the beacon station. The current is then low, and variations of input voltage cause very little change in current. This makes accurate reading of the meter difficult. To remedy this defect, a lower current meter provided with a relay-operated shunt to protect the meter at high current values may be used. This shunt may be calibrated, if desired, to read higher values of current. The meter may also be used as a tuning meter, though its use for this object is optional, the amplitude of reed vibration normally serving this purpose.

The greatest value of the automatic volume control is its use when the received signals are of high field intensity; that is, when the pilot is close to the beacon station. It is then that the adjustments of volume become so frequent that they are very troublesome, if not

impossible. The automatic volume control may be used, however, at all times save when the full sensitivity of the radio receiver is required. The sensitivity of the radio receiver is reduced slightly by the automatic control unit. This has been shown by the graphs of Figure 6. Since either automatic or manual control of volume may

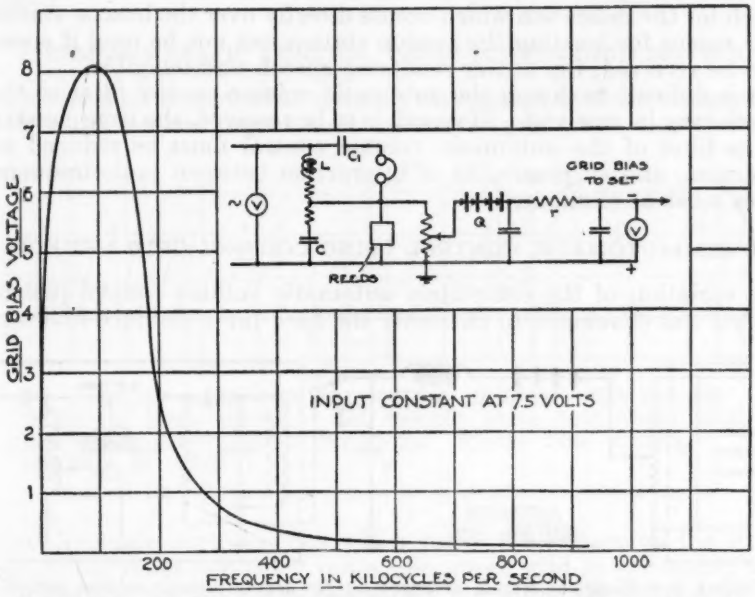

FIGURE 7.—*Variation of grid bias voltage with frequency for filter and automatic control units*

be used at will (by means of switch *S*, fig. 4) the pilot may use the type of control best suited to the occasion. Figure 7 is a graph in which the controlling voltage developed by the automatic volume control is plotted against frequency, when the filter previously described is used. The circuit arrangement is also shown in Figure 7.

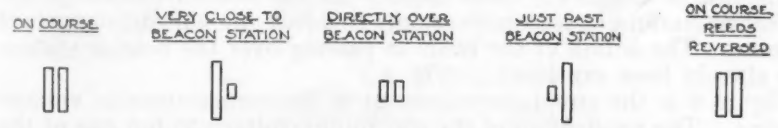

FIGURE 8.—*Localizing action of reed indicator over range-beacon tower*

The freedom from interfering signals obtained through the use of the filter circuit is apparent.

The usual zero-signal zone directly over the beacon station is modified when automatic volume control is used. When the pilot is nearly over the beacon station, one reed decreases in amplitude until it is at rest. As he passes over the loop antennas of the radio range beacon, the reeds reverse; that is, the reed formerly at rest rises to the amplitude of the vibrating reed, while the reed formerly vibrating decreases in amplitude until it is at rest. Then, as the pilot proceeds on the back course, the reeds become equal again. Figure 8 shows the

positions of the reeds, in the order named, as the pilot passes over the beacon station.

It is worthy of note that the flutter phenomenon previously described may be used to advantage in flying the visual radio range. If this flutter be introduced, and made to occur at the field intensity of the visual range beacon at 4 miles, the pilot is warned that he must watch for the indication which occurs directly over the beacon station. This means for locating the beacon station can not be used if speech is to be received, the flutter rendering speech unintelligible.

It is difficult to design the automatic volume-control filter so that speech may be received. If speech is to be received, the time constant of the filter of the automatic volume control must be reduced to a minimum, and all possibility of interaction between radio-frequency tubes must be eliminated.

3. SEMIAUTOMATIC CONTROL USING CONTROL-GRID METHOD

A variation of the completely automatic volume control just described was developed to eliminate the need for a distance indicator.

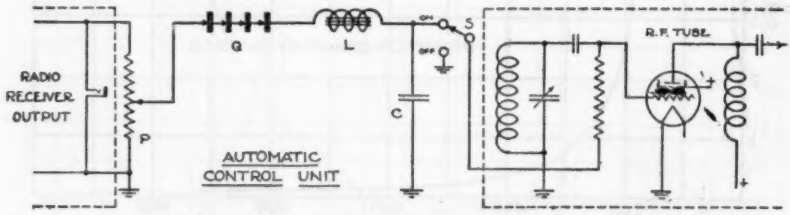

FIGURE 9.—*Electrical circuit arrangement for semiautomatic volume control operating on the control grids*

It is a semiautomatic volume control which does not change the operation of the radio receiver in any way, but supplements the manual volume control, reducing to approximately one-fifth the number of adjustments necessary over a given range of input voltage. It gives a very definite sense of approach to the beacon station without the use of the special distance indicator previously mentioned, since the reeds rise in amplitude more rapidly as the beacon station is approached, and necessitate increasingly frequent manual adjustments of volume. The action of the reeds in passing over the beacon station has already been explained. (Fig. 8.)

Figure 9 is the circuit arrangement of the semiautomatic volume control. The application of the controlling voltage to but one of the radio-frequency tubes eliminates any possible interaction between tubes. The filter of the automatic control unit consists of inductor L and condenser C, and has a low time constant (that is, time required for developing the control voltage). In all other respects the semiautomatic volume control is similar to the completely automatic volume control previously described. Since voltage divider P regulates the value of the controlling voltages, the extent to which the automatic control unit controls the volume may be varied at will. Figure 10 is a graph which gives the characteristics of the semiautomatic volume control when voltage divider P applies about one-third of the output voltage to the control unit. It is also a comparison of semi-

automatic and manual volume control in number of adjustments necessary to maintain a constant voltage output.

Any signal may be received with this semiautomatic volume control. The radio receiver sensitivity is not impaired. The radio receiver may be used either with or without semiautomatic volume control.

4. SEMIAUTOMATIC CONTROL USING SCREEN-GRID METHOD

This method is somewhat simpler, with regard to changes necessary in the radio receiver proper, than the control grid method. When the

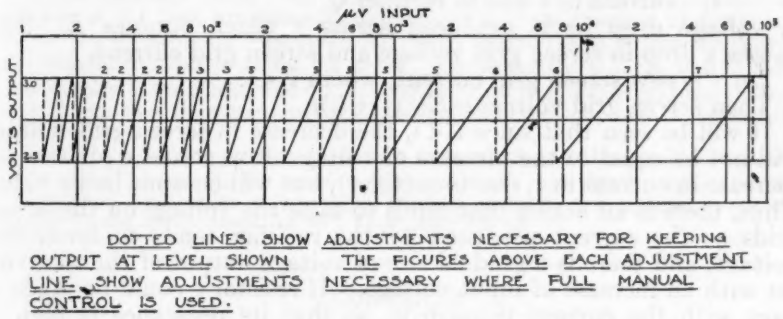
μV INPUT
VOLTS OUTPUT
DOTTED LINES SHOW ADJUSTMENTS NECESSARY FOR KEEPING OUTPUT AT LEVEL SHOWN THE FIGURES ABOVE EACH ADJUSTMENT LINE SHOW ADJUSTMENTS NECESSARY WHERE FULL MANUAL CONTROL IS USED.

FIGURE 10.—*Performance graphs for semiautomatic volume control*

manual volume control is one which varies the voltage on the screen grids of the radio-frequency tubes, the screen grid power supply lead is broken and the voltage developed by the automatic volume control is placed in series, but opposing the screen grid voltage. Figure 11 shows the circuit arrangement. Since the screen grids require current, care must be taken that the automatic volume control does not absorb too much power from the radio receiver output. A step-up

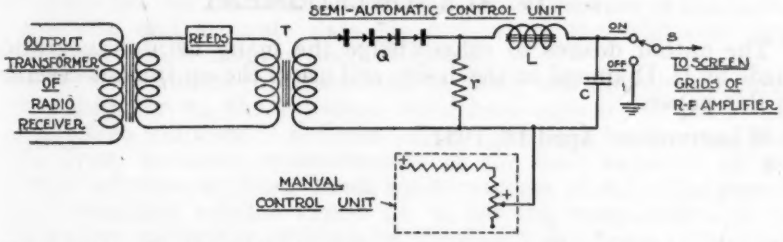

FIGURE 11.—*Electrical circuit arrangement for semiautomatic volume control operating on screen grids*

transformer T is placed in series with the output load. Since this transformer has low impedance and since it raises the output load impedence, the power loss due to the automatic volume control is small.

In Figure 11, the output of the rectifier Q is shunted by a resistor r. This resistor supplies a path for the screen grid current, and makes the load on the secondary of transformer T pure resistance. This is reflected back to the low impedance primary as a pure resistance load of low impedance. The voltage divider, used to determine the con-

trolling voltage of the automatic volume control is not used. The controlling voltage is determined by the constants of transformer T. The operation of this automatic volume control is similar to that previously described. In this method for automatically controlling the volume, there is an inherent characteristic which makes supplementary adjustment of volume necessary. It is best explained by reference to Figure 11.

Let E = voltage of movable arm of manual control unit.

i = screen-grid current when no current is produced by rectifier.

Screen grid voltage $= E - ir$.

i_1 = current in r due to rectifier Q.

A voltage drop $i_1 r$ is produced across r which opposes E. This causes a drop in screen grid voltage and screen grid current.

Let i' = new screen grid current, where $i' < i$.

Then screen grid voltage $= E - (i' + i_1)r$.

It will be seen that since $i' < i$, the decrease in screen-grid voltage will not be equal to the increase of voltage drop across r (due to the increase in current in r, due to rectifier), but will be some lesser value. Thus, there is an action that tends to raise the voltage on the screen grids as the current produced by the rectifier tends to lower this voltage, and there is a gradual rise of voltage output of the receiving set with an increase of input voltage. If resistor r could be made to vary with the current through it, so that its resistance is high at low-current values, and low at high-current values, it would tend to compensate for this tendency toward a rise of screen-grid voltage. A copper-oxide rectifier used as a resistor fulfills this requirement.

The volume control characteristics of this semiautomatic volume control are the same as the characteristics given in Figure 10 for the semiautomatic volume control using the control grid method. It may be used on any signal, and has little effect on the sensitivity of the radio receiver.

IV. ACKNOWLEDGMENT

The author desires to acknowledge the many helpful suggestions made by H. Diamond on the design and use of the equipment described in this paper.

WASHINGTON, April 18, 1931.

RP331

APPARENT AND PARTIAL MOLAL HEAT CAPACITIES IN AQUEOUS SOLUTIONS OF 19 UNI-UNIVALENT STRONG ELECTROLYTES

By Frederick D. Rossini

ABSTRACT

Φ_c, the apparent molal heat capacity of the solute, is shown, within the accuracy of the best experimental data, to be a linear function of the square root of the molality for aqueous solutions of uni-univalent strong electrolytes from infinite dilution to about 2.5 molal. Consequently, $\overline{C}_{p2}$, the partial molal heat capacity of the solute, and $\overline{C}_{p1}$, the partial molal heat capacity of the H_2O, are linear functions of the square root of the molality and the 3/2 power of the molality respectively.

In convenient form are tabulated data from which may be quickly computed values of Φ_c, $\overline{C}_{p2}$, and $\overline{C}_{p1}$ for aqueous solutions of the chlorides, bromides, iodides, nitrates, and hydroxides of hydrogen, lithium, sodium, and potassium for any molality in the given range, at 18°, 21.5°, and 25° C.

CONTENTS

		Page
I.	Introduction	47
II.	Treatment of the data	48
III.	Method of computing Φ_c, $\overline{C}_{p2}$, $\overline{C}_{p1}$, and C_p	53
IV.	Tabulated results	54
V.	Discussion	55

I. INTRODUCTION

The development of a complete set of correlated data on the heat changes associated with reactions involving aqueous solutions of strong electrolytes has been somewhat retarded because of the lack of appropriate and accurate data for computing the relatively large temperature coefficients of such reactions.

These temperature coefficients can be easily and directly computed from values for Φ_c, the apparent molal heat capacity of the solute, for the given solutions.[1] Reliable values for Φ_c can be obtained indirectly from accurate measurements of the heat capacity of any aqueous solution, or from direct measurements of Φ_c. The present writer, requiring reliable values for Φ_c for the computation of the temperature coefficient of heats of dilution [2] and heats of neutralization,[3] reviewed the data on heat capacities in aqueous solutions of uni-univalent strong electrolytes. Values of Φ_c were computed from the various data and plotted against $m^{1/2}$, the square root of the molality.[4]

[1] For a discussion of Φ_c, $\overline{C}_{p_2}$, and $\overline{C}_{p_1}$, the reader is referred to—
(*a*) Lewis and Randall, Thermodynamics, Chapter VIII, McGraw-Hill Book Co., New York; 1923.
(*b*) Randall and Ramage, J. Am. Chem. Soc., **51**, p. 323; 1929.
(*c*) Randall and Rossini, J. Am. Chem. Soc., **49**, p. 93; 1927.
(*d*) Rossini, B. S. Jour. Research, **4**, p. 313; 1930.
[2] Rossini, B. S. Jour. Research, **6**, p. 791; 1931.
[3] Rossini, B. S. Jour. Research, **6**, p. 847; 1931.
[4] Following Lewis and Randall, m is the molality in moles of solute per 1,000 g of H_2O.

II. TREATMENT OF THE DATA

The data [5] are plotted in Figures 1, 2, 3, and 4.

In all cases where the data were obtained at other temperatures the values were corrected to 25° or to 18° C.

An inspection of the plotted data, in which are included the actual experimental data of Randall and Rossini,[6] shows definitely that Φ_c can be represented, within the accuracy of the best experimental data, as a linear function of $m^{1/2}$, from the lowest measured concentration to about 2.5 molal.[7]

Randall and Ramage [8] found that the value of $\overline{C}_{p_2}$ for solutions of sodium chloride increased with temperature, but gave no quantitative information. Randall and Rossini,[9] from a comparison of their data with that of others at lower temperatures, estimated that the change in $\overline{C}_{p_2}$ or Φ_c with temperature was about 0.2 cal mole^{-1}°C^{-2}. From the data of Richards et al., Rossini [10] calculated for aqueous solutions of 3 uni-univalent strong electrolytes, in the region from infinite dilution to about 1 molal, that the change in Φ_c with temperature was 0.26 to 0.29 cal mole^{-1} °C^{-2}. From the data of Richards and Gucker,[11] who measured the specific heats of solutions of $NaOH \cdot 25H_2O$ and $NaC_2H_3O_2 \cdot 25H_2O$ at 16°, 18° and 20°C, the change in Φ_c with temperature over this range is computed to be 0.32 and 0.28 cal mole^{-1} °C^{-2}, respectively. For the purpose of the present work, $\frac{d\Phi_c}{dT}$ is taken as $\frac{2.0}{7}$ cal mole^{-1} °C^{-2}, for the temperature range 18° to 25° C. The same value is used for all the uni-univalent strong electrolytes from infinite dilution to about 2.5 molal and, while probably not strictly valid, this assumption is well within the accuracy of the experimental data.

Randall and Rossini [6] showed from their experimental data that $\overline{C}^{\circ}_{p_2}$ for individual ions is an additive property. This knowledge permits the accurate computation of Φ°_c (which is equal to $\overline{C}^{\circ}_{p_2}$) for a number of solutes for which no data are available in the dilute range of concentration, or for which the data are inadequate to permit reliable extrapolation to infinite dilution.

The curves for the various solutes were drawn in the following order, that the greatest advantage might be obtained in predicting

---

[5] (*a*) Richards and Rowe, J. Am. Chem. Soc., **43**, p. 770; 1921; **42**, p. 1621; 1920; Proc. Am. Acad., **49**, p. 173; 1913; on LiCl, NaCl, KCl, $LiNO_3$, $NaNO_3$, KNO_3, LiOH, NaOH, KOH, HNO_3, HCl, HBr, HI, 18° C.
(*b*) Richards and Hall, J. Am. Chem. Soc., **51**, p. 707; 1929; on NaOH, KOH, 18° C.
(*c*) Richards, Mair, and Hall, J. Am. Chem. Soc., **51**, p. 727; 1929; on HCl, 18° C.
(*d*) Richards and Gucker, J. Am. Chem. Soc., **51**, p. 712; 1929; **47**, p. 1876; 1925; on NaOH, NaCl, $NaNO_3$, KNO_3, 18° C.
(*e*) Randall and Rossini, J. Am. Chem. Soc., **51**, p. 323; 1929; Rossini, Thesis, University of California; 1928; on NaCl, KCl, NaBr, KBr, NaI, KI, $NaNO_3$, KNO_3, 25° C.
(*f*) Marignac, Ann. chim. phys., **8**, p. 410; 1876; on NaCl over the range 16° to 20° C., KCl at 17° to 22° C., $NaNO_3$ and KNO_3 at 18° to 23° C., NaBr, KBr, NaI, and KI at 20° to 51° C., HNO_3 at 21° to 52° C., HCl at 20° to 24° C.
(*g*) Thomsen, Thermochemische Untersuchungen, **1**, p. 38, Barth, Leipzig; 1882; on HCl, 18° C.
(*h*) Jauch, Z. Physik, **4**, p. 441; 1921; on LiCl, LiBr, LiI, 18° C.
(*i*) Thorvaldson, Brown and Peaker, J. Am. Chem. Soc., **52**, p. 3927; 1930; on HCl, 20° C.
(*j*) Wrewsky and Kaigorodoff, Z. physik. Chem., **112**, p. 83; 1924; on HCl, 20.5° C.

[6] See footnote 5 (*e*), p. 48.

[7] For solutions of HCl and NaCl, Randall and Ramage (see reference 1 (*b*), p. 47) reported $\overline{C}_{p_2}$ as a linear function of $m^{1/2}$, but their data were not precise enough to establish this fact.

[8] See footnote 1 (*b*), p. 47.

[9] See footnote 5 (*e*), p. 48.

[10] See footnote 1 (*d*), p. 47.

[11] See footnote 5 (*d*), p. 48.

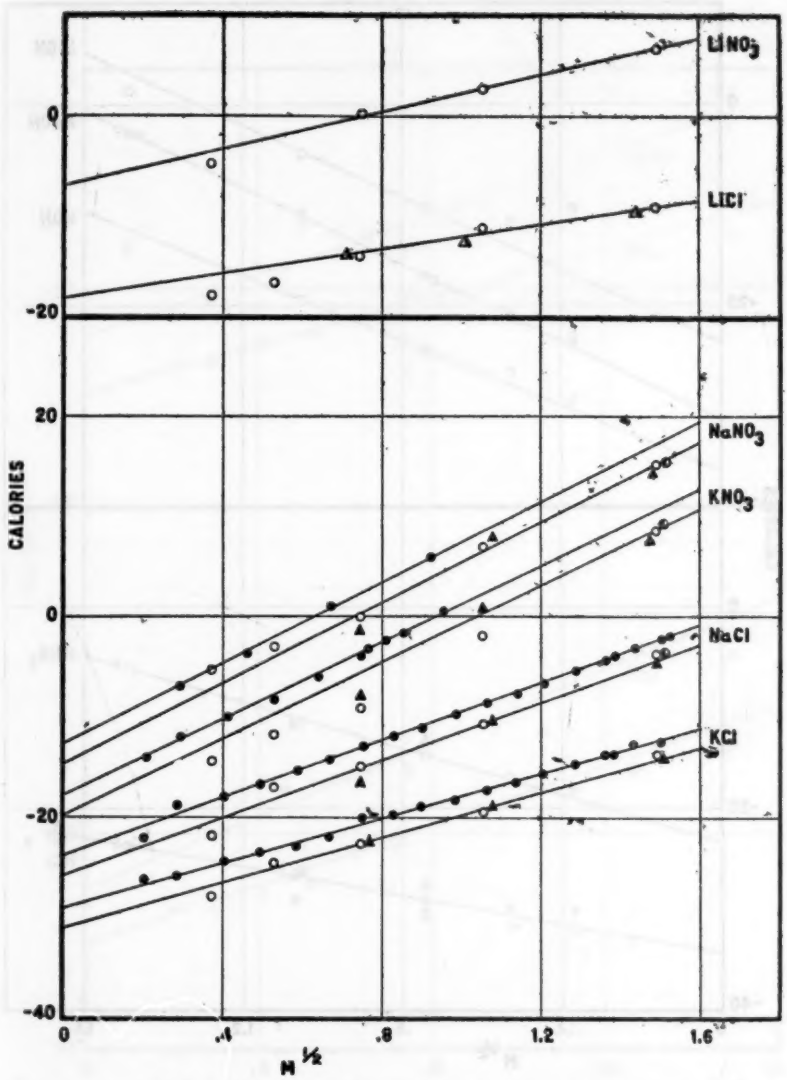

FIGURE 1.—*The apparent molal heat capacity of the solute in aqueous solutions of LiCl and $LiNO_3$ at 18° C., and NaCl, $NaNO_3$, KCl, and KNO_3 at 18° and 25° C*

The apparent molal heat capacity, in calories per mole, is plotted against the square root of the molality. Where two lines are drawn for one solute, the lower is for 18° C., and the upper for 25° C. The data of the various investigators are designated as follows:

- ● Randall and Rossini (25° C.).
- ○ Richards and Rowe (18° C.).
- ◐ Richards and Gucker (18° C.).
- ▲ Jauch (18° C.).
- ▲ Marignac (corrected from 16° to 23° to 18° C.).

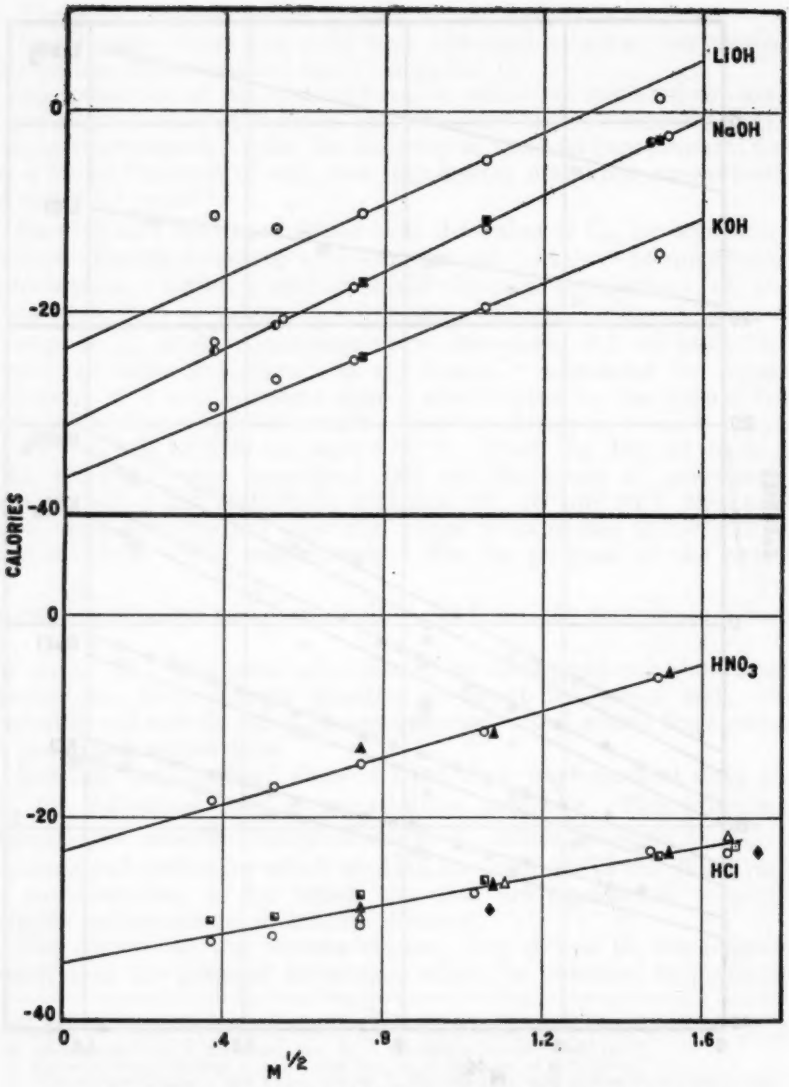

FIGURE 2.—*The apparent molal heat capacity of the solute in aqueous solutions of HCl, HNO_3, LiOH, NaOH, and KOH at 18° C.*

The apparent molal heat capacity, in calories per mole, is plotted against the square root of the molality The data of the various investigators are designated as follows:

○ Richards and Rowe (18° C.).
■ Richards and Hall (18° C.).
◱ Richards, Mair, and Hall (18° C.).
◐ Richards and Gucker (18° C.).
△ Thomsen (18° C.).
□ Thorvaldson, Brown, and Peaker (corrected from 20° to 18° C.).
◆ Wrewsky and Kaigorodoff (corrected from 20.5° to 18° C.).
▲ Marignac (data on HCl corrected from 22° to 18° C; on HNO_3 from 21° to 52° to 18° C.).

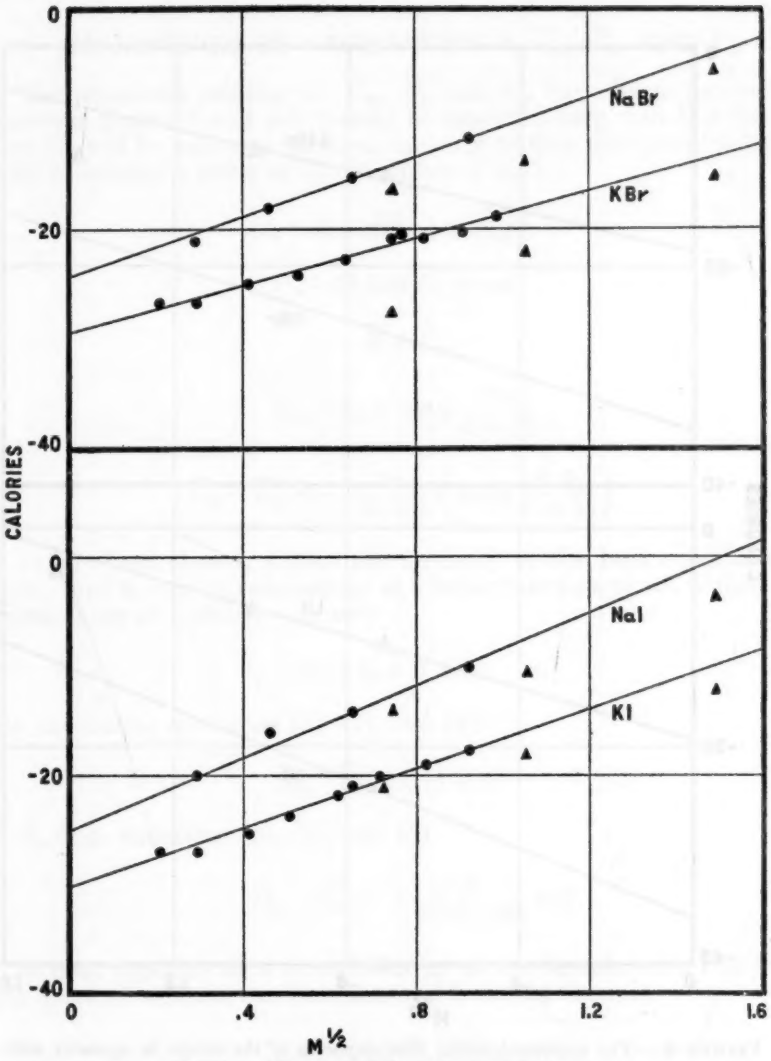

FIGURE 3.—*The apparent molal heat capacity of the solute in aqueous solutions of NaBr, KBr, NaI, and KI at 25° C.*

The apparent molal heat capacity, in calories per mole, is plotted against the square root of the molality. The data of the various investigators are designated as follows:

● Randall and Rossini (25° C.).

▲ Marignac (corrected from 25° to 51° to 25° C.).

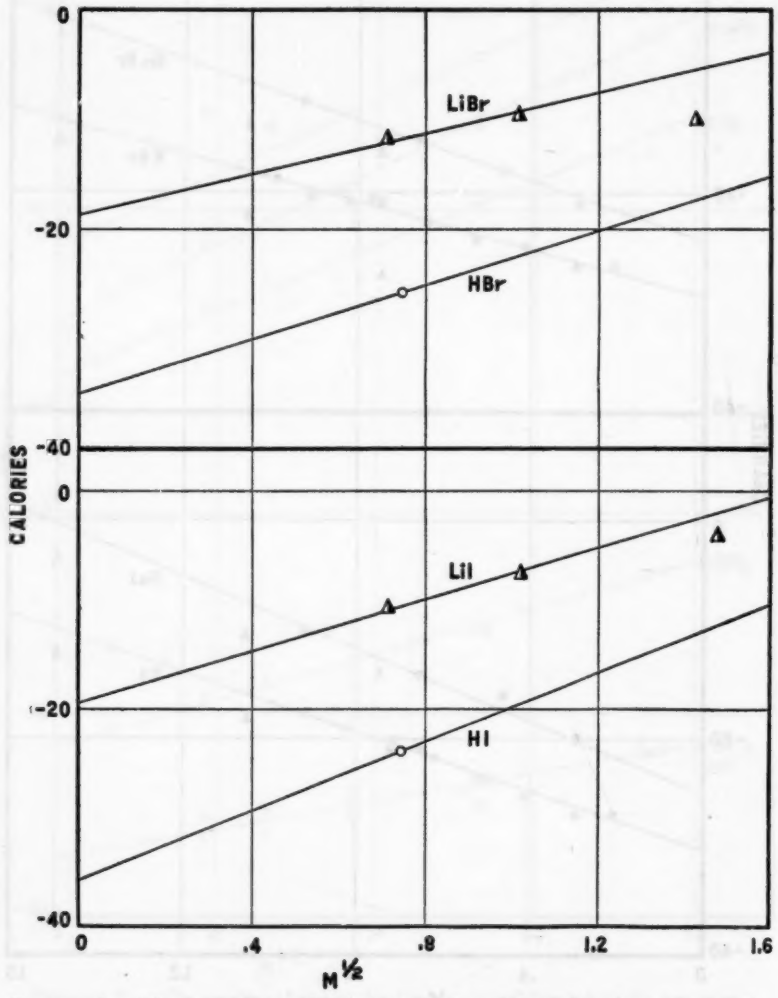

FIGURE 4.—*The apparent molal heat capacity of the solute in aqueous solutions of LiBr, LiI, HBr, and HI at 18° C.*

The apparent molal heat capacity, in calories per mole, is plotted against the square root of the molality. The data of the various investigators are designated as follows:

○ Richards and Rowe (18° C.).
△ Jauch (18° C.).

values for Φ_c for those substances on which the data are meager or unreliable: (1) NaCl; (2) KCl; (3) KNO_3 and $NaNO_3$; (4) LiCl and $LiNO_3$; (5) HCl and HNO_3; (6) NaOH; (7) LiOH and KOH; (8) KBr and NaBr; and (9) KI and NaI; (10) HBr, HI, LiBr and LiI.

III. METHOD OF COMPUTING Φ_c, $\overline{C}_{p_2}$, $\overline{C}_{p_1}$, AND C_p

The equations relating Φ_c, $\overline{C}_{p_2}$, $\overline{C}_{p_1}$ and C_p have been derived in previous papers [12] and will merely be repeated here. In this discussion C_p will be taken as the heat capacity of that amount of solution which contains 1,000 g or 55.508 moles of H_2O.

$$C_p = 55.508\overline{C}_{p_1} + m\,\overline{C}_{p_2} \tag{1}$$

$$C_p = 55.508\,\overline{C}^{\circ}_{p_1} + m\Phi_c \tag{2}$$

$$\Phi^{\circ}_c = \overline{C}^{\circ}_{p_2} \tag{3}$$

$$\overline{C}_{p_1} = \Phi_c + \tfrac{1}{2}m^{\frac{1}{2}}\frac{d\Phi_c}{d(m^{\frac{1}{2}})} \tag{4}$$

$$\overline{C}_{p_1} - \overline{C}^{\circ}_{p_1} = -\frac{m}{55.508}\left(\tfrac{1}{2}m^{\frac{1}{2}}\frac{d\,\Phi_c}{d(m^{\frac{1}{2}})}\right) \tag{5}$$

It has been shown, within the accuracy of the best experimental data, that Φ_c can be represented as a linear function of $m^{\frac{1}{2}}$ within the given range of molality. Hence

$$\Phi_c = \Phi^{\circ}_c + A\,m^{\frac{1}{2}} \tag{6}$$

By combining equations (6), (3), and (4)

$$\overline{C}_{p_2} = \overline{C}^{\circ}_{p_2} + \tfrac{3}{2}\,A\,m^{\frac{1}{2}} \tag{7}$$

and, from equations (6), (3), and (5)

$$\overline{C}_{p_1} - \overline{C}^{\circ}_{p_1} = -\frac{A}{2(55.508)}m^{\frac{1}{2}} \tag{8}$$

The heat capacity of a given solution at the temperature t in g-cal. per gram of solution can be computed from the formula

$$c_p = \frac{1{,}000 + m\Phi_c}{1{,}000 + mM} \tag{9}$$

where M is the molecular weight of the solute.

[12] See footnote 1, p. 47.

IV. TABULATED RESULTS

In Table 1 are given, for each of the 19 aqueous solutions, the following information:

1. The value of A, $3/2A$, and $-\frac{A}{2(55.508)}$. These values are the same for the three given temperatures, 18°, 21.5°, and 25° C.

2. The value of $\Phi_v^\circ (=\overline{C}^\circ_{p_2})$ for each of the three temperatures.

From these values one may compute, for any one of the 19 solutions, at any molality between 0 and 2.5, the values of the properties Φ_v, $\overline{C}_{p_2}$, $\overline{C}_{p_1}$, and C_p at 18°, 21.5°, and 25° C.

TABLE 1.—*Table of values for computing* Φ_v, $\overline{C}_{P_2}$ *and* $\overline{C}_{P_1}$

(In cal. mole^{-1}°C.$^{-1}$)

Solute	A	$3/2A$	$-\frac{A}{2(55.508)}$	$\Phi^\circ_v=\overline{C}^\circ_{p_2}$		
	18°–25° C.	18°–25° C.	18°–25° C.	18° C.	21.5° C.	25° C.
HCl	7.2	10.8	−0.065	−34.5	−33.5	−32.5
HBr	12.4	18.6	−.112	−35.0	−34.0	−33.0
HI	15.9	23.95	−.143	−35.7	−34.7	−33.7
HNO_3	11.5	17.25	−.104	−23.3	−22.3	−21.3
LiCl	6.1	9.15	−.055	−18.2	−17.2	−16.2
LiBr	9.2	13.8	−.083	−18.7	−17.7	−16.7
LiI	11.8	17.7	−.106	−19.4	−18.4	−17.4
$LiNO_3$	9.3	13.95	−.084	−7.0	−6.0	−5.0
LiOH	17.9	26.85	−.161	−23.6	−22.6	−21.6
NaCl	14.4	21.6	−.130	−25.8	−24.8	−23.8
NaBr	13.6	20.4	−.123	−26.3	−25.3	−24.3
NaI	16.6	24.9	−.150	−27.0	−26.0	−25.0
$NaNO_3$	20.0	30.0	−.180	−14.6	−13.6	−12.6
NaOH	19.0	28.5	−.171	−31.2	−30.2	−29.2
KCl	11.2	16.8	−.101	−31.0	−30.0	−29.0
KBr	10.8	16.2	−.097	−31.5	−30.5	−29.5
KI	13.6	20.4	−.123	−32.2	−31.2	−30.2
KNO_3	19.1	28.65	−.172	−19.8	−18.8	−17.8
KOH	16.1	24.15	−.145	−36.4	−35.4	−34.4

In Table 2 are given values for Φ_c°, which is equal to $\overline{C}_p^\circ$, for the individual ions at 25° C. These values have been computed by assuming Φ_c° for K^+ equal to Φ_c° for Cl^-. The temperature coefficient can be taken as half that for two ions.

TABLE 2.—*Values of* Φ°_v $(=\overline{C}^\circ_{p_2})$ *for individual ions at 25° C.*

(Computed by assuming $\Phi^\circ_v(K^+)=\Phi^\circ_v(Cl^-)$)

Ion	Φ°_v cal. mole^{-1} °$_v^{-1}$	Ion	Φ°_v cal. mole^{-1} °$_v^{-1}$
H^+	−18.0	Br^-	−15.0
Li^+	−1.7	I^-	−15.7
Na^+	−9.3	NO_3^-	−3.3
K^+	−14.5	OH^-	−19.9
Cl^-	−14.5		

NOTE.—The temperature coefficient of Φ°_v for a single ion can be taken as $\frac{2.0}{14}$ cal. mole^{-1} °C^{-1} at 18° to 25°C.

V. DISCUSSION

The accuracy of the present values for the apparent molal heat capacity can be judged from the figures. The data on NaCl at 25° C. and NaOH at 18° C. are the most consistent. The meager data on LiBr, LiI, HBr and HI indicate the need for accurate measurements at one or two concentrations, preferably at 1 and 2 molal. The data on HCl are at great variance, relatively. The line for HCl, drawn so as to be consistent with Φ°_c for HNO_3 and the known difference between Φ°_c for NO_3^- and for Cl^-, was passed through the middle of all the data. The resulting line, remarkably enough, passed almost directly through the three points from the data of Marignac. An inspection of the various plots shows that the data of Marignac, except, apparently, in the case of NaBr, KBr, NaI, and KI, are remarkably accurate. This was pointed out by Richards and Rowe.[13]

The values for Φ_c, $\overline{C}_{p_2}$ and $\overline{C}_{p_1}$ at 21.5° C. can be used to convert values for Φ_h, $\overline{H}_2$ and $\overline{H}_1$ from 18° to 25° C., or vice versa.

The desirability of having reliable values for Φ_c has already been discussed. $\overline{C}_{p_2}$ and $\overline{C}_{p_1}$ are, respectively, the temperature coefficients of $\overline{H}_2$ and $\overline{H}_1$, the partial molal heat content of the solute and the solvent. These properties occur frequently in thermodynamic equations involving solutions, as they serve to measure the change with temperature of $\overline{F}_2$ and $\overline{F}_1$, the partial molal free energy of the solute and the solvent, respectively.

WASHINGTON, March 27, 1931.

---

[13] See footnote 5 (a), p. 48.

MEASUREMENT OF LENARD RAYS

By Lauriston S. Taylor

ABSTRACT

An investigation is described in which the correct measurement of the electron output (Lenard current) from high-voltage cathode ray, or Lenard ray tubes, is attempted.

The evidence presented shows that a Faraday chamber of proper dimensions may be used to measure the Lenard ray current which at any point is shown to be a linear function of the total tube current. The open-plate method of measuring Lenard currents yields results which are consistently too low, although under the conditions here used bear a constant relationship to the Faraday chamber measurements. The open-plate measurements are, therefore, also a linear function of the total tube current. The condenser method of measurement (Thaller) yields measurements above or below those of the Faraday chamber, depending upon the relationship of the atomic numbers of the two plates. Moreover, the current measured by this method is not a linear function of the total tube current, and hence does not bear a constant relationship to the Faraday chamber measurements under the conditions used. Measurements of the range of scattered electrons from Lenard tubes operating at about 160 kv peak, indicate a maximum of about 15 mm in air, which is equivalent to an energy of about 60 electron kilovolts. By means of a variable Faraday chamber described, it is possible to obtain a measure of the velocity distribution of the scattered electrons.

CONTENTS

	Page
I. Introduction	57
1. Early use of Lenard tubes	57
2. Methods of measuring Lenard ray currents	58
II. Experimental investigation	60
1. Tubes and generating equipment	60
2. Apparatus used for comparing Lenard ray measurements	60
3. Measurement of total electron current	63
4. Comparison of open-plate and Faraday chamber methods	64
5. Comparison of condenser and Faraday chamber methods	67
6. Effect of changing the dimensions of Faraday chamber	69
III. Effect of electron scattering	70

I. INTRODUCTION

1. EARLY USE OF LENARD TUBES

In 1925 Coolidge described a high-voltage hot cathode tube of the Lenard type, by means of which high-speed electrons passed through a thin (0.0015 inch) metal window from the tube into the open air.[1] His principal improvement over the original Lenard tube lay in the very large increase in the number and speed of the electrons transmitted through the foil window. He has constructed a cascade tube operating at 900 kv and 2 ma on an induction coil. More recently

[1] W. D. Coolidge, J. Frank. Inst., 202, p. 693; 1926.

Slack [2] has developed a similar tube having a very thin (1 μ) concave glass window and operating up to at least 350 kv in a single stage.

Since the introduction of the Coolidge tube, a wide variety of investigations have been undertaken having in view its applications in the fields of physical, chemical, and biological research. Coolidge and Moore [3] made the first qualitative studies of various effects of the electrons upon substances in air as well as the effects upon animal tissue and bacteria. McLennan [4] and his coworkers have since carried out very extensive studies of their effect upon chemical reactions. In the biological field the most comprehensive studies have been carried out by Schaeffer and Witte,[5] and Baensch and Finsterbusch,[6] of whom the former made the first attempt to apply physical measurements of Lenard ray currents to biological reaction.

The greater part, however, of all of this work has been done with very little accurate knowledge of the magnitude of the Lenard ray quantities involved. The object of the present communication is to describe a study of several methods for measuring the current of the high-speed electrons in air under conditions suitable for general experimental application.

To avoid possible confusion in speaking of the various currents it is well to differentiate between them. By the total current is meant the electron stream leaving the filament irrespective of its ultimate destination. There is also a current composed of high-speed electrons in air, called the Lenard current. Its current density, which is directly proportional to the number density and velocity of the electrons, varies with distance and direction from the window. Most of the measurements described below are in terms of current density.

Experiment shows that it is insufficient and often misleading to measure the electron current at some point outside the tube in terms of the current through the tube and the voltage applied to the tube. While this may be satisfactory for reproducing conditions with a given set-up, many complicating factors render it useless from the viewpoint of reproduction under other slightly different conditions.[7]

2. METHODS OF MEASURING LENARD RAY CURRENTS

Three methods of measuring Lenard ray currents were announced almost simultaneously. Thaller [8] used a modification of a method described by Lenard [9] and shown diagrammatically in Figure 1 (*a*). The high-speed electrons *e* pass through a layer of noble metal *E*, about 0.001 mm thick, deposited on a somewhat thicker layer of copper oxide *C* or other insulating material, to the backing plate *P* and thence through a galvanometer to ground. The current through the galvanometer is then taken as the Lenard current.

The writer [10] has described some preliminary measurements made by the apparatus shown in Figure 1 (*b*) wherein the electrons were allowed to impinge upon a small aluminum plate *E* surrounded by an earthed guard plate *S*, so designed as to avoid error due to electrons

[2] C. M. Slack, J. Opt. Soc. Am., **18**, p. 123; 1929.
[3] W. D. Coolidge and C. N. Moore, J. Frank. Inst., **202**, p. 722; 1926.
[4] J. C. McLennan, Perrin, and Ireton, Proc. Roy. Soc., **125**, p. 246; 1929.
[5] W. Schaeffer and E. Witte, Strahlen., **31**, p. 415; 1929.
[6] W. Baensch and R. Finsterbusch, Strahlen., **33**, p. 399; 1929.
[7] It might be mentioned that, at the outset of this work, a number of erroneous results were obtained due to what later proved to be the improper measurement of the tube current.
[8] R. Thaller, Strahlen., **33**, p. 263; 1929.
[9] P. Lenard, Ann. Phys. u. Chem., **64**, p. 288; 1898.
[10] L. S. Taylor, Radiology, **12**, p. 294; 1929.

entering the space between E and S. The current from plate to ground as measured by the galvanometer was taken as the Lenard current.

Schaeffer and Witte [11] expressed their intensities in terms of the air ionization produced, having made the necessary corrections for the additional ionization produced by the associated X rays. This method aims to obtain a measure of the energy where the preceding deal only with the current; therefore, the measurements can not be directly compared.

The ionization currents produced by Lenard beams are relatively large. For example, consider an electron beam having a current density of only 8×10^{-8} amp/cm^2 (as in some of the work described below), and assume complete loss of velocity of all of the electrons which have an average speed of 125 kv. Using Eisl's [12] value of 32.2 volts loss of velocity to yield one pair of ions, it is found that 1.9×10^{15} ion pairs are formed per second by this stream, which should

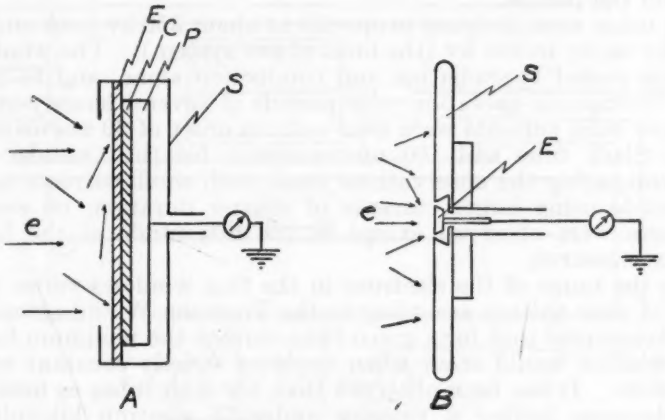

FIGURE 1.—*Lenard ray collectors*

(*a*) Schematic diagram of Lenard-Thaller condenser collector for measuring Lenard rays. (*b*) Cross section of Taylor open plate collector

give a saturation current of 3×10^{-4} amperes per square centimeter—4,000 times the initial electron current.

In spite of the advantage of yielding conveniently large currents, other experimental difficulties, discussed below, render the ionization method of Lenard ray measurement less satisfactory, however, than the electron-current method. In this study we have used a Faraday chamber method as a basis of comparing the first two methods above.

The Lenard current is measured in terms of the unit previously proposed by the author,[13] as that beam having an electron current density of one e. s. u. per square centimeter normal to the direction of the beam. This was called the "lenard" and was designated by the letter L. It is obvious that, due to scattering of the electrons in air, the current density will be essentially uniform only over a very small area. Hence, it was thought desirable to restrict the measurements to the current over an area only 1 cm in diameter rather than some 10 cm as in Thaller's system. The intensity of the beam

[11] W. Schaeffer and E. Witte, Strahlen., **31**, p. 415; 1929.
[12] A. Eisl, Ann. der Physik, **3**, p. 277; 1929.
[13] L. S. Taylor, Radiology, **12**, p. 294; 1929.

striking the center of such a large collector as Thaller's will be very different from that striking the edges, so that in effect he measures an average intensity. As mentioned, this type of measurement is not directly comparable with Schaeffer and Witte's.

II. EXPERIMENTAL INVESTIGATION

1. TUBES AND GENERATING EQUIPMENT

Two types of hot cathode Lenard tubes were used in this investigation. The first was the Coolidge type having a large flat metal foil window supported on a honeycomb grid. The foil was of nickel about 0.03 mm thick. The tube operated continuously on a metal 4-stage mercury diffusion pump. The second tube was of the Slack type having a drawn-in glass window about 0.002 mm thick with an effective opening of about 3 cm diameter. This tube was sealed off the pumps.

Both tubes were designed to operate at about 350 kv peak and were tested by us up to 325 kv (the limit of our system). The window of each was cooled by radiation and conduction alone, and to permit steady continuous operation over periods of several hours comparatively low tube currents were used—of the order of 20 microamperes for the Slack tube and 100 microamperes for the Coolidge tube. When comparing the observations made with small currents against those made using larger currents of shorter duration, no essential differences were observed except in the magnitude of the Lenard currents measured.

Since the range of the electrons in the thin windows varies as the square of their voltage according to the Thomson-Whiddington-Bohr law, it is obvious that for a given tube current the minimum heating of the window would occur when applying strictly constant voltage to the tube. It has been observed that, for such tubes as here used, most electrons having a velocity under 75 electron kilovolts are completely absorbed in the window, and hence are effective only in producing heat and a few X rays. Thus when applying other than constant voltage to the tube only that portion of the wave above 75 kv. is effective in producing the results sought.

Not having available a suitable constant voltage source for this work, a disk mechanical rectifier was used in which rectification occurred over approximately 15° to 20°. For convenience of measurement the anode and window of the tube were at ground potential and a maximum of about 160 kv was applied to the cathode.

Tubes, generating equipment and measuring apparatus were placed for safety in a large room lined with ¼-inch lead, and all controls and indicating instruments were brought outside and so arranged as to permit the variation and measurement of all quantities without the necessity for entering the room. This had the one undesirable feature of requiring very careful electrostatic shielding of all parts of the apparatus to prevent the sensitive galvanometers from picking up electrical disturbances from the mechanical rectifier and high-tension leads.

2. APPARATUS USED FOR COMPARING LENARD RAY MEASUREMENTS

In order to facilitate the comparison between the three systems outlined above, namely, Thaller's condenser system, Taylor's open

plate system and the Faraday chamber, a single Lenard ray collector was designed in such a manner as to readily measure the electrons according to any one of the methods.

The collector C in Figure 2 was mounted on a grounded track so as to be movable through a distance of about 25 cm from the tube window L in any direction from zero to an angle of 150° with the axis of the tube. The outer case of the collector, the copper gauze shield S_1, and the tube anode were connected together through a galvanometer G_T to ground. This system was surrounded by a second copper gauze shield S_2 which was grounded. Both S_1 and S_2 were so slotted as to permit the ready movement of the collector along the track.

Figure 3 shows a detailed diagram of the collector used as a basis of comparison. The inner cylinder D, carefully insulated from the

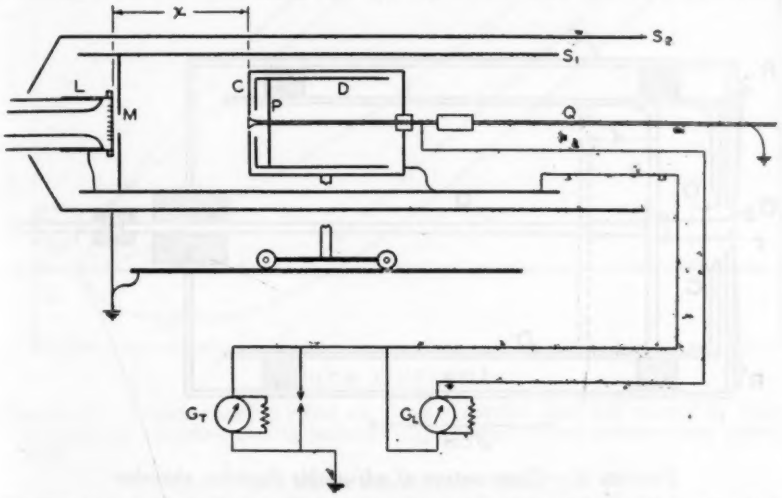

FIGURE 2.—*Diagram of experimental set-up for comparing the condenser, open plate and Faraday chamber methods of Lenard ray measurement*

case C, contained a plunger P which could be moved by means of the rod Q from outside the lead room. Both inner cylinder and plunger were connected through the galvanometer G_L to the galvanometer circuit G_T as indicated. Galvanometers, all lead wires, shunts, etc., were completely surrounded by earthed shielding. Thus the galvanometer G_T indicates the total electron current of the tube, made up in part of the small electron current to the Faraday chamber as measured by G_L. A current measuring system placed thus in the grounded circuit is preferable when dealing with currents as small as those here involved, since it does not measure any of the corona losses in the high-tension circuit.

The complete collector is essentially a large adjustable Faraday chamber. The plunger P supports a collector F of which the outer end having a diameter of 9.8 mm passes through the opening O_2 in the outer case C, with a clearance of 0.1 mm. The Faraday cylinder D has its front end G adjustable in position along the axis so as to vary the spacing between C and G. The openings O_1 in the Faraday

chamber and O_2 in the case are tapered in such a manner that all the electrons (except those at a glancing angle) incident on the plane of O_2 will pass into the chamber when the plunger is drawn back. On the front of the outer case is a thin tapered ring by means of which thin metal covers may be securely clamped over the opening O_2.

This system may be used for any of the three methods described above. By placing the collector F flush with the outer face of the case we have the open-plate system. By moving the plunger back into the cylinder D, a Faraday chamber is obtained. To obtain Thaller's condenser system, a thin metal foil and insulator may be clamped under the ring R and then F moved up to just bear on the insulator under the foil. Moreover, by moving the plunger back while the opening O_2 is covered we can effectively measure the transmission of the foil and insulator by the Faraday chamber method.

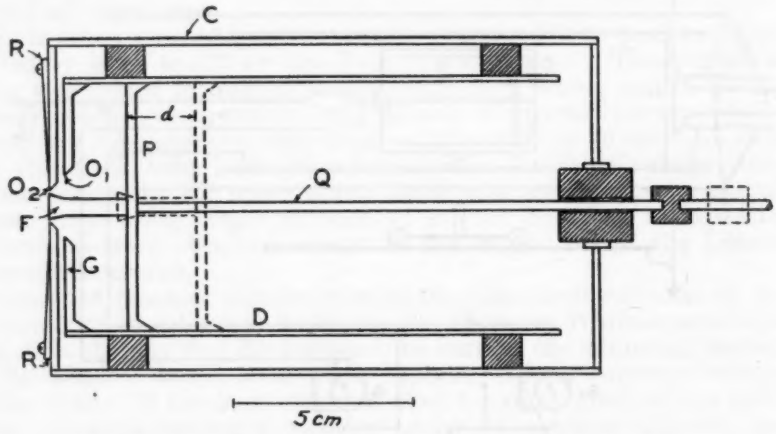

FIGURE 3.—*Cross section of adjustable Faraday chamber*

Broken lines indicate position of plunger when drawn back. (Cross section indicates hard rubber).

Care must be taken to properly identify any currents measured, since the total tube output may be considered as made up of a number of separate parts. A correct measure of the tube current is not obtained by measuring simply the current between anode and ground, since this does not measure the electrons that pass through the window. The total tube current consists of the following parts: (1) the current to the anode (including the window), of which a large part is due to electrons scattered from the primary cathode beam within the focusing tube; (2) the current to the diaphragm M (fig. 2); (3) the electrons scattered back of M striking the outer conducting wall of the tube; (4) the electrons striking the shield S_1 and the Faraday case front C; and (5) the electrons entering the Faraday cylinder D. If the shields S_1 and S_2 are removed the part 4 will be reduced while part 3 will be increased. Moreover, the amount of these changes will depend to a considerable extent upon the relative positions of the diaphragm M and the Faraday case C.

Figure 4 shows a series of curves of the Lenard current, measured with the open plate collector, as it varies with total tube current

for a fixed voltage on the tube. These are given to indicate, without going into detail, the necessity for careful shielding and the elimination of stray potentials in the system. Curves *a*, *b*, and *c* were taken with both shields S_1 and S_2 (fig. 2) removed: *a* with the center electrode at exactly the same potential as the case; *b* and *c* with the center electrode maintained at about 0.5 volt above and below the case potential respectively. The slight displacement from the origin was due to stray field disturbance. Curve *d*, taken with only S_2 removed, is linear, but passes far from the origin due to an excessively

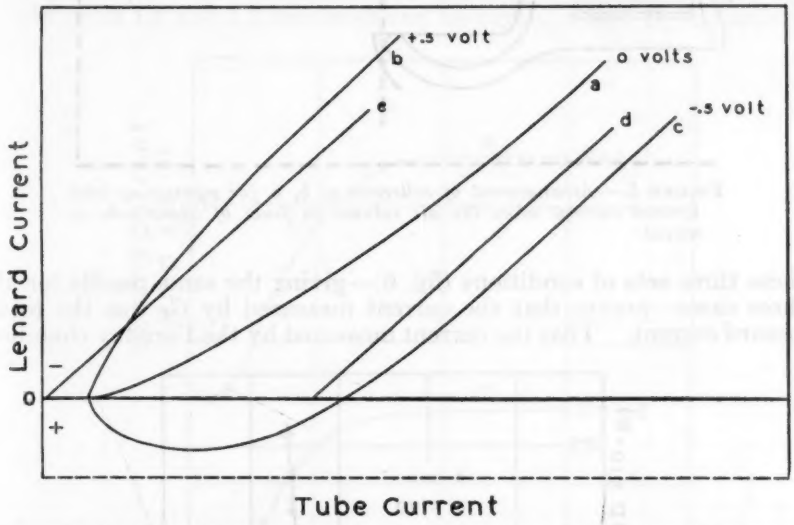

FIGURE 4.—*Curves showing effect on Lenard current readings caused by poor electrostatic shielding and by potential differences between collector and guard ring.*

Scales of same order as in later figures.

large field disturbance picked up by S_1. Curve *e* for a completely shielded system is linear and passes through the origin.

3. MEASUREMENT OF TOTAL ELECTRON CURRENT

The first point investigated was the correctness of the indications of the Faraday chamber. Since the entire space (outside and inside the chamber) is highly ionized it must be assured that the net flow of current to the collector is simply the primary electron current—that other positive and negative ions either recombine or reach the collector in equal numbers.

One way of testing this is by measuring the apparent total tube output current, say, as a function of the filament current, while varying over wide limits the air volume in front of the tube. This was accomplished in the case of the Slack tube by inserting first a closed lead cylinder *a* (fig. 5) into the window so that there was practically no volume of air to be ionized; second, covering the opening with a flat plate *b* so that only the space inside the mouth of the window was ionized; and third, inclosing a large volume of air in front of the tube

with a can *c*. With the Coolidge tube a can only was used. A plot of the total tube current as a function of the filament current for

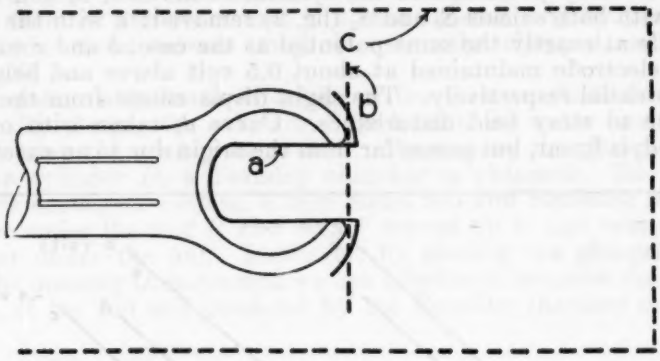

FIGURE 5.—*Arrangement of collectors a, b, c, for measuring total Lenard current when the air volume in front of Slack tube is varied*

these three sets of conditions (fig. 6)—giving the same results for all three cases—proves that the current measured by G_T was the total Lenard current. That the current measured by the Faraday chamber

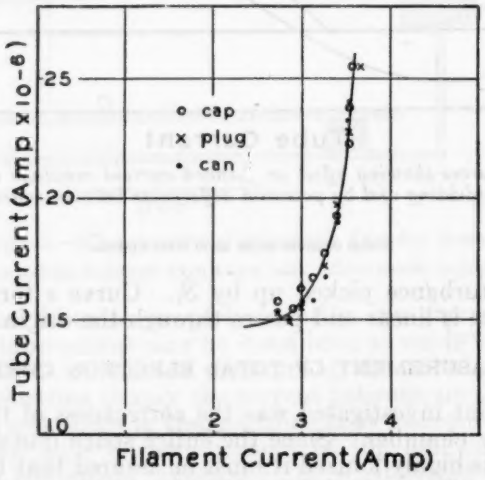

FIGURE 6.—*Total Lenard current as a function of filament current*

is a definite fraction of the total, is supported by mutually consistent results discussed below.

4. COMPARISON OF OPEN PLATE AND FARADAY CHAMBER METHODS

The next point investigated was the effect of moving the collector F back from the position where it was flush with the outer case. Two curves A and B (fig. 7) show the change in current to the Faraday chamber as a function of the distance d between F and the front face of the outer case C (fig. 3). It will be noticed that the current for

values of d greater than about 1.5 cm, is about 33 per cent greater than for conditions where F and C are flush.

To avoid confusion in speaking of the currents measured by G_L for different positions of the collector F, the currents will be identified as follows: (*a*) When the collector is flush with the outer case, as the plate or collector-plate current; (*b*) when the current no longer changes with d, as the complete or complete Faraday current; and (*c*) when the current is intermediate between the two cases above, as the intermediate current.

Two cases where the distance x between C and the Lenard tube window is 1.0 and 1.5 cm are shown by curves A and B, respectively.

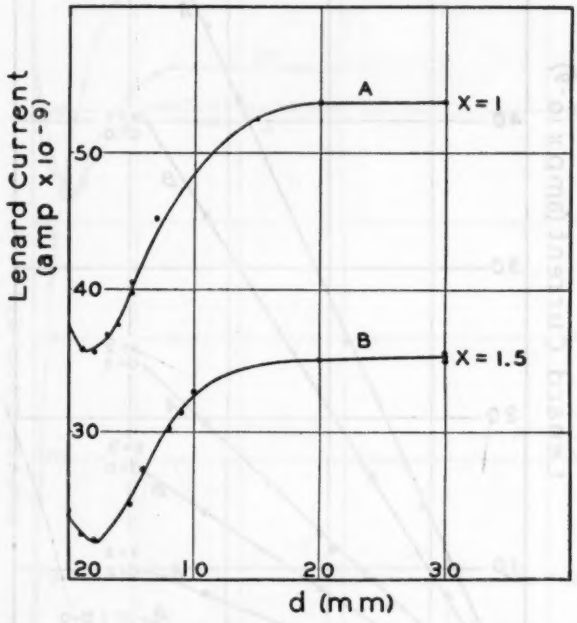

FIGURE 7.—*Lenard current as a function of the distance d which the plunger is withdrawn, for two distances x between collector face and tube window*

Other conditions remaining the same, the ratio between the plate and complete currents was approximately the same for all values of x and all tube potentials used. Since the velocity distribution of the electrons in the beam subtended by the opening O_2 will vary with both tube potential and the distance x—hence, the ionization-intensity distribution will vary with both—it may then be safely assumed that the form of the curves in Figure 7 is not due to positive or negative ions.

The minimum always appears at d about 2 to 3 mm and the saturation current is reached when d reaches 20 mm, for the particular arrangement of the inner cylinder. Both of these points may be shifted slightly by changing the size of O_1 or the distance between O_1 and O_2. The minimum may be explained as due to the fact that as the collector F recedes, the opening O_2 prevents electrons from striking it at the more grazing angles. The subsequent gradual approach to a complete Faraday current at $d = 20$ mm is due to the

gradual reduction in scattering of electrons from the face of F to the edges of the opening O_2, or even entirely out through O_2.

Figure 8 gives representative curves showing the current as a function of the total tube current for four different distances x (10, 20, 30, 40 mm) from the tube window and two different distances d (0, 30 mm) of the collector plate F for each value of x. Since from these it is seen that the ratio of the two currents at any one value of x is the same for all tube currents; and further, since it is found that

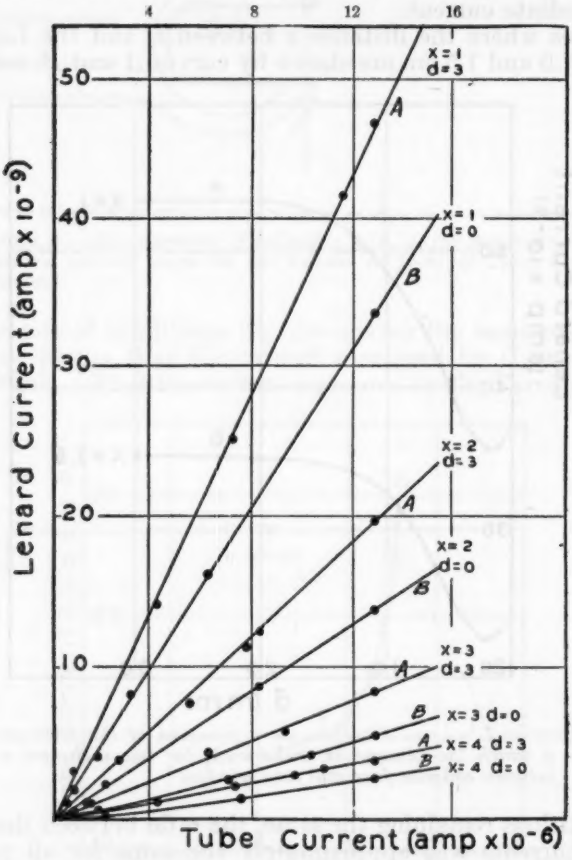

FIGURE 8.—*Lenard current as a function of tube current for different values of x and d*

The ratio of the *A* curves to the corresponding *B* curves is the same for all values of *x*. Values of *x* and *d* indicated in centimeters

the ratio of the two currents at any one value of d and any two values of x is the same for all tube currents, it is to be concluded that the ionization density in front of the collector, which must change greatly over this range of conditions, does not affect the measured magnitudes. Curve A, taken for $d=30$ mm is seen to be about 33 per cent greater than curve B taken with $d=0$, which is in good agreement with the curves shown in Figure 7.

We may conclude from these results, that the open plate measurement of any Lenard current bears a constant ratio to the Faraday chamber measurement.

5. COMPARISON OF CONDENSER AND FARADAY CHAMBER METHODS

To test the condenser method of Lenard current measurement (Thaller), the opening O_2 was covered with a 0.01 mm aluminum foil clamped in place by means of the ring R. (Fig. 3.) The collector F was then moved back just sufficiently to prevent contact with the foil (about 0.02 mm) forming a condenser with an air dielectric and having as plates the aluminum foil and the collector F. As seen by Curve I

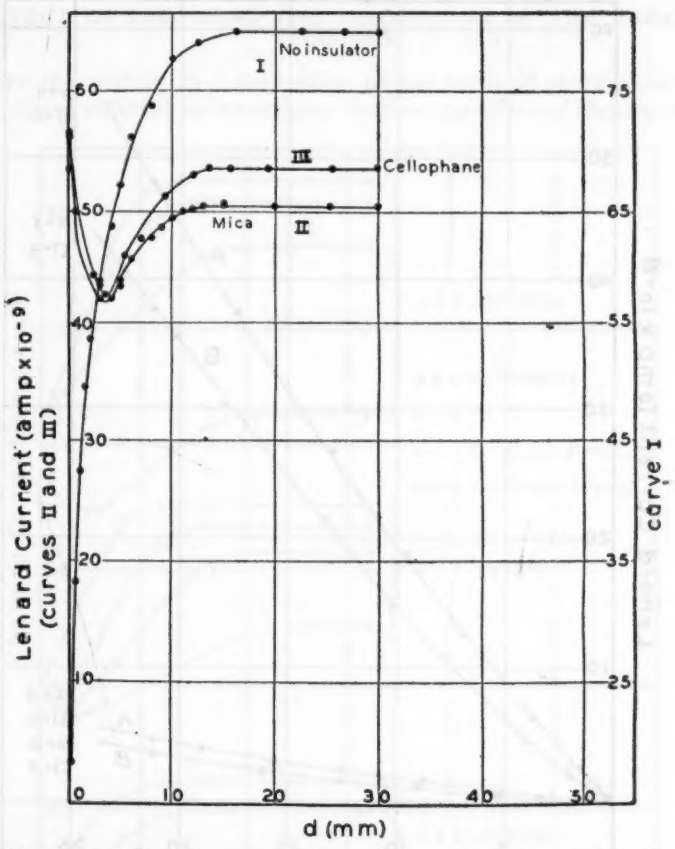

FIGURE 9.—*Lenard current as a function of the distance d for different dielectrics between the aluminum collector window and plunger*

in Figure 9 the Lenard current I_L for $d = 0.02$ mm. is very small, but increases rapidly to a complete value several fold larger at $d = 20$ mm.

To reproduce Thaller's method more closely, the alumium foil was backed with a mica sheet 0.015 mm thick to serve as a solid dielectric in place of the air, and the collector F then placed in close contact with the mica. Curve II in Figure 9 shows the Lenard current I_L as a function of d, whence it is seen that the complete value of I_L for this particular case is some 12 per cent lower than the plate ($d = 0$). It is also noticed that the intermediate current I_L passes through a minimum, as in the case of the open Faraday chamber. Curve III taken with a 0.027 mm layer of cellophane in place of the mica shows

a similar curve—reaching a minimum and complete value for exactly the same values of d. It should be pointed out that the equal values of I at the minimum is accidental and, in general, will differ for different thicknesses of the dielectric. Also the ratio of plate to complete value of I_L will vary with the dielectric thickness used.[14]

Contrary to the case of the open plate, the plate and complete currents are not linear functions of the tube current. Plotting, as in

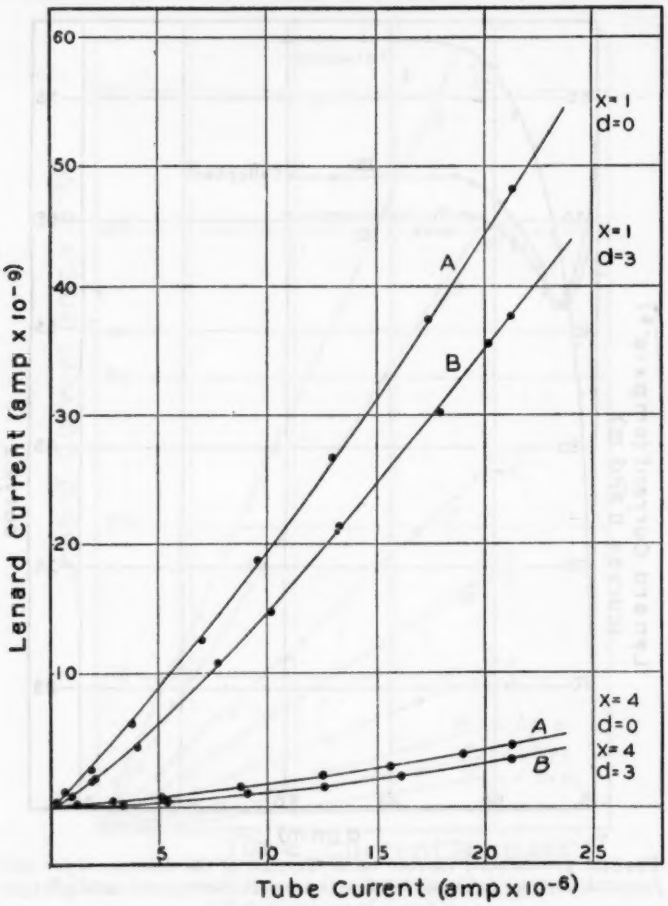

FIGURE 10.—*Lenard current as a function of the tube current for the condenser collector*

The ratio between curves A and B are the same only for the same values of the tube current; x and d are indicated in centimeters.

Figure 8, I_L, against the total tube current (as the filament current is varied) the curves shown in Figure 10 are obtained; curve A with $d=0$ and curve B with $d=30$ mm. The ratio is found to vary, however, but slightly as I_L increases. Compared, however, with the Faraday chamber or open plate method, the varying ratio eliminates

[14] It might be mentioned that whereas a single sheet of mica has lasted throughout these experiments, cellophane turns yellow and becomes very fragile with a few hours' use at the current densities here employed. As a result a new sample was used for each set of observations with the result that slight discrepancies exist between the curves.

the possibility of reliably determining Lenard currents by Thaller's method. This behavior is to be expected since in the condenser method, electrons will pass through the dielectric at various angles, the absorption in the material will depend upon the degree to which the electrons have a velocity normal to the collector. This will vary with the ionization density in front of the tube, which in turn will vary with the tube emission.

6. EFFECT OF CHANGING THE DIMENSIONS OF THE FARADAY CHAMBER

Before proceeding to a discussion of the form of the curves found above, it is of interest to investigate further the effect of the dimensions

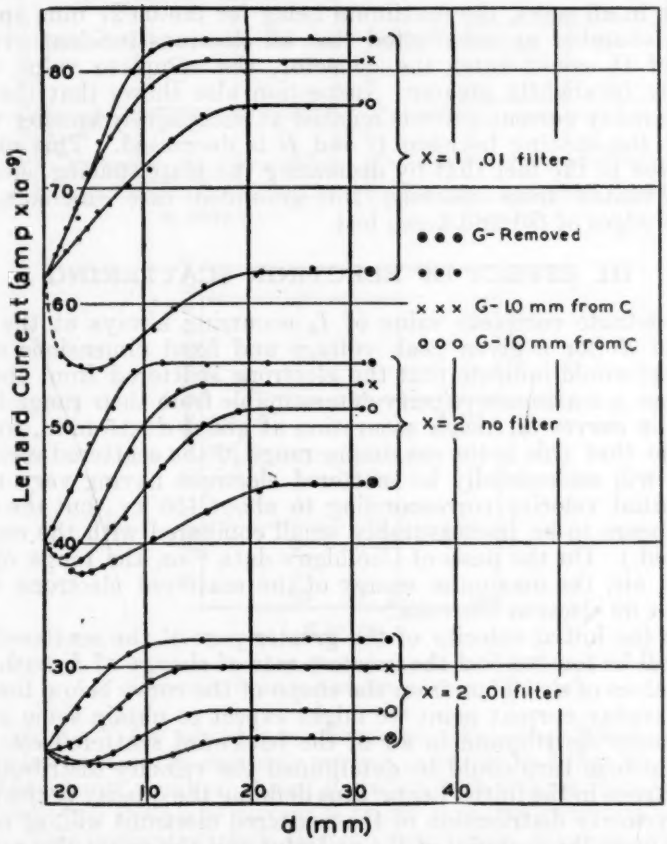

FIGURE 11.—*Lenard current as a function of d for various filters and for various positions of the diaphragm G. (fig. 3). Small solid dots represent G–0027 mm from C*

of the Faraday chamber upon the current measurements. Having found the effect of varying d, that of changing the position of the inner diaphragm G (fig. 3) with respect to the front cover C, using two different qualities of Lenard radiation and two distances x between Lenard tube and Faraday chamber, was sought. The radiation quality was changed by placing a 0.01 mm aluminum filter in the

beam at distances of 3 and 13 mm from O_2 the corresponding positions of the chamber being $x=10$ mm and $x=20$ mm, respectively. In both cases the current I_L to the Faraday cylinder was measured as a function of the displacement d of the collector. The spacing between the plates G and C (fig. 3) was made 10, 1, and 0.027 mm (held apart by a cellophane spacer near the periphery), and G removed entirely.

The resulting curves are given in Figure 11 and need little explanation. In all cases, the curves for G removed have a very much lower complete value than where it is in place. This is to be expected, since a large number of the electrons scattered from the chamber will strike the outer grounded cover C and not become a part of the collector current except for the few rescattered to the wall D of the chamber. As the plate G is moved closer to C the complete currents increase in all cases, the maximum being for the 0.027 mm. spacing. With a chamber so constructed that all electrons incident over the plane of O_2 could enter the collector, the complete value would probably be slightly greater. Inspection also shows that the complete Faraday current point is reached at successively smaller values of d as the spacing between C and G is decreased. This may be attributed to the fact that by decreasing the plate spacing, electrons are prevented from reaching the grounded case (including the beveled edges of O_2) and being lost.

III. EFFECT OF ELECTRON SCATTERING

The definite complete value of I_L occurring always at the same value of d (for a given peak voltage and fixed dimensions of the chamber) would indicate that the electrons scattered from the face of F have a maximum velocity determinable from their range in air. Since the curves all reach saturation at about $d=15$ mm., we may conclude that this is the maximum range of the scattered electrons. (There will undoubtedly be scattered electrons having very nearly their initial velocity corresponding to about 150 kv., but the quantity appears to be immeasurably small compared with the currents here used.) On the basis of Coolidge's data [15] on the range of electrons in air, the maximum energy of the scattered electrons would be about 60 electron kilovolts.

Since the initial velocity of the greater part of the scattered electrons will be low we find the greatest rate of change of I_L with d for small values of d. Thus from the shape of the curve below the complete Faraday current point we might expect to obtain some idea of the velocity distribution in air of the backward scattered electrons, from which in turn could be determined the velocity distribution of the electrons in the initial beam, thus defining the quality of the beam.

The velocity distribution of the scattered electrons will, of course, depend upon the material of the collector and the quantities actually measured will, in addition, depend upon the surrounding walls where rescattering occurs. Thus the quantity measured is the net result of a differential scattering. This is indicated by some of the curves in Figure 12, where I_L is plotted as a function of d. Group A was obtained using gold (atomic number $Z=79$), tin ($Z=50$), and aluminum ($Z=13$) as thin covers over the opening O_2. These covers had

[15] W. D. Coolidge, J. Frank. Inst., 202, p. 693; 1926.

different thickness and were themselves covered on the outer side by 0.027 mm. cellophane so that the absolute values of I_L are not comparable. The collector F was brass (Z about 30) as used heretofore. Electrons scattered from F are in part rescattered from and in part absorbed by the window.

Curve 1 for a gold window gives a very high plate current. Curve 2 for tin is similar in this respect, though relatively smaller than for

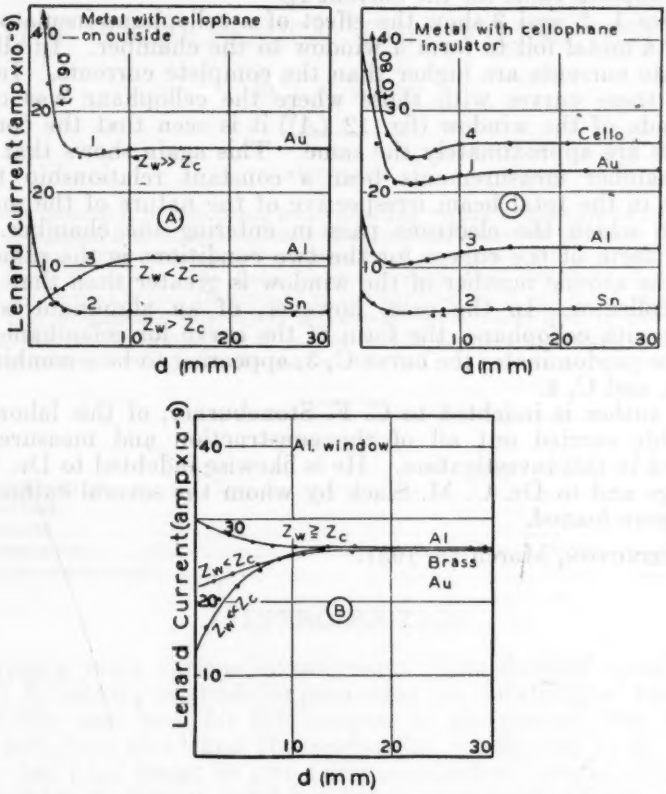

FIGURE 12.—*Curves showing effect on the measured Lenard current of different collector window and plunger materials*

gold. Curve 3 for aluminum shows, on the other hand, a plate current lower than the complete current; and, we find that, in general, when the atomic number, Z_W, of the window is greater than that, Z_C, of the collector the plate current is larger than the complete and vice versa. This indicates that the net scattering reverses with the relative position of the scatterers in the atomic number scale.

To check this as it affects the type of measurements here involved the curves in group B were obtained which seem to support this view. Here the window was of aluminum in all cases while the face of the collector F was covered successively with aluminum, brass, and gold. The relative plate and complete values of I_L occur in an order which is the reverse of that shown by curves A. The slight increase in the case of two aluminum scatterers may be attributed

to a small amount of brass exposed by the beveled edges under the aluminum window.

With a cover of cellophane or mica over O_2, the complete value of the current is less than the plate, and hence does not obey the relationship to atomic numbers found for the metal foils. Curve 4 in group C, showing the variation of I_L with d, for a cellophane window over the Faraday chamber, is seen to give a higher plate than complete value for the current I_L.

Curves 1, 2, and 3 show the effect of a cellophane insulator used behind a metal foil to form a window to the chamber. In all cases the plate currents are higher than the complete currents. In comparing these curves with those where the cellophane was on the outer side of the window (fig. 12 (*A*)) it is seen that the complete currents are approximately the same. This again shows that Faraday chamber measurements bear a constant relationship to the current in the total beam irrespective of the nature of the material through which the electrons pass in entering the chamber. The general form of the curves for the two conditions is the same only when the atomic number of the window is greater than that of the brass collector. In the case, however, of an aluminum window backed with cellophane, the form of the curve for cellophane alone seems to predominate; the curve C, 3, appearing to be a combination of A, 3, and C, 4.

The author is indebted to C. F. Stoneburner, of this laboratory, who ably carried out all of the construction and measurements involved in this investigation. He is likewise indebted to Dr. W. D. Coolidge and to Dr. C. M. Slack by whom the several cathode-ray tubes were loaned.

Washington, March 15, 1931.

A NEW TEST FOR PREDICTING THE DURABILITY OF VARNISHES

(THE PHOTOCHEMICAL EMBRITTLING TEST)

By J. H. Wilson

ABSTRACT

The test described in this paper for evaluating varnishes consists in two operations. A varnish film is first exposed to an intense source of light for a definite period of time, after which it is bent double at a prescribed temperature over a rod of fixed diameter. The data presented show that the more durable the varnish, the longer it may be exposed to the light before it will crack on bending. This text possesses a number of advantages over those now in use for this purpose, due to the simplicity of preparing the samples and making the test, and the speed with which results can be obtained.

CONTENTS

		Page
I.	Introduction	73
II.	Method	74
III.	Results	75
IV.	Conclusions	82
V.	Acknowledgment	83

I. INTRODUCTION

In recent years various investigators [1] have devoted considerable time to developing methods for predicting the durability of varnishes. The two tests used for this purpose at the present time are the kauri reduction test [2] and the accelerated weathering cycle. [3] The former has been found to give fairly satisfactory results when comparing the same type of varnishes, but is not suitable for the comparison, for instance, of a varnish made from a natural resin with one made from a synthetic resin. Came's [4] results show that little correlation exists between the durability of spar varnishes when exposed outdoors and their durability in the accelerated weathering cycle which has been used almost exclusively at this laboratory for paints. This cycle consists in a continuous exposure to a carbon arc light and subjection to a water spray every 20 minutes. How-

[1] See Bibliography in the paper Durability Tests of Spar Varnishes, by C. L. Came, B. S. Jour. Research 4, p. 247; 1930.

[2] The kauri reduction test consists in determining the maximum amount of kauri solution which can be added to the varnish, so that after baking a film of this mixture on metal and cooling it will show no cracks on bending over a 3 mm (one-eighth inch) rod. For a full description of this test, see A. S. T. M. Standards, Pt. II, p. 358; 1930.

[3] The accelerated weathering cycle consists in exposing the varnishes to conditions simulating actual outdoor weathering, but much more severe; as intense light, water, cold, etc., so that failure can be made to occur quickly. A typical cycle is described by Came. (See paper referred to in footnote 1.)

[4] See footnote 1.

ever, it is probable that by changing the cycle as has been done by W. R. Fuller [5] results more in accord with outdoor weathering could be obtained.

The opinions of a number of manufacturers and consumers of paint and varnish in regard to the kauri reduction test and the accelerated weathering test are expressed in the replies to a questionnaire [6] sent out by a committee of the Cincinnati-Dayton-Indianapolis Paint and Varnish Production Club. All of these replies agree that neither of these tests gives completely satisfactory results, although some indicate that under certain conditions the results are satisfactory in comparing materials of the same type.

It is the purpose of this paper to describe a new method, which may be termed the photochemical embrittling test, for evaluating the durability of varnishes and to give some results which show the correlation between this test and actual weathering.

II. METHOD

The new method takes one feature from each of the two tests already described. First, the varnish films are exposed to an intense source of light, as is done in the accelerated weathering cycle, causing the photochemical embrittling, and second, the films are tested for the degree of brittleness as is done in the kauri reduction test, by bending the varnish-coated panel over a mandrel.

In detail, the test is carried out in the following steps:

1. The varnish sample is flowed on a terneplate strip. (A size of 35 by 2.5 by 0.03 cm or 14 by 1 by 0.012 inch has been found to be satisfactory.)
2. The varnish is allowed to dry in an inclined position so that the excess will flow off.
3. The 14-inch strips are cut into short chips of about 1¼ to 1½-inch length, which are appropriately marked on the back.
4. The cut strips are placed in a suitable holder, which may be made from a strip of metal about 2 inches wide and long enough to extend around the tank surrounding the carbon arc light. About one-quarter inch of one side is bent through 180° thereby forming a pocket for the chips. This holder is situated directly opposite the center of the carbon arc light and about 15 inches from it. The apparatus is the same as that used in the accelerated weathering cycle described by Walker and Hickson.[7]
5. Every hour a chip of each varnish is removed from the light, cooled to a standard temperature, and bent double over a 3 mm. (one-eighth inch) rod.
6. The chips are examined closely for signs of failure.

Two distinct types of failure have been found to occur on bending the specimens in this test. Some varnishes failed by showing long easily visible cracks of the kind obtained in the kauri reduction test. Other varnishes failed by a change which has been called whitening in

[5] H. A. Gardner, Physical and Chemical Examination of Paints, Varnishes, Lacquers and Colors (5th ed.), p. 408; 1930; Institute of Paint and Varnish Research, Washington, D. C.

[6] The Evaluation and Compilation of the Methods Used in Accelerated Testing of Protective Coatings. Cincinnati-Dayton-Indianapolis Production Men's Club. Am. Paint & Varnish Mfrs. Assoc. Circ. No. 370, pp. 548-564; Am. Paint J., **14**, No. 52C, p. 25; Paint, Oil & Chem. Rev., **90**, No. 18, pp. 14-17; Oil, Paint & Drug Reporter, **118**, No. 19, pp. 63-4; 1930.

[7] P. H. Walker and E. F. Hickson, Accelerated Tests of Organic Protective Coatings, B. S. Jour. Research, **1**, p. 2; 1928.

this paper. This whitening is probably caused by the formation of a great many cracks, so fine that they can not be resolved by a microscope magnifying about 75 diameters. An apt comparison might be made to the bending of glass. At ordinary temperatures the glass will crack and shatter; at temperatures near the melting point it can be bent and still will remain clear and transparent; however, at an intermediate temperature the glass can be bent, but in so doing, it ceases to be transparent and reflects the light from countless newly formed surfaces, thus giving the whitened appearance.

In general, the poorest varnishes show no whitening but only the long visible cracks which on longer exposure shatter on bending. The better varnishes first become whitened and after some hours begin to crack. The condition grows steadily worse until they finally shatter. After a number of hours of light exposure the best varnishes begin to whiten. This effect gradually becomes worse and some cracking may occur after a very long exposure.

It is always desirable to run a standard varnish whose durability outdoors and elasticity after exposure to light are known along with the samples being tested, as a precaution against unknown variations, such as solarization of the glass chimney, slight changes in the radiation of the arc, possible changes in conditions at the time of bending, etc.

The only costly piece of apparatus required in this method is the carbon arc weatherometer light. It has been found possible to substitute an ordinary incandescent mazda light for the carbon arc, although a much longer exposure is required to give the same results. This comparison will be shown later in this paper.

A very useful accessory apparatus is a cabinet for obtaining any desired temperature for bending the strips. The cabinet in use in this laboratory is constructed of double windows on all sides with about three-eighths inch dead air space between the outer and inner windows. In the front of the cabinet is a board having two 6-inch holes to accommodate the operator's arms when working in the cabinet. Each hole is provided with a collapsible sleeve of insulating material so that when the arms are withdrawn, the openings can be closed. The desired temperature is obtained by running cold or hot water through a copper radiator inside the cabinet and by circulating the air with an electric fan. No difficulty is experienced in getting a temperature 10° C. below that of the room. The humidity may also be fixed, if desired, by introducing an open vessel containing a saturated salt solution of definite vapor pressure.

III. RESULTS

The type of results obtained is illustrated by tests of a set of seven varnishes submitted through the courtesy of W. R. Fuller, of the Pratt & Lambert Co., who also furnished us with their composition, kauri reduction values, and approximate outdoor durabilities. These data are given in Table 1. In order to insure an unbiased judgment, this latter information was withheld until after the completion of the tests. From the results shown in run 1 of Table 1 the varnishes were arranged in the following order: 1, 2, 3, 6, 4, 5, 7, while the order obtained from Mr. Fuller was 1, 2, 3, 4, 5, 6, 7 or, in other words, the photochemical embrittling test gave the cor-

rect order with the exception of No. 6, which was placed too low in the scale.

As stated previously the temperature at which the bending is done greatly affects the degree of cracking. This fact can be utilized to advantage by lowering the temperature of bending when it is desired to speed up a determination, as in the case of very good varnishes which do not fail in a working day, or to get an approximate idea of the number of hours that will be required before cracks will start to occur on bending at the specified temperature. This eliminates considerable useless work required in bending and examining very good varnishes in the early stages. Testing at approximately 0° C. can be done conveniently by placing the varnish specimen on a lump of ice in a closed container with the varnish side up, and after 15 or 20 minutes removing the chip and bending immediately. The results of the test made on the seven varnishes are given in run 2, Table 1 for comparison with run 1, Table 1. It will be noticed that in this determination varnish No. 6 falls in its correct position between No. 5 and No. 7.

Although the carbon arc light has been found to be satisfactory, it is quite expensive, and is now used by only a comparatively few laboratories. To make the test more available the substitution of mazda lamps for the carbon arc was tried out on the same seven varnishes. The results are shown in runs 3 and 4 of Table 1.

TABLE 1.—*Typical photochemical embrittling tests showing the effect of varying the temperature of bending and the type of lights*

Varnish No.	Run 1. A typical photochemical embrittling test									Run 2. Showing the effect of lowering the temperature of bending			Run 3. Showing the effect of substituting a 1,000-watt mazda light for the carbon arc				
	Hours in carbon arc light before bending at 22° C.									Hours in carbon arc light before bending at approximately 0° C.			Hours in mazda light before bending at 22° C.				
	0	1	2	3	4	5	6	7	8	0	2	4	3	20	26	44	68
1	O. K.	C_6	C_6	C_8	----	----	----	----	----	C_6	C_8	----	C_6	C_8	----	----	----
2	O. K.	C_2	W_6C_2	C_7	C_8	----	----	----	----	C_6	C_8	----	O. K.	C_6	C_8	----	----
3	O. K.	O. K.	W_3	W_4	W_7	W_7C_3	W_8C_6	----	----	C_3	W_7C_4	W_8C_5	O. K.	O. K.	C_1	C_5	C_5
4	O. K.	O. K.	W_1	W_3	W_3	W_6	W_7	W_8	----	O. K.	C_4	W_8C_5	O. K.	O. K.	O. K.	C_2	C_2
5	O. K.	O. K.	O. K.	O. K.	W_2	W_6	W_6	W_5	W_6C_5	O. K.	W_4	W_7	O. K.	O. K.	O. K.	O. K.	O. K.
6	O. K.	O. K.	W_2C_2	W_3C_2	W_6	W_6	W_6	W_3	----	O. K.	W_4	W_6	O. K.	O. K.	O. K.	O. K.	O. K.
7	O. K.	O. K.	W_2	W_2	W_4	W_5	W_5	W_5	W_6	O. K.	W_4	W_5	O. K.	O. K.	O. K.	O. K.	O. K.
	Strips were placed 15 inches from the light. The temperature registered by a thermometer next to the strips was 56° C.												Strips were placed 8 inches from the light. The temperature registered by a thermometer next to the strips was 60° C.				

TABLE 1.—*Typical photochemical embrittling tests showing the effect of varying the temperature of bending and the type of lights*—Continued

Varnish No.	Run 4. Showing the effect of substituting a 150-watt mazda light for the carbon arc					Compositions, kauri reductions and durabilities of the varnishes				
	Hours in mazda light before bending									
	Bent at 22° C.			Bent at −5° C.	Bent at 17° C.	Oil per 100 pounds of resin	Kind of oil	Kind of resin	Kauri reduction	Durability
	41 hours	65 hours	89 hours	113 hours	137 hours					
						Gallons			*Per cent*	*Months*
1	C_4	C_4	C_4	C_8	C_8	46.3	Tung	Rosin	40	3
2	C_2	C_2	C_2	C_8	C_8	45.8	do	Rosin and a small proportion of ester gum	50	3½
3	O. K.	O. K.	O. K.	C_8	C_8	45.5	do	60 per cent rosin 40 per cent ester gum	70	4
4	O. K.	O. K.	O. K.	C_8	C_2	49.25	Linseed and tung	Ester gum and a smaller amount of rosin	90	6½
5	O. K.	O. K.	O. K.	C_8	O. K.	63.3	Similar to No. 4, but containing additional linseed oil		120	8
6	O. K.	O. K.	O. K.	C_2	O. K.	50	Tung	Phenolformaldehyde resin	100	11
7	O. K.	O. K.	O. K.	O. K.	O. K.	50	do	Slightly more durable phenolformaldehyde resin than No. 6.	165	18+
	Strips were placed 7 inches from the light. The temperature registered by a thermometer next to the strips was 34° C.					The outdoor durability data refer to roof exposures at Buffalo, N. Y., at an angle of 45° facing south and are average figures for exposures at different periods of the year				

NOTE.—The letters C and W refer to cracking and whitening, respectively. The subscripts 1 to 8 refer to the degree of failure as follows: 1, Trace; 2, slight; 3, some; 4, definite; 5, considerable; 6, bad; 7, very bad; 8, shattered.

Here again it will be seen that the test has placed the varnishes in their correct order, although bending at a low temperature had to be resorted to in order to cause the best varnishes to fail. The time required for failure to occur is many times that required with the carbon arc. Since the 1,000-watt mazda produced a temperature near the samples which was slightly higher (4° C.) than that produced by the arc, the embrittlement of the film is not caused merely by heat. It is probably the effect of a photochemical reaction caused by a certain range of wave lengths in which the arc used had a much greater intensity than the 1,000-watt mazda lamp. The difference between the effects of the two mazda lamps is undoubtedly caused mainly by the difference in intensity of the light from the two sources, rather than a difference in spectral distribution.

The following suggested procedure might well be used in arranging a given set of varnishes in the order of their durabilities. The chips are placed in the carbon arc light and at the end of the first hour two chips of each varnish are removed. One of these chips is bent at a low temperature, say, 0° C.; the other is bent at a temperature near that of the room but preferably below 25° C. Those varnishes that crack at 0° C. are classed as poorer than those that only whiten or show no sign of failure. Thereafter the poorer varnishes by this separation are bent only at the higher temperature and are rated according to the number of hours of light exposure required before they crack. The better varnishes are bent at 0° C. until they crack and are rated by the same method. To get a finer distinction it may be necessary to select some other temperature for bending.

To illustrate the reliability of this test in rating the durabilities of a large number of varnishes, some representative results will be given. In Figure 1 are shown the results obtained with a set of 42 spar varnishes by the three quick tests [8] in comparison with the durability on outdoor exposure. The arrangement of the varnishes in the order of increasing durability shows a good distribution in the range of exposure of from 28 to 141 days before the varnish became definitely checked. This end point was considered to have been reached when checks all over the panel could easily be seen with the naked eye. The number of hours of sunshine rather than the number of days was chosen as ordinate, as this tends to eliminate discontinuities due to changes in climatic conditions. Obviously, the order of failure will be the same in both cases.

It is evident that the reliability of any test for determining durabilities should be measured by the degree with which the results obtained follow the course of those obtained by outdoor exposure. When the samples are plotted in the same order, as is done in Figure 1, the curve for each test should rise gradually from left to right. With a few exceptions this general trend is apparent in the photochemical embrittling test and the kauri reduction test, but no such relation exists for the accelerated cycle used, which consisted of exposure to a continuous carbon arc light and an intermittent water spray every 20 minutes.

By an inspection of Figure 1, it will be seen that, in general, the poorest varnishes failed by cracking only, the best varnishes failed

[8] C. L. Came, formerly of this laboratory, made the observations and determinations of the roof exposure, the kauri reduction, and the accelerated weathering cycle test.

by whitening only while the intermediate ones exhibited both types of failure.

This observation is utilized in rating the 50 varnishes of the set reported by Came.[9] These varnishes were classified into five groups as shown in Figure 2 ranging from those which failed by cracking only to Nos. 32 and 39 which showed no cracking or whitening on bending after an exposure to the light for 13 hours. Each group is divided into subgroups, underscored by a solid line, which are so similar in the embrittling test that it is impractical to try to differ-

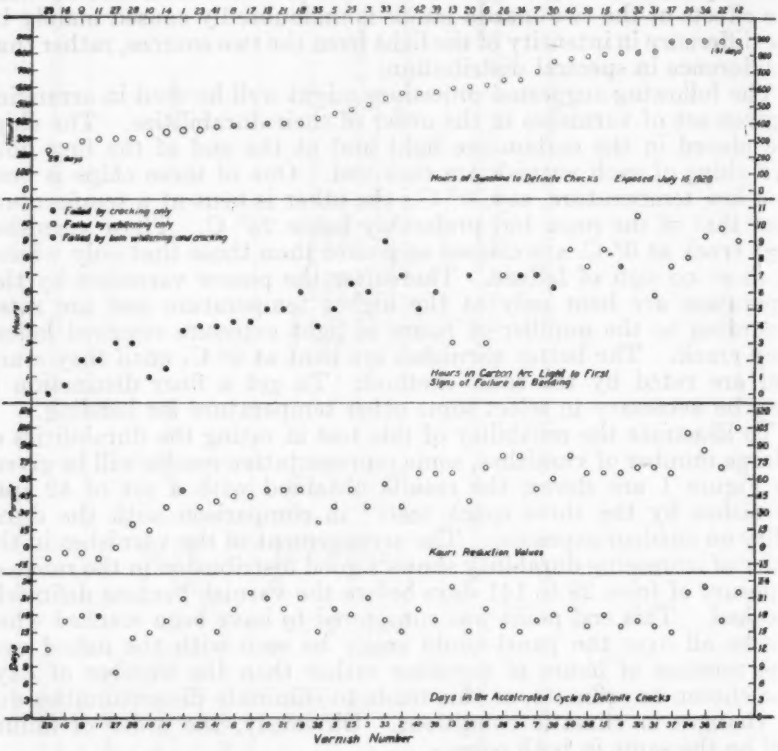
Hours of Sunshine to Definite Checks Exposed July 16 1928
Failed by cracking only
Failed by whitening only
Failed by both whitening and cracking
Hours on Carbon Arc Light to First Signs of Failure on Bending
Kauri Reduction Values
Days in the Accelerated Cycle to Definite Cracks
Varnish Number

FIGURE 1.—*A comparison of the reliability of the photochemical embrittling test, kauri reduction, and the accelerated weathering cycle for the prediction of the durability of spar varnishes*

entiate between them. However the subgroups themselves can be graded in the order indicated. As may be seen from the figure, the results of the photochemical embrittling test correspond rather well with the order of outdoor durability. Unfortunately the majority of the varnishes selected for this test had approximately the same durability instead of differing in fairly even increments as is the case in Figure 1. This made a differentiation in this region difficult and likewise rather immaterial. However, these results are included since the durabilities of the varnishes have been published previously.

[9] See footnote 1, p. 73.

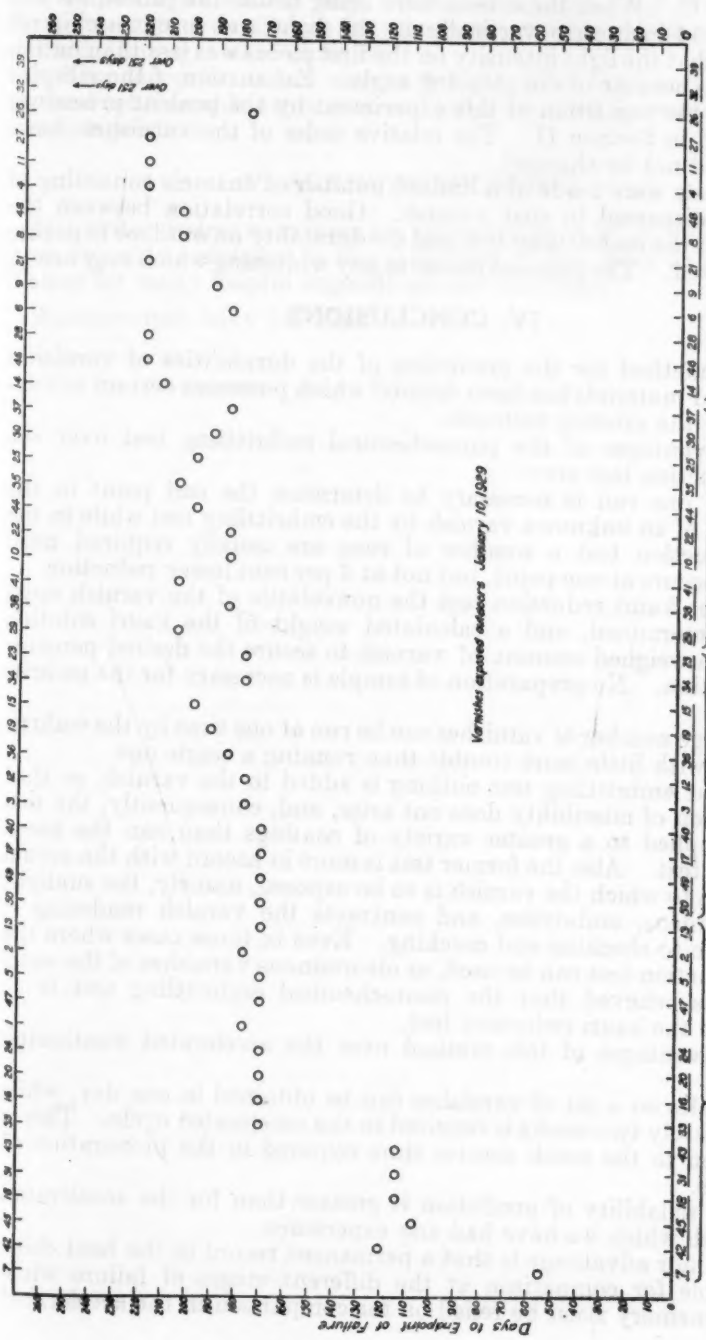
Over 251 days
Over 122 days
Varnishes exposed outdoors January 10, 1929
Days to Endpoint of Failure
Failed by cracking only
Failed mainly by cracking but some whitening
Failed mainly by whitening but some cracking
Failed by whitening only
O.K.
Varnish Number

FIGURE 2.—*A set of 50 spar varnishes arranged in the order of increasing durability by the photochemical embrittling test compared with their outdoor durabilities*

The bending of the varnish strips in both of these sets was done at 24° to 25° C. When these tests were being made, the procedure was to hang a 14-inch strip vertically in the light and to cut a chip off hourly so that the light intensity on the first pieces was less than on the later pieces because of the glancing angle. Exhaustion of the samples prevented the repetition of this experiment by the present procedure as outlined in Section II. The relative order of the varnishes, however, would not be changed.

Some tests were made of a limited number of enamels consisting of pigments dispersed in spar varnish. Good correlation between the cracking in the embrittling test and the durability on outdoor exposure was observed. The pigment obscures any whitening which may occur.

IV. CONCLUSIONS

A new method for the prediction of the durabilities of varnishes and related materials has been devised which possesses certain advantages over the existing methods.

The advantages of the photochemical embrittling test over the kauri reduction test are:

1. Only one run is necessary to determine the end point in the durability of an unknown varnish by the embrittling test while in the kauri reduction test a number of runs are usually required until cracking occurs at one point, but not at 5 per cent lower reduction.

2. In the kauri reduction test the nonvolatile of the varnish must first be determined, and a calculated weight of the kauri solution added to a weighed amount of varnish to secure the desired percentage reduction. No preparation of sample is necessary for the embrittling test.

3. A large number of varnishes can be run at one time by the embrittling test with little more trouble than running a single one.

4. In the embrittling test nothing is added to the varnish, so that the question of miscibility does not arise, and, consequently, the test can be applied to a greater variety of coatings than can the kauri reduction test. Also the former test is more in accord with the actual conditions to which the varnish is to be exposed, namely, the sunlight which hardens, embrittles, and contracts the varnish rendering it susceptible to checking and cracking. Even in those cases where the kauri reduction test can be used, as oleoresinous varnishes of the same type, it is believed that the photochemical embrittling test is as reliable as the kauri reduction test.

The advantages of this method over the accelerated weathering cycle are:

1. Results on a set of varnishes can be obtained in one day, while approximately two weeks is required in the accelerated cycle. This is in addition to the much shorter time required in the preparation of the panels.

2. The reliability of prediction is greater than for the accelerated cycles with which we have had any experience.

3. A minor advantage is that a permanent record in the bent chips is available for comparison at the different stages of failure while notes or memory must be relied on for comparison in the accelerated cycle.

The disadvantages of the photochemical embrittling test are:

1. It predicts checking only. While this is probably sufficient for varnishes, it is not sufficient for pigmented coatings which also fail by chalking, fading, loss of gloss, etc.

2. The end point is not always definite as in the kauri reduction test and considerable experience and judgment may be required for an accurate prediction.

V. ACKNOWLEDGMENT

The writer desires to express his appreciation to H. D. Bruce for his most valuable assistance in the early part of this work and to P. H. Walker for many helpful suggestions and criticisms.

WASHINGTON, May 14, 1931.

RP334

INTERPOLATION OF THE O. S. A. "EXCITATION" DATA BY THE FIFTH-DIFFERENCE OSCULATORY FORMULA

By Deane B. Judd

ABSTRACT

In order to compute the dominant wave length and purity of a color stimulus by means of the O. S. A. "excitation" data, two values must be obtained by interpolation. The adoption of the osculatory formula for this interpolation permits the computations to be made with perfect reproducibility. Each of the O. S. A. curves by this method is represented as a series of parabolas of the fifth degree which join at the values specified at every 10 mμ so as to have a common slope and curvature at the junction point. Interpolated values have been computed according to this formula for every millimicron.

Since 1922, colorimetric computation in America has been carried out mostly by means of the O. S. A. "excitation" data[1] in their extrapolated form.[2] In spite of the fact that these data are based on rather meager experimental measurements they represent the characteristics of the average normal eye with a satisfactory degree of approximation, and they have been used as the basis for extensive work in color standardization. In computing dominant wave length and colorimetric purity[3] by means of these data interpolated values are required, and have commonly been found from an interpolation graph.

It is not to be supposed, of course, that any form of interpolation, graphical or by formula, yields any information concerning the true course of the O. S. A. "excitation curves" between the specified points. Theoretically that course is wholly unspecified, and there are a large number of equally reliable curves to be drawn through the intervals. As in the case of the standard visibility function[4] it has been found convenient in the work of the National Bureau of Standards to adopt arbitrarily a single set of curves. The interpolated values adopted are found by a method superior to any graphical interpolation because the values may be reproduced at any time anywhere, and it is believed that the solution by fifth-difference, osculatory interpolation is more suitable than solutions by other formulas for interpolation because it combines continuity in function, in first derivative and in second derivative with considerable com-

[1] L. T. Troland, Report of Committee on Colorimetry for 1920-21, J. Opt. Soc. Am. and Rev. Sci. Inst., **6**, pp. 547-553; 1922.

[2] Spectrophotometry, Report of O. S. A. Progress Committee for 1922-23, J. Opt. Soc. Am. and Rev. Sci. Inst., **10**, p. 230; 1925.

[3] I. G. Priest, The Computation of Colorimetric Purity, J. Opt. Soc. Am. and Rev. Sci. Inst., **9**, pp. 503-520; 1924. D. B. Judd, The Computation of Colorimetric Purity, J. Opt. Soc. Am. and Rev. Sci. Inst., **13**, pp. 133-152; 1926.

[4] D. B. Judd, Extension of the Standard Visibility Function to Intervals of 1 Millimicron by Third-difference Osculatory Interpolation, B. S. Jour. Research, **6**, pp. 465-471; 1931.

putational convenience. Indeed, the ease of applying this method is so great that the labor involved is not much greater than that of the graphical method.

If λ be the wave length in millimicrons, λ_0, the value of the wave length at the beginning of the 10 mμ interval within which $f(\lambda-\lambda_0)$ is to be defined by interpolation, and if $\Delta_1 f(-20)$, . . . $\Delta_5 f(-20)$ be the five leading major differences, then the fifth-difference, osculatory interpolation formula may be written:

$$f(\lambda-\lambda_0)=f(-20)+k_1\Delta_1 f(-20)+k_2\Delta_2 f(-20)+k_3\Delta_3 f(-20)$$
$$+k_4\Delta_4 f(-20)+k_5\Delta_5 f(-20),\ \lambda_0<\lambda<\lambda_0+10$$

where the coefficients, k_1 to k_5, applied to the leading major differences are defined:

$$k_1\equiv(\lambda-\lambda_0+20)/10$$
$$k_2\equiv(\lambda-\lambda_0+20)\ (\lambda-\lambda_0+10)/200$$
$$k_3\equiv(\lambda-\lambda_0+20)\ (\lambda-\lambda_0+10)\ (\lambda-\lambda_0)/6{,}000$$
$$k_4\equiv(\lambda-\lambda_0+20)\ (\lambda-\lambda_0+10)\ (\lambda-\lambda_0)\ (\lambda-\lambda_0-10)/240{,}000$$
$$k_5\equiv(\lambda-\lambda_0)^3\ (\lambda-\lambda_0-10)\ (5\lambda-5\lambda_0-70)/2{,}400{,}000$$

This formula is another form of that derived in 1880 by Sprague.[5] Sprague's formula was restated in nearly the form used above by Karup [6] 20 years later who used, however, three of the central differences in place of three of the leading differences which we have used here with appropriate changes in the coefficients of these differences. Since this formula, applied interval by interval, yields a series of parabolas which join at the specified points so as to have common slopes and osculating circles at the junction points, it was called by Karup a formula for osculatory interpolation. Osculatory interpolation has attracted some attention [7] since its discovery, and, indeed, has been extensively used in the construction of the United States Life Tables.[8] Probably the best general treatment of osculatory interpolation is due to Glover.[9]

Although the formulas for osculatory interpolation have usually been applied in the past by computing the leading minor differences (that is, values which would be obtained by differencing the desired, evenly spaced, interpolated values) from the leading major differences, and then deriving the desired interpolated values by continuous addition, the interpolation of the O. S. A. "excitation" data has been accomplished by finding for each value the products indicated in the formula and actually taking their sum. With a computing

[5] T. B. Sprague, Explanation of a New Formula for Interpolation, J. Inst. Actuaries, **22**, pp. 270-285; 1880.

[6] J. Karup, On a New Mechanical Method of Graduation, Trans. Second International Actuarial Congress, p. 82; 1899.

[7] George King, On the Construction of Mortality Tables from Census Returns and Records of Deaths, J. Inst. Actuaries, **42**, pp. 238-246; 1908. James Buchanan, Osculatory Interpolation by Central Differences; with an Application to Life Table Construction, J. Inst. Actuaries, **42**, pp. 369-394; 1908. See also an appendix by G. J. Lidstone, Alternative Demonstration of the Formula for Osculatory Interpolation, pp. 394-397. George King, On a New Method of Constructing and of Graduating Mortality and Other Tables, J. Inst. Actuaries, **43**, pp. 109-184; 1909

[8] J. W. Glover, United States Life Tables, 1890, 1901, 1910, and 1901-1910, pp. 344-347, 372-388; 1921.

[9] J. W. Glover, Derivation of the United States Mortality Table by Osculatory Interpolation, Quarterly Publications of the American Statistical Association, **12**, pp. 87-93; 1910.

machine it was found possible to obtain nine interpolated values and to check them by an independent method in about 20 minutes;[10] it seems doubtful whether the continuous addition method would be much more expeditious.

We take, then, $\lambda-\lambda_0$ equal in succession to 1, 2 . . . 9, and $f(\lambda-\lambda_0)$ interval by interval equal to ρ_0, γ_0 and β_0 in succession, where ρ_0, γ_0, and β_0 are the O. S. A. "excitation curves" as extrapolated by Priest and Gibson.[11]

Table 1 shows by an example how to compute the leading, descending, major differences. We have taken $f(\lambda-\lambda_0)$ equal to ρ_0, and λ_0 equal to 580 mμ. The leading, descending, major differences appear in the first row.

Table 2 shows by the same example the computation of the leading ascending, major differences which were used in an independent check on the computation; the leading, ascending, major differences appear in the first row of this table.

Table 3 gives the values of the coefficients, k_1 to k_5, for $\lambda-\lambda_0$ equal to 1, 2, . . . 9.

Table 4 shows the details of the computation of the interpolated values according to the fifth-difference formula for the same interval and function referred to in Tables 1 and 2. The check by means of the ascending differences is also given for this interval and function.

Table 5 gives the results of these computations for ρ_0, γ_0, and β_0.[12] Since there was some rejection error in writing down the products (for example, the coefficients, k_1 to k_5, given in Table 3 were taken to the nearest fourth decimal), the values given in Table 5 are not quite what would be found by rigorous evaluation according to the formula for fifth-difference osculatory interpolation; they may be taken as correct, however, to within 3 in the second decimal. The values of Table 5 were further checked for clerical errors by computing the first and second minor differences.

TABLE 1.—*Computation of the leading descending major differences,* $\lambda_0 = 580$ mμ

$\lambda-\lambda_0$ in mμ	λ in mμ	$f(\lambda-\lambda_0)=\rho_0$	$\Delta_1\rho_0$	$\Delta_2\rho_0$	$\Delta_3\rho_0$	$\Delta_4\rho_0$	$\Delta_5\rho_0$
−20	560	466	+39	−24	+24	−64	+121
−10	570	505	+15	0	−40	+57	
0	580	520	+15	−40	+17		
10	590	535	−25	−23			
20	600	510	−48				
30	610	462					

[10] The check was carried out by taking the differences in the ascending order rather than in the descending order as indicated in the formula. See Tables 2 and 4. It might naturally be supposed that about twice the time to calculate nine values would be required to calculate and check them by an independent method, but this is not quite the case. The time actually required is considerably less than twice because the products found for checking the values in one interval may be used to calculate values in the four subsequent intervals.

[11] See footnote 2, p. 85. The values referred to here are included in Table 5 along with the values obtained from them by interpolation.

[12] The values for ρ_0 from 451 to 459 and from 461 to 469 mμ result from substituting in the formula $f(-20)$ equal to 4 and 1, respectively; that is, we have taken ρ_0 for 430 and 440 mμ equal to ρ_0 for 470 and 460 mμ, respectively, instead of zero as shown in Table 5. This choice was made in order to bring the interpolated function to zero at 450 mμ with a zero slope; then, for λ less than 450 mμ, ρ_0 is arbitrarily set at zero instead of at the values which would be obtained by mechanical application of the formula. Similarly for β_0 between 590 and 610 mμ, we choose β_0 in the formula as 1 and 2 for 620 and 630, respectively, although β_0 is given in Table 5 as zero for wave lengths greater than 610 mμ.

TABLE 2.—*Computation of the leading ascending major differences,* $\lambda_0 = 580\ m\mu$

$\lambda-\lambda_0$ in $m\mu$	λ in $m\mu$	$f(\lambda-\lambda_0)=\rho_0$	$\nabla_1\rho_0$	$\nabla_2\rho_0$	$\nabla_3\rho_0$	$\nabla_4\rho_0$	$\nabla_5\rho_0$
30	610	462	+48	−23	−17	+57	−121
20	600	510	+25	−40	+40	−64	
10	590	535	−15	0	−24		
0	580	520	−15	−24			
−10	570	505	−39				
−20	560	466					

TABLE 3.—*Coefficients,* k_1 *to* k_5*, for interpolation to tenths by fifth-difference osculatory interpolation*

$\lambda-\lambda_0$	k_1	k_2	k_3	k_4	k_5
1	+2.1	+1.155	+0.0385	−0.0086625	+0.00024375
2	+2.2	+1.320	+.0880	−.0176000	+.00160000
3	+2.3	+1.495	+.1495	−.0261625	+.00433125
4	+2.4	+1.680	+.2240	−.0336000	+.00800000
5	+2.5	+1.875	+.3125	−.0390625	+.01171875
6	+2.6	+2.080	+.4160	−.0416000	+.01440000
7	+2.7	+2.295	+.5355	−.0401625	+.01500625
8	+2.8	+2.520	+.6720	−.0336000	+.01280000
9	+2.9	+2.755	+.8265	−.0206625	+.00759375

TABLE 4.—*Example of interpolation to tenths by the fifth-difference osculatory formula, descending differences; check by ascending differences*

Take $\lambda_0=580$ mμ, and f $(\lambda-\lambda_0=\rho_0$; then from Table 1:

$$f(\lambda-\lambda_0)=466+39k_1-24k_2+24k_3-64k_4+121k_5$$

The coefficients, k_1 *to* k_5 may be found in Table 3.

λ in $m\mu$	$\lambda-\lambda_0$	$+39k_1$	$-24k_2$	$+24k_3$	$-64k_4$	$+121k_5$	$f(\lambda-\lambda_0)$
581	1	+81.90	−27.72	+0.92	+0.56	+0.02	521.68
582	2	+85.80	−31.68	+2.11	+1.13	+.19	523.55
583	3	+89.70	−35.88	+3.59	+1.68	+.52	525.61
584	4	+93.60	−40.32	+5.38	+2.15	+.97	527.78
585	5	+97.50	−45.00	+7.50	+2.50	+1.42	529.92
586	6	+101.40	−49.92	+9.98	+2.66	+1.74	531.86
587	7	+105.30	−55.08	+12.85	+2.57	+1.82	533.46
588	8	+109.20	−60.48	+16.13	+2.15	+1.55	534.55
589	9	+113.10	−66.12	+19.84	+1.32	+.92	535.06

Check by ascending differences: From Table 2 we may write:

$$f(\lambda-\lambda_0)=462+48k_1'-23k_2'-17k_3'+57k_4'-121k_5'$$

The coefficients, k_1' to k_5', may be found in Table 3 by reading the values of the coefficients, k_1 to k_5, for $10-\lambda+\lambda_0$ instead of for $\lambda-\lambda_0$.

λ in $m\mu$	$\lambda-\lambda_0$	$+48k_1'$	$-23\ k_2'$	$-17\ k_3'$	$+57\ k_4'$	$-121\ k_5'$	$f(\lambda-\lambda_0)$
581	1	+139.20	−63.36	−14.05	−1.18	−0.92	521.09
582	2	+134.40	−57.96	−11.42	−1.92	−1.55	523.55
583	3	+129.60	−52.79	−9.10	−2.29	−1.82	525.60
584	4	+124.80	−47.84	−7.07	−2.37	−1.74	527.78
585	5	+120.00	−43.13	−5.31	−2.23	−1.42	529.91
586	6	+115.20	−38.64	−3.81	−1.92	−.97	531.86
587	7	+110.40	−34.39	−2.54	−1.49	−.52	533.46
588	8	+105.60	−30.36	−1.50	−1.00	−.19	534.55
589	9	+100.80	−25.56	−.65	−.50	−.02	535.07

TABLE 5.—*The O. S. A. "excitation" data extended to values for every millimicron by fifth-difference osculatory interpolation*

Original values appear in bold-face type

λ in mμ	ρ_0	γ_0	β_0	λ in mμ	ρ_0	γ_0	β_0	λ in mμ	ρ_0	γ_0	β_0
410	**0**	**0**	**433**	**470**	**4**	**81**	**697**	**530**	**307**	**572**	**43**
1	0.00	0.05	450.34	1	4.55	85.30	678.06	1	314.02	576.22	41.46
2	.00	.11	466.85	2	5.16	89.54	658.31	2	320.98	580.13	39.96
3	.00	.19	482.53	3	5.83	93.74	637.78	3	327.91	583.77	38.48
4	.00	.27	497.65	4	6.57	97.88	616.48	4	334.76	587.14	37.03
5	.00	.37	512.88	5	7.41	101.97	594.40	5	341.50	590.26	35.62
6	.00	.49	528.98	6	8.39	106.01	571.56	6	348.14	593.18	34.24
7	.00	.61	546.72	7	9.50	110.01	547.94	7	354.62	595.90	32.88
8	.00	.73	566.71	8	10.81	114.01	523.60	8	360.94	598.44	31.56
9	.00	.86	589.18	9	12.31	118.00	498.58	9	367.06	600.81	30.26
420	**0**	**1**	**614**	**480**	**14**	**122**	**473**	**540**	**373**	**603**	**29**
1	0.00	1.15	640.68	1	15.88	126.02	446.93	1	378.78	605.02	27.76
2	.00	1.30	669.70	2	17.97	130.02	420.08	2	384.38	606.91	26.54
3	.00	1.47	701.04	3	20.28	134.01	392.56	3	389.80	608.68	25.36
4	.00	1.66	734.21	4	22.80	138.04	364.62	4	395.05	610.28	24.20
5	.00	1.85	768.20	5	25.50	142.24	336.87	5	400.15	611.64	23.06
6	.00	2.05	801.90	6	28.38	146.68	309.88	6	405.12	612.68	21.96
7	.00	2.28	834.20	7	31.38	151.50	284.32	7	409.98	613.29	20.90
8	.00	2.50	864.09	8	34.48	156.81	260.67	8	414.73	613.40	19.90
9	.00	2.74	891.04	9	37.69	162.64	239.24	9	419.40	612.97	18.92
430	**0**	**3**	**915**	**490**	**41**	**169**	**220**	**550**	**424**	**612**	**18**
1	0.00	3.28	936.48	1	44.44	175.86	202.72	1	428.50	610.54	17.12
2	.00	3.58	955.33	2	47.97	183.19	187.64	2	432.89	608.56	16.28
3	.00	3.91	971.38	3	51.62	191.02	174.83	3	437.16	606.01	15.48
4	.00	4.26	984.68	4	55.39	199.36	164.12	4	441.33	602.96	14.74
5	.00	4.64	995.42	5	59.32	208.20	155.18	5	445.44	599.46	14.02
6	.00	5.06	1003.81	6	63.47	217.55	147.56	6	449.51	595.60	13.34
7	.00	5.50	1010.18	7	67.88	227.42	140.83	7	453.59	591.47	12.72
8	.00	5.96	1014.76	8	72.60	237.79	134.60	8	457.69	587.15	12.12
9	.00	6.47	1017.68	9	77.64	248.66	128.66	9	461.83	582.66	11.54
440	**0**	**7**	**1019**	**500**	**83**	**260**	**123**	**560**	**466**	**578**	**11**
1	0.00	7.59	1018.48	1	88.64	271.80	117.84	1	470.18	573.13	10.49
2	.00	8.21	1015.95	2	94.59	284.06	113.19	2	474.44	568.08	10.01
3	.00	8.89	1011.45	3	100.82	296.78	108.98	3	478.76	562.88	9.57
4	.00	9.62	1005.18	4	107.34	309.88	105.16	4	483.11	557.50	9.16
5	.00	10.44	997.49	5	114.12	323.27	101.64	5	487.40	551.84	8.76
6	.00	11.33	988.76	6	121.13	336.84	98.40	6	491.54	545.84	8.38
7	.00	12.32	979.38	7	128.33	350.49	95.36	7	495.42	539.41	8.03
8	.00	13.43	969.69	8	135.74	364.11	92.46	8	498.98	532.47	7.68
9	.00	14.65	959.88	9	143.30	377.62	89.69	9	502.17	525.00	7.34
450	**0**	**16**	**950**	**510**	**151**	**391**	**87**	**570**	**505**	**517**	**7**
1	0.01	17.48	939.91	1	158.86	404.25	84.36	1	507.51	508.54	6.67
2	.05	19.06	929.69	2	166.89	417.40	81.69	2	509.64	499.62	6.34
3	.11	20.74	919.44	3	175.08	430.43	78.97	3	511.33	490.24	6.02
4	.20	22.54	909.12	4	183.38	443.22	76.20	4	512.68	480.41	5.71
5	.31	24.52	898.68	5	191.76	455.73	73.42	5	513.78	470.20	5.40
6	.43	26.68	888.06	6	200.16	467.80	70.70	6	514.78	459.67	5.10
7	.56	29.10	877.15	7	208.52	479.33	68.06	7	515.82	448.82	4.80
8	.70	31.78	865.86	8	216.80	490.24	65.55	8	517.02	437.74	4.52
9	.85	34.76	854.14	9	224.96	500.47	63.20	9	518.42	426.46	4.26
460	**1**	**38**	**842**	**520**	**233**	**510**	**61**	**580**	**520**	**415**	**4**
1	1.17	41.51	829.55	1	240.92	518.87	58.89	1	521.68	403.36	3.76
2	1.35	45.31	816.89	2	248.70	527.01	56.87	2	523.55	391.50	3.52
3	1.56	49.42	804.02	3	256.34	534.39	54.92	3	525.60	379.46	3.30
4	1.79	53.77	790.90	4	263.82	541.08	53.06	4	527.78	367.30	3.07
5	2.06	58.32	777.31	5	271.18	547.13	51.26	5	529.92	355.07	2.86
6	2.35	62.95	763.10	6	278.44	552.70	49.52	6	531.86	342.88	2.66
7	2.69	67.60	748.08	7	285.63	557.89	47.84	7	533.46	330.83	2.48
8	3.07	72.17	732.08	8	292.78	562.80	46.19	8	534.55	318.97	2.31
9	3.51	76.64	715.05	9	299.92	567.51	44.58	9	535.06	307.36	2.15

TABLE 5.—*The O. S. A. "excitation" data extended to values for every millimicron by fifth-difference osculatory interpolation*—Continued

λ in mμ	ρ_0	γ_0	β_0	λ in mμ	ρ_0	γ_0	β_0	λ in mμ	ρ_0	γ_0	β_0
590	**535**	**296**	**2**	**620**	**375**	**59**	**0**	**650**	**118**	**3**	**0**
1	534.44	284.89	1.87	1	365.85	55.08	0.00	1	111.72	2.67	0.00
2	533.34	274.08	1.75	2	356.74	51.42	0.00	2	105.74	2.37	0.00
3	531.64	263.58	1.65	3	347.73	48.01	0.00	3	100.08	2.12	0.00
4	529.40	253.40	1.55	4	338.79	44.84	0.00	4	94.72	1.90	0.00
5	526.72	243.47	1.46	5	329.92	41.88	0.00	5	89.64	1.70	0.00
6	523.69	233.74	1.38	6	321.05	39.09	0.00	6	84.82	1.54	0.00
7	520.44	224.18	1.30	7	312.16	36.43	0.00	7	80.28	1.40	0.00
8	517.05	214.70	1.20	8	303.17	33.87	0.00	8	75.96	1.25	0.00
9	513.58	205.30	1.10	9	294.12	31.40	0.00	9	71.87	1.12	0.00
600	**510**	**196**	**1**	**630**	**285**	**29**	**0**	**660**	**68**	**1**	**0**
1	506.26	186.84	0.89	1	275.86	26.69	0.00	1	64.36	0.89	0.00
2	502.42	177.80	.77	2	266.72	24.45	0.00	2	60.95	.77	0.00
3	498.47	168.90	.64	3	257.57	22.28	0.00	3	57.78	.66	0.00
4	494.40	160.16	.50	4	248.42	20.16	0.00	4	54.82	.53	0.00
5	490.10	151.58	.37	5	239.32	18.14	0.00	5	52.04	.41	0.00
6	485.46	143.26	.24	6	230.26	16.22	0.00	6	49.43	.30	0.00
7	480.41	135.21	.14	7	221.28	14.43	0.00	7	46.93	.20	0.00
8	474.82	127.47	.06	8	212.40	12.80	0.00	8	44.55	.12	0.00
9	468.68	120.07	.02	9	203.64	11.32	0.00	9	42.24	.05	0.00
610	**462**	**113**	**0**	**640**	**195**	**10**	**0**	**670**	**40**	**0**	**0**
1	454.85	106.24	0.00	1	186.49	8.82	0.00				
2	447.18	99.81	0.00	2	178.09	7.77	0.00				
3	439.00	93.69	0.00	3	169.83	6.86	0.00				
4	430.34	87.89	0.00	4	161.72	6.06	0.00				
5	421.35	82.39	0.00	5	153.78	5.38	0.00				
6	412.12	77.19	0.00	6	146.08	4.79	0.00				
7	402.78	72.26	0.00	7	138.62	4.26	0.00				
8	393.45	67.59	0.00	8	131.44	3.80	0.00				
9	384.19	63.18	0.00	9	124.57	3.38	0.00				

Figure 1 illustrates the smoothness of the interpolated values obtained by this method; it shows a portion of the ρ_0 curve near its maximum which possesses an irregularity of such nature that graphical interpolation is difficult.

It is to be noted that the interpolation has not been carried out beyond the limits 410 and 670 mμ; this serves to emphasize that the present plan is to refrain from using the interpolated values in obtaining the trilinear coordinates corresponding to a given spectral distribution of energy. There would now seem to be little need to make use of intervals smaller than 10 mμ for this purpose although advances in colorimetric technique may be made in the future which will require smaller intervals to be used. The interpolation of the O. S. A. curves by somewhat refined method does not presuppose this advanced technique; it is merely a question of adopting arbitrarily some one of the many equally reliable interpolations so that computed results via the O. S. A. "excitation" data which depend on interpolation may be perfectly intercomparable; the specific purpose, as previously stated, is to make possible the computation of rigorously comparable values of dominant wave length and colorimetric purity from given values of trilinear coordinates. The interpolated results given in Table 5 are sufficient to permit reproducible interpolation for dominant wave lengths to tenths of a millimicron merely from a table of values. If, for special purposes, a comparison of values to hundredths of a millimicron be desired it is probable that an inter-

polation graph based on the values of Table 5 would afford an adequate basis. It may be pointed out, too, that interpolations of any

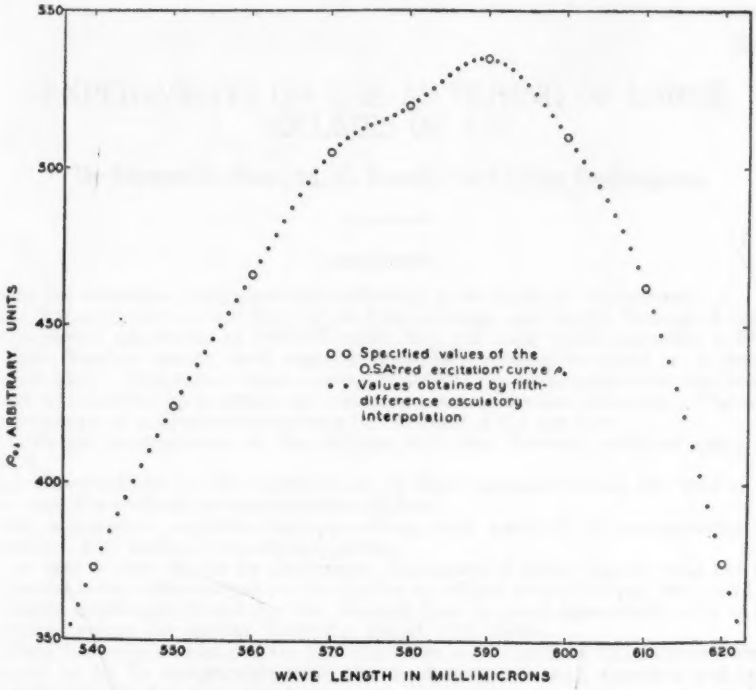

FIGURE 1.—*Example of interpolation of the O. S. A. "excitation" data by the fifth-difference, osculatory formula*

A portion of the red curve near its maximum is chosen for a demonstration of the smoothness of the interpolated values.

precision desired, however great, may be accomplished by carrying the appropriate number of decimal places in computing by the formula.

WASHINGTON, May 12, 1931.

EXPERIMENTS ON THE METERING OF LARGE VOLUMES OF AIR

By Howard S. Bean, M. E. Benesh,[1] and Edgar Buckingham

ABSTRACT

The investigation comprised the following three kinds of experiment:

(*a*) Experiments on the flow of air from a large gas holder through a rotary displacement gas meter of 200,000 cubic feet per hour rated capacity, a 24 by 12 inch Venturi meter, and various thin-plate orifices installed in a smooth 24-inch pipe. The rate of flow was determined from observations on the holder, which was flooded by a stream of water, to control the temperature. The average precision of a determination was better tnan ± 0.5 per cent.

(*b*) Series comparisons of the orifices with the Venturi, without using the holder.

(*c*) Observations on the distribution of static pressure along the wall of the pipe near the orifices, at various rates of flow.

The apparatus, experimental procedure, and methods of computation are described, and tables of results are given.

The rate of flow shown by the rotary displacement meter agreed with the rate computed from observations on the holder to within about 0.5 per cent; and the discharge coefficient found for the Venturi was in good agreement with earlier published values for similar Venturis, tested with water.

When the values obtained for the discharge coefficients of the orifices were so reduced as to be comparable with the most complete and accurate published values for water, the agreement was very satisfactory.

CONTENTS

		Page
I.	Preface	94
II.	Introduction	95
III.	General arrangement of the apparatus	96
IV.	Holder	96
	1. Measurement of the dimensions	96
	2. Height measurements	98
	3. Control and measurement of temperature	99
	4. Leakage test	100
V.	Orifice meter installation	100
	1. Orifices	100
	2. Pipe	101
	3. Honeycombs	101
	4. Pressure taps	101
	5. Water manometers	102
	6. Wet and dry bulb psychrometer	102
VI.	Rotary displacement meter	102
VII.	Venturi meter	103
VIII.	Auxiliary instruments and operations	103
	1. Regulation of the rate of flow	103
	2. Barometer	103
	3. Clock	103
	4. Photographic recording	104

[1] Chief gas research engineer, The People's Gas Light & Coke Co., Chicago, Ill.

	Page
IX. Variation of pressure along the pipe near an orifice	104
1. Experiments	104
2. Mode of representing the results	104
3. Tables of results	105
4. Variation of pressure distribution with speed of flow	111
5. Variation with diameter ratio	113
X Experiments with the holder	113
1. Procedure	113
2. Saturation in the holder	115
3. Computation of the rate of flow of dry air along the line	116
4. Computation of the density and rate of flow of moist air at any section of the line	117
5. Reduction of the observations on the orifices	119
6. Reduction of the observations on the Venturi	119
7. Reduction of the observations on the rotary displacement meter	120
XI. Results of the experiments with the holder	121
1. General characteristics of the runs	121
2. Results of the tests of the rotary displacement meter	122
3. Results of the tests of the Venturi meter	124
4. Discussion of the results obtained with the Venturi	125
5. Discharge coefficients of the orifices	126
XII. Comparison of the orifices with the Venturi	127
1. Experimental procedure	128
2. Computations	128
3. Results of the comparisons	129
XIII. Discussion of the results of the experiments on orifices	130
1. Reduction for change of tap location	130
2. Allowance for varying density; the expansion factor	132
3. Witte's values of K for smooth pipes	135
4. Comparison of the Chicago results for air with Witte's results for water	136
5. Conclusions from the foregoing comparison	138
6. Remarks	139
7. Graphical representation of Tables 16, 17, and 18	140
XIV. Summary	142
Note A—The adiabatic discharge coefficient	143
Note B—The Reynolds number	144

I. PREFACE

The investigation discussed in the following paper was initiated by the American Gas Association and was carried out, with the cooperation of the National Bureau of Standards, under the general oversight of a committee appointed by the association, on which the bureau was represented.

The work was done during the summer and autumn of 1924 at the Pitney Court Station of the People's Gas Light & Coke Co., of Chicago where a large gas holder and other important facilities were placed at the disposal of the committee. The company also furnished assistance of various kinds, and bore a large share of the cost of the operations.

The committee was indebted to the Builders Iron Foundry, of Providence, R. I., for the loan of a Venturi meter; to the Connersville Blower Co., of Connersville, Ind., for the loan of a rotary displacement meter; and to the Republic Flow Meters Co., of Chicago, Ill., for the loan, or the special construction, of numerous small but essential parts of the apparatus.

The National Bureau of Standards contributed in the matter of standardizing measuring instruments, and by advice or suggestions regarding experimental methods and the reduction of observations.

One of the present authors (Benesh), acting as chairman of the committee, made the detailed plans for the experiments and the work was carried out under his immediate supervision. Another of the authors (Bean) represented the bureau during the experiments, and participated in them as an observer. The remaining author (Buckingham) served as a member of the committee and as an adviser in theoretical matters. He is responsible for the form in which the results are presented, but in preparing the paper he has received much indispensable assistance from his two colleagues.

II. INTRODUCTION

The main object of the undertaking was to test the accuracy of several types of meter which are in common use for measuring large quantities of gas at pressures near atmospheric. The meters in question were: (*a*) A series of round, square-edged orifices installed concentrically, one at a time, in a straight, smooth pipe of 24 inches nominal diameter; (*b*) a rotary displacement meter of a rated capacity of 200,000 cubic feet per hour; and (*c*) a 24 by 12 inch Venturi meter.

A few tests were made on a large, wet drum, station meter, but they did not reveal anything of general interest. Observations were also made on a Thomas electric meter, but the method of operation was modified from standard commercial practice, and while the results were of interest to the makers of the meter, they might be misleading to others and will not be reported here.

The tests were made with air, and the large gas holder served as the absolute standard to which the other meters were referred; but in addition to the laborious and time-consuming experiments with the holder, a number of intercomparisons were made, without using the holder.

A third section of the investigation consisted in observations on the longitudinal distribution of pressure along the wall of the 24-inch pipe near the orifices. These were needed in order that the results obtained when using the orifices as meters might be compared with the published results of other observers.

The general scheme of the holder experiments was as follows: The inner lift of the holder, the only one used, was first filled with air by a centrifugal booster, warm water being sprayed into the intake to insure saturation. The connections were then changed and air was withdrawn from the holder by the booster and forced along the test line in which the meters were installed in series. From the dimensions of the holder and its rate of fall, together with observations of pressure and temperature, the mean rate of outflow of air was computed. This was then compared with the mean indications of the meters during the run and their correction factors or coefficients were thus determined with reference to the holder as the standard.

In the intercomparison tests and in the experiments on the longitudinal distribution of pressure near the orifices, the booster was disconnected from the holder and drew its air from outside.

III. GENERAL ARRANGEMENT OF THE APPARATUS

The arrangement of the line in which the meters were installed is shown schematically in Figure 1, the notation being as follows:

A = pipe leading from the holder to the booster.
B = the booster.
O = the pair of flanges for holding the orifice plates.
$R.\ D.$ = the rotary displacement meter.
$W.\ D.$ = the connections to the wet drum meter.
V = the Venturi meter.
T = a 20-inch Thomas electric meter.
$H_1 \ldots H_4$ = honeycombs.
$P_1 \ldots P_4$ = wet and dry bulb psychrometers.
t_1, t_2 = dry bulb thermometers.
M = the bank of water manometers.

Starting at the holder (off the sheet to the left), the pipe A ran underground for about half its length and then up to the second floor of the meter house, where the centrifugal booster was situated. From the booster, the piping led down to the ground floor, to the entrance of the first straight section of the test line proper, containing the orifice station, the lower line in Figure 1.

By means of details not shown in the figure, provision was made for changing the connections of the booster so as to permit of: (*a*) Filling the holder with air from outside, (*b*) withdrawing air from the holder and sending it along the test line through the meters, and (*c*) drawing air from outside and sending it directly into the test line.

The general appearance of the 41 by 90 foot first floor room may be gathered from the view in Figure 2, taken from a point near the middle of the lower edge of Figure 1. In the foreground are the water manometers and the cathetometers for reading them, and behind the manometers is the 24-inch pipe containing the orifice station. The line containing the Venturi meter was parallel to the orifice line, about 10 feet to the left and behind. The rotary displacement meter is shown in the right background. This meter could be either included in the line or by-passed, by shifting a blank plate from one flange joint to another.

The wet drum meter, which came next after the rotary displacement meter, was by-passed in all the experiments to be reported, and it is not necessary to describe the somewhat circuitous route by which the air reached the entrance to the straight pipe leading to the Venturi meter.

IV. HOLDER

1. MEASUREMENT OF THE DIMENSIONS

The mean radius of the inner lift of the holder was found by the following process: The distance from a mark at the center of the crown to a punch mark on each of the 21 columns of the surrounding framework was measured with a steel tape. By means of a plumb line, a second mark was located on each column, directly below the first at a convenient height for measuring the distance from the column back to the shell, and this distance was measured. Departures of the plating from verticality were determined along each

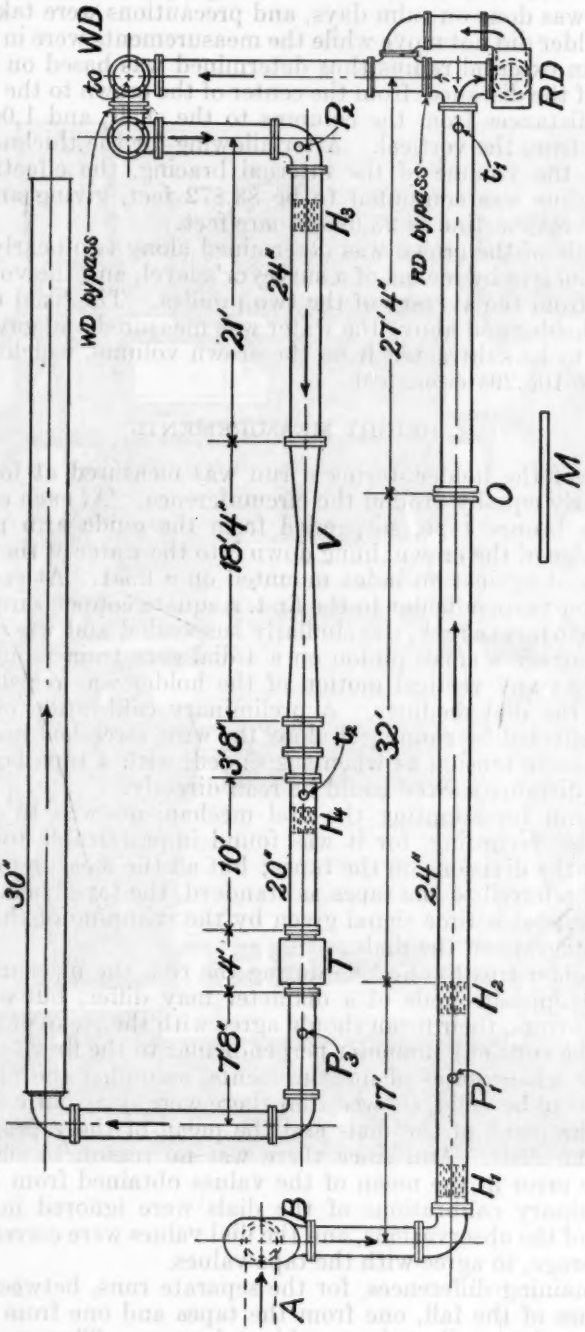

FIGURE 1.—*General arrangement of meters and auxiliary apparatus*

column by means of a surveyor's transit sighted on a rider which could be raised or lowered while bearing against the shell plates. This work was done on calm days, and precautions were taken to see that the holder did not move while the measurements were in progress.

The mean external radius thus determined was based on 42 measurements of the distances from the center of the crown to the columns; 63 of the distances from the columns to the shell; and 1,008 of the departures from the vertical. After allowing for the thickness of the plates and the volume of the internal bracing, the effective mean internal radius was computed to be 83.872 feet, giving an average horizontal cross section of 23,098 square feet.

The profile of the crown was determined along two nearly perpendicular diameters by means of a surveyor's level, and the volume was computed from the average of the two profiles. The fixed timbering inside the holder and above the water was measured and gave a small correction to be subtracted from the crown volume, which was thus found to be 106,294 cubic feet.

2. HEIGHT MEASUREMENTS

The fall of the holder during a run was measured at four points spaced nearly equally around the circumference. At each end of one diameter a bronze tape, suspended from the guide arm projecting from the edge of the crown, hung down into the water of the tank and could be read against an index mounted on a float. At each end of the diameter perpendicular to the first, a square copper wire, notched on one side to form a rack, was similarly suspended and was guided by rollers to engage a small pinion on a 4-dial gear train mounted on a float, so that any vertical motion of the holder was registered as a change of the dial readings. A preliminary calibration of the dial train was effected by running it along the wire, stretched horizontally under the same tension as when suspended, with a tape beside it on which the distance moved could be read directly.

The reason for adopting the dial mechanisms was to permit of photographic recording, for it was found impracticable to get clear pictures of the divisions on the tapes; but all the measurements were ultimately referred to the tapes as standard, the tapes being read by two observers at a time signal given by the snapping of the cameras which photographed the dials.

If the holder tips to one side during the run, the measurements of the fall at opposite ends of a diameter may differ, but aside from accidental errors, their mean should agree with the mean of the values found at the ends of a diameter perpendicular to the first. Examination of the whole series of measurements, assuming the preliminary calibrations to be valid, showed that there were systematic differences between the mean of the dials and the mean of the tapes, and also between the dials. And since there was no reason to suspect any systematic error in the mean of the values obtained from the tapes, the preliminary calibrations of the dials were ignored in the final reduction of the observations, and the dial values were corrected so as, on the average, to agree with the tape values.

The remaining differences, for the separate runs, between the two mean values of the fall, one from the tapes and one from the dials, were then to be attributed to accidental errors. They ranged from

B. S. Journal of Research, RP335

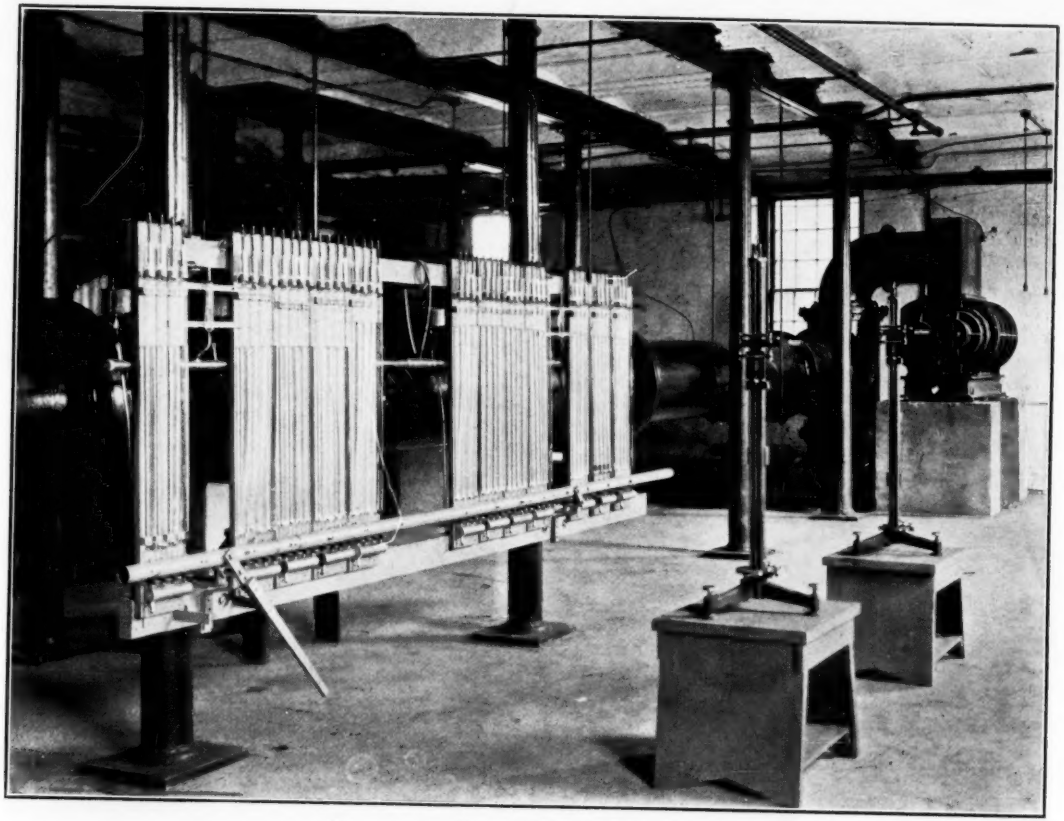

FIGURE 2.—*General view of laboratory*

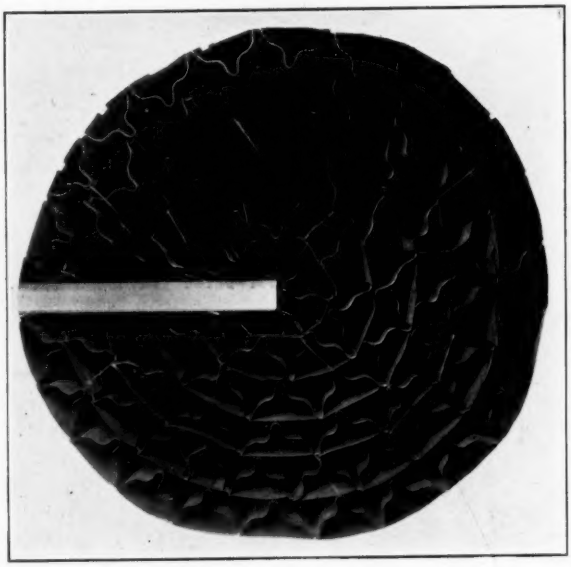

FIGURE 3.—*Honeycomb*

nothing up to 1.7 per cent of the fall, with an average of ±0.43 per cent, and may have been due partly to bending of the tapes or wires by wind.

The wires were, of course, held taut by weights on their lower ends, but there was no evidence of a progressive stretching during the course of the experiments.

During a few of the earlier runs, dial mechanisms were used at all four stations. The readings from the dials that were thereafter replaced by tapes were corrected by comparison with the corrected readings from the other pair of dial trains, which was used throughout.

In addition to the fall of the holder during a run, it is also necessary to know the absolute value of the initial or final height of the edge of the crown above the water in the tank. The zero correction to be applied to the tape readings for this purpose was found by running a level line out from the edge of the crown and taking a reading on the tape.

3. CONTROL AND MEASUREMENT OF TEMPERATURE

The temperature of the air in the holder was measured by four, or later only three, resistance thermometers. Two of these were hung from the crown near the NW. side, about 8 and 18 feet down, respectively; one was about halfway from the center to the SE. side, a few feet below the crown; and one was a few feet below the crown at the center. This last thermometer became defective during the course of the experiments and was not used during the later runs.

The first attempt to control the temperature was by means of some 20 garden spray nozzles distributed under the crown so as to give a fairly uniform shower; and when this proved unsatisfactory, the sprays were placed on top of the crown. Ultimately, the holder was virtually water jacketed by flooding it with water, pumped up from the tank and allowed to run down again over the crown and sides in as uniform a film as possible. It was found that with a flow of 700 to 1,000 gallons per minute, the temperature of the water flowing over the crown did not change more than 1 or 2 degrees F. from center to edge, even in a strong wind.

Uniformity of temperature was tested by means of a movable thermocouple. After the resistance thermometers had come to indicate uniformity within 0.5 degree, one junction of the couple was held near one of the resistance thermometers while the other was shifted about to a number of positions within the holder, and the difference in temperature of the junctions was found from the observed E. M. F. This was first tried on a cool, rainy, windy night without the flood in operation, and it was repeated on a rather cool calm night with a small flood stream. The greatest difference observed was about 1 degree F.

The experiments with the holder were made at night, most of them between midnight and 4 a. m., a time when the temperature of the outside air is usually falling slowly. If the temperature in the holder can not be held perfectly constant during the whole of a run, it is evidently desirable that it should fall rather than rise. For if the air is saturated at the start, it tends to remain saturated as it cools, whereas if the temperature rises, there is some doubt on this point unless the rise is very slow.

In preparing for a run, the holder was filled by the booster, while water, about 5 degrees warmer than the water in the tank, was sprayed into the intake. Thus the air entered the holder saturated (this was tested by a psychrometer) at a temperature somewhat above that already existing in the holder, and remained saturated as it cooled down. To assist mixing by convection currents and to prevent the formation of fog, the internal sprays were usually turned on for a time after the holder was filled and before the run was started.

4. LEAKAGE TEST

Before starting to use the holder for experiments with air, it was purged of gas and the inlet from the gas mains sealed. It was then thoroughly cleaned and the water in the tank was renewed. It was next examined for leaks and those found were calked, after which it was filled with air, sealed off, and left for five days, during which observations of height, temperature, and barometric pressure were made from time to time, so that the amount of air in the holder could be computed. This test showed that, to the degree of accuracy of the observations, the holder was tight and that no leakage correction would be needed, even in the longest runs made with it.

V. ORIFICE METER INSTALLATION

1. ORIFICES

The orifice plates were made of one-eight inch Monel metal, and the orifices were cylindrical holes with square, sharp corners at both faces of the plate. The edges were examined under the microscope and in a few cases, where the upstream corner appeared not to be quite perfect, it was retouched with an oilstone or a dead smooth file laid flat on the face of the plate.

Centering in the pipe was adjusted by measurement from the cylindrical outer edge of the plate to three flats, 120° apart on the upstream orifice flange, where the distances from the axis of the pipe were known.

The diameter of each orifice was measured in several azimuths by an inside micrometer, the range of the separate values obtained being of the order of ± 0.002 inch for the larger orifices and somewhat less for the smaller ones. Values of the mean diameter d are shown in column 2 of Table 1.

The mean of 11 measurements of the diameter of the pipe within 6 inches upstream from the orifice plate was $D = 23.311$ inches, the diameter on the downstream side being about 0.01 inch larger. Values of the diameter ratio of the orifices, $d/D = \beta$, are shown in column 3 of the table. For convenient reference, the orifice plates were designated by the approximate values of the area ratio expressed in per cent, which are given in the first column. The values of β^4 given in the last column were frequently needed during the analysis of the experimental results.

TABLE 1.—*Dimensions of orifices*

Area ratio	Diameter d	Diameter ratio β	β^4	Area ratio	Diameter d	Diameter ratio β	β^4
Per cent	*Ins.*			*Per cent*	*Ins.*		
5	5.213	0.2236	0.0025	50	16.489	0.7073	0.2503
10	7.374	.3163	.0100	55	17.299	.7421	.3033
20	10.429	.4474	.0401	60	18.061	.7748	.3603
30	12.776	.5481	.0902	65	18.800	.8065	.4230
35	13.798	.5919	.1227	70	19.509	.8369	.4906
40	14.748	.6327	.1602	75	20.187	.8660	.5624
45	15.628	.6704	.2020	80	20.858	.8946	.6404

2. PIPE

The straight run of smooth steel pipe ahead of the orifice, to the nearest fitting other than a simple flange joint, was 47 feet 2 inches; and on the downstream side it was 25 feet 6 inches. The first 10 feet on each side of the orifice consisted of two 5-foot lengths which had been machined smooth inside, the joints being dowelled so that they lined up within one thirty-second inch. The whole pipe, out to the distances mentioned above, was painted inside with graphite and oil and rubbed down, which gave it a very smooth surface.

3. HONEYCOMBS

To eliminate whirl or large eddies in the stream approaching the orifice, two honeycombs were mounted in the pipe. The first was near the entrance from the booster to the straight run of pipe, about 45 feet from the orifice, and the second was set with its downstream face 32 feet 2 inches or 16.5 D from the orifice.

The honeycombs were 12 inches long in the direction of flow and each contained about 160 parallel passages or cells. They were built up of alternate rings of flat and of doubly-corrugated, 30-gage galvanized iron. The appearance of one of the honeycombs is shown in Figure 3, and those placed in the line ahead of the Venturi and Thomas meters were of similar construction.

4. PRESSURE TAPS

The side holes drilled through the pipe for taking off the pressures were one-eighth inch in diameter and were rounded off on the inside of the pipe to a radius of one thirty-second inch. Nipples for rubber tubing were soldered over the holes on the outside and could be joined by short rubber connectors to lengths of copper tubing, of about ¼-inch bore, leading to the manometers.

In all the observations for determining the discharge coefficients of the orifices, the same pair of holes was used. They were, respectively, 12 inches upstream and 6 inches downstream from the face of the nearer of the two flanges holding the orifice plate.

In the investigation of longitudinal distribution of pressure, measurements were made simultaneously at 46 holes, 14 upstream and 32 downstream. The first 10 of the upstream holes were in a line along the top of the pipe. The eleventh, distant 2 inches from the plate, was offset 1 inch to one side; the twelfth, distant 1 inch from the plate, was similarly offset to the other side; and the thir-

teenth and fourteenth, also 1 inch from the plate, were at the ends of a horizontal diameter. The first 3 of the downstream holes corresponded in location to the last 3 of the upstream. The others were on 3 parallel lines, on top and 2 inches on either side, and were so arranged that no 2 holes on the same line were less than 4 inches apart. The longitudinal spacing of the holes used is shown in Tables 2 to 11.

5. WATER MANOMETERS

All the pressures to be observed were low enough to be measured on open-water manometers 36 inches high. The manometers were made up in units of 4 each, the vertical glass tubes being 1 inch in diameter but drawn down at the ends to facilitate making connections. The lower ends of the 4 tubes were connected through cocks to a short header and thence to a common reservoir or tank near the top of the tubes. This tank had a free-water surface 8 inches in diameter and was provided with a 1-inch gage tube for observing the level of the water in the tank. It had a tight cover, with a nipple which could either be left open to the atmosphere or connected to one of the pressure taps. The upper ends of the manometer tubes could be connected to any desired pressure taps.

For the experiments on pressure distribution, 12 such units were provided. They were set up in line, as shown in Figure 2, and the 48 cocks were connected by links to a long, horizontal bar, so that they could all be closed simultaneously by moving a single lever. The water columns were thereby locked in position and the levels could then be determined at leisure by means of the cathetometers provided for making the readings. When the manometers were being used in this way, the separate tanks were connected to a common header.

Thermometers hung near the manometers gave the temperatures of the water columns with sufficient accuracy for making the small reduction to standard temperature.

6. WET AND DRY BULB PSYCHROMETER

Two mercurial thermometers were inserted through a rubber stopper in a hole in the wall of the pipe, and a wick around one of them was fed with water from outside, by a device which prevented any escape of air. This consisted of a small electrically heated boiler followed by a condenser, from which the condensate was led to the wick through a small copper tube extending for some distance along the inside of the pipe, so as to equalize the temperature. By adjusting the heating current, the water supply could be made just sufficient to keep the wick properly moistened.

Similar psychrometers were used at the other points in the line indicated in Figure 1.

VI. ROTARY DISPLACEMENT METER

The location of the rotary displacement meter is shown in Figures 1 and 2. To give the temperature of the air entering it, a dry thermometer was inserted a few feet ahead of the meter at the point t_1 in Figure 1. The pressure was measured by one of the manometers connected to a tap some distance downstream from the orifice flanges,

the drop from this point to the rotary meter being negligible at the comparatively low rates of flow to which this meter was limited. The humidity of the air was determined by the psychrometer ahead of the orifice station.

VII. VENTURI METER

The Venturi tube used was the "Herschel standard Venturi tube" made by the Builders Iron Foundry. The holes into the piezometer rings were three-eighths inch in diameter and there were 12 at the entrance and 8 at the throat. The diameter at the entrance ring was 24.86 inches, and the throat diameter was 11.992 inches.

Ahead of the Venturi, there was a 19-foot straight run of 24-inch pipe to the flange of the next elbow, and a honeycomb was set with its downstream face 15.5 feet, or about 7.7 D from the upstream flange of the Venturi.

At the downstream end of the Venturi, a short nipple and a reducer, 3 feet 8 inches long together, led to a 10-foot length of 20-inch pipe and so to the Thomas meter.

The entrance and throat pressures were measured by a pair of the water manometers already described.

VIII. AUXILIARY INSTRUMENTS AND OPERATIONS

1. REGULATION OF THE RATE OF FLOW

The steam pressure at the turbine which drove the booster was not constant and the governor was rather sluggish; and since accuracy in the experiments required that the rate of flow along the test line should be constant during any one run, hand regulation was resorted to. An inclined draft gauge was set up near the turbine and connected to two taps near the orifice flange. An attendant, watching this gauge and with his hand on a lever attached to the throttle valve of the turbine, kept the gauge reading and therefore the rate of flow as constant as practicable during the course of any experiment.

2. BAROMETER

The barometer, of the Fortin type, was kept in a vault where the temperature was nearly constant. Its internal corrections had been determined by comparison with the standard barometer of the U. S. Weather Bureau Station in Chicago. Since the cistern of the barometer was 23 feet below the water level in the holder tank, a small altitude correction was applied in making computations that involved the absolute pressure in the holder.

The excess pressure inside the holder was read on a small, U-tube, water manometer at the center of the crown.

3. CLOCK

The time measurements needed in the experiments with the holder were made by means of a high-grade pendulum clock with sweep seconds hand, which ran within a few seconds a day and was amply accurate, in comparison with the unavoidable errors in other parts of the work.

4. PHOTOGRAPHIC RECORDING

Some of the more important readings were recorded photographically by cameras fitted with electromagnetically controlled shutters so that they could all be snapped at once by closing a single switch. By this means simultaneous pictures could be taken of the clock face, the dials on the mechanisms for measuring the fall of the holder, and the dials of the rotary displacement meter.

IX. VARIATION OF PRESSURE ALONG THE PIPE NEAR AN ORIFICE

1. EXPERIMENTS

The experimental procedure in this part of the investigation was very simple. With an orifice plate in position and the manometers connected to a series of taps along the pipe, the booster was started and brought up to a constant speed, drawing air from outside and forcing it along the line through the orifice. After waiting till the water columns had become as nearly steady as was to be expected, they were fixed by closing all the cocks simultaneously, and the readings were then made with the cathetometers. Zero readings were made on the open gauge tubes on the common header, and the gauge pressure at each tap could then be found by subtraction.

Barometer readings were taken, to permit of reducing the results to absolute pressures, if desired, and the temperature of the air in the pipe was also recorded. The water columns were all at nearly the same temperature and since only comparative values of the pressures were needed, reduction to standard temperature was superfluous.

At least two such sets of observations, or runs, at different rates of flow, were made with each of the orifices listed in Table 1.

2. MODE OF REPRESENTING THE RESULTS

If the pressures, observed in the foregoing manner near an orifice installed in a straight pipe, are plotted against distance from the orifice, the resulting points lie along a curve of the familiar shape illustrated qualitatively in Figure 4, which also shows the notation adopted here for representing the results.

Starting with a tap several pipe diameters ahead of the orifice and going on to taps successively farther downstream, the static pressure observed at the wall of the pipe at first decreases slowly, as it does in steady flow along any straight pipe, but near the orifice the pressure begins to rise as the stream piles up against the plate. This upstream part of the curve is represented by ABC in Figure 4.

At the rates of flow attained in these experiments, the preliminary fall was inappreciable except for the largest orifices, and the curve was sensibly a horizontal straight line for a considerable distance ahead of the point B where the obstruction offered by the orifice plate began to make itself felt. Still farther upstream, the observations at the first two taps, which were 56 and 44 inches from the orifice, gave abnormally low values as is indicated by the dotted piece of curve starting at A' in Figure 4. This was doubtless due to the proximity of a flange joint a little over 3 inches ahead of the first tap. There was probably a slight discontinuity in the line of the pipe

wall here, for although the two sections of pipe had been machined smooth they were not perfectly round, and there was also a small change of mean diameter, the upstream section being about 0.04 inch larger than the section next the orifice in which the tap holes were located.

On the downstream side of the orifice plate, after the sharp drop from C to D, the pressure falls to a minimum at E, rises to a maximum at F, and thereafter falls off slowly.

In order to compare the results obtained with any one orifice at different rates of flow with one another or with observations on other orifices, it is first necessary to reduce them all to some common basis, and this was done as follows:

The most probable value of the pressure p_2 at the downstream minimum, E, was found graphically by plotting and drawing a

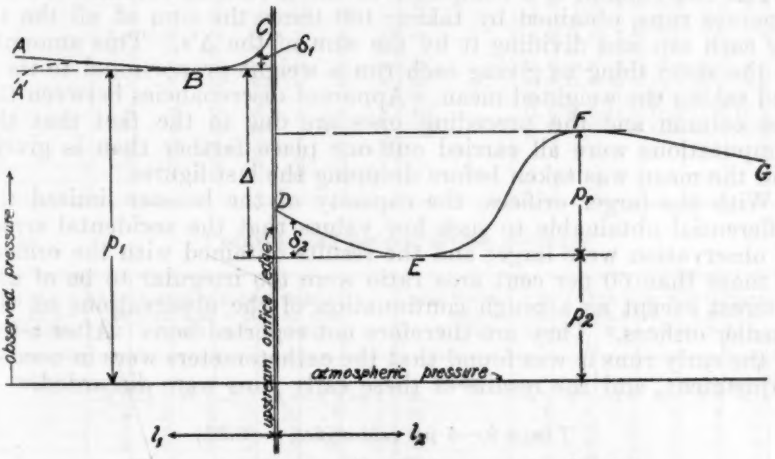

FIGURE 4.—*Pressure distribution curve (qualitative)*

smooth curve, which gave an estimate based on several neighboring points. This minimum pressure was then subtracted from the pressure observed at each of the downstream taps and the difference was denoted by δ_2, as illustrated in Figure 4.

For the upstream points, in the few instances in which there was a recognizable minimum at B, the minimum pressure p_1 was found graphically, as for p_2; but usually the readings were so uniform that this was unnecessary and p_1 was taken to be this uniform pressure. The value of p_1 was then subtracted from each of the observed upstream pressures and the difference denoted by δ_1.

When the values of δ_1 and δ_2 had been found, they were expressed as percentages of the difference of pressure, $p_1 - p_2 = \Delta$, between the upstream and downstream minima, and the various sets of observations were thus made comparable.

3. TABLES OF RESULTS

The results of the observations, expressed in the manner just described, are exhibited in Tables 2 to 11, which are all arranged in the same way.

The first column gives the distance in inches from the nearer face of the orifice plate to each of the taps at which the pressures were measured, starting with the tap farthest upstream. The decreasing numbers in the first part of the column refer to the upstream taps, and the increasing numbers in the second part to the downstream taps.

Each of the following columns, except the last, refers to a single run and gives the values found for $100\ \delta_1/\Delta$ or $100\ \delta_2/\Delta$, at the distances from the orifice shown in the first column. At the head of each of these columns certain data characteristic of the run are given, namely: (1) The differential $p_1 - p_2 = \Delta$ in inches of water; (2) the differential, expressed in per cent of the minimum upstream pressure, or $100\ \Delta/p_1 = 100\ x$; and (3) the Reynolds number R_d defined in note B, divided by 100,000.

The last column is a composite of the preceding columns for the separate runs, obtained by taking 100 times the sum of all the δ's for each tap and dividing it by the sum of the Δ's. This amounts to the same thing as giving each run a weight proportional to its Δ and taking the weighted mean. Apparent discrepancies between the last column and the preceding ones are due to the fact that the computations were all carried out one place farther than is given, and the mean was taken before dropping the last figures.

With the larger orifices, the capacity of the booster limited the differential obtainable to such low values that the accidental errors of observation were large; and the results obtained with the orifices of more than 60 per cent area ratio were too irregular to be of any interest except as a rough continuation of the observations on the smaller orifices. They are therefore not reported here. After a few of the early runs it was found that the cathetometers were in need of adjustment, and the results of these early runs were discarded.

TABLE 2.—*5 per cent orifice, $\beta = 0.224$*

Δ in. H_2O =	2.33	2.71	15.48	18.06	31.74	
$100\ x$ =	.58	.68	3.74	4.44	7.40	
$10^{-5} R_d$ =	1.6	1.7	4.2	4.4	5.8	
Inches						
56	−0.8	−0.3	−0.4	−0.3	−0.2	−0.3
44	−.7	.4	.2	−.1	−.1	.1
36	−.3	−.1	.1	.0	.0	.0
28	.0	−.1	.1	.0	.0	.0
24	.0	−.1	.1	.0	.0	.0
20	.0	−.1	.0	.0	.0	.0
16	−.2	.3	.0	.0	.0	.0
12	−.2	.3	.0	.0	.0	.0
8	.2	.3	.0	.0	.0	.0
4	.2	.3	.3	.0	.0	.1
2	−.2	.1	.3	.0	.0	.1
1	−.2	.1	.0	.1	.1	.1
1	.3	−.1	.4	.5	.5	.5
2	.5	.0	.3	.4	.5	.4
4	.5	−.3	.2	.3	.4	.3
6	.3	−.1	.1	.2	.4	.3
8	.0	−.4	.0	.1	.3	.2
10	.0	−.4	.0	.1	.3	.1
12	.0	−.7	.0	−.1	.2	.0
14	.0	−.3	.0	−.1	.2	.0
16	.0	−.1	.0	.0	.2	.1
18	.0	.1	.0	.0	.2	.1

Δ ins. H_2O =	2.33	2.71	15.48	18.06	31.74	
$100\ x$ =	.58	.68	3.74	4.44	7.40	
$10^{-5} R_d$ =	1.6	1.7	4.2	4.4	5.8	
Inches						
20	.0	.1	.0	.0	.1	.1
22	.0	.1	.0	.0	.1	.1
24	.0	.1	.0	.0	.1	.0
26	.0	.0	−.1	−.2	.0	.0
28	.0	.0	.1	.0	.0	.0
30	.0	.0	.0	.0	.0	.0
32	.0	.0	.0	.0	.0	.0
34	.0	.0	.0	.0	.0	.0
36	.0	.3	.3	.1	.2	.2
40	.0	.4	.4	.3	.3	.3
44	1.4	.6	1.0	.9	.7	.8
48	1.4	1.7	1.3	1.5	1.1	1.3
52	2.4	2.3	2.3	2.3	1.9	2.1
56	3.4	2.9	3.1	3.0	2.6	2.8
64	4.1	4.8	4.3	4.4	4.0	4.2
72	4.9	5.8	5.4	5.1	5.1	5.2
80	5.6	6.0	5.6	5.7	5.6	5.6
96	5.9	6.0	6.0	5.9	6.0	6.0
112	5.9	6.0	6.0	6.0	6.1	6.1
130	5.9	6.0	6.1	6.1	6.2	6.1

TABLE 3.—*10 per cent orifice, $\beta=0.316$*

Δ ins. H_2O =	3.85	4.48	18.70	19.03	32.24	32.31		Δ ins. H_2O =	3.85	4.48	18.70	19.03	32.24	32.31	
100 x =	.96	1.11	4.51	4.59	7.55	7.56		100 x =	.96	1.11	4.51	4.59	7.55	7.56	
10^{-3} R_d =	3.0	3.2	6.6	6.6	8.6	8.6		10^{-3} R_d =	3.0	3.2	6.6	6.6	8.6	8.6	
Inches								*Inches*							
56	−0.3	−0.1	−0.3	−0.4	−0.2	−0.3	−0.3	20	.8	.2	.1	.1	.0	.0	.1
44	.0	−.1	.0	−.3	.0	.0	.0	22	1.1	.4	.1	.1	.0	.0	.1
36	.0	.0	.0	.0	.0	.0	.0	24	.1	.4	.1	.1	.0	.0	.0
28	.0	.0	.0	.0	.0	.0	.0	26	−.1	−.4	.0	.0	.0	.0	.0
								28	.0	.0	.0	.0	.0	.0	.0
24	.0	.0	.0	.1	.0	.0	.0								
20	.1	.0	.0	.0	.0	.0	.0	30	.5	.1	.1	.0	.0	.0	.0
16	.1	.0	.0	.0	.0	.0	.0	32	.5	.4	.1	.1	.0	.0	.1
12	.3	.0	.0	.0	.0	.0	.0	34	.5	.8	.3	.1	.1	.0	.2
								36	1.0	.4	.6	.4	.7	.3	.5
8	.2	.2	.0	.0	.0	.0	.0	40	1.6	1.6	1.3	1.1	1.2	1.0	1.2
4	.2	.3	.0	.1	.1	.0	.1								
2	.2	.1	.0	.1	.1	.0	.1	44	2.7	3.3	2.1	2.1	2.0	1.9	2.1
1	.2	.1	.0	.1	.1	.1	.1	48	3.6	4.4	3.0	2.9	2.9	3.1	3.1
								52	5.8	5.8	4.2	3.9	4.1	4.4	4.3
1	1.6	1.0	.9	.9	.8	.6	.8	56	7.1	6.7	5.4	5.1	5.4	5.5	5.5
2	1.6	.9	.7	.8	.7	.4	.7	64	8.6	8.5	7.8	7.7	7.8	7.6	7.8
4	1.5	.9	.6	.7	.4	.3	.5								
6	1.4	.8	.5	.6	.3	.3	.5	72	10.4	9.3	9.7	9.0	9.7	8.1	9.1
8	1.1	.5	.5	.5	.0	.2	.3	80	10.9	11.5	10.6	10.2	10.3	9.3	10.1
								96	11.7	11.5	11.5	11.0	11.4	11.2	11.3
10	1.0	.4	.5	.4	.2	.0	.2	112	12.1	11.7	11.8	11.5	11.5	11.3	11.5
12	.7	.1	.4	.3	.1	.2	.2	130	12.1	11.7	11.8	11.6	11.7	11.3	11.6
14	.5	.1	.3	.2	.1	.2	.2								
16	.5	.1	.2	.2	.1	.0	.1								
18	.6	.2	.0	.1	.0	.0	.1								

TABLE 4.—*20 per cent orifice, $\beta=0.447$*

Δ ins. H_2O =	3.76	4.11	18.08	18.26	29.20	29.44		Δ ins. H_2O =	3.76	4.11	18.08	18.26	29.20	29.44	
100 x =	.94	1.02	4.39	4.43	6.92	6.98		100 x =	.94	1.02	4.39	4.43	6.92	6.98	
$10^{-3}R_d$ =	4.2	4.4	9.3	9.3	11.8	11.9		$10^{-3}R_d$ =	4.2	4.4	9.3	9.3	11.8	11.9	
Inches								*Inches*							
56	−0.5	−0.2	−0.4	−0.2	−0.3	−0.2	−0.3	20	−0.1	0.0	−0.2	0.1	0.0	0.0	0.0
44	−.2	.0	.0	.0	.0	.0	.0	22	.1	.0	−.2	.0	.0	.0	.0
36	.1	.0	.0	.0	.0	.0	.0	24	.2	.0	.0	.0	.0	.0	.0
28	.0	.0	.0	.0	.0	.0	.0	26	.7	.6	.1	.0	.0	.0	.1
								28	.7	1.0	.3	.3	.3	.3	.3
24	.0	.1	.0	.0	.0	.0	.0								
20	−.1	.0	.0	.0	.0	.0	.0	30	.8	1.5	.6	.9	.7	.9	.8
16	−.2	.0	.0	.0	.0	.0	.0	32	2.4	2.3	1.2	1.3	1.1	1.1	1.2
12	−.1	.1	.0	.0	.0	.0	.0	34	2.8	3.4	2.2	2.1	1.9	1.8	2.1
								36	3.8	4.3	2.8	3.4	4.0	2.9	3.4
8	−.1	.1	.2	.0	.1	.1	.1	40	6.3	6.1	4.9	4.7	4.4	4.4	4.7
4	.2	.3	.4	.1	.3	.4	.3								
2	.2	.4	.5	.3	.4	.4	.4	44	9.2	8.5	7.0	6.7	6.3	6.4	6.7
1	.0	.4	.4	.4	.5	.4	.4	48	11.3	10.2	8.9	9.0	8.3	8.3	8.7
								52	13.2	12.1	11.0	10.9	10.4	10.0	10.6
1	1.1	.6	1.2	.7	.9	1.1	1.0	56	16.4	15.2	12.9	13.0	12.4	12.2	12.8
2	1.0	.6	.9	.7	.8	.9	.8	64	17.5	17.9	16.3	16.5	15.6	15.6	16.0
4	.6	.5	.6	.6	.6	.8	.6								
6	.4	.7	.5	.5	.4	.7	.5	72	20.6	19.8	18.5	18.9	18.5	18.4	18.7
8	.0	.7	.4	.5	.3	.5	.4	80	21.3	21.0	20.4	20.1	19.7	19.8	20.0
								96	22.0	21.5	21.4	21.8	21.4	21.5	21.5
10	.3	.6	.5	.4	.2	.4	.4	112	22.1	21.6	21.8	22.2	21.7	22.0	21.9
12	−.3	.3	.3	.4	.1	.3	.3	130	21.9	21.6	21.7	22.3	21.9	22.0	22.0
14	−.1	.3	.3	.4	.1	.3	.2								
16	.0	.0	.2	.2	.1	.2	.2								
18	.3	.0	.1	.0	.0	.1	.1								

TABLE 5.—*30 per cent orifice, $\beta=0.548$*

Δ ins. H_2O=	3.63	15.36	15.58	19.19	19.91		Δ ins. H_2O=	3.63	15.36	15.58	19.19	19.91	
100 x=	9.1	3.65	3.78	4.63	4.83		100 x=	.91	3.65	3.78	4.63	41.83	
$10^{-4}R_d$=	5.2	10.8	10.9	12.1	12.3		$10^{-4}R_d$=	5.2	10.8	10.9	12.1	12.3	
Inches							*Inches*						
56	−0.7	−0.3	−0.4	−0.3	−0.3	−0.3	20	1.0	.3	.0	.1	.1	.2
44	−.2	.0	−.1	.0	−.1	−.1	22	1.0	.3	.2	.3	.4	.3
36	.0	.0	.0	.1	.0	.0	24	2.6	.8	.7	.8	.9	.9
28	.0	.0	.0	.0	.0	.0	26	4.1	1.5	1.9	1.4	1.7	1.7
							28	5.4	2.7	2.6	2.6	2.7	2.3
24	.1	.0	.0	.0	.0	.0							
20	−.1	.0	.0	.0	.0	.0	30	6.5	4.0	4.0	4.0	4.1	4.2
16	−.1	.0	.0	.0	.0	.0	32	7.5	5.6	5.5	5.1	5.3	5.5
12	−.3	.1	.1	.0	.1	.0	34	10.5	7.3	7.1	6.6	6.8	7.1
							36	11.5	9.0	8.7	8.2	8.7	8.8
8	.0	.4	.2	.3	.4	.3	40	13.3	11.4	11.2	11.5	11.3	11.4
4	.0	.8	.7	.8	.9	.8							
2	.0	1.1	1.0	1.0	1.0	.9	44	18.0	14.2	13.8	13.8	13.8	14.1
1	.0	1.2	1.0	1.0	1.1	1.0	48	19.9	16.7	16.8	16.6	16.8	16.9
							52	21.2	19.1	19.4	19.1	19.4	19.3
1	.9	1.4	1.2	1.3	1.2	1.2	56	23.1	21.6	21.5	21.1	21.3	21.4
2	.0	.9	.7	1.1	.9	.9	64	25.5	25.1	25.3	24.6	25.4	25.1
4	1.0	.7	.7	.9	1.0	.8							
6	.7	.5	.6	.6	.7	.6	72	27.7	28.3	27.9	28.0	27.9	28.0
8	.2	.4	.5	.4	.6	.5	80	28.6	29.5	29.4	29.4	29.7	29.4
							96	29.4	31.2	31.2	31.1	31.2	31.1
10	.1	.3	.3	.3	.4	.3	112	29.6	31.8	31.6	31.6	31.7	31.5
12	.0	.2	.3	.1	.3	.2	130	29.6	31.8	31.6	31.6	31.8	31.6
14	−.1	.0	.2	.1	.1	.1							
16	.1	.0	.2	.0	.1	.1							
18	.0	−.2	.0	.0	−.1	−.1							

TABLE 6.—*35 per cent orifice, $\beta=0.592$*

Δ ins. H_2O=	3.34	3.35	12.35	15.41		Δ ins. H_2O=	3.34	3.35	12.35	15.41	
100 x=	0.84	0.84	3.03	3.74		100 x=	0.84	0.84	3.03	3.74	
$10^{-4}R_d$=	5.6	5.6	10.7	11.9		$10^{-4}R_d$=	5.6	5.6	10.7	11.9	
Inches						*Inches*					
56	−0.4	−0.6	−0.4	−0.3	−0.3	20	2.1	1.7	.4	.9	.9
44	.0	−.6	.0	−.1	−.1	22	3.2	3.5	1.1	1.3	1.6
36	.0	.0	.0	.1	.0	24	4.7	4.5	2.1	2.7	2.7
28	.0	.0	.1	.1	.1	26	6.3	6.5	3.8	4.0	4.3
						28	8.1	8.1	5.7	5.6	5.9
24	.0	−.2	.0	.0	.0						
20	.0	.0	.0	.0	.0	30	9.7	9.5	7.5	7.5	7.7
16	.2	.0	.0	.0	.0	32	11.2	11.5	8.7	9.0	9.1
12	.2	.0	.0	.0	.0	34	13.4	13.8	10.9	11.3	11.3
						36	15.0	16.7	13.0	12.9	13.1
8	.5	.0	.4	.4	.4	40	18.9	18.7	16.4	15.8	16.2
4	.6	1.1	1.2	1.2	1.1						
2	.6	1.6	1.5	1.3	1.3	44	22.4	22.0	19.9	18.8	19.3
1	1.3	1.3	1.5	1.4	1.4	48	24.4	24.2	22.9	20.2	22.3
						52	26.2	26.9	25.4	24.6	24.6
1	2.3	1.7	1.4	1.4	1.5	56	27.9	28.6	27.9	26.3	26.5
2	1.7	1.7	.9	1.1	1.1	64	31.0	30.6	31.4	30.3	30.0
4	1.7	1.0	.7	.8	.8						
6	1.2	1.0	.4	.7	.6	72	33.7	33.0	34.7	32.9	32.7
8	.9	.2	.3	.5	.4	80	34.8	35.0	36.6	33.7	34.4
						96	35.3	35.7	38.2	36.0	35.7
10	.4	.2	.4	.2	.3	112	35.6	35.9	39.0	36.4	36.2
12	.2	.0	.2	.3	.2	130	35.5	36.1	39.0	36.4	36.2
14	.1	.0	−.1	.2	.0						
16	.1	.0	.2	.1	.1						
18	.2	.2	.1	.0	.1						

TABLE 7.—*40 per cent orifice, $\beta=0.633$*

Δ ins. H_2O=	2.89	3.95	9.74	10.64		Δ ins. H_2O=	2.89	3.95	9.74	10.64	
100 x=	.73	.99	2.42	2.61		100 x=	.73	.99	2.42	2.61	
$10^{-4}R_d$=	5.7	6.6	10.4	10.9		$10^{-4}R_d$=	5.7	6.6	10.4	10.9	
Inches						*Inches*					
56	−1.2	−0.2	−0.2	−0.2	−0.3	20	1.8	1.9	1.2	1.3	1.4
44	−.5	−.1	−.1	−.1	−.1	22	3.7	4.2	2.8	2.8	3.1
36	.0	.0	.1	.0	.0	24	5.0	6.0	4.7	4.5	4.8
28	.0	.0	.1	.0	.0	26	7.1	7.7	6.6	6.4	6.7
						28	9.7	9.5	8.5	8.5	8.8
24	.0	.0	.0	.0	.0						
20	−.1	.1	.0	.0	.0	30	11.3	11.9	11.0	10.5	10.9
16	−.1	.1	.0	.0	.0	32	12.1	14.0	13.1	12.8	13.0
12	−.1	.1	.0	.0	.0	34	14.8	16.5	15.1	14.6	15.1
						36	17.6	17.5	16.8	16.8	17.0
8	.1	.3	.3	.4	.3	40	18.5	22.5	20.5	20.4	20.5
4	1.4	1.2	1.5	1.6	1.5						
2	1.4	1.3	1.7	2.0	1.7	44	25.0	25.4	23.6	23.9	24.1
1	1.9	1.6	1.9	2.1	1.9	48	27.1	27.6	26.8	27.0	27.0
						52	29.1	30.4	29.6	29.5	29.6
1	2.7	1.8	1.6	1.4	1.7	56	31.8	32.6	32.0	31.2	31.8
2	2.4	1.2	1.2	1.0	1.2	64	34.0	35.8	35.0	34.5	34.8
4	1.6	.8	.6	.6	.7						
6	1.2	.7	.5	.4	.6	72	36.3	38.0	37.3	37.5	37.4
8	.8	.1	.5	.3	.4	80	38.1	39.2	39.1	38.9	38.9
						96	39.2	40.6	40.6	40.2	40.3
10	.5	.1	.3	.2	.3	112	39.9	41.1	41.0	40.8	40.8
12	.3	.1	.2	.1	.2	130	39.9	41.0	41.0	40.8	40.8
14	.1	.1	.0	.1	.1						
16	.0	.3	−.1	.0	.0						
18	.3	.8	.0	.2	.2						

TABLE 8.—*45 per cent orifice, $\beta=0.670$*

Δ ins. H_2O=	2.81	2.99	6.85	8.04		Δ ins. H_2O=	2.81	2.99	6.85	8.04	
100 x=	.72	.76	1.69	2.00		100 x=	.72	.76	1.69	2.00	
$10^{-4}R_d$=	5.9	6.3	9.5	10.2		$10^{-4}R_d$=	5.9	6.3	9.5	10.2	
Inches						*Inches*					
56	−0.4	−0.7	−0.5	−0.5	−0.5	20	5.3	5.9	3.9	3.8	4.3
44	.0	.0	−.3	−.4	−.2	22	8.3	8.2	6.0	6.0	6.5
36	.0	−.1	.0	.0	.0	24	10.8	10.3	8.3	8.7	9.0
28	−.1	.0	.0	.0	.0	26	13.0	11.6	10.9	10.6	11.1
						28	15.9	16.1	13.5	13.5	14.1
24	.0	.0	.0	.0	.0						
20	.0	.0	.0	−.1	.0	30	18.5	17.9	15.3	16.1	16.3
16	.3	−.1	−.1	.0	.0	32	19.0	20.4	18.2	18.3	18.5
12	.1	.0	−.1	.0	.0	34	23.1	22.6	20.9	20.0	20.9
						36	24.3	24.3	22.9	22.4	22.9
8	.1	.1	.3	.4	.3	40	27.3	27.4	26.4	26.2	26.3
4	2.1	1.7	1.4	2.0	1.8						
2	1.8	2.1	2.3	2.6	2.3	44	31.7	30.8	29.2	29.6	29.7
1	2.5	2.2	2.5	2.6	2.5	48	36.5	33.4	32.2	32.6	32.8
						52	36.5	35.3	34.6	35.3	34.9
1	1.7	1.7	1.6	1.4	1.5	56	38.9	37.1	37.3	37.7	37.3
2	1.4	.9	.5	.9	.8	64	41.8	41.4	40.2	40.3	40.3
4	1.4	.7	.3	.5	.6						
6	1.0	.4	.2	.0	.3	72	44.1	42.5	42.9	42.9	42.6
8	.0	.1	.1	.0	.0	80	45.5	43.9	44.6	44.7	44.2
						96	46.0	44.6	45.4	46.1	45.2
10	.0	.0	.0	.0	.0	112	46.0	45.6	45.8	46.6	45.7
12	.0	.0	.0	.1	.0	130	46.0	45.4	45.7	46.4	45.5
14	.3	.3	.0	.0	.1						
16	2.1	1.6	1.0	.4	1.0						
18	3.5	3.8	1.9	1.6	2.2						

TABLE 9.—*50 per cent orifice, $\beta=0.707$*

Δ ins. H_2O=	2.21	2.33	5.56	5.94	5.99		Δ ins. H_2O=	2.21	2.33	5.56	5.94	5.99	
$100x$=	.56	.59	1.39	1.48	1.48		$100x$=	.56	.59	1.39	1.48	1.48	
$10^{-5}R_d$=	5.8	6.0	9.2	9.6	9.6		$10^{-5}R_d$=	5.8	6.0	9.2	9.6	9.6	
Inches							*Inches*						
56	−0.4	0.3	−0.6	−0.3	−0.3	−0.3	20	7.1	6.6	6.9	7.1	6.8	6.7
44	.0	.2	−.4	−.1	−.1	−.1	22	9.4	9.0	9.6	9.2	8.9	9.2
36	.0	.5	.1	−.1	−.2	.0	24	12.1	11.8	12.5	12.0	12.1	12.1
28	.2	.2	−.1	.0	.1	.1	26	15.3	14.5	15.7	15.1	15.0	15.1
							28	18.4	18.8	18.7	18.2	17.9	18.5
24	.0	.2	.1	.0	.0	.0							
20	.0	.0	−.1	−.1	.1	.0	30	20.7	20.6	21.1	20.7	20.3	20.6
16	.0	.0	−.1	−.1	.1	.0	32	23.5	24.2	23.4	23.1	23.0	23.3
12	.0	−.2	.1	−.1	.9	.2	34	27.3	26.7	25.6	26.2	25.5	26.0
							36	28.7	28.1	27.9	27.9	27.8	27.9
8	.0	−.2	.8	.3	.9	.5	40	32.4	32.5	31.7	31.5	30.9	31.5
4	2.1	.5	2.5	2.6	2.7	2.4							
2	2.7	2.7	3.0	2.9	3.4	3.0	44	35.1	35.4	35.1	34.7	35.0	34.9
1	2.7	2.4	3.6	3.4	3.8	3.4	48	36.1	37.5	38.2	37.9	37.8	37.7
							52	39.9	39.4	40.4	40.0	40.2	40.0
1	1.2	1.5	2.1	1.6	1.4	1.7	56	43.7	41.1	42.1	41.3	42.5	42.0
2	1.4	1.2	1.2	.8	1.1	1.1	64	43.8	44.0	44.6	44.4	45.0	44.5
4	1.2	.3	.4	.4	.1	.5							
6	.4	.0	.0	−.1	.1	.1	72	45.4	46.5	46.3	46.5	45.9	46.4
8	.4	.2	.1	.0	.0	.2	80	46.7	48.1	47.9	48.0	48.2	47.9
							96	47.6	48.2	49.2	49.3	49.7	49.1
10	.2	.2	.4	.0	.0	.2	112	48.3	48.2	50.1	49.4	50.1	49.4
12	.2	.0	.2	.0	.0	.1	130	47.8	48.4	49.3	49.4	50.1	49.2
14	−.2	.0	.0	.0	.2	.0							
16	.5	1.5	1.4	1.6	1.8	1.5							
18	3.7	2.0	3.5	3.4	3.4	3.3							

TABLE 10.—*55 per cent orifice, $\beta=0.742$*

Δ ins. H_2O=	3.22	3.31	5.26	5.84		Δ ins. H_2O=	3.22	3.31	5.26	5.84	
$100x$=	.81	.84	1.32	1.45		$100x$=	.81	.84	1.32	1.45	
$10^{-5}R_d$=	7.6	7.7	9.7	10.2		$10^{-5}R_d$=	7.6	7.7	9.7	10.2	
Inches						*Inches*					
56	−0.7	−0.8	−0.5	−0.8	−0.7	20	11.5	12.1	12.2	10.8	11.6
44	−.4	−.2	.0	−.3	−.2	22	14.5	14.9	15.1	14.8	14.8
36	.0	.2	.3	−.1	.1	24	18.3	18.8	18.7	18.6	18.6
28	.0	.2	.3	.0	.1	26	22.5	21.9	21.8	22.4	22.1
						28	25.9	24.3	24.9	25.0	25.0
24	.0	.2	.2	.0	.1						
20	.0	.1	.0	.0	.0	30	27.8	27.6	28.1	29.5	28.0
16	−.2	.0	.0	.1	.0	32	30.2	31.0	30.6	30.5	30.6
12	.0	.0	.2	−.1	.0	34	32.4	32.4	32.4	32.7	32.5
						36	35.2	34.7	34.8	34.9	34.9
8	1.0	.6	.6	.5	.6	40	38.3	38.6	38.0	38.3	38.3
4	2.8	2.2	3.0	2.9	2.8						
2	4.0	4.1	4.0	3.9	4.0	44	41.6	41.1	41.3	41.5	41.4
1	4.8	5.1	4.7	4.6	4.8	48	44.0	43.8	43.8	43.9	43.9
						52	46.0	45.4	45.6	45.5	45.6
1	2.1	2.4	1.6	2.1	2.0	56	47.5	47.4	47.2	47.7	47.5
2	1.0	1.0	.8	.5	.8	64	49.3	49.7	49.7	49.7	49.7
4	.5	.4	.0	.5	.3						
6	.0	.4	−.1	.3	.1	72	50.9	51.4	51.8	51.4	51.4
8	.0	.2	.1	.1	.1	80	52.1	52.6	52.7	52.4	52.5
						96	53.2	53.3	54.0	53.4	53.5
10	.2	−.1	.1	−.5	−.1	112	54.0	54.1	54.5	54.3	54.3
12	.4	.1	.4	.5	.4	130	52.9	53.3	53.8	53.7	53.5
14	1.1	.8	1.7	1.3	1.3						
16	4.8	4.5	4.9	4.4	4.6						
18	7.1	7.3	7.6	6.5	7.1						

TABLE 11.—*60 per cent orifice, $\beta=0.775$*

Δ ins. H_2O=	1.25	1.64	4.24	4.46		Δ ins. H_2O=	1.25	1.64	4.24	4.46	
$100x$=	0.31	0.41	1.04	1.10		$100x$=	0.31	0.41	1.04	1.10	
$10^{-5}R_d$=	5.1	5.9	9.4	9.7		$10^{-5}R_d$=	5.1	5.9	9.4	9.7	
Inches						*Inches*					
56	−0.6	−1.4	−0.7	−1.0	−0.9	20	18.6	20.1	18.3	16.6	17.8
44	.3	−.5	.1	.0	.0	22	22.0	24.2	21.5	20.3	21.4
36	.6	.0	.2	.6	.4	24	24.2	28.1	25.9	23.6	25.0
28	.0	.0	.2	.4	.2	26	29.9	31.9	29.1	26.9	28.7
						28	31.8	34.8	32.8	29.6	31.6
24	.0	.0	.1	.4	.2						
20	.0	.0	.0	.0	.0	30	34.3	37.2	36.0	33.7	34.9
16	−.3	.2	.1	.0	.0	32	37.7	39.1	37.1	35.6	36.7
12	.3	.0	.1	.0	.1	34	39.9	41.2	40.0	38.0	39.3
						36	41.5	42.9	41.9	39.8	41.1
8	.6	.2	.1	.8	.4	40	43.7	45.8	44.6	42.4	43.7
4	3.8	3.8	3.6	3.5	3.6						
2	5.7	4.8	5.7	6.0	5.7	44	47.8	48.9	47.5	45.2	46.7
1	6.9	6.5	6.1	6.4	6.4	48	49.4	50.6	49.1	46.3	48.6
						52	50.0	51.1	51.3	49.0	50.1
1	2.8	1.7	3.0	2.6	2.5	56	50.9	53.5	52.8	50.3	51.6
2	1.9	1.0	.4	1.2	.9	64	52.2	54.4	54.1	52.3	52.1
4	.9	.0	.0	.0	.0						
6	.6	.0	.1	.0	.0	72	52.2	55.6	55.9	53.6	54.5
8	.0	.2	.2	.0	.0	80	58.2	56.6	56.7	54.8	56.0
						96	56.9	56.8	58.2	55.5	56.7
10	.0	.5	.4	.0	.1	112	58.2	56.8	58.4	56.1	57.2
12	.9	2.2	1.6	.9	1.2	130	58.2	56.6	57.5	55.1	56.4
14	3.5	5.5	3.6	3.3	3.6						
16	7.2	10.1	9.6	8.7	9.0						
18	12.0	14.6	13.2	11.1	12.4						

4. VARIATION OF PRESSURE DISTRIBUTION WITH SPEED OF FLOW

If the data obtained in the different runs with any one orifice are plotted in the form

$$\frac{100\delta}{\Delta}=f\,(l)$$

where l= distance from the orifice plate, it is found that the upstream parts of the resulting curves do not show any certain variation with Δ. If there is any systematic variation within the range of differentials and speeds covered in these experiments, it is masked by the accidental errors of measurement which are evident in the irregularities of each series of points.

On the downstream side, however, the systematic change of the curve with increasing Δ is quite clear. It is illustrated by the two curves of Figure 5, each of which represents the mean of two runs at nearly the same Δ, with the 45 per cent orifice.

As the differential and the speed through the orifice are increased, the minimum corresponding to the point E of Figure 4 is blown farther downstream and the subsequent rapid rise occurs a little later. At points between the orifice plate and the downstream minimum, increasing Δ lowers the value of $100\delta_2/\Delta$, although the change is not great within the range of these experiments.

Both these effects are more pronounced for large than for small diameter ratios, and a given change of Δ has more effect when Δ is still small than when it is larger. One gets the impression that as Δ increases, the curves for any one orifice tend to approach a final form asymptotically.

With a given gas flowing through any one orifice, the curve of pressure distribution along the wall of the pipe is fixed by the values of the Reynolds number and the fractional differential, $\Delta/p_1 = x$. In the present experiments, the Reynolds number was always so high as to

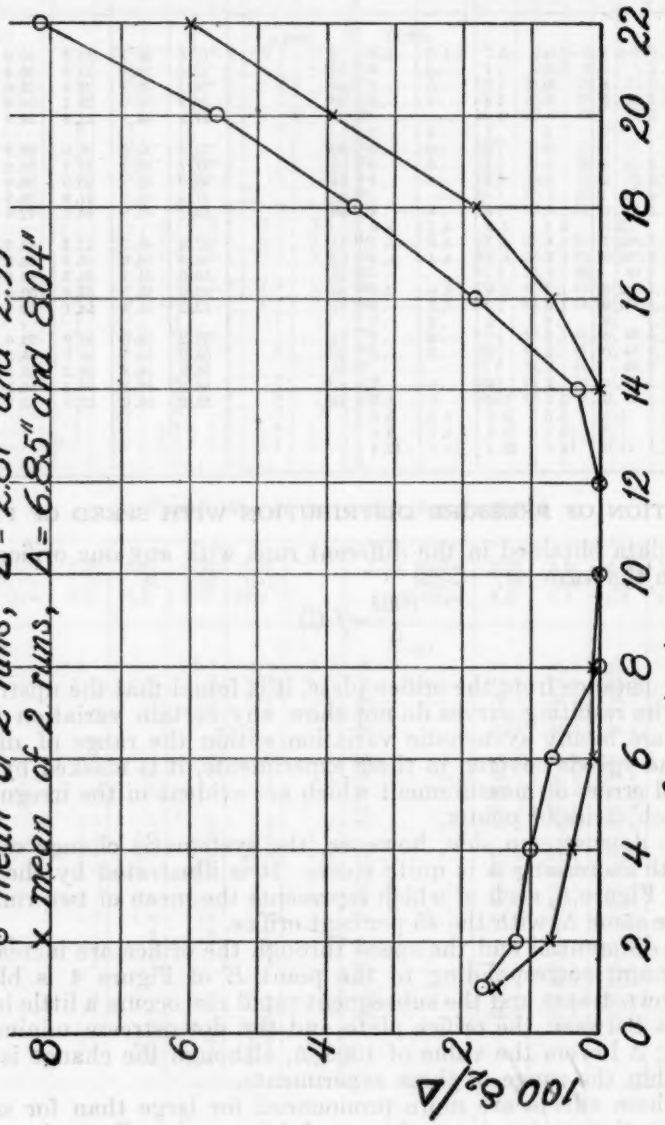

FIGURE 5.—*Downstream pressure curves for 45 per cent orifice, β=0.670*

make the effects of viscosity insignificant; and the change of the downstream part of the curve with Δ—or with x, since p_1 was nearly constant—is probably to be attributed to the same cause as the simultaneous change of the adiabatic discharge coefficient, namely, the lateral expansion of the gas in the jet after passing the orifice, due to the excess of static pressure at the axis of the jet over that at the

boundary.[2] This view of the matter is consistent with the fact that the upstream part of the pressure curve is much less affected by changes in Δ than the downstream part.

5. VARIATION WITH DIAMETER RATIO

If points are plotted from the composite data in the final columns of Tables 2 to 11, smooth mean cuves drawn through the points are of the same general shape as found by other observers. Sample plots are given in Figure 6 for the 20 and 40 per cent orifices ($\beta = 0.447$ and 0.633) from $l_1 = 20$ inches to $l_2 = 28$ or 52 inches. Since δ_1 is measured from the upstream and δ_2 from the downstream minimum, and since the difference between these minimum pressures is $\Delta = 100$ on the given scale, a consistent picture of the distribution of pressure over the whole length of the figure would require that the ordinates of the upstream points be increased by 100.

As the diameter ratio, β, is increased, the downstream minimum becomes more pronounced and moves up toward the orifice, in the well-known manner; and the following maximum moves in the same direction, though it is so flat as to be difficult to locate at all closely.

For area ratios up to $\beta^2 = 0.6$, the rise of pressure from the downstream minimum to the maximum, expressed as a fraction of the drop from the upstream to the downstream minimum (p_r/Δ in fig. 4), is roughly equal to β^2 or "the restoration of pressure is equal to the area ratio," a convenient practical rule which we have not seen stated in just this form.

X. EXPERIMENTS WITH THE HOLDER

1. PROCEDURE

After the holder had been filled with air, in preparation for a run, and the connections of the booster rearranged, the resistance thermometers were read continuously, in rotation, until they showed that the temperature had become nearly uniform and constant. The booster was then started and brought up to the speed necessary to give the desired rate of flow along the line, and the attendant at the turbine throttle kept this rate as nearly constant as practicable throughout the ensuing run.

Since the mean rate of outflow of air was to be computed from the initial and final states of the holder, no intermediate observations on the holder were needed if all went well. But to avoid having to waste a whole run of which only a part was for any reason unsatisfactory, each run was divided into five periods with records of the height taken at six known instants, so that those periods for which the observations on the holder and on the meters under test were satisfactory could be utilized and the others discarded.

The resistance thermometers were read at about the times when the height was measured. The readings of each thermometer were plotted against the times when they were made, a mean curve was drawn, and the mean temperature in the holder at the instant of taking each height record was found from this curve.

[2] E. Buckingham, Note on Contraction Coefficients of Jets of Gas, B. S. Jour. Research, 6; May, 1931; or Techn. Mech. u. Thermodyn., May, 1931.

Barometer readings were made occasionally, and if they changed enough during the run to make it worth while, the corrected values of the pressure were plotted against the times, and the pressures at the times of taking the height records were found graphically. The excess

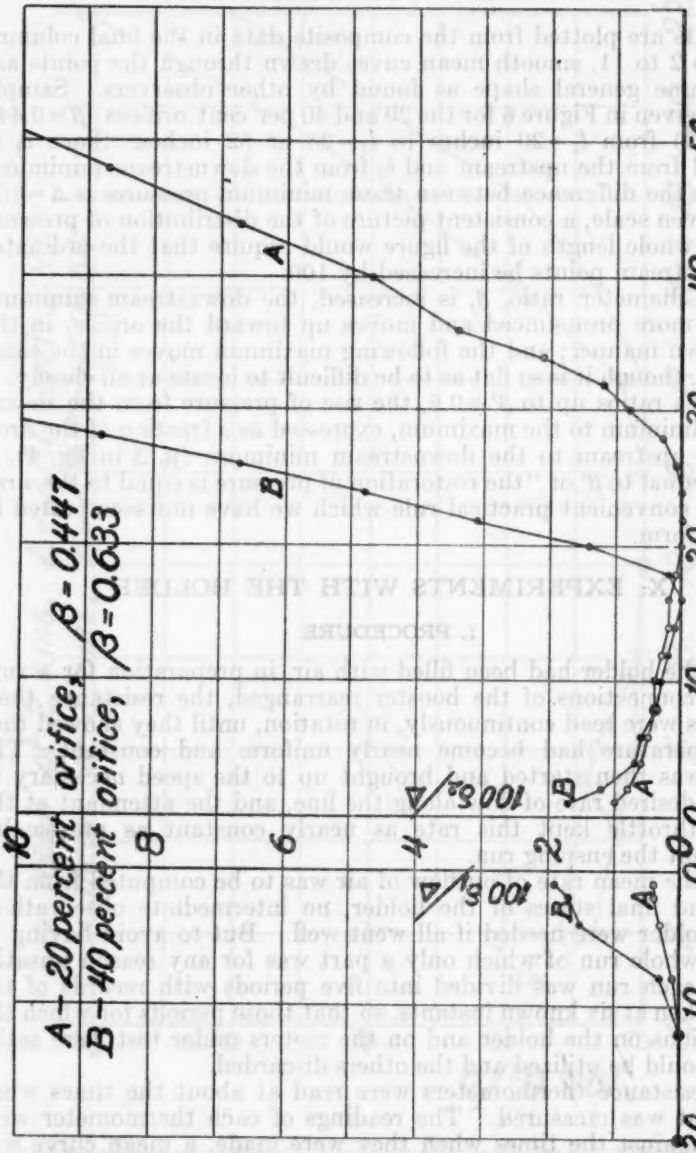

FIGURE 6.—*Average variations of pressure on the upstream and downstream sides of two orifices*

pressure inside the holder, shown by the gauge on the crown, was sensibly constant throughout the experiments.

When an orifice or the Venturi was under test, it was desirable to have as many readings as possible of the differential, so as to average

out the accidental fluctuations due to the unavoidable slight unsteadiness of the rate of flow. Measurements were therefore made continuously, as often as an observer, or sometimes two observers, could sight and read the cathetometers. The temperatures of the wet and dry bulb thermometers changed slowly and regularly and did not need to be read so often—the average interval between readings was about 11 minutes. The computations relating to the Venturi and the orifices were based on the averages of the observed values of the differential, the static pressure, and the wet and dry bulb temperatures.

Since the rotary displacement meter registers the total volume passed and not the instantaneous rate, all that was needed for comparison with the observations on the holder was the mean density of the air entering the meter and the photographs of its dials, taken simultaneously with the measurements of the height of the holder. The mean density was computed from the average values of the static pressure and the wet and dry bulb temperatures.

2. SATURATION IN THE HOLDER

In computing the mass of air in the holder, it has to be assumed that the air is saturated with water vapor, and it is important that the assumption be as nearly true as possible. Initial saturation was ensured by spraying warm water into the intake of the booster while filling the holder, but if the temperature of the air had risen much during a run, the evaporation from the tank might not have been rapid enough to maintain saturation. In most of the runs to be reported on, the mean temperature in the holder either fell or remained constant, and in the remainder, the most rapid rate of rise was 1.0 degree per hour.

In the first reduction of the observations, immediately after the experiments, the values found for the discharge coefficient of the Venturi varied irregularly by much more than could possibly be attributed to the accidental errors of observation at the Venturi, and the indications seemed to be that there must have been errors of 5 degrees or more in the measurements of the mean temperature of the holder. After the care that had been taken, such errors seemed not merely very disappointing, but quite incredible, and an indirect check on the holder temperatures was therefore carried out.

In passing through the booster, the air from the holder was heated much more than enough to offset the simultaneous compression, and when it entered the line it was considerably less than saturated. At the beginning of a run, the inside of the booster was still wet from the water sprayed in while filling the holder, but it dried off as the run proceeded, and the pyschrometers along the line showed that the vapor content of the air, after first decreasing, reached a constant value, indicating that the drying was complete.

It seemed safe to assume that when this steady state of partial saturation had been attained, the air was neither depositing nor taking up any appreciable amount of water since leaving the holder, and that the percentage composition of the air-vapor mixture was the same in the line as it had been in the holder. On this assumption, it was very easy to calculate from the wet and dry bulb temperatures and the pressure at any point in the line, together with the known pressure in the holder, what the vapor pressure in the holder

must have been, and thence, by means of the vapor pressure curve, to find what the temperature must have been if the air was saturated. This could then be compared with the temperature indicated by the resistance thermometers, and the agreement was found to be quite as good as could be expected.

In a few cases, the wet bulb readings were very irregular and indicated that the water supply to the wick had been deficient; but omitting these exceptional cases, the remaining 29 computations gave a maximum difference of 2.3 degrees between observed and calculated holder temperatures, and an average difference of only 0.63 degree.

The success of this check restored our confidence in the measurements of the temperature in the holder, and it was soon thereafter discovered that the discrepancies that had led to the check were spurious and due to a systematic mistake in one part of the computations.

3. COMPUTATION OF THE RATE OF FLOW OF DRY AIR ALONG THE LINE

In general, the mass of moist air that leaves the holder during any interval of time is not equal to the decrease of the mass contained in the holder. For if the temperature falls, vapor is precipitated and vanishes into the tank without having gone out through the booster; and if the temperature rises, vapor which did not exist at the start appears, from nowhere, as it were, by evaporation from the water in the tank. Furthermore, some vapor is added after the air leaves the holder by the drying out of the booster during the initial stages of a run, as mentioned above. But the mass of dry air that leaves the holder is equal to the difference of the masses present at the beginning and end of the run, and this same mass is discharged through each of the meters installed in series in the line. It is therefore most convenient to base all the computations on masses of dry air, and we have first to find the mass of dry air contained in the holder at any instant for which the temperature, pressure, and volume are known from observation.

Let

t (°F.) = the temperature of the air in the holder;
p (inch Hg, 32°) = its absolute pressure;
e_s (inch Hg, 32°) = the saturation pressure of water vapor at t°;
ρ_a (lbs./ft.^{3}) = the density of dry air at p, t;
V (ft.^{3}) = the volume of the holder at the observed height; and
W_a (lbs.) = the mass of dry air contained in it.

On the assumption that the air is saturated, the partial pressure of the dry air is $(p-e_s)$, and if the vapor were all removed by absorption, without changing the temperature or the volume, the pressure of the remaining dry air would be $(p-e_s)$. If the volume were then reduced, isothermally, in the ratio $(p-e_s)/p$, the pressure would increase to p and the resulting density would be ρ_a. Hence the mass of dry air (which has not been changed by these operations) is

$$W_a = \frac{p-e_s}{p} V \rho_a \qquad (1)$$

Now let subscripts 1 and 2 refer to conditions at the beginning and end of a run.

Let

z (minutes) = the duration of the run; and

M_a (lbs./sec.) = the mean rate of outflow of dry air.

Then evidently

$$M_a = \frac{(W_a)_1 - (W_a)_2}{60z} \tag{2}$$

or by (1)

$$M_a = \frac{V_1X_1 - V_2X_2}{z} \tag{3}$$

where

$$X = \frac{(p - e_s)\rho_a}{60p} \tag{4}$$

Values of X may be tabulated in terms of p and t as arguments and, after the table has been constructed, the values of X_1 and X_2 may be found by interpolation.

The required values of e_s were taken from the Wärmetabellen issued by the Reichsanstalt in 1919, and the values of ρ_a were found as follows. The density of dry air containing the normal amount of CO_2, at 32° F. and under a pressure of 29.921 inches of mercury, at 32° and with $g = 32.161$ ft./sec.^{2}, as at Chicago, was taken to be 0.08070 lb./ft.^{3} This value was deduced from the results of Ph. A. Guye's discussion of the best available data, as summarized in Landolt and Börnstein's Tables, 5th ed., 1923, vol. 1, p. 43. The mean coefficient of expansion of dry air at atmospheric pressure between 32° and 122° F., in terms of the volume at 32° is very close to 1/490 (not 1/492). Hence we have, for the density of dry air at t° F. and an absolute pressure of p inches of mercury at 32°, at Chicago,

$$\rho_a = \frac{0.08070 \times 490\ p}{29.921\ (458 + t)} = \frac{1.3216\ p}{458 + t} \tag{5}$$

And upon combining this with (4) we have the equation

$$X = 0.022026 \frac{p - e_s}{458 + t} \tag{6}$$

by means of which the table to be used with equation (3) was computed.

4. COMPUTATION OF THE DENSITY AND RATE OF FLOW OF MOIST AIR AT ANY SECTION OF THE LINE

Let

t (°F.) = the temperature of the air at the given section;

p (inch Hg) = the static pressure there;

e (inch Hg) = the partial pressure of the water vapor;

ρ (lbs./ft.^{3}) = the density of the moist air; and

M (lbs./sec.) = the rate of flow of moist air past the section.

The value of t is given by the dry bulb thermometer, and e is found from p, t, and the wet bulb depression, by means of Table 75 in Smithsonian Meteorological Tables (4th ed.), 1918.

Taking the ratio of the molecular weights of water vapor and air to be $18.02/28.95=0.622$, and using the same fundamental data as for equation (5), we have

$$\rho=\frac{1.3216\ (p-0.378e)}{458+t} \tag{7}$$

The rate of mass flow of the mixture of dry air and vapor is greater than that of the dry air alone by the amount of vapor carried along with the air. The pressure of the mixture being p, the partial pressure of the dry air in it is $(p-e)$ and the ratio of the mass of vapor to the mass of air in any quantity of the mixture is $0.622e/(p-e)$. Hence the mass of the mixture is greater than the mass of the dry air contained in it, in the ratio

$$\frac{p-e+0.622e}{p-e}=\frac{p-0.378e}{p-e}$$

and the rate of mass flow of the mixture past the point in question is

$$M=M_a\frac{p-0.378e}{p-e} \tag{8}$$

where M_a is the mass flow of dry air computed from the observations on the holder by means of equations (3) and (6).

In addition to the rate of flow in pounds per second, it is convenient to have the rate also expressed in the more roundabout, but more familiar way as cubic feet per hour under standard conditions, and this may be accomplished as follows.

Let Q (ft.^{3}/hour) be the volume rate of flow past a section of the line where the temperature is t, the static pressure p, and the vapor pressure e, measured at the density ρ corresponding to these conditions. Then evidently

$$Q=\frac{3{,}600M}{\rho} \tag{9}$$

and upon substitution of the values of M from (8) and ρ from (7) this takes the form

$$Q=\frac{3{,}600\ (458+t)}{1.3216\ (p-e)}M_a \tag{10}$$

Now let the standard conditions be $t=60$ (°F.), $p=30$ (inches Hg), and $e=0.26$ (inches Hg), which corresponds to 50 per cent relative humidity at 60°. Then if Q_s is the value Q would have if standard conditions prevailed at the section in question, and if we substitute the standard values in equation (10), the result is

$$Q_s(\text{ft}^3/\text{hour})=47{,}450M_a(\text{lbs./sec.}) \tag{11}$$

and Q_s is the volume flow of moist air under the standard conditions that would carry the actual mass flow of dry air computed from the observations on the holder.

In the gas industry, "standard conditions" are usually understood to be 30 inches, 60°, and complete saturation. For these conditions, the figure 47,450 should be increased by about 0.9 per cent.

5. REDUCTION OF THE OBSERVATIONS ON THE ORIFICES

The results of the tests of the orifices will be given as values of "the hydraulic discharge coefficient, based on the upstream density and with the approach factor included." This coefficient, which was denoted by C'_1 in B. S. Research Paper No. 49[3], will be denoted here by C. It may be defined, in terms of British absolute units, by the equation

$$M = C\frac{\pi}{4}d^2\sqrt{2\rho_1\Delta} \tag{12}$$

in which, M = the rate of flow, in lbs./sec.; d = the diameter of the orifice, in feet; ρ_1 = the density of the moist air, in lbs./ft.^{3} at the upstream pressure, temperature, and humidity; and Δ = the differential in poundals per square foot.

In practice, the diameter d was measured in inches, and the cathetometer scales were graduated in centimeters, so that the differential was read in centimeters of water at the prevailing temperature. Upon introducing these units and supposing the differential to have been reduced to cm. of water at 32° F., equation (12) may be put into the form

$$C = \frac{15.975M}{d^2\sqrt{\rho_1\Delta}} \tag{13}$$

And after introducing the values of M from equation (8), and of ρ_1 from equation (7), we have

$$C = \frac{13.896M_a}{d^2\,(p-e)}\sqrt{\frac{(p-0.378e)\;(458+t)}{\Delta}} \tag{14}$$

in which:

M_a (lbs./sec.) = the mass flow of dry air computed from the observations on the holder, as described above under 3;
d (inches) = the diameter of the orifice;
t (° F.) = the temperature shown by the dry bulb thermometer ahead of the orifice;
p (inches Hg, 32°) = the absolute pressure at the upstream tap;
e (inches Hg, 32°) = the partial pressure of the water vapor as found from p, t, and the wet bulb depression; and
Δ (cm H_2O, 32°) = the observed differential, after reduction to 32° F.

6. REDUCTION OF THE OBSERVATIONS ON THE VENTURI

The observations on the Venturi may be reduced in the same way as those on the orifices, and the results will first be given as values of C computed by means of equation (14), with d representing the diameter of the Venturi throat.

They will also be given as values of the "adiabatic" discharge coefficient because this permits of more direct comparison with

[3] B. S. Jour. Research, 2, p. 561; March, 1929.

values for water; and since the adiabatic coefficient is usually understood not to include the factor which allows for the speed of approach, it will be given in that form. It is then to be computed from the values of C already found from equation (14) by means of the equation (see note A)

$$C_a = C\left[\frac{2(1-r)\ (1-\beta^4 r^{2/3})}{7(r^{2/3}-r^{2/3})}\right]^{\frac{1}{2}} \tag{15}$$

in which $r = p_2/p_1$ and $\beta = d/D$, D being the diameter of the Venturi at the entrance section, where the upstream pressure p_1 is observed.

7. REDUCTION OF THE OBSERVATIONS ON THE ROTARY DISPLACEMENT METER

The results of the tests of the rotary displacement meter may be stated most conveniently by giving the values found for the quantity

$$C_d = \frac{M}{M_d} \tag{16}$$

in which M is the mean rate of mass flow through the meter, computed from the observations on the holder, and M_d is the mean rate indicated by the displacement meter. It may be called the coefficient of the meter, and it is evidently the factor by which the rate shown by the meter must be multiplied to make it agree with the rate computed from the observations on the holder, which is treated as the absolute standard.

The "dial factor" of the meter, or the volume of gas taken in per revolution, was given by the makers as 9.6789 cubic feet per revolution. Hence if the photographs of the dials taken at the beginning and end of a run of z minutes duration showed a difference of n revolutions, the mean rate of volume flow indicated by the meter was

$$V = \frac{9.6789n}{60z} (\text{ft.}^3/\text{sec.}) \tag{17}$$

measured at the upstream density at which the gas was taken in.

The expression for this upstream density is given by equation (7) and we therefore have

$$M_d = \frac{9.6789n}{60z} \times \frac{1.3216\ (p-0.378e)}{458+t} \tag{18}$$

The mass flow computed from the observations on the holder is given by equation (8) and upon combining equations (8), (16), and (18) we have

$$C_d = 4.6907\ \frac{M_a z\ (458+t)}{n\ (p-e)} \tag{19}$$

in which

M_a (lbs./sec) = the mass flow of dry air;
z (minutes) = the duration of the run;
n = the difference of the initial and final dial readings;
t (°F.) = the mean temperature of the air entering the meter;
p (inches Hg 32° F.) = its mean absolute static pressure; and
e (inches Hg 32° F.) = the mean partial pressure of the vapor in it.

XI. RESULTS OF THE EXPERIMENTS WITH THE HOLDER

1. GENERAL CHARACTERISTICS OF THE RUNS

Table 12 gives certain information regarding the 43 separate runs made with the holder, the runs being numbered and listed approximately in the order of increasing rate of flow, shown in column 3 in thousands of cubic feet per hour at standard density.

TABLE 12.—*Characteristics of the holder runs*

Number of run	Date, 1924	Rate of flow $\frac{Q_s}{1,000}$	Duration of run z	Fall of holder H_1-H_2	$\frac{100\epsilon}{H_1-H_2}$	Fall of temperature t_1-t_2	$\frac{100\delta\Delta}{\Delta}$
1	2	3	4	5	6	7	8
	Mo. Day		*Minutes*	*Feet*		°*F.*	
0.B	8 28	22.7	300	5.4	0.13	0.5	23.1
1	8 29	34.2	120	3.2	.31	.5	2.1
2	9 6	35.2	200	5.4	.04	.6	1.1
3	8 20	37.9	240	7.2		.2	
4	9 7	38.8	270	8.6	−.38	1.3	.6
5	9 10	52	105	4.2	−.83	−.5	3.0
6	9 11	55	100	4.3	1.69	−.2	.6
7	9 8	59	180	8.3	.33	.0	1.4
8	9 5	62	234	11.4	−.55	2.1	1.4
9	9 10	72	60	3.5	.08	.1	.9
10	8 27	74	210	12.4	.16	.8	10.8
11	9 5	80	150	9.5	−.26	1.9	3.4
11.B	8 29	84	150	9.9		.2	.9
12	8 21	104	180	14.7		−.1	
13	8 24	109	210	18.1		.9	
14	9 10	110	80	6.8	.40	−.3	2.2
15	8 11	110	150	13.0		.4	
15.B	8 25	114	150	13.5	−.29	−.1	1.4
16	8 31	127	135	13.7	−.51	.4	11.1
17	8 22	138	135	15.0		1.2	
18	8 23	151	135	16.2		.5	
19	8 26	173	100	13.7		.4	1.6
19.B	8 31	174	90	12.5		1.0	.4
20	9 4	184	125	17.9	−.40	.4	1.6
21	8 30	208	90	14.8	−.32	.1	.5
22	9 4	216	75	12.6	T	.4	.8
23	9 13	307	75	18.0	T	−.1	1.6
24	8 31	310	75	18.3	−.37	−.1	.3
25	9 11	310	60	14.5	.25	−.3	.3
26	9 3	318	60	14.7	−.53	−.2	1.0
27	9 12	319	60	15.1	.78	−.4	.6
27.B	9 3	338	51	13.5	−.52	.0	28.3
28	9 3	377	52	15.2	−.27	1.3	.5
29	9 1	393	59	18.3	−.20	−.4	1.3
30	9 9	394	40	12.2	.52	.4	2.4
31	9 11	406	45	14.3	.57	−.2	.8
32	9 13	418	44	14.3	T	−.7	.8
33	9 9	462	22	7.9	.43	.0	.7
34	9 2	464	40	14.5	−.45	.2	.6
35	9 12	485	28	10.6	T	.4	.7
36	9 12	486	38	14.5	.53	.0	1.6
37	9 1	501	36	14.2		−.5	1.3
38	9 3	612	34	16.2	−.26	−.2	5.5

Columns 4 and 5 give the duration of the run and the approximate value of the fall of the holder. Since the absolute error of a determination of the height does not depend on the magnitude of the preceding or following fall of the holder, the percentage error of (H_1-H_2) is

likely to be less for large than for small falls; but on the other hand, in a run of the long duration needed for a large fall at a low rate, the outside temperature may change enough to make the temperature control inadequate and the mean temperature uncertain, so that very long runs are undesirable. It thus appears that a smaller holder would have been more suitable for measuring the lower rates of flow and that higher accuracy in the results is to be expected at the higher rates of flow than at the lower.

In column 6, ϵ denotes the difference between the two mean values of the fall (H_1-H_2) found from the measurements at the two pairs of stations at the ends of two perpendicular diameters of the holder; and $100\,\epsilon/(H_1-H_2)$ is the percentage difference between the two estimates of (H_1-H_2). Where no value is given, only one pair of measurements was available; the letter T indicates that they were made by observation of the tapes at stations 1 and 3, and a blank means that they were made with the dial mechanisms at stations 2 and 4. If all the measurements were accurate, these accidental differences would vanish and, on the whole, the smaller the discrepancy between the two values of (H_1-H_2) the nearer their average is likely to be to the true value.

Column 7 gives the change of the observed mean temperature in the holder during the run. In 15 of the 43 cases the temperature rose a little, but it does not seem probable that there was ever any serious deficiency of saturation.

The numbers in column 8 serve as a criterion for estimating the constancy of the rate of flow in those runs in which an orifice was under test; they are to be interpreted as follows: The observed values of the differential Δ across the orifice were averaged for each of the periods into which the run was subdivided, usually 5 in number, and the difference between the highest and lowest of these averages is denoted by $\delta\Delta$. The percentage difference, $100\delta\Delta/\Delta$, is a measure of the inconstancy of the differential, aside from the more rapid fluctuations occurring within each period, and the accompanying variations of the rate of flow are about half as large as those of the differential.

It will be noticed that the variations were large in runs 0.B, 10, 16, and 27.B, and data on the Venturi or an orifice obtained in these runs must be regarded as of no value.

Where no figure is given in column 8, the rotary displacement meter was under test, and constancy of the rate of flow is less important for this than for the Venturi or an orifice.

In the case of run 7, the data on the holder are somewhat uncertain, the records not being clear, so that results from this run are also to be looked on with suspicion.

2. RESULTS OF TESTS OF THE ROTARY DISPLACEMENT METER

The results of the eight experiments in which air from the holder was discharged through the rotary displacement meter are exhibited in Table 13, in which the third column gives the values found for the correction factor or coefficient C_d. The mean value 0.994 indicates that, on the average, the meter ran 0.6 per cent fast in comparison with the holder. The departures of the individual values from the mean are shown in the last column; they average ± 0.4 per cent and do not appear to be systematically related to the rate of flow, given in the second column, or to the duration of the run or the fall of the holder, given in columns 4 and 5 of Table 12.

TABLE 13.—*Rotary displacement meter*

Number of run	Rate $\frac{Q}{1,000}$	C_d	$C_d - 0.994$
3	38	0.990	−0.004
12	104	.996	.002
13	109	1.001	.007
15	110	.985	−.009
15.B	114	.995	.001
17	138	.997	.003
18	158	.999	.005
19	173	.992	−.002
		.994	±.004

Table 14 contains the same results arranged chronologically, together with the temperature, t°F, of the air entering the meter (column 4); its absolute static pressure, p, in inches of mercury (column 5); and the approximate value of the pressure drop Δp across the meter, in inches of water (column 6).

TABLE 14

Number of run	Date, September, 1924	C_d	t	p (in Hg)	Δp (in Hg)
1	2	3	4	5	6
			° F.		
15	11	0.985	69.3	29.46	0.45
3	20	.990	66.7	29.30	.2
12	21	.996	66.5	29.34	.4
17	22	.997	74.8	29.26	
18	23	.999	71.4	29.50	1.0
13	24	1.001	71.4	29.32	.55
15. B	25	.996	70.1	29.39	.72
19	26	.992	70.7	29.35	1.23

There is no systematic relation between the variations of C_d and those of t, p, and Δp, but there seems to be a distinct run with the date, as given in column 2, the values of C_d increasing from the eleventh to the twenty-fourth of August, and decreasing on the two following days.

If this apparent connection between the value of C_d and the time when it was measured were real, it would indicate either a systematic change in the operation of the meter or a contrary change in the operations of measuring the outflow from the holder. If the change of C_d were simply progressive and always in the same direction, some interpretation might suggest itself, but we are inclined to regard the apparent connection as purely fortuitous.

If the measurements of rate of flow by the holder could be regarded as exact, the departures given in column 4 of Table 13 would have to be regarded as accidental errors of the rotary meter due to irregular running. But it seems much more likely that the apparent departures of C_d from its mean value represent, at least in the main, accidental errors in determining the rate of flow by means of the holder.

3. RESULTS OF THE TESTS OF THE VENTURI METER

The results of the tests of the Venturi meter are summarized in Table 15. Column 3 gives the approximate average value of the differential throughout the run, expressed in inches of water; column 4 gives it as a percentage of the absolute static pressure at the entrance to the Venturi; column 5 gives the value of the Reynolds number referred to the diameter and speed at the throat, as defined in note B; column 6 gives the values of C, the hydraulic discharge coefficient based on the upstream density and with the approach factor included; column 7 gives the corresponding values of the adiabatic coefficient C_a found from those of C by means of equation (15); and column 8 gives the departures of the separate values of C_a from the mean value of 0.990.

TABLE 15.—*Tests of the Venturi meter*

Number of run	Rate $\frac{Q_r}{1{,}000}$	Δ (in. H_2O)	$100\,x$	$\frac{Rd}{100{,}000}$	C	C_a	$C_a-0.990$
1	2	3	4	5	6	7	8
19	173	0.83			1.051		
19.B	174	0.91			0.996		
20	184	0.95			1.018		
21	208	1.07			1.089		
22	216	1.28			1.024		
23	307	2.76	0.69	6.6	1.016	0.992	0.002
24	310	2.88	0.73	6.6	1.012	.988	−2
25	310	2.82	0.70	6.6	1.012	.988	−2
26	318	2.96	0.74	6.8	1.010	.987	−3
27	319	2.98	0.75	6.8	1.021	.997	7
28	377	4.24	1.04	8.0	1.011	.987	−3
29	393	4.66	1.16	8.3	1.009	.988	−2
30	394	4.56	1.13	8.4	1.012	.991	1
31	406	4.95	1.23	8.6	1.010	.989	−1
32	418	5.10	1.27	9.2	1.015	.994	4
33	462	6.25	1.54	9.9	1.006	.988	−2
34	464	6.44	1.59	9.9	1.005	.986	−4
35	485	7.05	1.75	10.6	1.004	.987	−3
36	486	7.04	1.75	10.4	1.011	.993	3
37	501	7.58	1.87	10.3	1.004	.987	−3
38	611	11.25	2.76	12.9	1.005	.993	3
Means.				8.7		0.990	±0.003

In runs 19 to 22 the differential was too low to be measured at all accurately, as is evident from the large irregular variations of C; and 13 further values from tests at rates of flow below 130,000 cubic feet per hour varied still more. The Venturi was, in fact, too large to be used satisfactorily at rates below about 300,000 cubic feet per hour, under working conditions which did not permit of keeping the flow absolutely steady, and we shall therefore ignore all these runs up to No. 22 and confine our attention to those from No. 23 onward.

Run 27.B is also omitted from the tabulation because the rate of flow was very far from constant, as shown in column 8 of Table 12: it gave $C=0.665$.

The mean of the remaining 16 values of C_a is 0.9897. The departures of the separate values from 0.990 are given in column 8: they

average a little less than ± 0.003 and do not show any systematic variation with the rate of flow.

It will be noticed that 9 of the 16 values lie within the limits 0.987 to 0.989 and this makes it appear probable that if there had been a much larger number of experiments the mean would have been a little lower than 0.990. There are also other indications pointing in this direction.

In run 27, which gives the greatest departure from the mean, there was also the greatest discrepancy between the mean values of $(H_1 - H_2)$ for the two pairs of measuring stations at the holder. (See Table 12.) Furthermore, the discharge coefficient of the 20 per cent orifice, which was measured during this run, also came out higher than would be expected from comparison with neighboring values, so that it seems probable that the error of the holder measurement in this run was rather larger than usual. The value for run 38 is also under suspicion because the rate of flow was much more variable than in the other runs listed in Table 15. (See Table 12 column 8.)

There is no obviously valid principle for assigning weights to the various values, but if we omit runs 27 and 38 altogether, the remaining 14 values give a mean of 0.9889 with a mean departure from the mean of ± 0.002.

If we further confine our attention to those runs in which there were height measurements at all four stations and the agreement of the two means was as good as or better than the average, we have Nos. 24, 25, 28, and 29, for which the values of C_a are 0.988, 0.988, 0.987, and 0.988.

Thus everything points to the conclusion that the mean value 0.990, obtained by treating all the 16 values as of equal weight, is a little high, and we shall adopt the value $C_a = 0.989$ as being probably as close to the truth as can be got from these experiments.

The accidental variations of C_a shown in column 8 of Table 15 are the joint results of errors in the measurements at the holder and errors in the observations at the Venturi, especially in the measurement of the differential. It is impossible to separate the two kinds of error so as to estimate their relative importance, but it seems safe to conclude that neither kind of error was often greater than ± 0.3 per cent.

4. DISCUSSION OF THE RESULTS OBTAINED WITH THE VENTURI

A discharge coefficient is, by definition, the ratio of an observed rate of flow to a "theoretical" rate. In computing the theoretical rate of flow of a liquid through a Venturi, the density is treated as constant. In computing the theoretical rate of flow of a gas, by the thermodynamic method which leads to the definition of the adiabatic discharge coefficient C_a, the variation of density accompanying the change of pressure from entrance to throat is taken account of in the equations, by the aid of certain assumptions which are known to be very nearly true and need not detain us here. In both cases, the dissipation of energy by turbulence and skin friction is ignored, and the unavoidable presence of dissipation in any real experiment is the main reason for the failure of the theory, in either case, to represent the observed facts exactly.

Now the dissipation is due almost exclusively to the existence of viscosity; and the effect of viscosity on the nature of the motion of a fluid through a Venturi is fixed by the value of the Reynolds number. Hence we conclude that if a Venturi is tested with both air and water at the same value of the Reynolds number, the value of C_a found in the experiment on air should be very nearly identical with the coefficient $C_w = C/\sqrt{1-\beta^4}$, or the discharge coefficient with the approach factor not included, found in the experiment on water.

The particular Venturi now in question was tested only with air, but it is of some interest to compare the results with those of previous tests of similar Venturis with water; and for this purpose we may use a curve constructed by one of the present authors [4] in 1921, from the rather scanty published data then available regarding the discharge coefficients of Venturis for water. The curve, which represents C_w as a function of log R_d, is reproduced on a small scale in the Report of the A. S. M. E. Special Research Committee on Fluid Meters, 3d ed., p. 67, 1931; and the statement is there made that: "The curve represents the general run of the values of C (denoted here by C_w), and it seems likely that values read from it will always be accurate within 1 per cent."

In the present instance, the mean value of R_d was 870,000 (Table 15, column 5) and at this point the reading from the curve is $C_w = 0.9874$ as compared with our mean value $C_a = 0.990$ or the more probable value 0.989.

At the limiting values $R_d = 660{,}000$ and 1,290,000, the curve gives $C_w = 0.9864$ and 0.9887; and in view of the accidental errors shown by column 8 of Table 15, it is not surprising that our values of C_a should fail to show any evidence of systematic variation with the rate of flow.

5. DISCHARGE COEFFICIENTS OF THE ORIFICES

Only the four smallest orifices were tested against the holder, and the results obtained are collected in Tables 16 and 17. They are given as values of "the hydraulic discharge coefficient based on the upstream density with the approach factor included"; that is, values of C computed by means of equation (14) of Section X, 5.

The differential, in per cent of the upstream absolute static pressure, is given as 100 x. Since one atmosphere is equivalent to about 1,030 cm. of water and the static pressure was never far from atmospheric, the differentials, as actually measured in centimeters of water, were about ten times the values given for 100 x. If expressed in inches of water, they would be about four times the values of 100 x.

Values of C from runs 0.B, 10, 16, and 27.B are omitted as worthless because the rate of flow was very inconstant. (See Table 12, column 8.) A value from run 7 is also omitted because the records of the measurements on the holder are not clear.

The three values in parentheses are also to be disregarded—in run 1, because there was evidently some mistake of recording, though it could not be found and corrected; and in runs 11 and 15.B, because the differential (about 0.8 inch) was too small for accurate measurement.

[4] E. Buckingham.

In order to compare the remaining values of C with the results of other observers, further computations are necessary but they will not be given till a later section.

TABLE 16.—*Discharge coefficients of 5 and 10 per cent orifices*

Run	Rate $\frac{1{,}000 \text{ cu. ft.}}{\text{hour}}$	5 per cent		10 per cent	
		C	$100\,x$	C	$100\,x$
1	34	(0.366)	1.85		
2	35	.582	.76		
4	40	.589	.93		
5	52			0.597	0.38
6	55	.600	1.65		
8	62	.601	2.03		
9	72	.602	2.69		
11 B	84	.591	3.95		
14	110			.597	1.59

TABLE 17.—*Discharge coefficients of 20 and 30 per cent orifices*

Run	Rate $\frac{1{,}000 \text{ cu. ft.}}{\text{hour}}$	20 per cent		30 per cent	
		C	$100\,x$	C	$100\,x$
11	87	(0.632)	0.21		
15 B	114			(0.628)	0.19
19	174	.605	1.07		
19 B	175	.610	1.00		
20	184	.614	1.07		
21	209	.610	1.38		
22	216	.617	1.42		
23	307			.633	1.34
24	311	.608	3.27		
25	311	.609	3.22		
26	319	.608	3.35		
27	320	.612	3.43		
28	378	.604	4.68		
29	395	.603	5.17		
30	396	.606	5.07		
31	407	.605	5.47		
32	418			.633	2.43
33	463			.630	2.91
34	466			.629	2.99
35	485			.628	3.29
36	488			.630	3.32
37	503			.618	3.49
38	614			.627	5.05

XII. COMPARISON OF THE ORIFICES WITH THE VENTURI

The time during which the holder was available for experimental work was not long enough for making absolute tests of all the orifices, so a more expeditious method had to be adopted. It consisted in running air though an orifice and the Venturi in series and treating the Venturi as a secondary standard, its discharge coefficient having been determined in the tests against the holder.

1. EXPERIMENTAL PROCEDURE

The intake of the booster was disconnected from the holder and left open so that air from outside could be forced into the line, and the rotary displacement and wet drum meters were by-passed, to avoid pulsations in the flow. The orifice to be tested was put in position; a pair of the water manometers was connected to the pressure taps 12 inches upstream and 6 inches downstream; and a second pair was connected to the entrance and throat piezometer rings of the Venturi.

After these preliminaries, the booster was started and brought up to a constant speed; and as soon as a steady state had been established, with the water columns as nearly at rest as could be hoped for, the manometers were shut off simultaneously. The wet and dry bulb temperatures and the pressures were then read and recorded, together with the barometric pressure.

These operations were repeated once or twice before changing the speed of the booster or going on to a different orifice, and the average of the results was treated as a single test or run.

2. COMPUTATIONS

Similar observations are made at the orifice and at the Venturi, and symbols that refer to the Venturi may be distinguished by subscript v. At the orifice, let:

p = the absolute static pressure at the upstream tap;
t = the dry bulb temperature;
ρ = the density of the air at p, t;
Δ = the differential;
d = the diameter of the orifice; and
C = the hydraulic discharge coefficient, based on the upstream density and with the approach factor included.

Let the corresponding quantities for the Venturi be denoted by p_v, t_v, etc., d_v being the diameter of the throat. The value of C_v is assumed to be known from the holder experiments, and C is the quantity sought.

When the flow is steady, it is the same at both places and we have

$$C\frac{\pi}{4}d^2\sqrt{2\rho\Delta}=C_v\frac{\pi}{4}d_v^2\sqrt{2\rho_v\Delta_v},$$

or

$$C=C_v\left(\frac{d_v}{d}\right)^2\sqrt{\frac{\rho_v\Delta_v}{\rho\Delta}} \tag{20}$$

The diameters, d and d_v, have been measured, once for all. The observed differentials, Δ and Δ_v, appear only in a ratio so that with the manometers all at nearly the same temperature, no reduction to standard temperature is needed.

The ratio of the densities is found by means of the equation

$$\frac{p}{\rho T}=\text{constant} \tag{21}$$

This would not be permissible if the vapor content of the air varied between the orifice and the Venturi; but the psychrometers showed

that the air was always less than saturated, so that condensation was impossible; and, on the other hand, no water could be taken up because the line was dry; the composition of the mixture was therefore constant.

Upon setting $T=(458+t)$ in equation (21) (see Section X, 3) we now have

$$\frac{\rho_v}{\rho}=\frac{p_v(458+t)}{p(458+t_v)} \tag{22}$$

and it remains only to consider the value of C_v.

Assuming the constant mean value $C_a=0.989$ obtained from the tests of the Venturi against the holder (Section XI, 3), we have by equation (15) (Section X, 6)

$$C_v=0.989\left[\frac{3.5\,(r^{1.2}-r^{1.4})}{(1-r)\,(1-\beta^4 r^{1.2})}\right]^{1/2} \tag{23}$$

in which $\beta=0.4823$ is the diameter ratio of the Venturi and, in our present notation,

$$r=\frac{p_v-\Delta_v}{p_v} \tag{24}$$

with p_v and Δ_v expressed in the same units.

Upon making these various substitutions in equation (20), we obtain the required value of C.

3. RESULTS OF THE COMPARISONS

In testing the smaller orifices, the differential was lower at the Venturi than at the orifice and with the large orifices this relation was inverted. In either case, the precision of the result was limited by the accuracy with which the smaller of the two differentials could be measured. There were, in all, 42 of these comparison tests, comprising 124 separate sets of readings, but those in which the smaller differential was less than 1.56 cm or 0.6 inch have been discarded as too unreliable to be worth reporting. The results of the remaining 26 runs are shown in Table 18.

TABLE 18.—*Orifices v. Venturi*

1	2	3	4	5	1	2	3	4	5
Area ratio × 100	Number of run	C	$100\,x$	Δ or Δ$_v$ cm H_2O	Area ratio × 100	Number of run	C	$100\,x$	Δ or Δ$_v$ cm H_2O
	10	0.595	2.98	1.56	40	30	0.681	0.62	6.42
	11	.592	5.14	2.77		31	.657	1.76	18.09
10	12	.589	5.74	3.13					
	13	.596	6.91	3.91	45	32	.681	.67	6.94
	14	.591	7.35	4.11		33	.679	1.73	18.46
	22	.609	1.52	3.25	50	34	.706	.38	4.01
20	23	.608	3.03	6.65		35	.702	1.34	14.22
	24	.601	6.47	14.90					
	25	.632	.90	4.64	55	36	.728	.37	3.85
30	26	.629	2.43	12.91		37	.729	1.00	10.63
	27	.627	3.51	19.03					
					60	38	.760	.79	8.33
					65	39	.801	.66	7.01
					70	40	.827	.51	5.34
					75	41	.909	.39	4.13
					80	42	1.005	.28	2.95
35	28	(.464)	(2.03)	(7.74)					
	29	.640	2.87	22.02					

The first two columns give the area ratio of the orifice, in per cent, and the serial number of the run. The third and fourth columns show the values found for C and the percentage differentials at which they were found. The last column gives the lower of the two differentials, expressed in centimeters of water, as measured.

In run 28 there was evidently a mistake in reading or recording the differential across the orifice, and the value of C may be disregarded.

XIII. DISCUSSION OF THE RESULTS OF THE EXPERIMENTS ON ORIFICES

Accurate standardization tests of a set of orifices are valuable to anyone who is to use these particular orifices for metering purposes. But however carefully the work may have been done, the results of a comparatively small number of tests, such as have been reported here, are of little general interest except as they confirm, correct, or extend the body of information about the discharge coefficients of orifices which is already publicly available. We have therefore to compare the discharge coefficients obtained in the present investigation with some of those already published by others.

In the present instance, the pipe was smooth and the orifices were carefully finished. Furthermore, the orifices were large, their diameters ranging from 5.2 inches upward, so that the remaining imperfections of the edges were very small relatively to the absolute sizes of the orifices. In the vital matter of geometrical shape, our apparatus was thus very closely comparable with the apparatus used by Witte [5] in some of his admirable experiments with water, and our results will therefore be compared with his.

Before this comparison can be instituted, some preliminary reductions are needed; for although the similarity of shape of the apparatus appears satisfactory, the experimental conditions differed in two respects.

In the first place, the points where the pressures were measured were not similarly situated. In Witte's experiments, the pressure connections were made in the corners between the wall of the pipe and the faces of the orifice plate, whereas in the present experiments, the pressures were taken off at points 12 inches upstream and 6 inches downstream. To make the results comparable, this difference must be allowed for by utilizing the observations on the longitudinal distribution of pressure, described above in Section IX.

In the second place, the discharge coefficient of an orifice for a gas varies with the pressure ratio. Hence it is necessary to allow for this effect of changing density by extrapolating from values measured at various finite values of the fractional differential, $\Delta/p_1=x$, to find the limiting value at $x=0$, which represents what would have been obtained if the density had remained constant during the flow through the orifice, as it does with water.

1. REDUCTION FOR CHANGE OF TAP LOCATION

In a given test, let Δ' be the observed differential, ρ' be the density at the observed upstream pressure, and C' be the discharge coefficient,

[5] R. Witte, Durchflusszahlen von Düsen und Staurändern, Techn. Mech. u. Thermodynamik, **1** Nos. 1, 2, 3; 1930.

computed from Δ' and ρ', together with the observed mass flow, M, and the known diameter, d. Let Δ'', ρ'', and C'' be the values that would have been obtained in the same test if a different pair of taps had been employed. Then we have, by definition,

$$M = C' \frac{\pi}{4} d^2 \sqrt{2\rho'\Delta'} = C'' \frac{\pi}{4} d^2 \sqrt{2\rho''\Delta''} \tag{25}$$

or

$$\frac{C''}{C'} = \sqrt{\frac{\rho'\Delta'}{\rho''\Delta''}} \tag{26}$$

Now the longitudinal variations of the upstream static pressure, within a few pipe diameters of the orifice, are, at most, only a few per cent of the drop through the orifice (see Tables 2 to 11); and in the present experiments, that drop was never as much as 8 per cent of the absolute static pressure. Hence the percentage difference of the two upstream static pressures was insignificant and for our present purposes equation (26) may be simplified to the form

$$\frac{C''}{C'} = \sqrt{\frac{\Delta'}{\Delta''}} \tag{27}$$

If the curve of pressure distribution, qualitatively illustrated in Figure 4, has been determined by experiment, the difference of pressure, Δ', between two taps at any distances from the orifice plate within the range of the experiments may evidently be found, in terms of the difference between the upstream and downstream minima, by readings from the curve. The same is true of the differential Δ'' between any second pair of taps, and we can thus find the ratio Δ'/Δ'' for any two pairs of taps. This may then be substituted in equation (27) and if one of the two discharge coefficients has been determined, the other may be computed from it.

The observations did not cover a sufficient length of pipe to give any information about the arrangement commonly known as "pipe taps," in which the pressure connections are made at points 2.5 D upstream and 8 D downstream, D being the pipe diameter; and our further considerations relate only to the region from 1 D upstream to 0.5 D downstream.

For this region, the composite data given in the final columns of Tables 2 to 11 were plotted against distances, as in Figures 5 and 6, and smooth curves were drawn through the two sets of points, for each orifice. Values of Δ'/Δ were read from the curves at several pairs of distances, the values for each pair were plotted against the area ratios of the orifices, and a second set of smooth curves was drawn. The two sets of curves were then readjusted until they appeared to give a representation of the observed facts which was as free as practicable from the influence of accidental errors of measurement.

Values of the reduction factor $\sqrt{\Delta'/\Delta''}$, required for use with equation (27), were obtained from these adjusted curves and the results are exhibited in Table 19, in which the notation is as follows:

C (12, 6) represents the value of the hydraulic discharge coefficient, based on the upstream density and with the approach factor included, as observed with the pressure taps 12 inches upstream and 6 inches downstream from the orifice.

C (24, 12) is the value that would have been found if the distances had been 24 inches and 12 inches, or approximately 1 D and 0.5 D; this combination has been called "throat taps."

C (3, 3) is the value that would have been found with the taps 3 inches or $D/8$ on each side of the orifice plate; this corresponds to the "flange taps" in B. S. Research Paper No. 49.[6]

C (1,1) is the value that would have been obtained if the taps had been 1 inch from the orifice plate; since we had no taps that were less than 1 inch, or $D/24$, from the orifice plate, this arrangement was the nearest we had to taking off the pressures right in the corner.

It may be noted that the values in Table 19 were obtained from the composite values in Tables 2 to 11, and that each one should not, in reality, be quite constant, because the pressure distribution curves varied with the rate of flow, as was illustrated by Figure 5. But over the length of pipe now in question, and over the range of differentials for which the reduction factors in Table 19 have been deduced, these variations are small and probably altogether insignificant in comparison with other unavoidable errors.

2. ALLOWANCE FOR VARYING DENSITY; THE EXPANSION FACTOR

Let us suppose that an orifice is tested with a liquid, and let K denote the discharge coefficient with the approach factor included, defined in terms of normal units by the equation

$$M = K\frac{\pi}{4}d^2\sqrt{2\rho\Delta} \tag{28}$$

in which M, d, ρ, and Δ have their usual meanings, but ρ does not require any identifying subscript because it is sensibly constant for any one liquid.

At low values of the Reynolds Number (small orifice, low speed, high viscosity) K varies with the rate of flow; but at high values, where the effects of viscosity are negligible, the value of K is constant and no longer dependent on the rate of flow.

If the same orifice is tested with a gas, such as air, we have (see equation 12, Section X, 5)

$$M = C\frac{\pi}{4}d^2\sqrt{2\rho_1\Delta} \tag{29}$$

but even though the Reynolds Number be so high as to make viscosity of no importance, C is not constant but decreases as the differential and the rate of flow are increased.

TABLE 19.—*Reduction factors for change of tap location*

Area ratio β^2	$\frac{C(24.12)}{C(12,6)}$	$\frac{C(3,3)}{C(12,6)}$	$\frac{C(1,1)}{C(12,6)}$
0.05	0.999	1.000	1.001
.10	.999	1.000	1.001
.20	.999	.999	1.000
.30	.998	.997	.999
.35	.998	.996	.998
.40	.998	.994	.997
.45	.999	.992	.995
.50	1.000	.989	.991
.55	1.002	.986	.987
.60	1.005	.982	.981
.65	1.012	.976	.975

[6] See footnote 3, p. 119.

If tests are carried out over a sufficient range of values of the fractional differential, $\Delta/p_1 = x$ (but all at high values of the Reynolds Number, where the effects of viscosity are insensible, as was true of all the tests recorded here), the results show that as x decreases, the values of C tend toward the fixed value K as a limit. It is therefore convenient to represent C in the form

$$C = KY \tag{30}$$

in which K is the constant discharge coefficient found by testing the orifice with water, and Y is the variable "expansion factor," introduced into the literature by E. S. Smith [7] to take account of the effect of the variations of density during flow through an orifice, which occur with a gas but are absent in the simpler case of a liquid.

The experiments described in this paper did not cover a sufficient range of values of x to permit of determining the form of Y, but we may utilize later information obtained from experiments on natural gas, conducted at Los Angeles in 1929 by one of us,[8] as part of an investigation being carried out by a committee of the natural gas department of the American Gas Association, in cooperation with the National Bureau of Standards.

Similar information is contained in B. S. Research Paper No. 49[9] but the Los Angeles results are to be preferred, because the working conditions were more favorable as regards steadiness of flow and permitted of higher precision in the measurements.

In the Los Angeles experiments, the orifices were tested in new commerical steel pipes of 16, 8, and 4 inch nominal diameter, with honeycombs of smaller pipes placed from 10 D to 15 D ahead of the orifices; and pressure measurements were made at taps distant 1 inch from the orifice plates.

So far as concerns the expansion factor, the results of the tests in the 16 and 8 inch pipes were consistent, and the change of relative tap distance from $D/16$ to $D/8$ made no appreciable difference: but the further change to $D/4$ did appear to have a slight effect, and we shall confine our attention to the tests in the two larger pipes. These were carried out on 17 orifices with diameter ratios from 0.124 to 0.869, or area ratios between 1.5 and 76 per cent.

When the values of C for each orifice were plotted against the values of x at which they were measured, the result was a diagram, such as is illustrated, qualitatively, by Figure 7.

For the two orifices with diameter ratios below $\beta = 0.2$ the curves were sligltly convex upward, but for the remaining 15, for which $0.3 < \beta < 0.87$, the series of plotted points showed no evidence of systematic departure from straight lines. The expansion factor was therefore of the form

$$Y = 1 - Bx$$

with B a constant for each orifice but increasing with β.

Table 20 gives the diameter ratios, the number of tests on each orifice, and the range of values of x over which the tests were distributed.

[7] Ed S. Smith, jr., "Quantity-Rate Fluid Meters," paper presented at the annual meeting of the A. S. M. E., New York, December, 1929. Trans. A. S. M. E. paper No. HYD-52-7b, 52, No. 30.
[8] H. S. Bean.
[9] See footnote 3, p. 119.

TABLE 20.—*Los Angeles tests*

Pipe diameter D (inches)	Diameter ratio β	Number of tests	x	
			Minimum	Maximum
15.38	0.390	26	0.009	0.46
	.553	27	.010	.40
	.650	21	.007	.26
	.699	21	.006	.20
	.748	14	.009	.13
	.796	11	.014	.11
	.829	18	.02	.08
	.861	11	.02	.06
8.05	.310	21	.03	.47
	.497	21	.02	.48
	.621	21	.02	.44
	.683	28	.02	.51
	.745	29	.02	.53
	.807	31	.02	.57
	.869	29	.02	.65

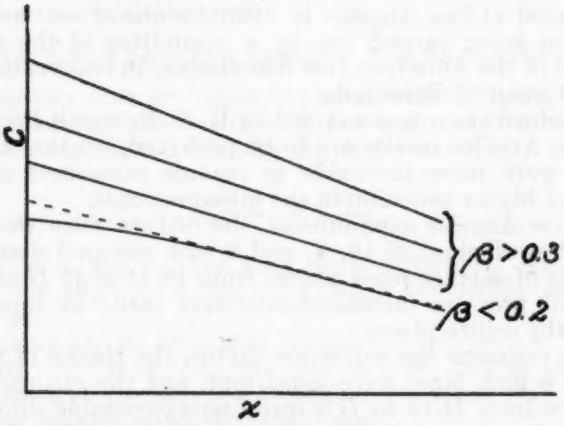

FIGURE 7.—*Qualitative relation between the discharge coefficient C and the differential-static pressure ratio x*

The slopes of all the 15 straight lines obtained from these tests may be represented, within the precision of the measurements, by setting

$$Y=1-(0.31+0.35\beta^4)x \tag{31}$$

but this equation is not directly applicable to experiments on air; for the expansion factor depends on the specific heat ratio, $C_p/C_v=\gamma$, as well as on x, according to some equation

$$Y=f(x, \gamma) \tag{32}$$

and the specific heat ratio of the Los Angeles gas was computed from the average chemical analysis to be 1.283, whereas for air it is 1.40.

It may be shown,[10] however, that when x is small, equation (32) is, very nearly, of the more definite form

$$Y=\psi\left(\frac{x}{\gamma}\right) \tag{33}$$

[10] See note 7, p. 133.

and this means that equation (31) may be regarded as a special case of the more general equation

$$Y = 1 - 1.283(0.31 + 0.35\beta^4)\frac{x}{\gamma}$$

or

$$Y = 1 - (0.40 + 0.46\beta^4)\frac{x}{\gamma} \tag{34}$$

applicable to all nearly ideal gases.

In the case of air, with $\gamma = 1.40$, the general equation reduces to

$$Y = 1 - (0.29 + 0.33\beta^4)x \tag{35}$$

and this equation will be used for finding values of K from our observed values of C.

3. WITTE'S VALUES OF K FOR SMOOTH PIPES

The experiments now in question, which are only a small part of Witte's extensive researches on nozzles and orifices, were carried out in smooth pipes, and the orifice plates were finished with great care to have the upstream corner of the hole perfectly square and sharp. The results are so important that it is advisable to quote them here and they are given in Table 21, the figures in colums 1, 2, 4, and 5 being copied directly from Table 7 of the original paper.[11]

The four pipes used were of approximately 2, 4, 8, and 12 inches in diameter, and the 24 orifices tested had the area ratios shown in column 2 of Table 21. Each orifice was tested at various rates of flow, the numbers of separate tests being given in column 4, and the resulting average values of K in column 5.

TABLE 21.—*Witte's values of K for perfect orifices in smooth pipes*

Diameter of pipe [mm]	Area ratio	Diameter ratio	Number of tests	K (obs.)	$0.599 + 0.39\,\beta^4 = K$ (calc.)	K(obs.) $-K$(calc.)
1	2	3	4	5	6	7
	Per cent	β				
	9.2	0.303	7	0.602	0.602	0.000
310	23.4	.484	12	.621	.620	.001
	33.7	.580	12	.642	.643	−.001
(12″.2)	46.8	.684	9	.685	.684	.001
	55.0	.742	6	.717	.717	.000
	5.1	.226	22	.599	.600	−.001
	9.9	.315	25	.602	.603	−.001
	20.2	.450	17	.615	.615	.000
200	30.3	.550	15	.6365	.635	.001
	39.7	.630	7	.661	.660	.001
(7″.9)	49.0	.700	17	.693	.693	.000
	49.5	.703	6	.693	.694	−.001
	64.2	.801	30	.770	.760	.010
	70.1	.837	21	.808	.791	.017
100	36.5	.604	10	.651	.651	.000
	56.9	.754	5	.726	.725	.001
(3″.94)	61.0	.781	12	.749	.745	.004
	70.5	.840	12	.812	.793	.019
	17.6	.420	22	.613	.611	.002
	41.0	.640	13	.663	.665	−.002
50	51.9	.720	29	.704	.704	.000
	60.9	.780	29	.749	.744	.005
(1″.97)	70.7	.841	26	.812	.794	.018
	81.0	.900	14	.907	.855	.052

[11] See note 5, p. 130.

If all the measurements were exact, the points obtained by plotting the values of K against any power of the area ratio should evidently lie on some smooth curve; and when the observed values of K are plotted against β^4, or the square of the area ratio, the points for all diameter ratios up to $\beta=0.75$ do lie extremely close to the straight line represented by the equation

$$K(\text{calc.})=0.599+0.39\beta^4 \tag{36}$$

Values computed from equation (36) are shown in column 6 of the table and the differences, $K(\text{obs.})-K(\text{calc.})$, in column 7. Up to $\beta=0.75$, the greatest departure of the observed values from the linear equation (36) is one-third per cent, and the average departure is only about 0.1 per cent.

The equation

$$K=0.598+0.40\beta^4 \tag{37}$$

is about as good as equation (36) for medium values of β, but the straight line is a little too steep and the coefficient of β^4 is slightly but distinctly too high.

Since the diameter ratios of Witte's orifices did not correspond exactly to those of the orifices used in our experiments, a comparison between the two sets of results requires the use of some sort of interpolation formula, and for this purpose equation (36) will be taken as representing the aggregate of Witte's results, for $\beta \leqq 0.75$, within their experimental accuracy.

4. COMPARISON OF THE CHICAGO RESULTS FOR AIR WITH WITTE'S RESULTS FOR WATER

To make one of our values of C comparable with the corresponding value of K obtained by Witte, it has first to be multiplied by $C(1, 1)/C(12, 6)$ to take account of the difference of tap location; this product has then to be divided by the expansion factor Y, so as to give the value of

$$K=C(12, 6)\times\frac{C(1, 1)}{C(12, 6)}\div Y \tag{38}$$

The mean values of C from the holder tests, reduced in this manner, are exhibited in Table 22. Columns 3 and 4 give the mean values of C and 100 x, found by averaging the separate values in Tables 16 and 17; column 5 gives the factor for change of tap location, from Table 19; column 6 gives the value of the expansion factor for the given values of β and x, computed from equation (35); column 7 gives the resulting value of K for taps distant $D/24$ from the orifice plate; and column 8 gives the value of K from equation (36), which represents Witte's results for taps in the corner.

TABLE 22.—*Orifice coefficients measured by the holder, compared with Witte's results for water*

Area ratio	Number of tests averaged	$C(12, 6)$	$100\,x$	$\frac{C(1, 1)}{C(12, 6)}$	Y	K (obs.)	K Witte equ. (36)
1	2	3	4	5	6	7	8
Per cent							
5	6	0.594	2.00	1.001	0.9942	0.598	0.600
10	2	.597	0.99	1.001	.9971	.599	.603
20	13	.6085	3.05	1.000	.9908	.614	.615
30	8	.6285	3.10	0.999	.9901	.634	.634

Our values of C, and therefore of K, are much less reliable for the two smaller than for the two larger orifices; for the holder was better adapted to testing the 20 and 30 per cent orifices and there were more tests. The values of K, computed in accordance with equation (38) from the mean values of C, are thus intrinsically more probable than for the two smaller orifices, and they are in very good agreement with Witte's values as represented by equation (36).

The values of C obtained from the comparison runs in which the Venturi was used as the standard have also been reduced in the manner described above, and the resulting values of K for the 10 to 65 per cent orifices are exhibited in Table 23.

TABLE 23.—*Orifice coefficients measured by the Venturi meter compared with Witte's results for water*

Area ratio	Number of tests averaged	C (12, 6)	$100\,x$	K (obs.)	K (calc.) by equation (36)	K (calc.) by equation (39)	K (calc.) by equation (40)
1	2	3	4	5	6	7	8
Per cent							
10	5	0.5926	5.62	0.603	0.603	0.601	0.602
20	3	.6060	3.67	.613	.615	.613	.614
30	3	.6293	2.28	.633	.634	.634	.634
35	1	.640	2.87	.645	.647	.647	.647
40	2	.669	1.19	.670	.661	.663	.662
45	2	.680	1.20	.680	.678	.680	.679
50	2	.704	.86	.700	.697	.700	.699
55	2	.7285	.68	.721	.717	.721	.719
60	1	.760	.79	.748	.737	.745	.742
65	1	.801	.66	.783	.764	.770	.767

Columns 3 and 4 contain the means of the separate values of C and of $100\,x$ in columns 3 and 4 of Table 18; and the values of K deduced from these means are given in column 5. Column 6 gives the values of K computed from equation (36) or

$$K = 0.599 + 0.39\,\beta^4 \tag{36}$$

which represents Witte's results up to $\beta = 0.75$; and columns 7 and 8 give the corresponding values from the slightly modified equations

$$K = 0.597 + 0.41\,\beta^4 \tag{39}$$

and

$$K = 0.598 + 0.40\,\beta^4 \tag{40}$$

Our mean values of K from both Table 22 and Table 23 are plotted against values of β^4 in Figure 8, in which the two straight lines represent equations (36) and (39).

Table 23 and Figure 8 do not include values of K for the 70, 75, and 80 per cent orifices, although observed values of C are given in Table 18. Our failure to get satisfactory observations of the longitudinal

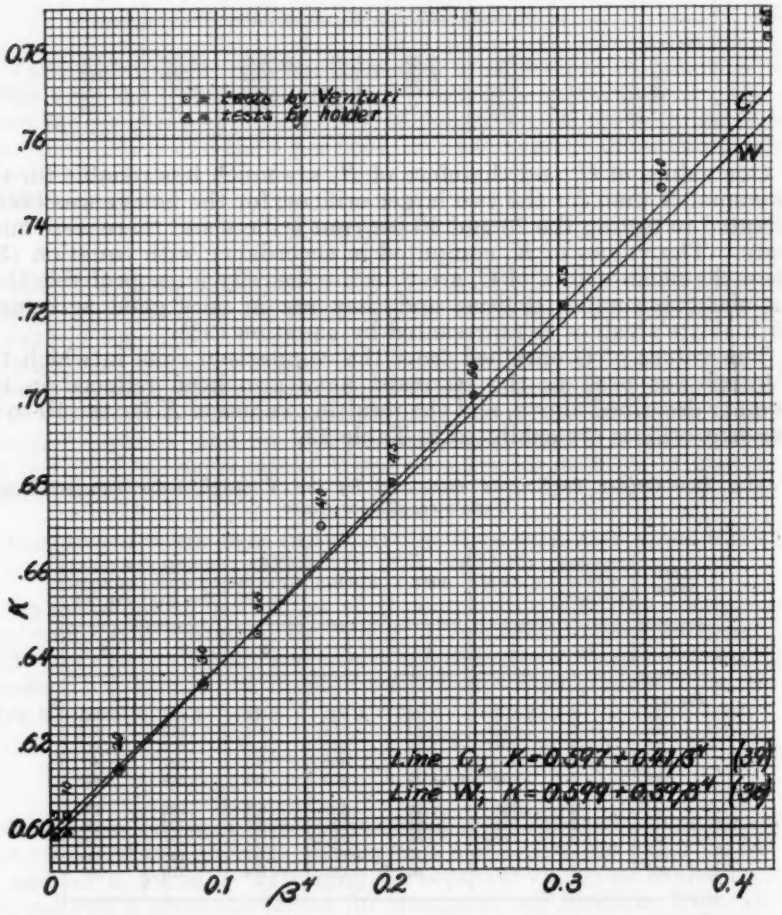

FIGURE 8.—*Results of orifice coefficient determinations by Chicago tests compared with the line W, representing the results of Witte's tests*

distribution of pressure with these large orifices made it impossible to extend Table 19 beyond the 65 per cent orifice.

5. CONCLUSIONS FROM THE FOREGOING COMPARISON

Examination of Tables 21, 22, and 23 and Figure 8 leads to the following conclusions:

(*a*) The values of K, deduced from our experiments with the holder by utilizing the observations on the longitudinal distribution of

pressure and the information regarding the expansion factor furnished by the Los Angeles experiments with natural gas, agree with the values of K from Witte's experiments with water, within the accidental errors of experiment. The agreement is closest for our 20 and 30 per cent orifices, and these are the ones on which our tests were most numerous and most reliable. This comparison does not go beyond an area ratio of 30 per cent, for which $\beta = 0.548$.

(*b*) When the tests on the larger orifices, with the Venturi as the standard, are also taken into account, it appears that, up to and including the 55 per cent orifice, equation (39) reproduces our results somewhat better than equation (36); or, graphically, the best straight line through our points is a little steeper than the best line through Witte's points.

(*c*) The value of K for our 40 per cent orifice is based on the mean of two rather discordant values of C (see Table 18), of which at least one must have been affected by some unusually large error. Omitting this value, we have for the remaining 8 orifices, up to and including the 55 per cent orifice, 4 values of K from experiments with the holder and 7 values from comparisons with the Venturi. There are also the 17 values given in Table 21 from Witte's experiments with area ratios up to 56.9 per cent. The mean equation (40) reproduces all these 28 values of K with an extreme departure of 0.5 per cent, for one of Witte's orifices and one of ours, and an average departure of somewhat less than 0.2 per cent.

(*d*) As the area ratio increases beyond about 57 per cent ($\sqrt{0.57} = 0.75+$), the value of K increases faster than before and the simple linear relations (36) and (39) no longer hold. This is evident from the data in Tables 21 and 23.

6. REMARKS

The difference between the lines W and C of Figure 8 appears to be significant and not merely accidental, but we are not, at present, able to interpret this difference with certainty.

Increasing the roughness of the wall of the pipe increases the slope of the line, and it is possible that our 24-inch pipe was rougher than the pipes used by Witte, to a sufficient degree to account for the difference mentioned; but this interpretation does not seem satisfactory. For aside from the fact that our pipe was actually very smooth, increasing the roughness of the pipe not only makes the line $K = f(\beta^4)$ steeper, but shifts it bodily upward, whereas the lines W and C of Figure 8 cross at the point where our observations are most trustworthy.

We are more inclined to attribute the difference of slopes to the different locations of the pressure connections, for the following reasons:

In an earlier paper,[12] Witte gives the results of measurements of the rise of pressure from the upstream minimum to the plate, and of the fall from the plate to the downstream minimum. The values are given only in the form of small-scale curves, but we can get from them approximate values which correspond to a continuation, right up to the faces of the plate, of our observations on the longitudinal distribution of pressure which stopped 1 inch away.

[12] Z. V. D. I., 72, No. 42, p. 1493, 1928.

On the downstream side, the points thus obtained lie on entirely natural extrapolations from our series of observed points; but on the upstream side there is a systematic difference. For the small diameter ratios, Witte's points are lower than would be expected from a tentative extrapolation of our curves, whereas at the large diameter ratios they are much higher. The indications are that shifting the pressure taps from our last position, 1 inch from the plate, to Witte's position, in the corner, will decrease the observed differential, slightly for small area ratios but increase it considerably for large ratios.

The values of C or K computed from the observed differentials will, of course, be affected in the opposite sense; and this is the sense in which Witte's values of K, represented by line W in Figure 8, differ from ours, which are represented by line C.

It is not possible to pursue this analysis quantitatively, without further detailed investigation of the variations of pressure close to the plate, but it is evident that such investigations are highly desirable.

7. GRAPHICAL REPRESENTATION OF TABLES 16, 17, AND 18

Tables 22 and 23 and Figure 8 deal only with mean values, and to give an idea of the consistency of our separate determinations of the discharge coefficients with one another and with the results of the Los Angeles experiments, embodied in equation (35), Figure 9 has been prepared.

The ordinates are values of $C \equiv C\ (12, 6)$, observed with the pressure taps 12 inches upstream and 6 inches downstream; and the abscissas are the values of 100 x at which the observations were made.

Each point represents a single value of C; the points surrounded by triangles are values obtained in the tests with the holder, and their coordinates are taken from Tables 16 and 17; and the points in the circles are values from the comparison runs against the Venturi, their coordinates being taken from Table 18. The points for each orifice are grouped, more or less closely, about a straight line; and the number at the right-hand end of the line is the area ratio of the orifice, in per cent.

The intercept and slope of the line for each orifice were determined as follows : It was first assumed that if the taps had been 1 inch from the plate, the value of

$$K \equiv K\ (1, 1) = \text{limit of } C\ (1, 1) \text{ as } x \doteq 0$$

would have satisfied equation (39), represented by line C in Figure 8; and the value of K (1, 1) was computed for the given value of β, from equation (39).

The corresponding value of

$$K(12, 6) = \text{limit of } C(12, 6) \text{ as } x \doteq 0$$

was then found from the relation

$$K(12, 6) = K(1, 1) \div \frac{C(1, 1)}{C(12, 6)}$$

by taking the value of $C(1, 1)/C(12, 6)$ from the last column of Table (19). This gave the required intercept of the straight line on the C axis.

The expansion factor at $x=0.1$ was next computed from (35), and when multiplied by the value of $K(12, 6)$ already found, this gave the ordinate of the line at $x=0.1$. The two points thus determined, for $x=0$ and $x=0.1$, were then plotted and the straight line was drawn through them.

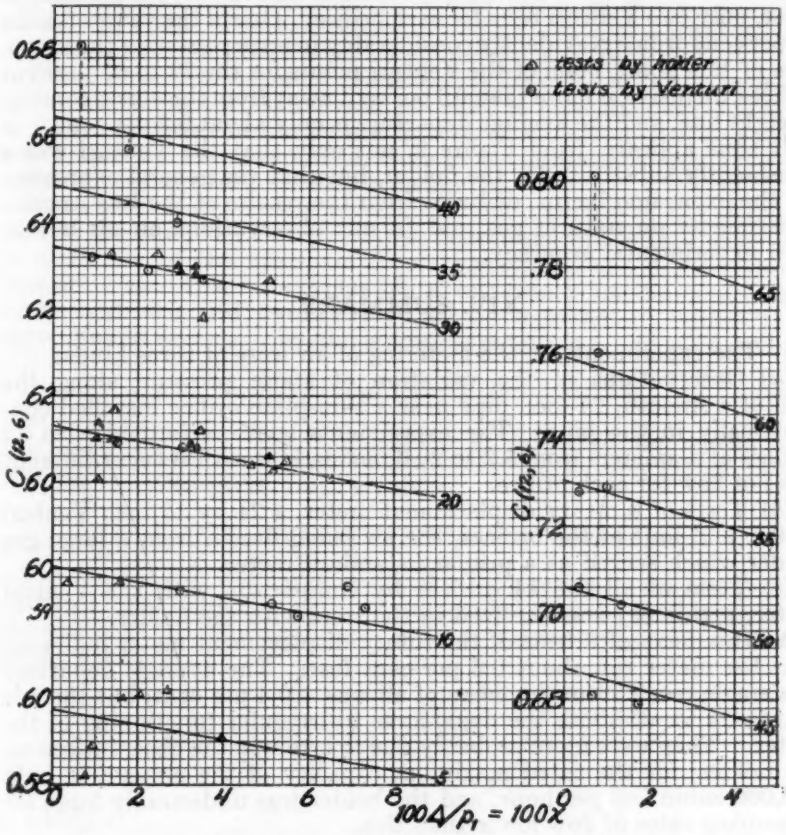

FIGURE 9.—*Actual test results plotted from Tables 16, 17, and 18*

The numbers at the right of the slanting lines are values of $100\beta^2$.

For the 5 per cent orifice ($d=5.2$ inches), the rate of flow attainable was limited by the maximum pressure the booster could give, and the greatest differential that could be reached at the Venturi was less than 0.3 inch. Since this was too low for accurate measurement, the Venturi tests were worthless and are not shown. The rates of flow were also too low to be measured satisfactorily with so large a holder, and the points from the holder runs are considerably scattered.

For the 10, 20, and 30 per cent orifices, there are points representing the results of both kinds of test. The higher rates of flow were more favorable to accuracy, and the points are less scattered than for

the 5 per cent orifice. Two of the Venturi points for the 10 per cent orifice are rather far out of line with the others; but the greatest differential at the Venturi was less than 1.7 inches, and the greatest departure of any of the points from the straight line corresponds to an error of only about 0.04 inch in reading this differential.

Aside from these two points, the Venturi and holder points are mixed indiscriminately, for all three orifices, and the use of the Venturi as a secondary standard, after calibration by the holder, is justified.

For the larger area ratios, there are no tests with the holder and, at most, only two Venturi tests for each orifice. One of the values for the 40 per cent orifice is evidently considerably in error; but with the exception of this point, none of the Venturi points for the 20 to 60 per cent orifices, inclusive, is more than 0.6 per cent away from the corresponding straight line, and the average departure is only about 0.2 per cent.

It thus appears, from Figure 9, not only that the Venturi was a satisfactory substitute for the holder, but that the general expression for the expansion factor, deduced from the results of the Los Angeles experiments on natural gas, did fit our observations on air within their experimental accuracy.

XIV. SUMMARY

1. The experiments on the metering of air were of three kinds:

(*a*) Observations of the variation of static pressure along the wall of a smooth, 24-inch pipe near a thin-plate orifice installed concentrically in the pipe. The experiments were performed with 14 orifices of diameters from 5.2 to 20.6 inches, and with several different rates of flow for each orifice.

(*b*) Tests of a rotary displacement meter, a 24 by 12 inch Venturi meter, and four of the orifices, the air being drawn from a large gas holder which served as a primary standard meter.

(*c*) Tests of all the 14 orifices by comparison with the Venturi meter, previously standardized in the tests with the holder.

2. The mean of 8 tests of the rotary displacement meter indicated that the meter ran about 0.6 per cent fast. The average departure of a single result from the mean of all was ± 0.4 per cent, but there is no reason to attribute the departures to irregular functioning of the meter. They were more probably due to errors in the observations on the holder; for the rated maximum capacity of the meter was only 200,000 cubic feet per hour, and the holder was undesirably large for measuring rates of flow lower than this.

3. The results of the comparisons of the Venturi with the holder, at rates of flow between 300,000 and 600,000 cubic feet per hour, indicated that within this range, a determination of rate of flow from observations on the rate of fall of the holder which appeared intrinsically satisfactory, was usually accurate to about ± 0.3 per cent. This corresponded to an accuracy of somewhat better than ± 2 degrees F. in the temperature, but in reality the limit of accuracy was set by errors in measuring the height rather than the temperature.

4. The results of the comparisons of the orifices with both the holder and the Venturi have been expressed as values of the discharge coefficient C, defined by the equation

$$M = CA\sqrt{2(p_1 - p_2)\rho_1}$$

in which M lbs./sec. is the rate of flow as measured by the fall of the holder or by the standardized Venturi; A square feet is the area of the orifice; p_1 and p_2 poundals per square foot are the pressures observed at the upstream and downstream pressure taps; and ρ_1 lbs./ft.^{3} is the density of the air at the pressure p_1 and at the upstream temperature.

By utilizing the results of the experiments of group A and of later experiments on natural gas, the values of C have been so reduced as to be comparable with the values for water obtained by R. Witte with apparatus that was very nearly, though not exactly, geometrically similar to ours. The agreement of the two sets of values is very close in the region where our own values are most reliable.

There appear to be small systematic differences, which increase to about 0.7 per cent when the ratio of orifice to pipe diameter is as large as 0.75, but they can not be interpreted or explained with any confidence until the variations of pressure in the immediate vicinity of the orifice plate have been further investigated.

If we let $\beta \equiv d/D$ denote the ratio of the diameter of the orifice to that of the pipe, and $x \equiv (p_1 - p_2)/p_1$ denote the differential expressed as a fraction of the upstream absolute pressure; and if the pressure taps are 1 inch from the orifice plate, our results for diameter ratios between $\beta = 0.3$ and $\beta = 0.77$ may all be represented, within their experimental accuracy, by the empirical equation

$$C = (0.597 + 0.41\beta^4)[1 - (0.29 + 0.33\beta^4)x]$$

The experiments did not go beyond $x = 0.08$, but the equation is probably valid for considerable higher values of x. For higher values of β, the equation gives too low values.

Note A.—THE ADIABATIC DISCHARGE COEFFICIENT

The "adiabatic discharge coefficient" C_a results from computing the theoretical mass flow on the assumptions that the fluid is an ideal gas and that the expansion from p_1 to p_2 is isentropic. It is defined by the equation

$$M = C_a \frac{\pi}{4} d^2 \left[\frac{2\gamma}{\gamma - 1} p_1 \rho_1 \frac{\left(\frac{p_2}{p_1}\right)^{\frac{2}{\gamma}} - \left(\frac{p_2}{p_1}\right)^{\frac{\gamma+1}{\gamma}}}{1 - \beta^4 \left(\frac{p_2}{p_1}\right)^{\frac{2}{\gamma}}} \right]^{\frac{1}{2}}$$

in which

M = the mass flow;
d = the diameter of the Venturi throat;
p_1, p_2 = the observed upstream and downstream pressures;
ρ_1 = the upstream density;
$\beta = d/D$ = the diameter ratio; and
$\gamma = C_p/C_v$ = the specific heat ratio.

The hydraulic discharge coefficient C, based on the upstream density and with the approach factor included, is defined by the equation

$$M = C \frac{\pi}{4} d^2 \sqrt{2\rho_1 (p_1 - p_2)}$$

By equating these two expressions for M we get the relation

$$\frac{C_a}{C}=\left\{\frac{\gamma-1}{\gamma}\cdot\frac{\left(1-\frac{p_2}{p_1}\right)\left[1-\beta^4\left(\frac{p_2}{p_1}\right)^{\frac{2}{\gamma}}\right]}{\left(\frac{p_2}{p_1}\right)^{\frac{2}{\gamma}}-\left(\frac{p_2}{p_1}\right)^{\frac{\gamma+1}{\gamma}}}\right\}^{\frac{1}{2}}$$

Or if we let $p_2/p_1=r$ and set $\gamma=1.4$ as for air, we have

$$\frac{C_a}{C}=\left[\frac{2(1-r)\left(1-\beta^4 r^{\frac{10}{7}}\right)}{7\left(r^{\frac{10}{7}}-r^{\frac{12}{7}}\right)}\right]^{\frac{1}{2}}$$

or equation (15) of Section X, 6.

Note B.—THE REYNOLDS NUMBER

In the case of a stream of fluid along a round pipe, the Reynolds number is usually defined as the value of the expression

$$R_D=\frac{DS_1\rho_1}{\mu} \tag{1}$$

in which D = the diameter of the pipe; S_1 = the mean linear speed along the pipe; ρ_1 = the density of the fluid; and μ = its viscosity. All the quantities are understood to be measured by some system of normal units, such as the British absolute or the cgs., and since the expression is of zero dimensions, its numerical value is the same in all such systems.

The mean speed has to be determined indirectly from the rate of discharge M, by means of the equation

$$M=\frac{\pi}{4}D^2S_1\rho_1 \tag{2}$$

and equation (1) might be written in the form

$$R_D=\frac{4M}{\pi D\mu} \tag{3}$$

but the traditional form equation (1) is retained here as more familiar.

As is well known, the effects of viscosity on the nature of the fluid motion depend on the value of R_D, which serves as a criterion, or an independent variable, in discussing these effects on skin friction, etc.

If a Venturi of throat diameter $d=\beta D$ is included in the pipe line, its discharge coefficient depends on the motion in the approaching stream and therefore on the value of R_D; but it is more natural to adopt as the independent variable or Reynolds number, the analogous expression

$$R_d=\frac{dS_2\rho_2}{\mu} \tag{4}$$

in which ρ_2 and S_2 are the density and mean speed at the throat; and this second form of Reynolds number is physically more signifi-

cant than the first, because the nature of the motion through the throat is more influenced by the size of the throat than by the size of the pipe.

Equation (4) may also be written in the form

$$R_d = \frac{4M}{\pi d\mu} \tag{5}$$

corresponding with equation (3); and since M is the same in both equations, and the viscosity is nearly the same at the throat as in the approach pipe, comparison of equation (3) with equation (5) gives the approximate relation

$$R_D = \beta R_d \tag{6}$$

and either form of the Reynolds number may be found from the other.

Similarly, for an orifice of diameter d installed in a pipe of diameter D, the nature of the motion and the value of the discharge coefficient, in so far as they are influenced by the viscosity of the fluid, may be regarded as dependent on either R_D or $R_d = R_D/\beta$.

In any event, and whether it is an orifice, a Venturi, or a straight pipe that is under consideration, the effects of viscosity on the motion of the fluid become negligible when the viscosity itself is sufficiently low; and since these effects are not determined merely by the value of μ, but by the value of the Reynolds number as a whole, they become insignificant when either R_D or R_d is made very large.

For further information on the experimental side of this subject the reader may be referred to papers by J. L. Hodgson,[13] R. Witte,[14] and F. C. Johansen.[15]

WASHINGTON, May 13, 1931.

---

[13] Inst. Civ. Eng., Selected Engineering Papers, No. 31, 1925.
[14] See footnote 5, p. 130 and 12, p. 139.
[15] Proc. Roy. Soc. London, A **126**, p. 231, 1929.

A COURSE INDICATOR OF POINTER TYPE FOR THE VISUAL RADIO RANGE-BEACON SYSTEM

By F. W. Dunmore

ABSTRACT

A form of tuned-reed radio range-beacon course indicator is described, called a reed converter, in which the course indications are not given by observing the two reed motions as heretofore, but by means of a zero-center pointer type indicating instrument. The motion of the two reeds generates small alternating voltages, which when rectified by oxide rectifiers and passed in opposing polarities through a zero-center indicating instrument, serve to give course indications by the deflection of the indicating instrument needle in the direction of deviation of the airplane from the course.

The reed converter consists of two reed units, two oxide rectifiers, and the course-indicating instrument. The driving coils of the two units are connected in series to the output of the aircraft radio receiving set.

Each reed converter unit consists of a polarized reed tuned to one of the beacon modulation frequencies. The reed vibrates between a set of driving coils which are supplied with the signal from the radio range. The same reed extends between a set of pick-up coils, the motion of the reed generating a voltage in these coils.

Since a null method of course indication is used, it is necessary to provide a signal-volume indicator in the form of a 0–500 microammeter in the output circuit of the oxide rectifiers. It is connected so that the output from each rectifier deflects the instrument pointer in the same direction. It not only serves to enable a pilot to tune in the beacon signal and to control the volume, but also indicates a cessation of this signal or a failure of any part of the radio receiving set or reed converter units.

Several forms of converter selector-switch circuit arrangements are shown whereby it is possible to use the reed converter course indicator on any course of a 4 or 12 course radio range beacon. By setting a pointer to the color of the range beacon to be flown and the direction of flight on it, the proper two-reed units are selected by this switch, and their outputs connected in the correct polarity to the course-indicating instrument so that its pointer will deflect in the same direction as the deviation of the airplane from the course.

As the course-sharpness indications depend upon the signal level delivered to the indicating instrument, this sharpness may be controlled at will.

The combination of this course indicator and the high-frequency fog landing beam course indicator into one indicating instrument is described. This instrument, when provided with a suitable switch, may be made to give two more indications; main radio range-beacon course and signal volume indication.

The advantages and disadvantages of the reed converter as compared to the tuned-reed indicator are discussed.

CONTENTS

	Page
I. Introduction	148
II. The tuned-reed converter unit	149
1. Principles of operation	149
2. Details of design	151
(*a*) The reed-converter unit design	151
(*b*) The reed-converter unit mounting	153
(*c*) Sensitivity	153
(*d*) Sharpness of resonance	154

Page

III. The course-selector switch, deviometer, volume indicator, and course-sharpness control 156
1. Reed converter applied to a 4-course radio range beacon 156
2. Use of the deviometer, volume indicator, and course-sharpness control 158
(*a*) The deviometer 158
(*b*) The volume indicator 159
(*c*) The course-sharpness control 160
3. Reed converter applied to 4- or 12-course beacon 161
(*a*) Two-unit plug-in arrangement 161
(*b*) Three-unit dual-control arrangement 164
(*c*) Three-unit single-control arrangement 165
IV. Applications of the reed-converter course indicator 165
1. As a main airways beacon course indicator 165
2. Use in holding an airplane automatically on a radio-beacon course 165
3. Use as a course indicator on the runway localizing beacon for blind-landing purposes 166
4. Combination with turn indicator 168
V. Comparison of reed converter with reed indicator 169
1. Advantages of reed converter 169
2. Disadvantages of reed converter 169
VI. Conclusion 169

I. INTRODUCTION

The tuned-reed type of visual indicator [1] is used to give a pilot a visual indication as to whether or not he is flying on a specified double-modulation radio range-beacon course and, if not, to which side and how much he has deviated. This type of tuned-reed indicator gives the course indication continuously by means of two vibrating reeds, the relative amplitudes of which indicate the position of the airplane with respect to the beacon course. In order to observe the reed vibration, each reed carries a white tab on its free end. These two tabs produce two adjacent white lines when the reeds vibrate. It is the relative length of these two lines which the pilot observes. Each reed is tuned to one of the frequencies of modulation used at the radio range beacon. The course is a zone in space where the strengths of the beacon-modulation frequencies are equal, each zone being indicated to the pilot by amplitude equality of the two vibrating reeds. A deviation from the course is indicated by an increase in that reed amplitude on the side to which the airplane has deviated and an equivalent decrease in the other reed amplitude.

The development of a form of reed indicator is described in this paper in which the course indications are not given by observing the reed motions, but by means of a zero-center pointer-type instrument. The motions of the two reeds generate small alternating voltages, which, when rectified and passed in opposing polarities through the zero-center indicating instrument, serve to give course indications by the deflection of the indicating instrument needle in the direction of the airplane's deviation from the course. A form of course-selector switch is also described which makes possible the use of this type of visual course indicator on any one of the courses of a 4 or 12 course radio range beacon in such manner that the instrument needle deflects in the same direction as the deviation of the airplane from the course,

[1] J. H. Dellinger, H. Diamond, and F. W. Dunmore, Development of the Visual Type Airway Radio Beacon System, B. S. Jour. Research, **4** (RP159), p. 425; March, 1930; Proc. I. R. E., **18**, p. 796; May, 1930.
F. W. Dunmore, A Tuned Reed Course Indicator for the 4 and 12 Course Aircraft Radio Range. B. S. Jour. Research, **4** (RP160), p. 461; April 1930; Proc. I. R. E., **18**, p. 963; June, 1930.

regardless of which course is being flown or the direction of flight. It is only necessary for the pilot to set the pointer of the switch to the color of the beacon course he is to fly, and to the direction of flight along this course; that is, to "To" or "From" the readiobeacon. This switch selects the two proper reed-converter units, and connects their outputs in the proper polarity to the zero-center indicating instrument, thus causing the needle to deflect in the direction of deviation of the airplane from the course. In its complete form the reed converter consists of three units, one tuned to 65 cycles, another to 86.67, and the third to 108.33 cycles. In this form it is applicable for use on the 12-course visual type radio range beacon or on 4-course beacons having different combinations of the above frequencies.

II. THE TUNED-REED CONVERTER UNIT

1. PRINCIPLES OF OPERATION

The tuned-reed converter in its simplest form is shown in Figure 1. It consists of a polarized metal reed vibrating between two sets of

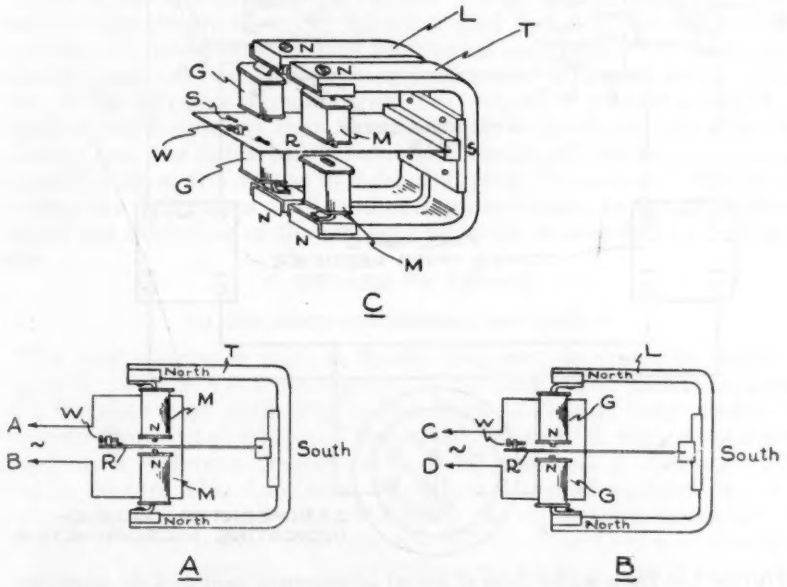

FIGURE 1.—*Tuned-reed converter illustrating method of operation*

electromagnet coils, one set being supplied with an alternating current of the frequency to which the reed is tuned, thus causing it to vibrate, and the other set, by virtue of the changing magnetic flux caused by the vibrating reed, generates an alternating voltage of the same frequency. At *A* (fig. 1) is shown a simple reed driving unit, the magnet *T* polarizing the reed *R* with a south pole, and the pole pieces of the electromagnets *M* with a north pole. With the electromagnet coils connected in series in the proper electrical polarity; that is, so that current flowing through them in series will tend to produce opposite magnetic polarities at the pole tips, the reed will, during one-half

cycle of the driving current, be attracted by the upper electromagnet and repelled by the lower one, thus moving up. During the second half cycle of the driving current the net driving force reverses. Thus when an alternating current of the natural frequency of the reed is applied at *AB* the reed will vibrate in synchronism.

Consider this same reed, now in motion, to be moving also between a second set of electromagnet coils *G*, as shown at *B* (fig. 1). As the reed moves up the flux in the upper coil will increase, thus producing an e. m. f. at the upper coil terminals, and the flux in the lower coil

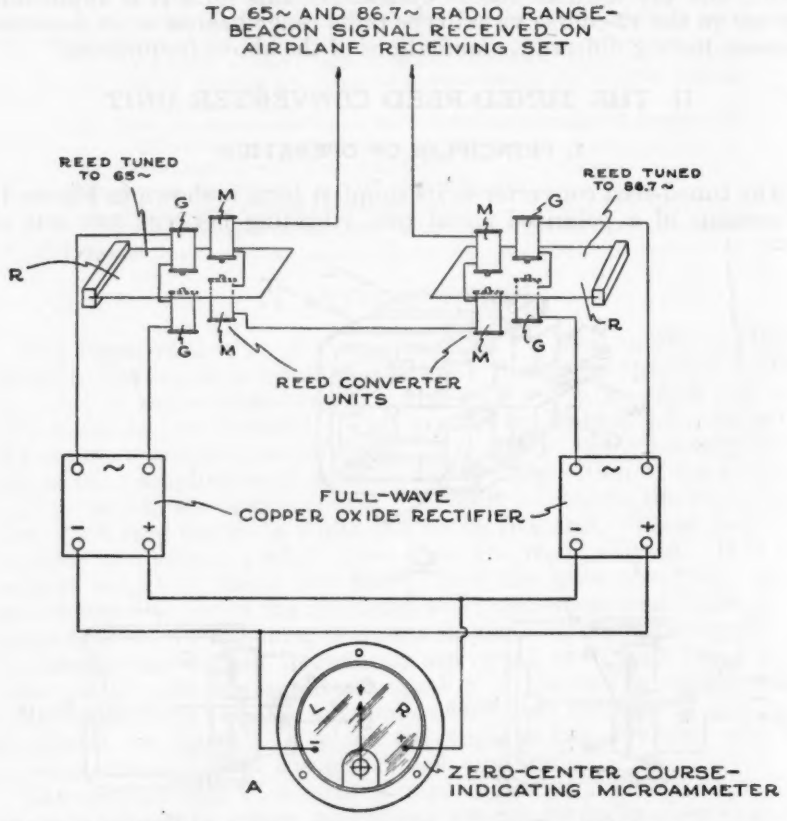

FIGURE 2.—*The simplest form of circuit arrangement used with the tuned-reed converter*

will decrease, thus producing an e. m. f. at the lower coil terminals. If connected in the proper polarity, these e. m. f.'s will add and a voltage will be produced at the terminals *C–D*. When the reed goes down, a voltage of opposite polarity is produced at *C–D*. Thus the vibrating reed produces an alternating-current voltage of the frequency of vibration of the reed.

The reed converter was made by combining the one reed *R* as shown at *C* (fig. 1) with the two sets of permanent magnets *T* and *L*. One set of coils *M* is supplied with the radiobeacon signal modulated at the frequency to which the reed is tuned, thus causing the reed to vibrate,

and thereby generating in the other set of coils G a voltage of the frequency of the vibrating reed. This reed converter, therefore, acts as a mechanical filter, allowing practically nothing but one frequency, that to which the reed is tuned, to pass through it.

In flight on a given radio-range beacon course, two units of the type shown in Figure 1, C are used, the reed in one unit being tuned to, say, 65 cycles, with the reed in the second unit tuned to, say, 86.67 cycles. The outputs from the coils G in each unit are rectified by means of oxide rectifiers and the rectified voltages applied in opposition to a zero-center microammeter, as shown in Figure 2. This tuned-reed converter unit is operated on the airplane by means of signals from the double-modulation type of radiobeacon, in which one carrier frequency is transmitted directively from two coil antennas oriented at right angles. The carrier radiated from one coil antenna is modulated at 65 cycles, the carrier radiated from the other coil antenna is modulated at 86.7 cycles. The course is along a line of direction in space where the two modulation frequencies are present in equal intensities. Off the course the intensity of one modulation frequency is greater than that of the other.

Thus when the airplane is on the course the 65 and 86.7 cycle received signals are of equal intensity and the d. c. output voltages from the two oxide rectifiers will be of equal amplitudes but of opposite polarity, and the course-indicating instrument will read zero. However, if the airplane deviates from the course, a greater strength of signal of one frequency than the other will be received, upsetting the balance, and the indicating-instrument needle will deflect an amount depending upon the degree of deviation from the course. Means for keeping the deflections of the indicating instrument in the same direction as the deviation of the airplane from the course will be discussed later.

2. DETAILS OF DESIGN

(a) THE REED CONVERTER UNIT DESIGN

The reed converter unit, as finally designed, is shown in detail in Figure 3. Figure 4 is a photograph of the unit. The unit is mounted on a bakelite base with plug connections so that it may readily be removed from its shock-proof base (not shown), so that a reed unit tuned to a different frequency may be inserted if desired. This plug-in feature also facilitates checking the reed calibration, as a spare unit may be easily inserted while the calibration check on the old unit is being made. The copper-oxide rectifier O is also arranged to plug in to the circuit. This rectifier, which is of the type used in a. c. indicating instruments, is mounted in a small bakelite case for protection, a lock nut and screw being employed for holding the case in place. Since the rectifier operates on the output of the reed converter, it can never be overloaded, as it is rated at 5 milliamperes, and the maximum possible input which occurs as the reeds bump the pole pieces, is about 500 microamperes.

The permanent magnets T and L are made from a chromium-nickel iron alloy known as 36 per cent "Cobaltcrom." They are magnetized with a polarity as indicated in Figure 3. Two are used to keep the driving and pick-up magnetic circuits separated to prevent coupling and to increase the sensitivity. The electromagnet coils M and G are similar to those used on the Western Electric type 509–W

head telephones. The pick-up coils G are connected in series in the proper polarity, and the reed driving coils M are connected either in series or in parallel in the proper polarity, depending upon the impedance desired in order to match that of the receiving set output. The two pick-up coils are placed 1 inch from the base of the reed and the two driving coils eleven-sixteenths inch from the base.

The reed R is made of an alloy known as Allegheny electric metal. It has a magnetic permeability as good as that of steel, is rust proof, and has a modulus of elasticity, which, although not entirely independent of temperature, is sufficiently so to allow of its use, especially with the broadness of tuning of the reed as used in this converter unit.

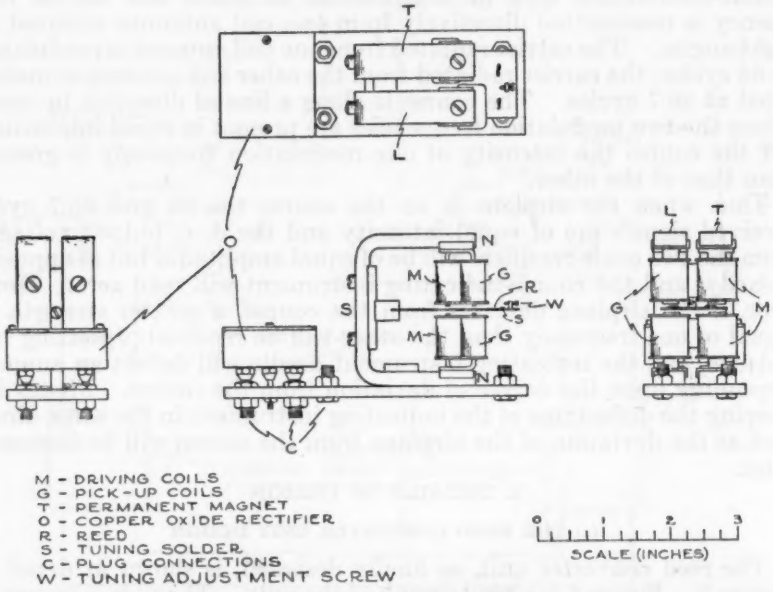

FIGURE 3.—*Schematic diagram showing construction of tuned-reed converter unit with oxide rectifier*

This material is noncorrosive in ordinary climates so that its weight does not change during use. Any change in weight will, of course, throw the reed out of tune. The 65-cycle reed is 2 inches long, 1 inch wide, and 0.013 inch thick. The 86.66-cycle reed is 1¾ inches long with the other dimensions the same as above. The 108.3-cycle reed is the same thickness and width but 1⅝ inches long. The proper size and shape of a reed for a given frequency may be determined mathematically.[2] The reeds are tuned approximately to the desired frequency by means of solder (S, fig. 3) on the end of the reed. The final tuning is done by adjusting screw W (figs. 3 and 4), which is made to turn very tightly in its threaded socket so that it can not be moved except with a screw driver. The screw and mounting are of noncorrosive material. It allows of a variation of 1 per cent in the tuning of the reed.

[2] G. L. Davies, Theory of Design and Calibration of Vibrating Reed Indicators for Radio Range Beacons, B. S. Journ. Research, 7 (RP338), p. 195; July, 1931.

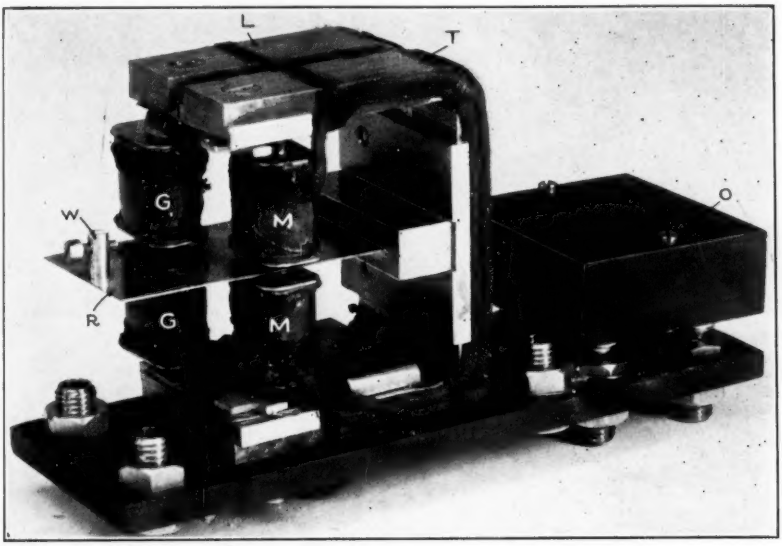

FIGURE 4.—*A plug-in tuned-reed converter unit with plug-in oxide rectifier*

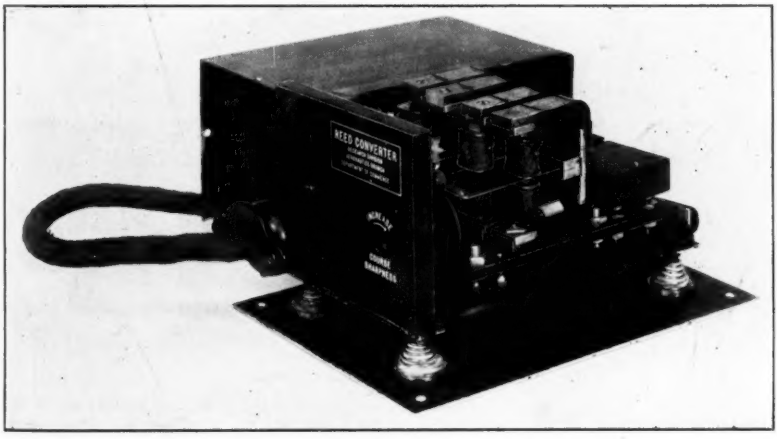

FIGURE 5.—*Tuned reed converters in a 2-unit shock-proof mounting*

UNIV. OF MICH.

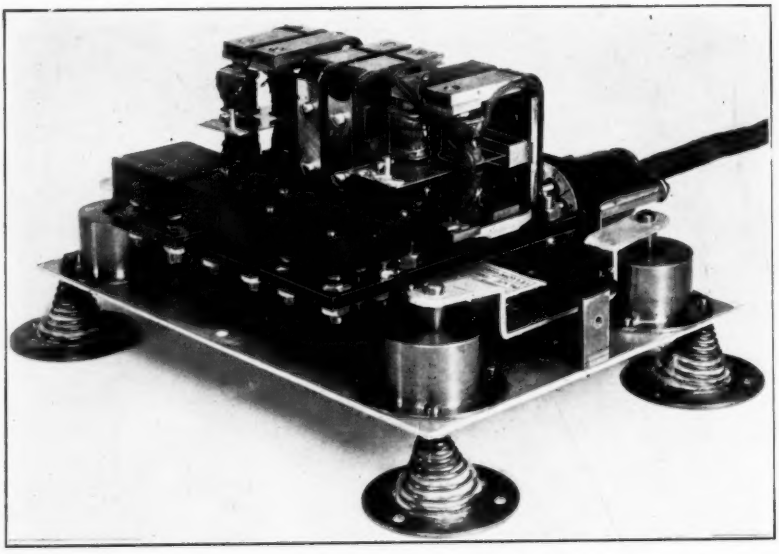

FIGURE 6.—*Tuned reed converters in a 3-unit shock-proof mounting*

The gaps between the two pole pieces of the driving electromagnets M control to a large degree the sensitivity of the indicator, while the gap between the pick-up coil pole pieces G controls the reed damping as well as the sensitivity. For one set of reed converter units constructed, in which the two driving coils were connected in parallel, 0.5 volt input to these two coils gave a deflection of 200 microamperes on the course-indicating instrument. The sharpness of resonance was about 40. (See Fig. 8.) In these units the gap between the electromagnet pole pieces varied between 0.04 and 0.06 inch.

At this point it might be well to mention the effect of direct coupling between the driving coils and the pick-up coils. Separate permanent magnets for the driving and pick-up coils solved the coupling problem as the two magnetic circuits are thus practically segregated. At the frequencies used, 65, 86.7, and 108.3, the direct magnetic coupling between these coils, with the reed held stationary, is so small that it can not be measured on a 0–200 microammeter; this is with the normal input voltage to the reed converter unit which can not be exceeded due to the automatic volume-control feature used on the receiving set output.[3] Should an excessive interfering signal of, say, 1,000 cycles be impressed on a converter unit, there is some appreciable coupling, but since two converter units are always used in series, and the output of the oxide rectifiers connected in opposing polarity, any effect from such a signal would be present in equal amounts in each converter unit and would, therefore, balance out. Furthermore, when used in a receiving circuit for reception from the simultaneous telephone and beacon type of signal,[4] all frequencies above, say, 200 cycles are cut off from the reed converter input and are sent to the head telephones, and are, therefore, not present in the reed converter circuits.

(b) THE REED-CONVERTER UNIT MOUNTING

Since the least motion of the reeds in this type of reed converter induces a voltage in the pick-up coils, due to the small clearance between the reed and pole pieces, it is important that the reed be moved only by the driving coils and not by any mechanical vibration. The reed converter units are, therefore, placed on a base which in turn is mounted on conical springs, stuffed with cotton for damping, as shown in Figure 5. The 2-unit mounting shown in Figure 5 contains the plug terminals for receiving the reed converter units and the 7-terminal socket for making the necessary external connections by means of a 7-terminal plug. The 3-unit mounting requires a 10-terminal plug connection. Such a mounting containing three converter units is shown in Figure 6. The resistance for adjusting the course sharpness (to be described later in this paper) is also placed on this mounting. It can only be adjusted by means of a screw driver, since when once set to give the desired course sharpness it should not be moved.

(c) SENSITIVITY

The gaps between the driving electromagnetic pole pieces are adjusted for each tuned-reed converter unit so that the three units will be of equal sensitivity. This adjustment is made at a normal course indicator operating current of, say, 200 microamperes. Figure

[3] W. S. Hinman, jr., Automatic Volume Control for Aircraft Radioreceivers, B. S. Jour. Research, 7 (RP330), p. 37; July, 1931

[4] F. G. Kear and G. H. Wintermute, A Simultaneous Radiotelephone and Visual Range Beacon for the Airways, B. S. Jour. Research. This will appear in the August issue.

7 shows the sensitivity curves for the three unit combinations. The a. c. input voltage was measured across two units in series, as they are used in this way in practice. The two driving coils in each unit were connected in parallel. In the region of operation of the reeds, that is, 100 to 300 microamperes, a linear relation exists between the input voltage and output current, and the slopes of the curves are about the same, which feature provides true course deviation indications as the relative value of the input voltage varies. The power input on one frequency to the two reed converters in series is about 1.0 milliwatt when an output current of 200 microamperes is obtained. This

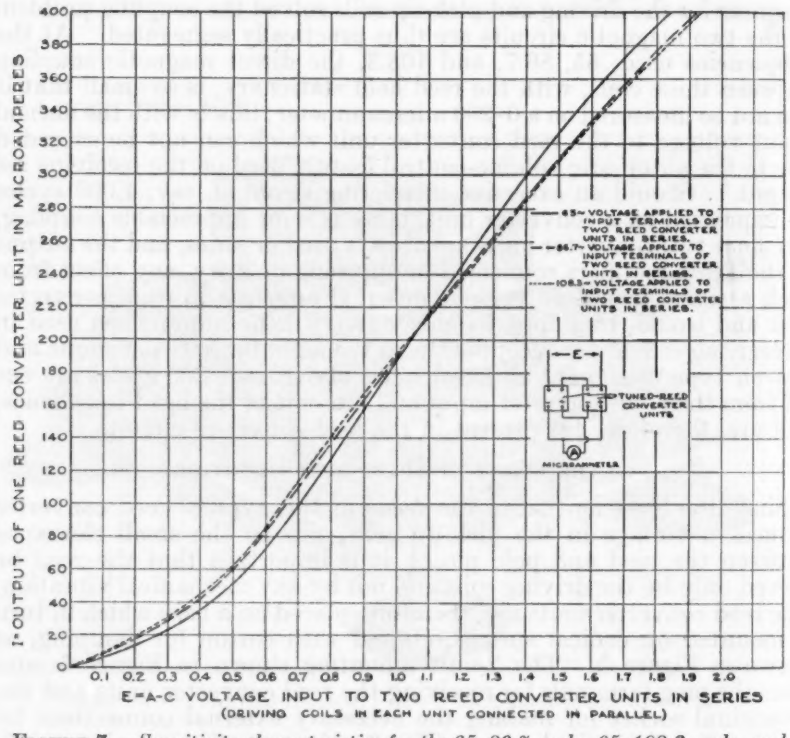
I=OUTPUT OF ONE REED CONVERTER UNIT IN MICROAMPERES
E=A-C VOLTAGE INPUT TO TWO REED CONVERTER UNITS IN SERIES
(DRIVING COILS IN EACH UNIT CONNECTED IN PARALLEL)
65~ VOLTAGE APPLIED TO INPUT TERMINALS OF TWO REED CONVERTER UNITS IN SERIES.
86.7~ VOLTAGE APPLIED TO INPUT TERMINALS OF TWO REED CONVERTER UNITS IN SERIES.
108.3~ VOLTAGE APPLIED TO INPUT TERMINALS OF TWO REED CONVERTER UNITS IN SERIES.
E
TUNED-REED CONVERTER UNITS
A
MICROAMMETER

FIGURE 7.—*Sensitivity characteristics for the 65–86.7 cycle, 65–108.3 cycle, and 86.7–108.3 cycle-reed converter course indicators*

sensitivity, which is about equivalent to that of the ordinary tuned-reed indicator, has been obtained with over twice the amount of damping in the reeds. The advantage of this increased damping is discussed under (*d*) Sharpness of resonance.

(d) SHARPNESS OF RESONANCE

While the tuned-reed converter is about equal in sensitivity to that of the tuned-reed indicator, the amount of damping possible at this sensitivity is over twice as great. This damping, a large proportion of which is caused by the load introduced by the pick-up coils, is, of course, an advantage, since the modulation frequencies at the beacon need not be held to the accurancy required for the tuned-reed indicator.

The damping is so proportioned that the output from the three reed converters will not change appreciably even though the frequency varies as much as ±1 per cent. The resonance curves for the three reed converter units are shown in Figure 8. Since the three frequencies of modulation at the radio range beacon are obtained in most cases from three generators with 6, 8, and 10 poles, respectively, and with a common shaft connected to a synchronous motor driven from the 60-cycle line, the three frequencies must vary in the

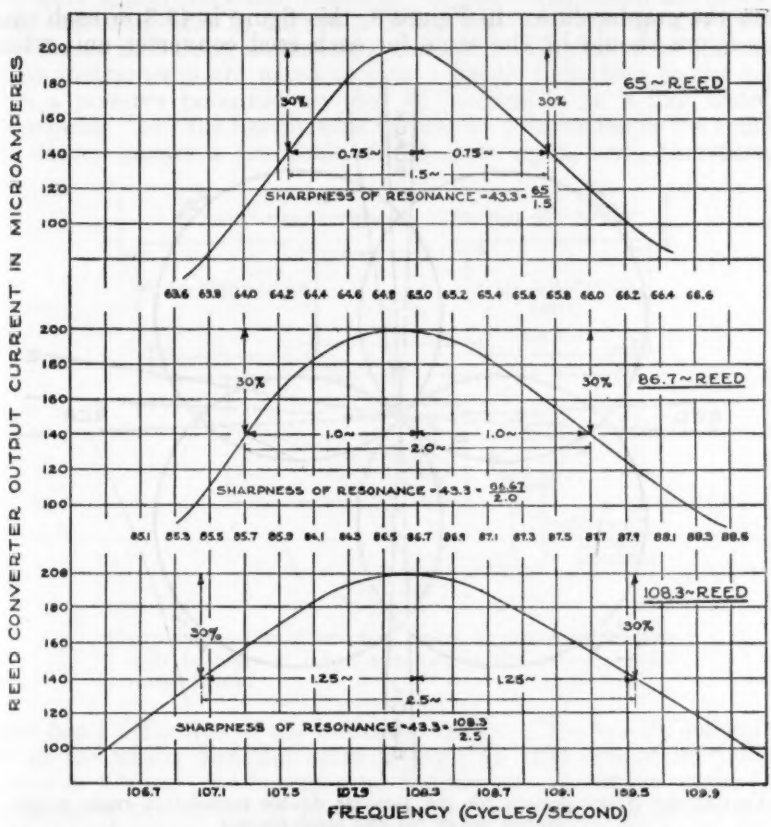

FIGURE 8.—*Resonance curves for the three reeds in the reed-converter units, showing effect of correctly proportioning the damping to keep converter outputs the same with the same percentage change in frequency*

ratio of 6:8:10. Therefore, if a 0.75-cycle variation occurs in the 65-cycle frequency, a 1.0-cycle variation will occur in the 86.7-cycle frequency and a 1.25-cycle variation will occur in the 108.3-cycle frequency. From the graphs in Figure 8 it will be seen that for such a variation in each frequency, each reed converter output drops by the same amount; that is, 30 per cent, or from 200 microamperes to 140 microamperes. Since the relative outputs of the reed converters do not change, no apparent shift in course is caused by a variation in the 60-cycle power line frequency by as much as ±1 per cent. A more conservative figure would be ±0.75 per cent, however, since

the resonance curves for a given reed converter may change slightly with time due to aging of the permanent magnets, etc.

A convenient method for expressing the sharpness of resonance of a tuned reed by a simple numeral has been adopted:

$$\text{Sharpness of resonance} = \frac{\text{Resonance frequency in cycles}}{\text{Band width in cycles at 30 per cent drop in converter output from that at resonance}}$$

From the graphs shown in Figure 8, this figure is 43.3 in each case. This figure should be the same for each reed converter unit when-

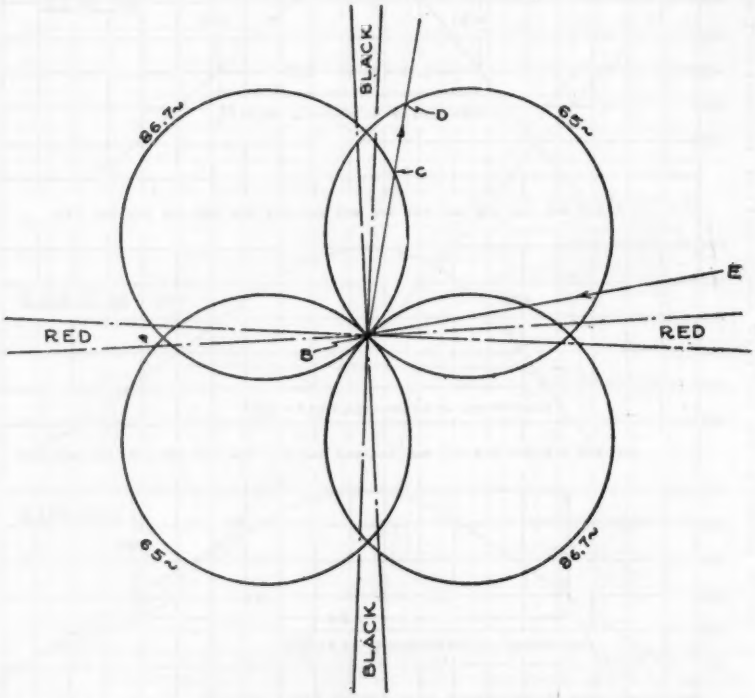

FIGURE 9.—*Space pattern for the 4-course double modulation radio range beacon giving red and black courses*

ever two units are used together, as they always are in practice. For the standard tuned-reed indicator (not the reed-converter type), this figure runs around 90.

III. THE COURSE-SELECTOR SWITCH, DEVIOMETER, VOLUME INDICATOR, AND COURSE SHARPNESS CONTROL

1. REED CONVERTER AS APPLIED TO A 4-COURSE RADIO RANGE BEACON

In order to show the application of the reed converter to the radio beacon courses, a typical space pattern for a 4-course radio range beacon with red and black courses is shown in Figure 9. The radio range is located at *B*. Modulation frequencies of 65-cycle and 86.7-

cycle are used on these courses. It is evident that the simple circuit arrangement shown in Figure 2 makes the reed converter applicable to but one direction of flight on each of these courses, if the needle of the zero-center indicating instrument *A* is to deflect in the same direction as the deviation of the airplane from the course. Thus when going "from" the beacon on a black course, if the airplane deviates to the right and flies along some course such as *BD*, the 65-cycle signal will predominate by an amount proportional to *CD*, as shown in Figure 9, and since the + side of the oxide rectifier in the 65-cycle reed converter unit in Figure 2 is connected to the + side of the zero-center indicating instrument, the needle will deflect to the right. (Such instruments are wired to give a needle deflection to the right with a positive potential on the + terminal.) In a like manner, when going "to" the beacon on a red course, a deviation to the right of the course causes a predominant 65-cycle signal and, therefore, a

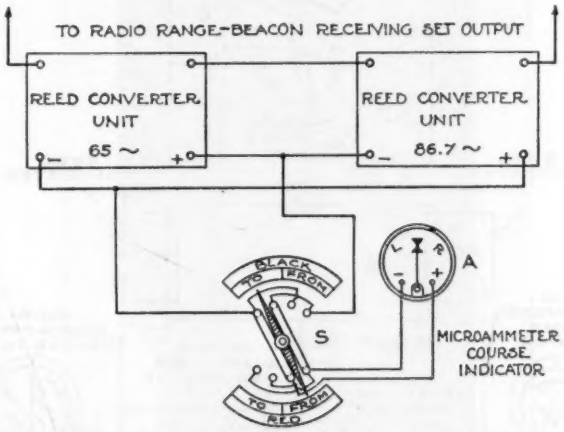

FIGURE 10.—*Use of reversing switch in reed-converter outputs in order to adapt converter to the 4-course radio range beacon*

right-hand deflection of the indicator needle. The needle deflections are in the wrong direction when flying "to" the beacon on a black course or "from" the beacon on a red course. A simple method for overcoming this difficulty is to put a reversing switch between the oxide rectifier outputs and the zero-center indicating instrument, as shown in Figure 10.

A color system is chosen such that the indicator needle deflection is always in the same direction as the deviation of the airplane from the course when flying in either direction on either the red or black courses. If the circuits in Figure 10 are checked through in conjunction with Figure 9, it will be found that if the reversing switch *S* is set to any desired direction of flight on either of the courses (red or black) and the airplane deviates, say, to the right, the resultant polarity of the voltage impressed at the terminals of indicating instrument *A* will cause it to deflect to the right. In Figure 10 the pointers on switch *S* are set for flying either "to" the beacon on a black course or "from" the beacon on a red course.

2. USE OF THE DEVIOMETER, VOLUME INDICATOR, AND COURSE-SHARPNESS CONTROL

(a) THE DEVIOMETER

Before going into the application of the reed converter to the 12-course beacon, the use of the deviometer, volume indicator, and course sharpness control will be discussed. The deviometer is used with the reed converter in the same way as with the tuned reed indicator, its function being to enable a pilot to fly along an off-course route, yet allowing the zero-center indicating instrument to read zero when the airplane is on this off-course route. Any deviations from this route are thus indicated in the usual way. Such off-course routes

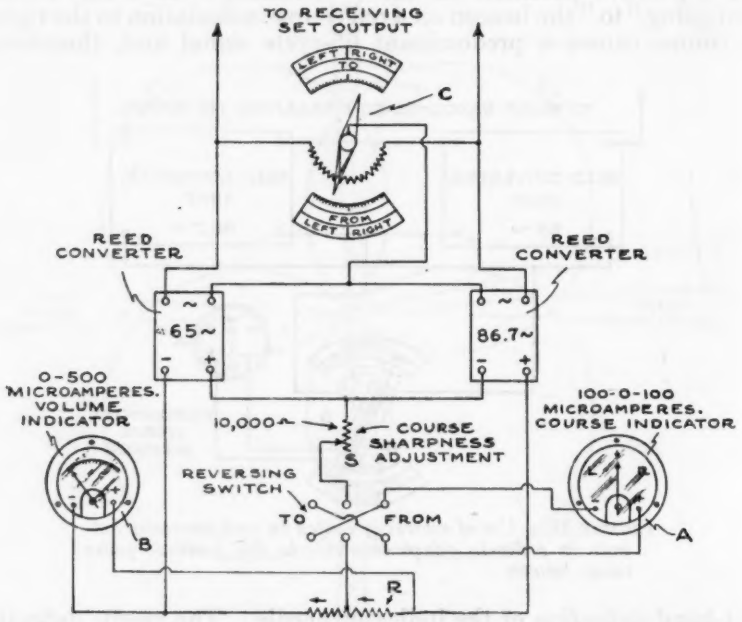

FIGURE 11.—*Simple deviometer and volume indicator circuit arrangements for using the reed converters on a red course*

may be flown along any line making an angle of up to 15° on either side of the equisignal course. The deviometer shown at *C* (fig. 11) consists of a 10,000 to 20,000 ohm resistor shunted across the two converter driving coils, with the sliding contact connected to the common connection between the two sets of driving coils. The arrangement at *C* (fig. 11) is for a red course only. Such a double pointer and wording arrangement is necessary, since the direction of movement of the sliding contact on the resistor reverses for a reversal of the direction of flight. Referring to Figure 9, assume a pilot desired to fly along an off-course line, such as *BE*, on the right of the red course going "to" the beacon. In order to keep the zero-center course indicating instrument from deflecting to the right due to an increase of the 65-cycle signal along this route, the effective sensitivity of the 65-cycle converter driving coils is reduced by lowering the deviometer shunting resistance across these coils. This is done by moving one of

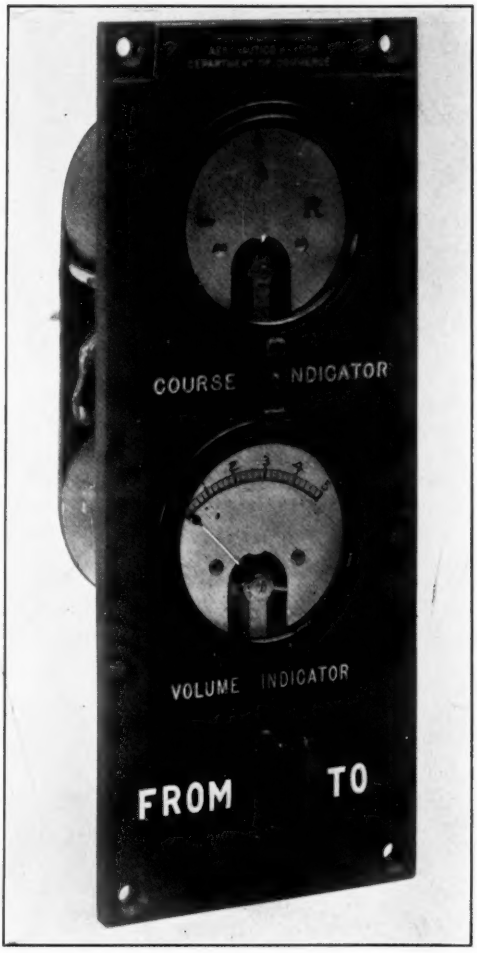

FIGURE 12.—*Course and volume indicating instruments with reversing switch for use with reed converter on a red, brown, or yellow radio-beacon course*

UNIV. OF

FIGURE 13.—*Reed converter-course indicating microammeter in plug-in shock-proof mounting*

FIGURE 14.—*Reed converter-course indicating microammeter showing plug-in feature and shock-proof mounting*

the deviometer pointers (fig. 11) to point, on the "To" scale, to the segment marked "Right." The amount of movement of deviometer *C* should be sufficient to reduce the indicating instrument deflection at *A* to the zero center when the airplane is on the new course, *BE*. The application of the deviometer and reed converter to all courses of the 4 or 12 course beacon will be discussed below.

(b) THE VOLUME INDICATOR

One seeming disadvantage of the reed-converter type of beacon course indicator is that a null method of course indication is used, which means that the beacon signal may be off, or the receiving set not functioning, yet the course indicating needle will read "on course." This can not happen with the tuned-reed indicator as the moving reeds are always visible, indicating the presence of a beacon signal as well as the volume output of the receiving set.

A method of overcoming this difficulty is to use a second indicating instrument with a range of about 0–500 microamperes as a volume indicator. The method of connecting this instrument in the reed-converter circuit is shown in Figure 11 at *B*. A center-tap resistor *R* of about 100 ohms is so connected to the oxide rectifier outputs that the *RI* drops across this resistance are additive so that both rectifier outputs deflect the needle of instrument *B* in the same direction. Such a system gives a positive indication that both modulation signals from the beacon are present in the reed-converter circuits. Furthermore, instrument *B* indicates the volume of signal output from the receiving set; thus a beacon signal may be tuned in by watching instrument *B* until it reads a maximum as the receiving set is tuned. A normal reading for *B* is about 250 microamperes. This output level may be held in flight either by an occasional adjustment of the volume control on the receiving set or by one adjustment in the automatic volume control unit, if such a unit is used.

There are several advantages in locating the volume-indicating instrument in the position in the circuit, as shown in Figure 11, and not in the output of the receiving set or elsewhere in the receiving set circuits. First, it is located at the very end of the whole receiving-circuit arrangement, including the reed-converter circuits, so that it will indicate a malfunctioning of any part of the complete beacon receiving system, and, secondly, instrument *B* is operated only by the tuned-reed outputs so that the mechanically tuned selectivity of the reeds prevents any interfering signal from operating it.

Figure 12 is a photograph of a panel containing the course and volume indicating instruments and a reversing switch. The reversing switch is of the snap type, and may be either thrown toward the word "From" (when flying "from" the beacon) or to the word "To" (when flying "to" the beacon). The panel is wired for use when flying in either direction on a red course. It may also be used on a brown or yellow course with the proper reed converters. By reversing the leads to the course-indicating instrument, this panel may be used on a black, blue, or green course. These new courses will be discussed below.

The two indicating instruments in figure 12 plug into iron cans supported on the panel, making the necessary electrical connections.

The cans are iron to keep strong magnetic fields from the instruments from affecting the airplane's magnetic compass. The lower can contains the resistance *R*. (Fig. 11.)

As the indicating instruments are the most fragile part of the reed-converter apparatus, it is preferable to mount them on springs. Such a spring mounting for the course indicating microammeter is shown in Figure 13. Figure 14 shows a rear view of the instrument removed from its iron case holder, showing the electrical plug connections. In case an instrument is found to be defective a new one may be immediately plugged into the holder.

(c) THE COURSE-SHARPNESS CONTROL

Unlike the tuned-reed indicator the course-sharpness indication given by the reed converter is a function of the beacon signal level delivered to it or to the course-indicating instrument. An unbalance in the course indicator with two strong output signals from the reed converter, gives a much greater deflection and, consequently, an apparently sharper course. The degree of sharpness may be set to suit the pilot, either by adjusting the automatic volume control on the receiving set (or hand volume control) to change the signal level delivered to the converter or, assuming a given signal level, the course sharpness may be controlled to a large extent by means of a 10,000-ohm resistance *S* (fig. 11), which is connected in series with the course-indicating instrument *A*. The value of this resistance depends upon the sensitivity of the instrument used. By decreasing this resistance or increasing the beacon signal delivered to the reed converter, an apparent sharpening of the beacon course is brought about. However, in so doing, the useful portion of the beacon space pattern is reduced, since a deviation of only 10° from the course may throw a 100–0–100 microampere course indicator off scale with a strong beacon signal level impressed on the reed converter, while with a weak signal and broad course indications, the needle will stay on scale for a 45° deviation from the course. In other words, the useful width of the beacon space pattern may be increased at a sacrifice of course sharpness. An advantage of the tuned-reed indicator over the reed converter is that it gives useful course indications up to the full width of the beacon space pattern. A method of partially overcoming this disadvantage in the reed converter is to have a course-indicating instrument with a more open scale. Such instruments are now made with 270° of scale in place of the customary 100°.

The effect of the apparent variation of the course sharpness with beacon signal strength input to the reed converter is shown in Figure 15. The data for these curves were taken on the National Bureau of Standards' visual type beacon at College Park, Md. The test circuit arrangement used is as shown in Figure 15. It will be noted that with a beacon signal input voltage to the reed convertors of 3.5 volts, the effective width of the beacon space pattern is only 10° when using a 100–0–100 microammeter and about 24° when using a 250–0–250 microammeter, while with a voltage input of 1.5 volts the width is 27° with the 100–0–100 instrument and the full width of 90° with the 250–0–250 instrument. Thus, when using a 100–0–100 microammeter and an input voltage of 3.5 volts, the pilot can not deviate

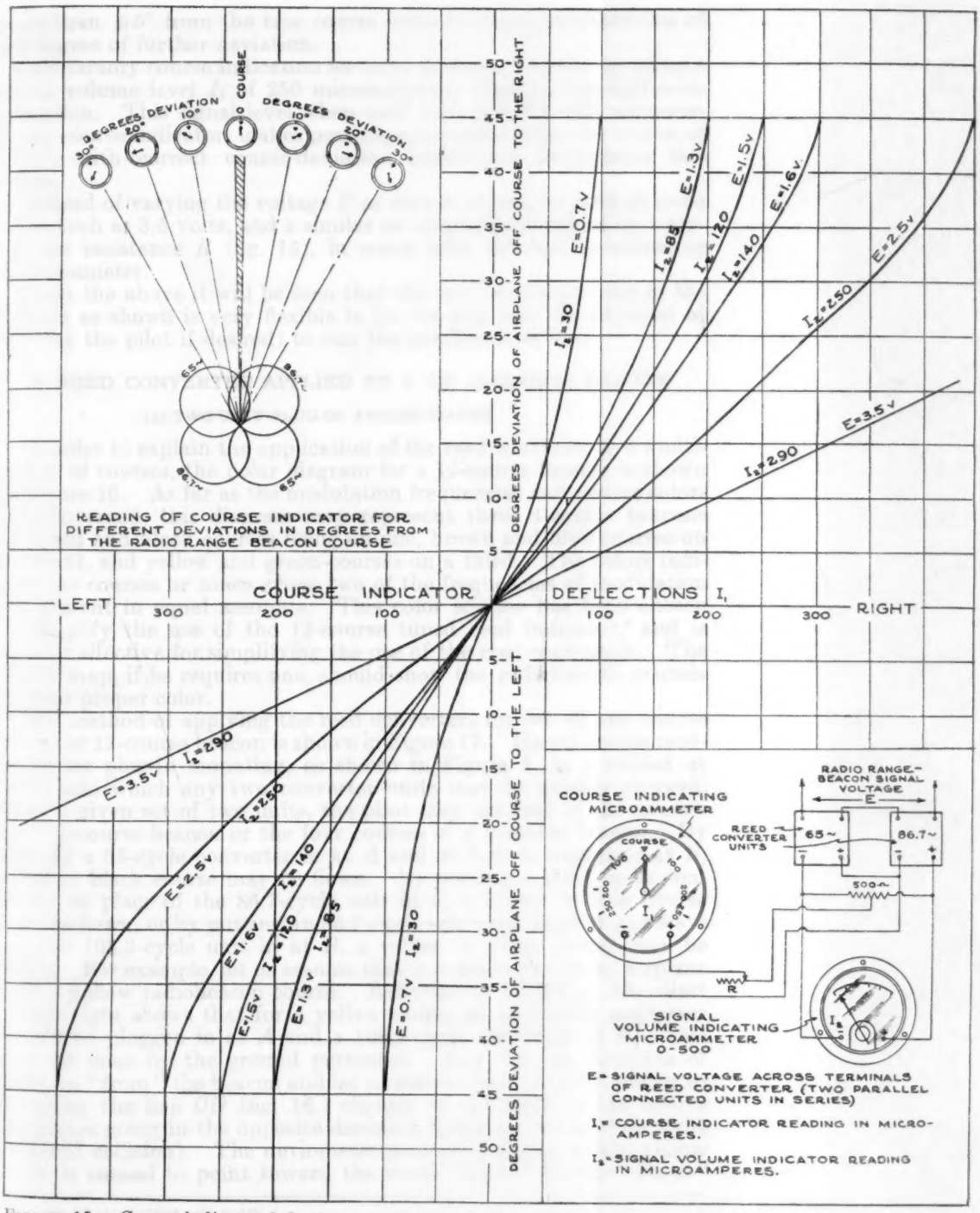

FIGURE 15.—*Course indicator deflections as airplane deviates from the course using different beacon signal levels impressed on the reed converter, illustrating course sharpness variations with signal level*

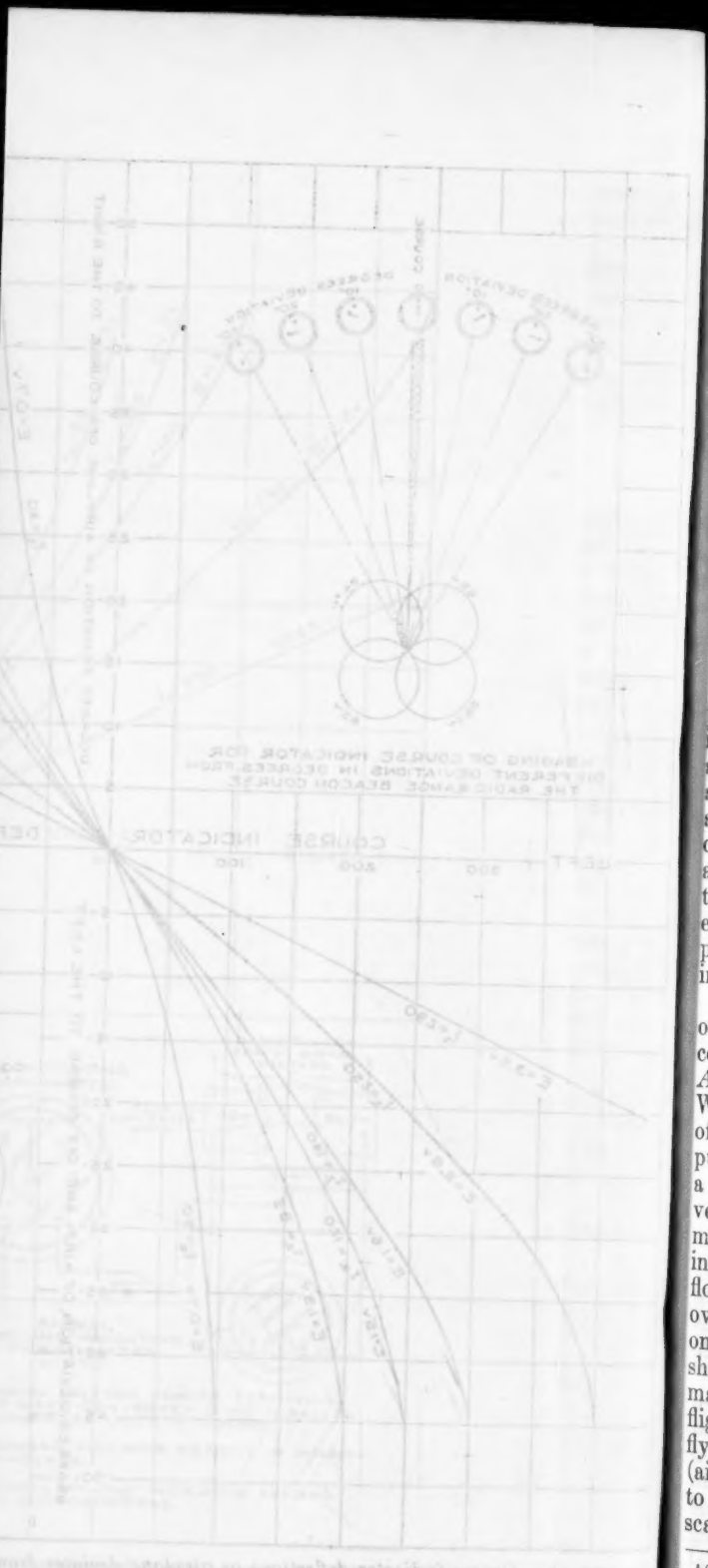

more than ±5° from the true course without losing an indication of the degree of further deviation.

Satisfactory course indication for most purposes is given by using a signal volume level I_2 of 250 microamperes, which is one-half-scale deflection. This signal level when used with a 250–0–250 microammeter course indicator, makes possible a deviation from the course of ±21°, with correct course-deviation indications throughout this range.

Instead of varying the voltage E as shown, it may be held at some value such as 3.5 volts, and a similar set of graphs obtained by varying the resistance R (fig. 15), in series with the course-indicating microammeter.

From the above it will be seen that the reed converter used in the circuits as shown is very flexible in its use and may be adjusted at will (by the pilot if desired) to suit the conditions of use.

3. REED CONVERTER APPLIED TO 4- OR 12-COURSE BEACON

(a) TWO-UNIT PLUG-IN ARRANGEMENT

In order to explain the application of the reed converter to a multiplicity of courses, the polar diagram for a 12-course beacon is shown in Figure 16. As far as the modulation frequencies and course colors are concerned, this diagram may represent three 4-course beacons also; red and black courses being on one, brown and blue courses on a second, and yellow and green courses on a third. The colors indicate the courses or zones where two of the frequencies of modulation are present in equal amounts. This color scheme has been chosen to simplify the use of the 12-course tuned reed indicator,[5] and is equally effective for simplifying the use of the reed-converters. The pilot's map, if he requires one, should show the radiobeacon courses in their proper color.

One method of applying the reed converters for use on any course of a 4- or 12-course beacon is shown in Figure 17. Here a double reed-converter plug-in mounting, as shown in Figure 5, is provided at A–B, into which any two converter units may be quickly plugged. With a given set of two units, the pilot may use four of the courses of a 12-course beacon or the four courses of a 4-course beacon. By putting a 65-cycle converter in at A and 86.7-cycle converter at B, a red or black course may be flown. By putting a 108.3-cycle converter in place of the 86.7-cycle unit in B, a brown or blue course may be flown, or by putting an 86.7-cycle converter in at A and leaving the 108.3-cycle unit in at B, a yellow or green course may be flown. For example, let us assume that it is desired to fly an airplane over a yellow radiobeacon course. Referring to Figure 17, the chart on the right shows that for a yellow course an 86.7-cycle converter should be plugged in at A and a 108.3-cycle converter at B. This may be done by the ground personnel. Now, let the direction of flight be "from" the beacon and let us assume that the pilot wishes to fly along the line OD (fig. 16,) slightly to the right of the course (airplanes going in the opposite direction flying a little to their right to avoid collision). The deviometer pointer, pointing to the yellow scale, is turned to point toward the word "Right" on the" From"

[5] See second paper of foot note, p. 148.

scale. This increases the sensitivity of the 86.7-cycle reed at A and decreases the sensitivity of the 108.3-cycle reed at B. It will be noted from Figure 16 when going "from" the beacon (the beacon being at the intersection of all courses at O) on a yellow course, when deviating to the right along the line OD, the 108.3-cycle signal becomes greater than the 86.7-cycle signal by an amount proportional to EF, so it must be cut down to make them equal. This is what occurs when the

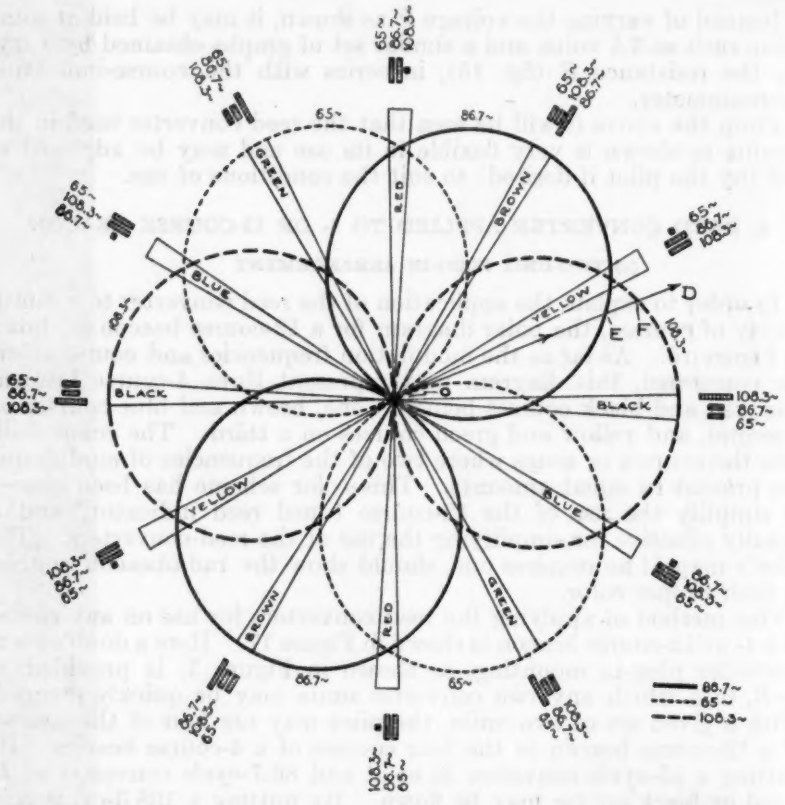

FIGURE 16.—*The 12-course radio range-beacon transmission characteristic*

The colors indicate the courses where two modulation frequencies are of equal strength and reed-converter outputs are equal, producing an on-course reading on the course indicator.

deviometer pointer is moved as stated above, since a lower resistance is shunted across B or the 108.3-cycle reed, thus cutting down its sensitivity, and a higher resistance is shunted across A, the 86.7-cycle reed, thus increasing its sensitivity.

The course-selector switch must also be set so that the pointer on the yellow scale points to "From." In this position it will be noted that the positive output of the 108.3-cycle converter at B is connected to the + side of the course-indicating instrument, thus causing it to deflect to the right, as the 108.3-cycle signal predominates over the 86.7-cycle signal. From Figure 16, it will be seen that when flying on the yellow course "from" the beacon that the 108.3-cycle signal predominates when the airplane deviates to the right. Thus the course

indicator needle deflects in the direction of deviation of the airplane from the course.

By taking any course and any desired direction of flight and using Figures 16 and 17, it can be shown as above that when the proper two

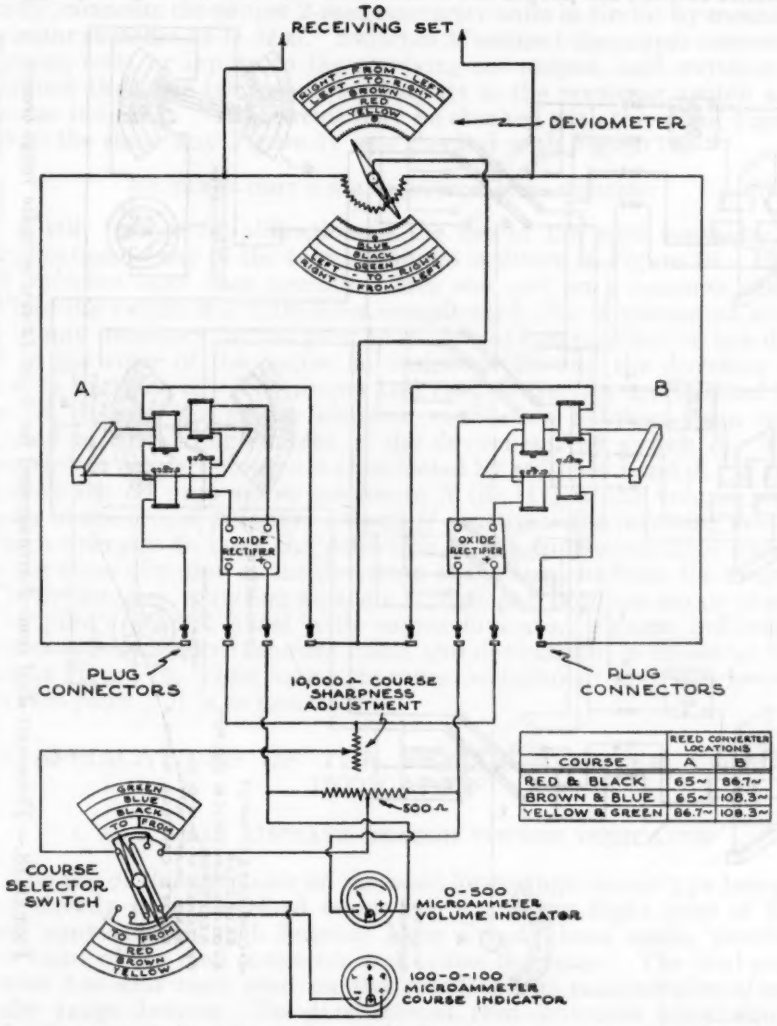

COURSE	REED CONVERTER LOCATIONS A	B
RED & BLACK	65~	86.7~
BROWN & BLUE	65~	108.3~
YELLOW & GREEN	86.7~	108.3~

FIGURE 17.—*Deviometer and course-selector switch with color system and converter plug-in arrangement for adapting the reed converter for use in any direction of flight on any course of a 4- or 12-course beacon.*

reed-converter units are plugged into circuit and the deviometer and course-selector switch set properly, correct course-deviation indications will be obtained.

The 2-unit plug-in converter arrangement shown in Figure 17 is applicable where a given airplane is flown over the routes of 4-course beacons with the same colored courses or from one 12-course beacon

to another on the same color and 90° color routes; for example, airplanes flying on a transcontinental air route or on a north and south route would probably use the same color course all the way, in which case this circuit arrangement would be useful. Should the airplane fly other routes, the proper set of reed-converter units may be plugged

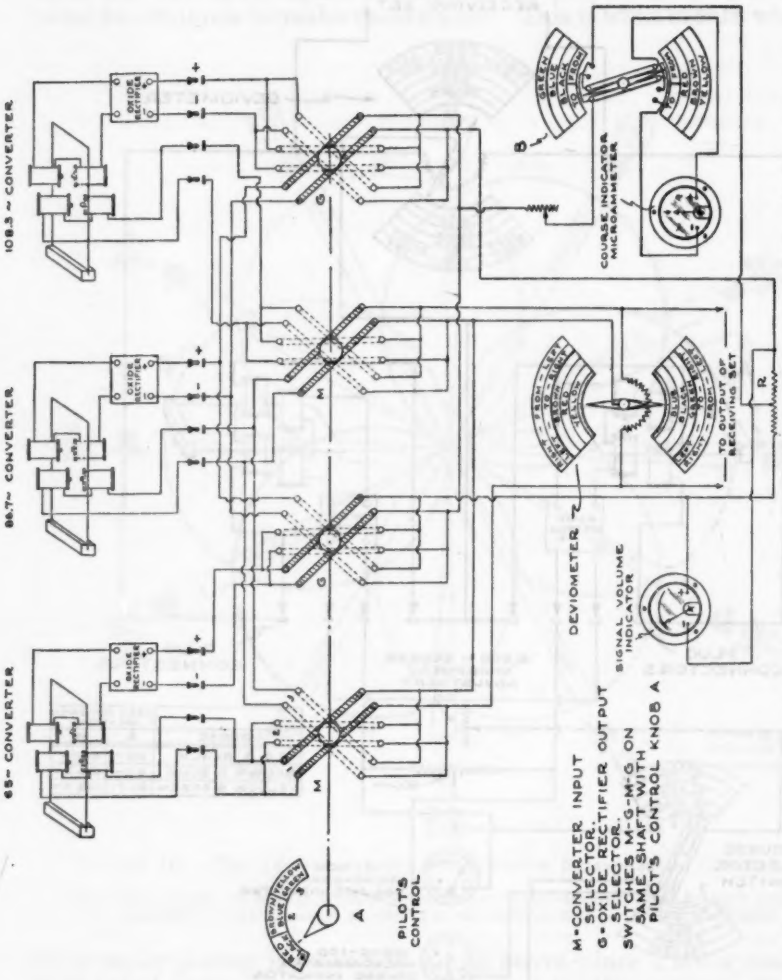

FIGURE 18.—*Three-unit dual control arrangement for 4- or 12-course radio range beacon*

By setting dial *A* to the color of the course to be flown the proper 2-reed converters are automatically connected in circuit. *B* is the reversing switch for the course indicating instrument.

in, thereby adapting the course indicator for use on these routes. An advantage of this circuit with plug-in arrangement is that a simple form of course-selector switch may be used as shown in Figure 17.

(b) THREE-UNIT DUAL-CONTROL ARRANGEMENT

(b) In order to make a single reed-converter installation useful on any course of a 4 or 12-course beacon at all times without any plugging in of reed-converter units by the pilot or ground personnel, a 3-unit circuit arrangement shown in Figure 18 has been worked out. The selector or reversing switch and deviometer shown in Figure 17 have

been retained, but a second selector switch containing the dial *A* and switches *M-G-M-G* on a common shaft has been added. The three converter units are left permanently in circuit, although they are still of the plug-in type so as to be quickly removed for replacement if necessary. The dial *A* when set to the color of the course the pilot desires to fly, connects the proper 2-reed converter units in circuit by means of selector switches *M-G-M-G*. Switches *M* connect the proper converter driving coils or inputs to the receiving set output, and switches *G* connect the same two converter outputs to the reversing switch and course indicator. This circuit may be checked with the aid of Figure 16 in the same way Figure 17 was checked with Figure 16.

(c) THREE-UNIT SINGLE-CONTROL ARRANGEMENT

A still further simplification in the use of the reed converter in application to any of the 4- or 12-courses is shown in Figure 19. Here all switches have been combined into one unit on a common shaft. While the switch is a little more complicated, this is warranted since it is only necessary for the pilot to set one of two pointers on one dial *D* to the color of the course he desires to fly and the direction he desires to fly on it. The proper two reed converters are selected by switch *E*, and the proper common connection between them connected to the sliding contact of the deviometer by switch *F*. The proper two converter outputs are selected by switches *I* and *J*. *J* also applies the *RI* drop across resistance *R* (fig. 11) to the volume indicator in the proper polarity. *G* and *H* constitute the reversing switch which operates to keep the deflection of the course-indicator needle in the same direction as the deviation of the airplane from the course. The deviometer, requiring separate adjustment, is on a separate shaft. The pilot's control panel with course indicator, volume indicator, course selector switch, control knob, and deviometer, is shown at the left in Figure 19. The course sharpness adjustment may also be put on this panel if it is so desired.

IV. APPLICATIONS OF THE REED-CONVERTER COURSE INDICATOR

1. AS A MAIN AIRWAYS BEACON COURSE INDICATOR

The use of this indicator on the main long-range visual-type beacon has already been described under III, 3. Many flight tests of the reed converter on such beacons have already been made, proving the value of the reed converter as a course indicator. The reed converter has also been used on the simultaneous radiotelephone and radio range beacon. To date several reed-converter installations have been made and have proven satisfactory.

2. USE IN HOLDING AN AIRPLANE AUTOMATICALLY ON A RADIO-BEACON COURSE

An early application of the reed converter was realized to be that of holding an airplane automatically on a given radiobeacon course. While the details of this application have not been tried, the fact that the reed converter produces a varying current output with a polarity, depending upon the direction of deviation of the airplane

from the course, makes it possible to use this current for control purposes, the airplane thereby being guided automatically in a horizontal plane along the radiobeacon course.

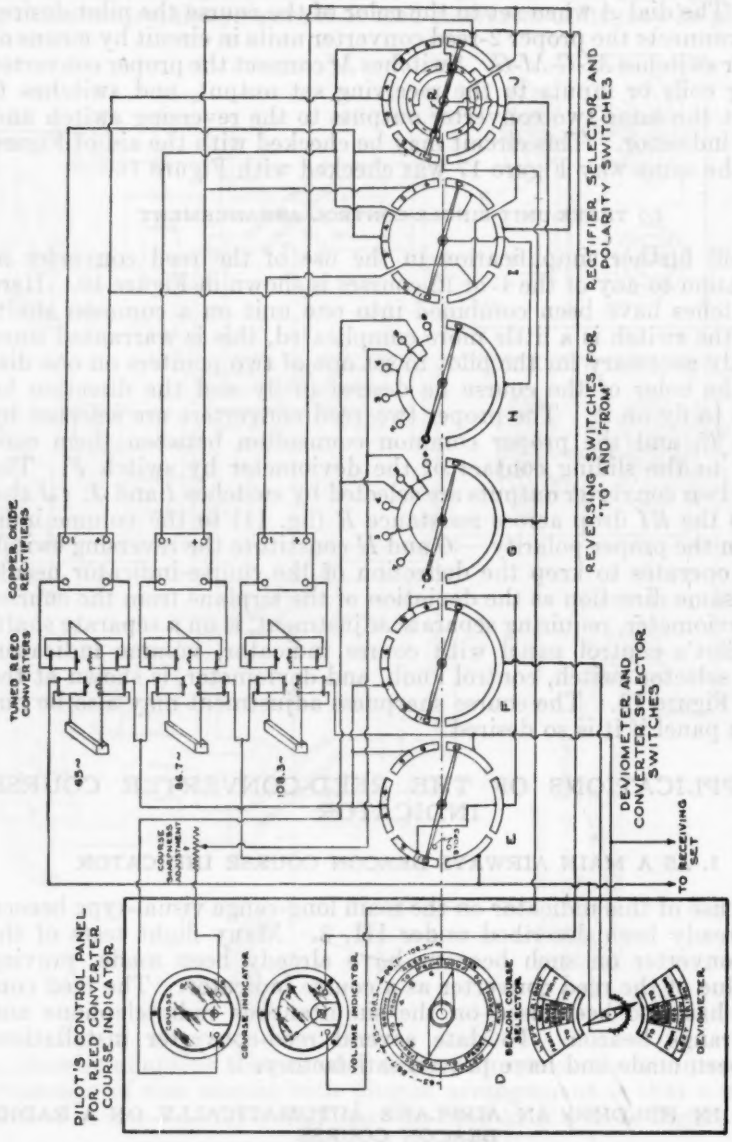

FIGURE 19.—*Three-unit single-control arrangement for the 4- or 12-course range beacon*

In this arrangement both the selector switch and the indicating instrument reversing switch are operated by one control.

3. USE AS A COURSE INDICATOR ON THE RUNWAY LOCALIZING BEACON FOR BLIND-LANDING PURPOSES

A valuable application of the reed converter has been found in the radio system of blind-landing aids developed by the National Bureau

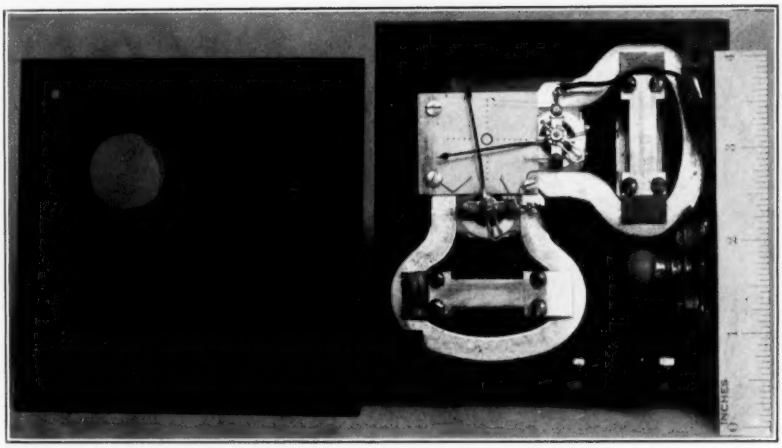

FIGURE 20.—*Tuned-reed converter course indicating instrument combined with the fog landing beam indicating instrument*

The point of intersection of the pointers indicates the position of the airplane with respect to both the runway course and high-frequency landing beam path. The intersection shown indicates that the airplane is too low and off to the left.

of Standards.[6] Here the reed converter is used as a runway-localizer course indicator giving indication that the airplane is over the runway (along which the runway beacon course is oriented). Since vertical guidance is obtained by flying in on the underside of a high-frequency radiobeam, using as the indicator a 0–500 microammeter mounted horizontally, it has been found possible to combine the reed-converter runway course-indicating instrument and the fog-landing beam-indicating instrument into one unit, as shown in Figure 20. Here the vertical needle is the 100–0–100 microammeter reed-converter runway-course indicator giving horizontal guidance, and the horizontal needle the high-frequency landing-beam course indicator giving vertical guidance. With the landing airplane on both courses, the two needles intersect over the circle. The needle intersection in Figure 20 shows that the airplane is below the proper glide path of the high-frequency landing beam, as the horizontal needle is below the circle, and off to the left of the runway course, as the vertical needle is

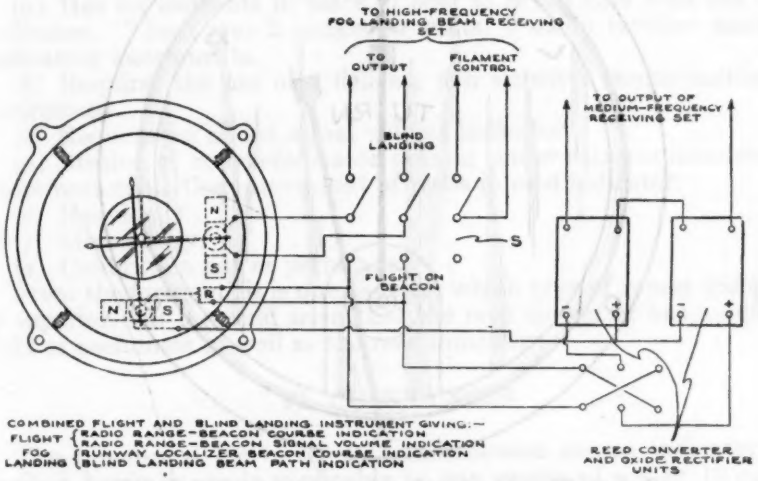

FIGURE 21.—*Combined flying and landing instrument as shown in Figure 20, and connected to give: (1) main beacon-course indications; (2) signal-volume indications; (3) runway-course indications; (4) landing beam-path indications*

to the left of the circle. This type of combined instrument has been found by numerous flights to be much easier to use than two separate instruments. The instrument may be made much smaller than that shown in Figure 20 and put in a round case by turning the permanent magnets (with the screws holding the pole pieces acting as a pivot) until they extend to the rear, perpendicular to the face of the instrument.

An advantage of the use of this combined instrument is that the 0–500 microammeter which is used to indicate the landing-beam path may perform a dual function, as shown in Figure 21. By means of a double-pole double-throw switch this instrument may be connected either to the output of the high-frequency fog landing beam receiver

[6] H. Diamond and F. W. Dunmore, A Radio Beacon and Receiving System for Blind Landing of Aircraft, B. S. Jour. Research, **5** (RP238); October, 1930. Proc. I. R. E., **19**, p 585; April, 1931.

and used as the landing-beam course indicator when landing in fog, or it may be connected across resistance R (see also fig. 11) in the output of the oxide rectifiers, and thus may serve as the signal-volume indicator. Since the signal-volume indicator is not necessary when landing, the combined instrument is thus made to take the place of three instruments. Thus when flying on the main radio range beacon the vertical pointer gives course indication and the horizontal needle signal-volume indication. When landing in fog, the same two pointers are used, the vertical one now giving runway-course indication, since the receiving set is tuned to the runway-localizer beacon, and the horizontal pointer correct landing-beam path indications. By making

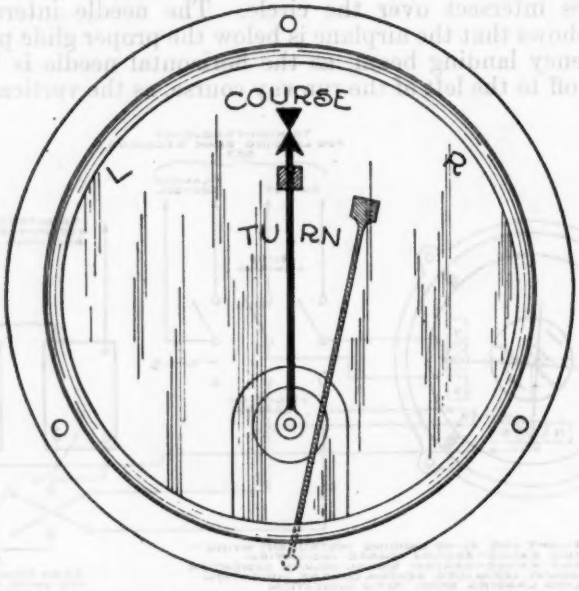

FIGURE 22.—*The tuned-reed-converter course-indicating instrument combined with the turn indicator, giving both indications on one dial*

the switch of the 3-pole double-throw type as shown at S (fig. 21), it may be made to turn on the landing-beam receiving set at the same time the instrument is connected to this set.

4. COMBINATION WITH TURN INDICATOR

Another combination of aircraft instruments made possible with the reed-converter type of indicator is that of the turn indicator and the reed-converter course-indicating instrument. Such a combination is shown in Figure 22, where the turn indicator is mounted in the rear of the zero-center beacon course indicator with a pointer on an extended shaft, traveling over the same instrument face as the pointer of the course indicator. The pointers are quite different in form to avoid confusion, and travel over different scales but on the same face. This combination greatly facilitates the use of the two instruments and saves panel space.

V. COMPARISON OF REED CONVERTER WITH REED INDICATOR

1. ADVANTAGES OF REED CONVERTER

(*a*) Gives sharper course indications.
(*b*) More easily adapted in combination with other aircraft and radio instruments.
(*c*) Greater damping of reeds allows greater variation in the modulation frequencies at the beacon.
(*d*) More easily adapted to the 12-course radio range beacon.
(*e*) Pointer type of course indications easier to see.
(*f*) Adapted to holding an airplane automatically on the course.
(*g*) Easier to tune the reed to the required frequency.

2. DISADVANTAGES OF REED CONVERTER

(*a*) Has six elements in place of one, as is the case with the reed indicator. These are: 2 connector units, 2 oxide rectifier units, 2 indicating instruments.
(*b*) Requires the use of a delicate and sensitive course-indicating instrument.
(*c*) Requires an added signal volume indicator.
(*d*) Motion of course-indicator pointer under extreme interference more noticeable than movement of reeds in reed indicator.
(*e*) Heavier.
(*f*) More costly.
(*g*) Calibration not as permanent.

From the foregoing it is questionable which type of course indicator is superior, but it would seem that the reed converter has a definite field of usefulness as well as the reed indicator.

VI. CONCLUSION

The tuned-reed converter as a radiobeacon course indicator described herein is made applicable to any course of a 4 or 12 course beacon by means of suitable selector switches, deviometer, volume indicator, and course sharpness adjustment. The converter consists of a common polarized tuned reed vibrating between two sets of electromagnets, one set being for driving the reed and the other set the pick-up or generating coils. The selector switch picks out the proper two reed-converter units for a given radio range beacon course and connects their outputs in the proper polarity to a zero-center course indicating instrument. A volume indicator is provided to indicate the presence of the beacon signal and the proper functioning of the receiving circuits. A color and wording system on the dial of the selector switch has been worked out so that when the pilot sets a pointer to the color of the course he is to fly and the direction he is to fly on it, the course deviations of the course indicator will be correct.

The zero-center course indicator is readily adapted in combination with other indicating instruments, especially the fog-landing indicator and the turn indicator. The combination with the fog-landing indicator makes a single instrument which serves as a main beacon course

indicator, signal volume indicator, runway course indicator, and landing beam path indicator.

The author is indebted to H. Diamond for helpful suggestions in connection with the reed-converter circuit arrangements, and to G. L Davies for suggestions relative to the design of the reed in the converter unit.

WASHINGTON, April 18, 1931.

RP337.

THE VISIBLE AND ULTRAVIOLET ABSORPTION SPECTRA OF CAROTIN AND XANTHOPHYLL AND THE CHANGES ACCOMPANYING OXIDATION

By H. J. McNicholas

ABSTRACT

The absorption spectra of equal molecular concentrations of pure carotin and xanthophyll in alcohol-ether solution are studied throughout the visible and ultraviolet spectral range, and the changes in these spectra are followed as the pigments oxidize slowly in solution.

The frequencies of the absorption bands for each pure unoxidized pigment appear to form a regular sequence extending throughout the observed spectral range and converging toward the lower frequencies in accordance with a simple parabolic law for each pigment. The imposition of a periodic variation in intensity on this progression of bands gives the appearance of three adjacent spectral regions of selective absorption which are partially resolved into overlapping component bands.

During oxidation of the pigments both spectra pass through the same characteristic series of changes, which are such as to indicate two very definite stages in the oxidation process for each pigment. Carotin is not oxidized to xanthophyll in this process, as contended by some previous investigators. The stages of oxidation are closely related to the two stages of hydrogenation described by Zechmeister and his associates. The oxidation data confirm the contentions of Schertz and others that the different xanthophylls described by Tswett may represent distinct stages in the oxidation of a single pigment.

CONTENTS

		Page
I.	Introduction	171
II.	Methods and nomenclature	173
III.	Preparation and exposure of the solutions	174
	1. Choice of solvent	174
	2. Experimental procedure	175
IV.	Absorption spectra of the pure pigments	176
V.	Oxidation in solution	185
	1. Experimental data	185
	2. Test for oxidation	188
VI.	Bearing of the oxidation experiments on the work of other investigators	188
VII.	Concluding remarks	191

I. INTRODUCTION

The wide distribution of the chloroplast pigments [1] in the tissues of plants and animals has attracted the attention of biologists since earliest times. Much progress has been made in the isolation,

[1] The chloroplast pigments constitute a group of four pigments which are always found closely associated in the chloroplastids of plant cells. These pigments are carotin, xanthophyll, chlorophyll-*a*, and chlorophyll-*b*. Other closely related pigments such as lycopin (an isomer of carotin), fucoxanthin, and some chlorophyll derivatives, are also found under certain conditions in the plastids of various plant cells.

identification, and classification of these pigments, but our knowledge of their significance, relationship, or function, in the metabolism of plant and animal life, has hardly progressed beyond the realms of speculation. A comprehensive discussion of the subject is contained in the books by Willstatter and Stoll,[2] Palmer,[3] and Spoehr.[4]

Carotin and xanthophyll are the two yellow chloroplast pigments occurring in relatively large quantities along with chlorophyll in green plants. Carotin is a highly unsaturated hydrocarbon, $C_{40}H_{56}$, and one of the few naturally occurring "colored" hydrocarbons. Xanthophyll is very similar to carotin in its physical and chemical properties, and has the atomic composition $C_{40}H_{56}O_2$. The molecular structure of these pigments is not definitely determined. Their isolation and the study of their physical and chemical properties is fraught with many difficulties, owing, in part, to the ease with which the pigments take up oxygen, either in solution or in the solid state. Some of their most characteristic properties undergo a marked alteration even in the earliest stage of oxidation. This is true of the spectral absorptive properties, which have long been a valuable aid in the identification and quantitative estimation of the pigments.

Many attempts have been made by various investigators to explain the presence and mysterious associations of these yellow pigments. Thus, the close correlation between carotin pigmentation and vitamin A content of plant tissues and the presence of carotin in milk and xanthophyll in egg yolks has led to much controversial discussion of the probable significance of these associations. Hypothetical relationships between the chloroplast pigments and theories of the interconversion of these pigments in the process of photosynthesis have all been advanced from time to time. Usually these speculations have not been substantiated by careful and thorough experimentation. From the standpoint of molecular structure and possible function in the living plant the great affinity of carotin and xanthophyll for oxygen is a matter of considerable interest. It has been contended that these pigments may play a respiratory rôle or aid in the regulation of oxygen pressure in the plant cells.

Aside from the academic and biological interest which may be attached to a study of the absorptive properties of the chloroplast pigments, the information thereby obtained is of value in the manufacture, purification, and bleaching of vegetable oils and other natural food products, such as flour, the color of which is a matter of considerable commercial importance. It is known that carotin, xanthophyll, and chlorophyll or its derivatives, are present in varying proportions in these materials and often play the chief rôle in determining the color of the finished product.

In the course of some studies of the chloroplast pigments, conducted at the Bureau of Plant Industry, United States Department of Agriculture, preparations of pure carotin and xanthophyll were made by Dr. F. M. Schertz, who also studied some of the physical and chemical properties [5] of these materials and applied colorimetric and spectrophotometric methods in their quantitative estimation.[6] Through

[2] Investigations on Chlorophyll. Authorized English translation from the German by F. M. Schertz and A. R. Merz. Published by F. M. Schertz, 1305 Farragut Street, NW., Washington, D. C.
[3] Carotinoids and Related Pigments. The Chemical Catalogue Co. (Inc.); 1922.
[4] Photosynthesis. The Chemical Catalogue Co. (Inc.); 1926.
[5] J. Agri. Research, **30**, p. 469; 1925 (carotin), **30**, 575; 1925 (xanthophyll).
[6] J. Agri. Research, **26**, p. 383; 1923 (carotin), **30**, 253; 1925 (xanthophyll).

the generosity of Doctor Schertz, freshly prepared crystals of pure carotin and xanthophyll were obtained for the present investigation. The author wishes to acknowledge his indebtedness to Doctor Schertz for his whole-hearted interest and assistance in the work and for his painstaking efforts to supply materials of the highest possible purity.

In the present investigation the absorption spectra of pure carotin and xanthophyll are studied throughout the visible and ultra-violet spectral range, and the changes in these spectra are followed as the pigments oxidize slowly in solution. The oxidation data afford the principle subject for discussion, inasmuch as they have an important bearing on some experimental results and conclusions of other investigators. The structure of the absorption spectrum of each pure unoxidized pigment is fully described, but a detailed discussion of the significance of this structure, or its implications regarding possible structural relations of carotin and xanthophyll to other chloroplast pigments, must await the further development of absorption theory and the completion of much more experimental work on these materials.

II. METHODS AND NOMENCLATURE

Detailed descriptions of the methods and apparatus used in the present investigation have been given in other publications. The visual method,[7] using the Koenig-Martens spectrophotometer,[8] and the photoelectric method[9] have been used to supplement and extend the photographic method[10] in the visible spectrum. All measurements in the ultra-violet were made by the photographic method, in which the underwater spark is used with a Hilger sector photometer and quartz spectrograph.

In each of these methods the transmission of a cell containing the solution is compared at different spectral frequencies (or wave lengths) with the transmission of a duplicate cell containing the solvent. If the transmissions of the cells containing the solution and solvent are represented by T_{sol} and T_{sov}, respectively, the absorbancy[11] is then defined by the following relation,

$$\text{Absorbancy} \equiv -\log_{10} \frac{T_{sol}}{T_{sov}} = bc\mathbf{k}$$

wherein b is the thickness of the absorbing layer, c is the concentration of the absorber, and $\mathbf{k}$ is the specific absorptive index. The latter quantity is a function of the frequency (or wave length) and is a characteristic property of the absorber and its immediate environment. The environmental effects of usual interest in these measurements are determined by the temperature, the nature of the solvent, and the concentration of the absorber. The temperature coefficient of change is usually small, and in the present investigation measurements were made at ordinary room temperatures without specific con-

[7] McNicholas, B. S. Jour. Research, **1**, p. 793; 1928.
[8] Martens and Grünbaum, Ann. der Phys. (4), **12**, p. 984; 1903.
[9] Gibson, J. Opt. Soc. and Rev. Sci. Inst., **7**, p. 693; 1923.
[10] Howe, Phys. Rev. (2), **8**, p. 674; 1916. B. S. Sci. Papers (No. 440), **18**, p. 121; 1922: B. S. Jour. Research, **1**, p. 939; 1928.
[11] For previous use of this term see R. Davis and K. S. Gibson, Filters for the Reproduction of Sunlight and Daylight and the Determination of Color Temperature. B. S. Miscellaneous Publication, No. 114, p. 39.

trol. Likewise, for the range of relatively low concentrations covered, the specific absorptive index may be considered independent of the concentration, so that, for a given solvent, the absorbancy is simply proportional to the product *bc*. This condition is generally expressed as Beer's law of absorption.

In the present work a convenient molecular concentration is chosen arbitrarily as the unit. This unit, for carotin, is 0.80 cg of the pure pigment in 1 liter of the solution. The same (unit) molecular concentration of xanthophyll, then, is 0.85 cg of the pigment in 1 liter of the solution. The pure crystals were known to contain no solvent molecules of crystalization. Taking the unit of thickness as the centimeter, measurements were made for values of the product *bc* equal to 1, 5, and 10. In the graphical presentation of the absorption spectra (figs. 1, 2, 4, and 5) the absorbancy for the above given values of *bc* is shown as a function of the frequency with the unit of frequency chosen as one vibration cycle per micro-micro-second (10^{-12} sec.). Hence

$$\text{Frequency} = \frac{\text{Vibrations}}{\text{sec.} \times 10^{12}} = \frac{3 \times 10^5}{\text{Wave length in millimicrons}}$$

III. PREPARATION AND EXPOSURE OF THE SOLUTIONS

1. CHOICE OF SOLVENT

In order to extend the absorption measurements as far as possible into the ultra-violet it is of importance to consider the absorptive properties of the organic solvents available for carotin and xanthophyll. As shown by Brode [12] the majority of these solvents, such as carbon disulphide, acetone, benzene, carbon tetrachloride, chloroform, and petroleum ether, exhibit strong general absorption in the far ultra-violet and are for this reason unsuited for the present work. Pure ethyl alcohol and ethyl ether, on the other hand, are quite transparent up to frequencies of 1,250 or 1,300, and were therefore selected for this investigation.

Different samples of alcohol or ether, however, may differ widely in their absorptive properties in the far ultra-violet, because of impurities which are usually present in small amounts, but which may exhibit, nevertheless, very strong selective or general absorption in this region. It is known that oxidation products may gradually form in alcohol and ether. Other impurities, such as benzene, may be present when this substance is used to dehydrate the alcohol. Although these impurities may be of no consequence in the usual chemical applications of these solvents, they are obviously of considerable importance in the absorption measurements. It is necessary to work with carefully purified or freshly distilled materials, free from sharp absorption bands or strong general absorption, and always to use the same batch of solvent in the solvent cell as used in the preparation of the solution.

It has been shown by Clover [13] that when a glass-stoppered bottle of ethyl ether is allowed to stand for several months, it acquires oxidizing properties which may be attributed to the formation of

[12] J. Phys. Chem., 30, p. 61; 1926. [13] J. Am. Chem. Soc., 44, p. 1107; 1922.

ethyl peroxide. This oxidation of the ether is accelerated by the action of light. The experiments of Schertz [14] have shown that both carotin and xanthophyll oxidize quite readily in pure, freshly distilled ethyl ether, but are comparatively stable in petroleum ether and alcohol solutions. It is probable that the formation of the peroxide in ethyl ether is responsible for the more rapid oxidation of the pigments in this solvent.

It seemed desirable to use ether as a solvent for the oxidation experiments. The pigments are also more soluble in ether than in alcohol. The high volatility of ether, however, introduced some difficulties in the absorption measurements, because of the occasional leakage of the ether from the particular type of absorption cell used in this work.[15] To meet in the most satisfactory manner these and other conditions arising in the preparation, measurement, and exposure of the solutions, the pigments were exposed to oxidation agencies in a fairly concentrated solution containing a high percentage of ether, and the solution then diluted with alcohol for the absorption measurements. All of the alcohol and ether used was previously redistilled and tested for the presence of any unusual absorption in the far ultra-violet. Sufficient volumes of each of these solvents were then set aside to supply all needs in the work.

2. EXPERIMENTAL PROCEDURE

The work on carotin was undertaken first. Having determined by preliminary trials the concentrations most suitable for the measurements, 2.00 cg of the freshly prepared crystals were weighed at the Bureau of Plant Industry and immediately transported to the National Bureau of Standards under a little absolute ethyl alcohol, sufficient to completely cover the crystals and thus to prevent undue exposure to oxidizing agencies. At the National Bureau of Standards the alcohol was increased to 50 ml and sufficient absolute ethyl ether was added to dissolve the crystals completely and to make up exactly 250 ml at the proper temperature, as designated for the graduation mark on the flask. The result was a stock solution of carotin, with a molecular concentration of 10 units, in a solvent consisting of 20 per cent alcohol and 80 per cent ether.

The preparation of the crystals and the solution occupied the greater part of one day. The solution was then stored in a cool, dark place and absorption measurements made on the following day. For these measurements the following dilutions were made:

Solution No. 1.—To 10 ml of the stock solution 30 ml of alcohol was added making a concentration of 2.5 molecular units in a solvent consisting of 80 per cent alcohol and 20 per cent ether. This solution was used in thicknesses of 2 and 4 cm ($bc = 5$ and 10, respectively) for measurements in the ultra-violet region of the spectrum.

Solution No. 2.—To 10 ml of solution No. 1, 40 ml of a mixture of 80 per cent alcohol and 20 per cent ether was added, making a molecular concentration of 0.5 unit in a solvent consisting, as before, of

[14] J. Agr. Research, **30**, pp. 469, 575; 1925.

[15] The construction of the cell is described in B. S. Sci. Paper No. 440. (See footnote 10.) The glass end plates are replaced by quartz plates for the ultra-violet measurements. These plates are clamped tightly against the finely ground plane-parallel ends of a glass tube. If the plates and ends of the tube do not make exceptionally good contact, highly volatile solvents, such as ether, will gradually leak out.

80 per cent alcohol and 20 per cent ether. This solution was used in a thickness of 2 cm ($bc=1$) for measurements in the visible and near ultra-violet.

All data obtained on the pure pigment in solution are given in Figure 1, and are discussed later in Section IV.

After solutions Nos. 1 and 2 were prepared, the stock solution, contained in a tightly-stoppered colorless-glass bottle, was placed on a shelf near a south window of the laboratory. The solution was thus exposed to diffused light from the walls of the room and to direct light from the southern sky, after transmission by the window glass and glass wall of the container. No direct sunlight was at any time incident on the solution. Two colorless-glass bottles, containing, respectively, pure alcohol and the 80:20 alcohol-ether mixture, were exposed with the stock solution to the same conditions of temperature and illumination. These bottles held sufficient volumes of the two solvents to supply all needs in future dilutions of the stock solution and for use in the solvent cell. No record was kept of weather conditions during the period of exposure.[16] The absorption spectrum of the slowly oxidizing material was redetermined at intervals of four or five weeks, the same experimental procedure being followed in each redetermination as described above for the pure pigment. The resulting absorption curves, with the record of exposure times, are shown in Figure 4 and are discussed in Section V.

The solution of xanthophyll was prepared and the absorption measurements begun approximately four months after the first measurement had been made on carotin. The procedure in making the solution and in carrying out the measurements was the same as that just described for carotin. The results are shown in Figures 2 and 5 and are discussed in Sections IV and V.

In order to work with molecular concentrations of xanthophyll, equal to the concentrations previously chosen for carotin, 2.12 cg of the freshly prepared crystals were weighed and dissolved in the alcohol-ether solvent. Different stocks of alcohol and ether were used for this series of measurements, but were selected, as before, with due regard to ultra-violet transparency. The stock solution was exposed at the same location in the laboratory, but the exposure periods were not simultaneous with those of carotin, of course, being made during different months of the year. (See legends of figs. 4 and 5.) The rates of oxidation of the two pigments are, therefore, not strictly comparable.

IV. ABSORPTION SPECTRA OF THE PURE PIGMENTS

The visible and ultra-violet absorption spectra of pure carotin and xanthophyll in equal molecular concentrations are shown in Figures 1 and 2. Values of absorbancy, as read from the curves, are also listed in Table 1.

In the early studies of these absorption spectra the various investigators recorded only two or three bands for each pigment, and sometimes a fourth band for xanthophyll. These bands are the definitely resolved components of the strong group of bands in the blue and violet regions of the visible spectrum. All the early work was done by

[16] These records are obtainable from the U. S. Weather Bureau. See dates of exposure in legends to Figures 4 and 5.

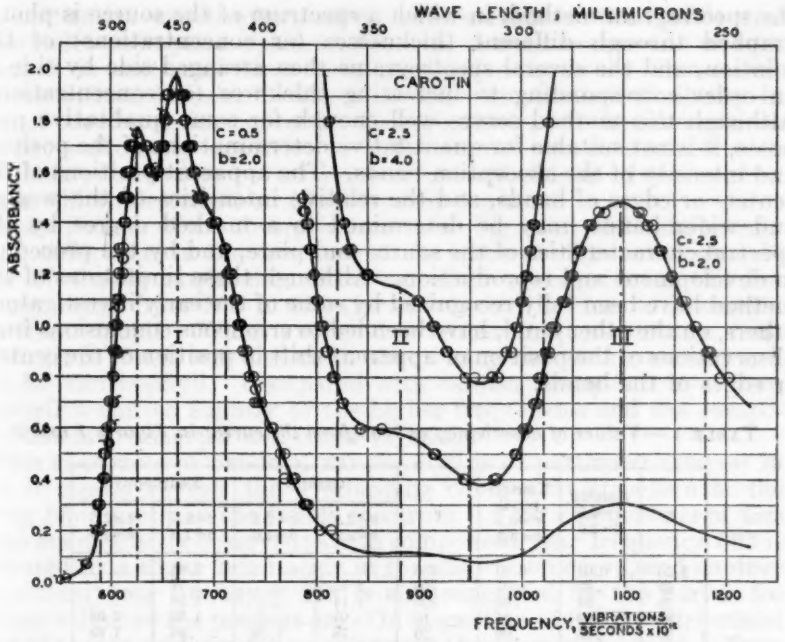

FIGURE 1.—*Visible and ultra-violet absorption spectrum of carotin*

Solvent: 80 per cent alcohol+20 per cent ether. Unit concentration (*c*) is 0.80 cg/l; unit thickness (*b*) is 1 cm. Methods: Open circles, photographic; hooked circles, visual.

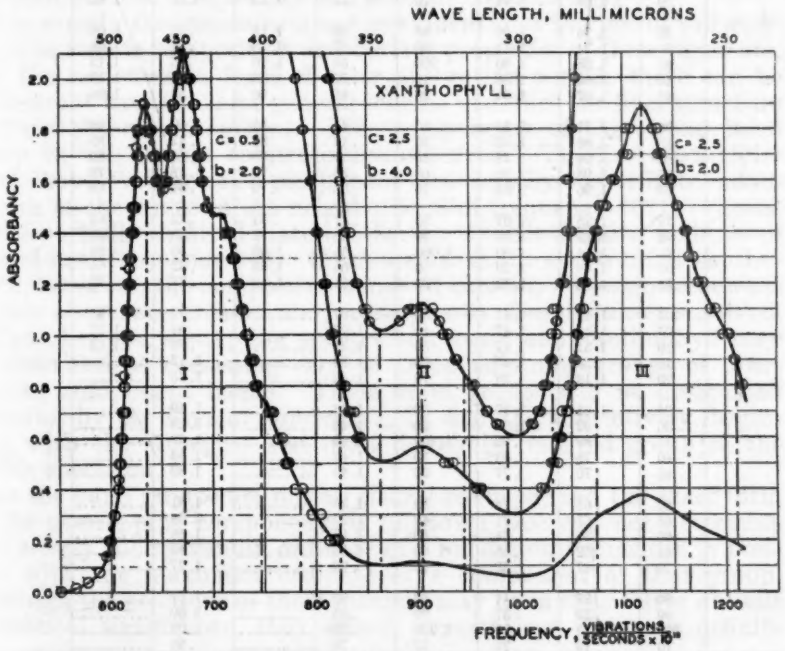

FIGURE 2.—*Visible and ultra-violet absorption spectrum of xanthophyll*

Solvent: 80 per cent alcohol+20 per cent ether. Unit concentration (*c*) is 0.85 cg/l; unit thickness (*b*) is 1 cm. Methods: Open circles, photographic; hooked circles, visual; filled circles, photo-electric.

the spectrogram method, in which a spectrum of the source is photographed through different thicknesses (or concentrations) of the solution, and the several spectrograms then arranged side by side in an order corresponding to increasing thickness (or concentration). Although this method serves well enough for some qualitative purposes, it is not suitable for quantitative determinations of the position and intensity of the absorption bands. The apparent positions of the centers or edges of bands, and the relative intensities of the weaker and wider bands, may be determined to a marked degree by the spectral characteristics of the source and plate, and by the procedure in development and reproduction. Although these limitations of the method have been fully recognized by some of the early investigators, others, on the other hand, have been led to erroneous conclusions from observations of the position or apparent shift in position of the centers or edges of the bands.

TABLE 1.—*Values of absorbancy as read from the curves in Figures 1 and 2*

ν	Carotin $c=0.5$ $b=2.0$	Xantho-phyll $c=0.5$ $b=2.0$	ν	Carotin		Xanthophyll	
				$c=2.5$ $b=2.0$	$c=2.5$ $b=4.0$	$c=2.5$ $b=2.0$	$c=2.5$ $b=4.0$
5.50	0.01	0.00	780	----------	----------	2.04	----------
60	.02	.01	790	1.45	----------	1.77	----------
70	.04	.02	800	1.14	----------	1.48	----------
80	.09	.05	10	.93	----------	1.19	2.08
90	.35	.09	20	.78	1.59	.94	1.88
600	.68	.22	30	.67	1.35	.74	1.44
05	.95	.32	40	.62	1.24	.61	1.21
10	1.21	.55	50	.60	1.20	.54	1.07
15	1.50	.99	60	.60	1.18	.51	1.02
20	1.68	1.34	70	.59	1.16	.51	1.02
25	1.76	1.60	80	.58	1.15	.52	1.04
30	1.74	1.83	90	.57	1.13	.54	1.08
35	1.68	1.90	900	.55	1.10	.56	1.12
40	1.60	1.83	10	.52	1.04	.55	1.10
45	1.57	1.64	20	.48	.96	.53	1.06
50	1.71	1.54	30	.44	.89	.50	.96
55	1.86	1.62	40	.42	.83	.47	.88
60	1.94	1.79	50	.39	.79	.43	.82
65	1.98	1.96	60	.38	.78	.39	.76
70	1.90	2.09	70	.38	.79	.34	.68
75	1.75	2.07	80	.41	.84	.32	.64
80	1.63	1.96	90	.46	.92	.30	.61
85	1.54	1.80	1,000	.55	1.09	.30	.60
90	1.49	1.59	10	.65	1.32	.32	.64
95	1.45	1.50	20	.81	1.62	.37	.73
700	1.41	1.47	30	.97	----------	.47	.91
05	1.37	1.47	40	1.09	----------	.64	1.17
10	1.31	1.47	50	1.21	----------	.81	1.63
15	1.23	1.40	60	1.33	----------	1.12	----------
20	1.13	1.29	70	1.42	----------	1.35	----------
25	1.01	1.17	80	1.46	----------	1.49	----------
30	.92	1.04	90	1.48	----------	1.58	----------
35	.82	.92	1,100	1.49	----------	1.69	----------
40	.76	.83	10	1.47	----------	1.83	----------
45	.70	.77	20	1.43	----------	1.89	----------
50	.65	.74	30	1.36	----------	1.81	----------
55	.61	.71	40	1.27	----------	1.66	----------
60	.56	.64	50	1.17	----------	1.54	----------
65	.52	.58	60	1.08	----------	1.43	----------
70	.47	.53	70	.99	----------	1.27	----------
80	.37	.44	80	.92	----------	1.17	----------
90	.29	.37	90	.85	----------	1.09	----------
800	.23	.30	1,200	.79	----------	1.01	----------
10	.19	.24	10	.74	----------	.91	----------
20	.16	.19	20	.70	----------	.75	----------

Quantitative spectrophotometric observations of the visible and ultra-violet absorption spectra of carotin in cyclohexane and of xanthophyll in methanol have been recorded recently by Pummerer, Rebmann, and Reindel.[17] The data show the general similarity in form of the absorption curves for these pigments, but the observations are not sufficiently extensive and the curves not determined with sufficient precision to reveal some structural details of the spectra which will be described on the following pages.

A comparison of the absorption curves in Figures 1 and 2 shows only minor differences in the structure of the spectra. The mean absorbancy of the equimolecular solutions, when averaged over the frequency range from 550 to 850 (for $bc=1$) is 0.82 for both carotin and xanthophyll. When averaged over the frequency range from 850 to 1,220 (for $bc=5$) the mean absorbancy is 0.86 for carotin and 0.88 for xanthophyll. Compared with carotin the spectrum of xanthophyll is shifted slightly to the higher frequencies and the component bands are sharper and closer together.

This sharpness of bands of xanthophyll is of particular interest in that it clearly reveals the overlapping component structure of the strong band group in the visible spectrum. Four components of this group are distinctly observed; a fifth component near frequency 602 is indicated by a slight indentation in the absorption curve, and another component near frequency 823 is also suggested by the curves for greater values of the product bc. On inspection of the far ultra-violet band the same evidence for a component structure is observed. Even the weaker ultra-violet band at frequency 903, which is further developed during the oxidation process (fig. 5), shows definite evidence of components near frequencies 945 and 987, respectively.

For carotin the structure is not so evident; but in view of the similarity in atomic composition and various properties of these pigments, and the sameness in form of their absorption curves, there can be little doubt that the same general scheme underlies the finer structure of their absorption spectra. Five components of the strong band group in the visible spectrum are observed. The far ultra-violet band shows evidence of a component structure by the definite indentations of the curve in the neighborhood of frequency 1021. Again, in the partially oxidized material (fig. 4), there is definite evidence of a band near frequency 949. Compared with the spectrum of xanthophyll, however, the component bands of carotin, although somewhat farther apart, are broader and, consequently, less definitely resolved.

The observed absorption spectra of carotin and xanthophyll may be described as consisting each of three adjoining groups of overlapping component bands. These band groups will be designated hereafter by the Roman numerals I, II, and III, respectively, beginning with the strongest and most definitely resolved group in the visible spectrum.

As the band groups are not all clearly resolved, and the exact form of the overlapping components is unknown, one can not determine how closely the maximum ordinate of a band group coincides in position with the maximum ordinate of a component of that group. Although the positions of these maxima may be in themselves of little theoretical significance, they afford, nevertheless, the only definite

[17] Ber. d. Deut. Chem. Gesell., **62**, p. 1411; 1929.

means for locating the bands in the spectrum. In the further description and discussion of these spectra it will be assumed that the maximum ordinates of the different band groups give the true relative positions of the strongest components of these groups. These maximum ordinates are taken, furthermore, to define the positions of the groups in the spectrum.

It is observed that the band groups of xanthophyll are not equally spaced, but the separation of Groups I and II is from 15 to 16 frequency units greater than the separation of Groups II and III. With the exception of the two sharp components of Group I, which are separated by approximately 36 frequency units, any assignment of frequency differences between adjacent components of the group must necessarily be highly conjectural. One can not determine precisely whether they are equally spaced in each group or whether they form a slightly converging sequence. The spacing of the components in Group III is definitely greater than the spacing in Group I. The band groups of carotin appear equally spaced and separated by the same frequency interval (216 units) as observed between Groups II and III of xanthophyll. The spacing of the two definitely resolved components of Group I is approximately 41 frequency units.

A close inspection of the absorption curves suggests the possibility that the entire observed spectrum of each pigment might be represented as a single regular sequence of component bands converging toward the lower frequencies. Then, the imposition of a periodic variation in intensity on the progression of component bands gives rise to the appearance of definite band groups in the spectrum and the characteristic form of the absorption curves.

It is found that the observed progression of bands, for each pigment, is, indeed, well represented by the parabolic equation

$$\nu - \nu_o = a\ (n - n_o)^2 \qquad (1)$$

wherein ν_o, n_o, and a are constants determined from the experimental data and the required frequencies ν are given by successive integral values of n. The axis of this parabola is parallel to the axis of frequencies and the coordinates of the vertex are ν_o and n_o. In the evaluation of the constants of equation (1) only the frequencies of the maximum ordinates of the three band groups were used. The absolute integral values of n are arbitrary, but relative values for the three band groups are determined definitely by the form of the absorption curves, which indicate how many component bands must be arranged in regular sequence, including the strongest components of each group. In this manner the following equations were obtained, in which the vertex of the parabola is placed at $n_o = -1/2$:

Carotin: $n = 6, 7, 8$, etc.

$$\nu - 480.2 = 2.57142(n + 1/2)^2 \qquad (2)$$

Xanthophyll: $n = 40, 41, 42$, etc.

$$\nu + 93.0 = 0.42353\ (n + 1/2)^2 \qquad (3)$$

TABLE 2.—*Calculated frequencies of the absorption bands*

Carotin (by equation (2))		Xanthophyll (by equation (3))	
n	ν	n	ν
6	589	40	602
7	625	41	636
8	666	42	672
9	712	43	708
10	764	44	746
11	[1] 820	45	[1] 784
12	882	46	823
13	949	47	[1] 863
14	1, 021	48	903
15	1, 098	49	945
16	[1] 1, 180	50	987
		51	1, 030
		52	1, 074
		53	1, 119
		54	1, 165
		55	1, 212

[1] Bands not indicated in Figures 1, 2, 4, or 5 by definite indentation in absorption curve.

The frequencies of the component bands, as given by these equations,[18] are listed in Table 2. They are also indicated in Figures 1 and 2 by dash-dot ordinates, from which the degree of agreement with the experimental data may be adjudged.

The provisional structures which are thus assigned to the absorption spectra of carotin and xanthophyll are most clearly represented by the schematic diagrams in Figure 3. For comparison, a similar diagram for the absorption spectrum of lycopin (an isomer of carotin), dissolved in methyl-cyclohexane, is also presented in the figure. The data are taken from the work of Pummerer, Rebmann, and Reindel.[19]

The general form of the absorption curve for lycopin is very similar to that for carotin. The entire spectrum is shifted, however, toward the lower frequencies, and an additional absorption region is observed in the far ultra-violet. Four components of the strong band group in the visible spectrum are indicated by the form of the absorption curve, but the curve in the ultra-violet is not determined with sufficient precision to reveal any details of a finer structure.

In explanation of the spectral diagrams we may recall a well-known experimental fact that the frequencies of the lines in atomic and molecular absorption or emission spectra may always be represented as differences between sets of frequencies which are known as spectral terms. The horizontal lines in the spectral diagrams represent the terms for the absorption spectra of these pigments. Differences

[18] The half-integral values for $n-n_s$ follow directly from the following relation, which is obtained from equation (1) and the absorption curves:

$$\Delta_2/2a=(2q-r)\ (n_I-n_s)+\tfrac{1}{2}\ (2q^2-r^2)$$

In deriving this relation let n_I, n_I+q, and n_I+r be the values of n for the strongest components of Band Groups I, II, and III, respectively, and Δ_2 the second difference between the corresponding frequencies of these three components. $2a$ is the constant second difference between the frequencies of adjacent component bands. In a preliminary determination of the constants of equation (1) it was noted that the best representation of the experimental data was obtained when the ratio $\Delta_2/2a$ was approximately zero, for carotin, and approached closely the integral value 36 for xanthophyll. For reasons which will appear later in discussion of Figure 3, the exact values 0 and 36 were subsequently imposed on the above ratio, for carotin and xanthophyll, respectively, in a final adjustment of the constants. The imposed condition that $\Delta_2/2a$ is an integer leads to exact half-integral values for $n-n_s$.

[19] Ber. d. Deut. Chem. Gesell., **62**, p. 1411, 1929. The positions of the bands were estimated from the published absorption curve, and are not known to a degree of accuracy comparable with corresponding data herein presented for carotin and xanthophyll.

between the terms give the observed frequencies of the absorption bands.

On the basis of the quantum theory of absorption spectra the spectral terms are interpreted as representing different discrete energy states, or energy levels, of the absorption mechanism. Accompanying the absorption of radiant energy of a definite frequency the absorption mechanism may pass from the normal unexcited state (represented by the lower heavy level in the diagram) to one of the higher energy levels. The heavy horizontal lines correspond to component bands of maximum intensity in each group and are used to indicate the energy separation of the groups. They may be designated as group levels in contradistinction to the parabolic set of component

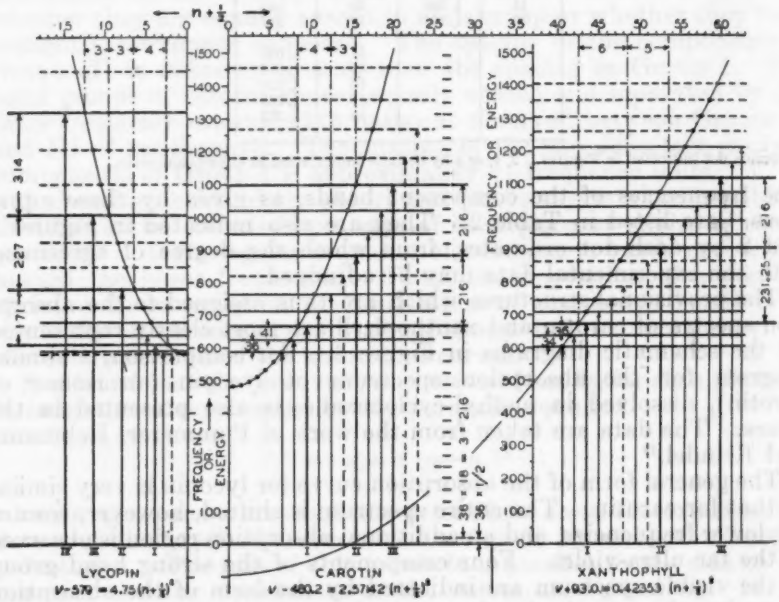

FIGURE 3.—*Schematic representation of the absorpiton spectra*

band levels. Only levels which are indicated by observed absorption bands are represented by continuous lines. Broken lines show levels suggested by the theoretical scheme.

The absorption spectrum of each pigment is thus represented by a single set of energy levels for the excited states combined with a single energy level for the normal state. The relative intensities of the absorption bands involve the respective probabilities of transitions from the normal to the corresponding excited states. These probabilities must be governed by peculiar conditions which determine the observed variations in intensity.

It is perhaps of further interest to point out certain structural regularities which appear in this schematic representation of the absorption spectra:

1. The observed group-levels for carotin may be equally subdivided and extended to the normal state. The subdivisions of the group

levels are then represented by the simple formula $\nu_m = 36\left(m+\frac{1}{2}\right)$, in which m takes successive integral values beginning with zero and the observed group-levels are given by successive values (for $m=3$, 4, 5) of 6 m. It is quite possible, however, that the indicated relation is an entirely fortuitous numerical combination arising from the circumstance that the frequency 666 of the first band group happens to be divisible by 216 with a remainder of 18, and the numbers 6, 18, and 36 are each a factor of 216. If the relation truly follows from some structural condition in the molecule, the spectral arrangement then suggests the possibility that the observed variation in intensity within the sequence of component bands may be related to the periodic coincidence or resonance of two distinct but mutually coupled sets of energy levels in the molecule. In this connection it would be of considerable interest to know if an absorption maximum exists for carotin at a frequency of 1,458, for here the two sets of energy levels as depicted in the diagram are again in exact coincidence. No observations have been made in this region of the spectrum, mainly because of the strong absorptive properties of the solvents used. It is observed that lycopin exhibits a region of selective absorption which would correspond to a fourth band group for carotin.

The group levels for lycopin and xanthophyll are not equally spaced and the number of observed levels is not sufficient to determine any regularity which might exist corresponding to the possibility suggested for carotin. A special attempt was made to find a region of selective absorption for xanthophyll in the frequency range from 430 to 250 (wave length 700 to 1,200 millimicrons.) For this experiment a nearly saturated solution in the alcohol-ether solvent was measured in a thickness of 10 cm using a sensitive thermoelectric method.[20] No trace of a band was found. It is obviously of considerable importance to extend the work on the absorptive properties of these pigments farther into the higher frequencies.

2. Another point of interest is the occurrence of multiples or submultiples of 36 in the frequency relations. This is particularly marked in the spectrum of carotin, but in the spectra of both pigments the sequence of component bands does not begin on the low frequency side until the frequency separation of the component-band levels is approximately 36. Again (see footnote, 18), the second difference between the frequencies of the three observed group levels in xanthophyll is $36a$, or eighteen times the constant second difference ($2a$) between the frequencies of adjacent component bands. The frequency interval of 36 units corresponds to a definite energy unit which may be of some special significance in the theory of these spectra.

3. The direction of convergence of the group levels changes progressively in passing from lycopin[21] through carotin to xanthophyll. For lycopin the convergence is toward the lower frequencies, for xanthophyll the direction of convergence is reversed, whereas for carotin the group levels appear to be equally spaced.

[20] Gibson, J. Opt. Soc. and Rev. Sci. Inst., **7**, p. 693; 1923.

[21] In making comparisons of the three spectra in Figure 3 it must be borne in mind that lycopin was studied at a concentration and in a solvent both different from the concentration and solvent used for carotin and xanthophyll. Hence, the environmental conditions of the absorption mechanism were not comparable for the three pigment molecules.

4. The rapidity of convergence of the component band levels, and the value of the constant a, both increase progressively with the shift of the vertex ν_0 toward the higher frequencies.

5. The value of the constant a for carotin is approximately six times its value for xanthophyll.

In consideration of these results it should be borne in mind that the definition of the absorption bands, and the extensiveness and accuracy of the experimental data, are such that the indicated structure of the absorption spectra is not established with a high degree of certainty. It is possible that the suggested numerical relations are entirely fortuitous. It may be recalled that the entire scheme is based on the assumption that the poorly defined and partly resolved component bands between the three maximum ordinates of the absorption curve are closely related to one another through the absorption mechanism and form a regular sequence extending throughout the spectrum. The procedure then was to assume the simplest law which would represent this sequence within the limits of uncertainty of the measurements. It is urgently recommended that these observations and speculations be confirmed and tested by further and more extensive studies of the absorptive properties of these pigments. If the numerical relations truly represent some structural conditions in the molecule they may be expected to hold also, with appropriate changes in the constants, at different temperatures and in different solvents or for other changes in the environmental conditions of the molecule. One may ask if the alterations in spectral structure brought about by different solvents or at different temperatures can be represented by corresponding shifts in the origin of the band series, by changes in the relative intensities of the component bands, or by changes in value of a. Being no longer in a position to carry on this work the author herein presents such observations and discussion as would seem to be of interest to others in the further study of these molecular spectra.

The molecular spectra of these yellow pigments, and the spectra of other chloroplast and related pigments, offer an interesting field for further investigation, not only from the viewpoint of the biologist, but also as a problem in absorption theory. Further studies may well include extensive measurements of other optical properties, such as rotatory power and fluorescence. Some chemical properties of considerable interest in this connection will be discussed in the Sections V and VI. Xanthophyll is known to have a high specific rotation. Conflicting reports on the rotation of carotin are found in the literature. Both pigments are fluorescent with a greenish hue, as would be expected if the fluorescence spectra are interpreted as emission spectra accompanying the return of the absorption mechanism from the excited energy states to the normal unexcited state. The absorption and fluorescence spectra may, perhaps, be recorded with greater precision if observations are made at very low temperatures. Under this condition it is known that the broad and apparently continuous absorption and fluorescence bands are often resolved into separate components. In the case of carotin, xanthophyll, lycopin, and other pigments (as shown by the spectograms of Willstatter), the broad absorption bands are already partly resolved at ordinary temperatures. At very low temperatures, therefore, a further resolution may be

expected so that the relative positions of the bands and the finer structure of the spectra could be observed with greater precision.

V. OXIDATION IN SOLUTION

1. EXPERIMENTAL DATA

An inspection of the curves in Figures 4 and 5 shows the same sequence of changes in the absorption spectrum of each pigment dur-

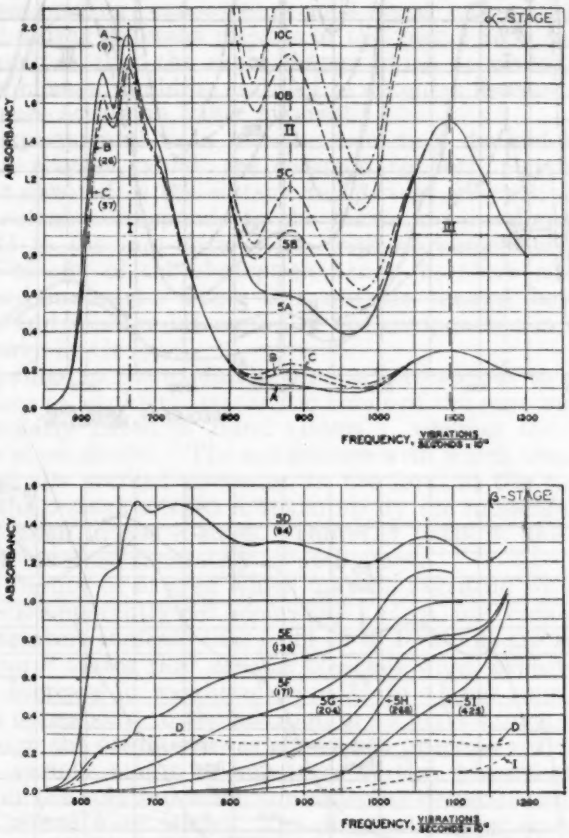

FIGURE 4.—*Changes in carotin spectrum, accompanying oxidation*

Upper set of curves shows α-stage; lower set shows β-stage. Curve *A* (upper) represents spectrum of pure unoxidized pigment, as reproduced from Figure 1. These measurements were made on March 10, 1922. Curves *B* to *I* show changes after successive periods of exposure to oxidizing agencies. Numbers in parentheses give total exposure time in days. Numbers 5 and 10 preceding letters on curves are values of *bc* used in the experimental determinations (see fig. 1), and (by Beer's law) are also multipliers of corresponding curves of the set *A* to *I* (for *bc*=1).

ing the slow auto-oxidation process in solution. The rapid development in the intensity of Band Group II is particularly noteworthy in each case. This change is accompanied by a decrease in the intensity of Group I, the rate of change being somewhat greater for the components of lower frequency. This apparent shift in the relative

intensities of the overlapping components may be partly the result, however, of a broadening of each component. Group III is practi-

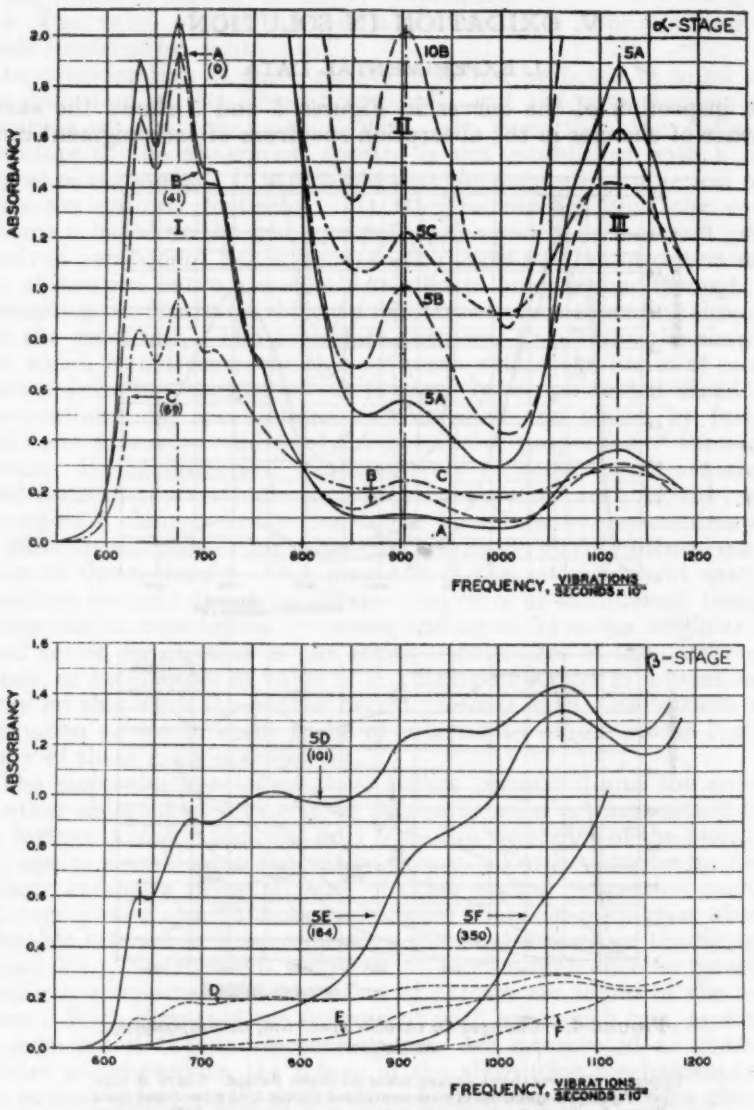

FIGURE 5.—*Changes in xanthophyll spectrum, accompanying oxidation*

Upper set of curves shows *α*-stage; lower set shows *β*-stage. Curve *A* (upper) represents spectrum of pure unoxidized pigment, as reproduced from Figure 2. These measurements were made on July 21, 1922. Curves *B* to *F* show changes after successive periods of exposure to oxidizing agencies. Numbers in parentheses give total exposure time in days. Numbers 5 and 10 preceding letters on curves are values of *bc* used in the experimental determinations (see fig. 2), and (by Beer's law) are also multipliers of corresponding curves of the set *A* to *F* (for $bc=1$).

cally unchanged for carotin, but decreases perceptibly in intensity for xanthophyll.

These changes progressed gradually for each of the pigments until some time after the second month of exposure to the oxidizing agencies.

Then a relatively rapid change took place, the original characteristic bands of the pure pigments fading rapidly with perhaps a simultaneous broadening of the components. The apparent shift of the intensity maximum of Group III toward the lower frequencies is noticed, until it appears centered at a frequency of 1,065 for each pigment.

Further changes in the absorption curves now progress more slowly, with a gradual disappearance of all indications of the original bands.

It may be emphasized that the sequence of these changes with time followed roughly the same course for each pigment, even though the corresponding exposure periods were not simultaneous but occurred during different months of the year. It is highly improbable, therefore, that the rapid change which occurred, following the first slow change, could be ascribed to a sudden increase in the oxidizing agencies acting on either pigment.

The experimental data indicate two very distinct stages in the oxidation process, which are common to both pigments, and are hereafter denoted as the α-stage and β-stage, respectively.

The α-stage corresponds to the maximum development of Band Group II in the mid-ultra-violet, with no perceptible shift in the position of any of the absorption bands, as observed for the pure unoxidized material. There is a notable change, however, in the absolute and relative intensities of the components in other groups, particularly in Group I.

The β-stage in the oxidation process corresponds to the rapid disappearance of all the characteristic bands of the pure material. This is particularly noted in Band Group I, whereas the other groups decrease more slowly. The suddenness with which this change takes place and the marked alteration in the form of the curves suggests that in the β-stage oxygen is taken up by the molecule in a manner different than in the α-stage. Different parts of the molecule are probably involved separately in each stage.

The quantity of oxygen which may be taken up by each pigment molecule is apparently not accurately known, but various statements in the literature indicate that from 10 to 15 atoms are added. Thus, Willstatter [22] states that carotin bleaches when exposed to dry air, with an increase in weight of from 35 to 41 per cent. These percentages correspond to the addition of 11 or 12 atoms of oxygen.

Although the oxidation was allowed to progress very slowly, molecules in various stages or substages of this process probably were present in the solution when the different determinations of the absorption curve were made. The observations, of course, represent the average effect of all the molecules. The process was slow enough, however, to detect the two main stages described above. Other less definite stages may possibly exist with less characteristic differences in the corresponding absorption curves, so that they would not be clearly indicated in the present experimental work. With a better control of the oxidation process, and more frequent observations of the spectral changes, the existence of other stages might be detected. In the case of xanthophyll a measurement was made fortunately during the period of most rapid change in its absorption curve, after the β-stage was well under way. (Curve C, fig. 5.) The rapid fading of Band Group I is clearly observed. Group II has passed its maximum development and is also fading rapidly. The broadening and initial

[22] Investigations on chlorophyll, English translation, p. 219.

shifting of Group III to lower frequencies is evident. In the case of carotin this change had progressed even further before a measurement was made. Because of the similarity in the sequence of changes for each pigment, the entire set of curves in Figures 4 and 5 may be taken to illustrate the progressive changes occurring during the oxidation of either pigment.

Although xanthophyll has been regarded by some investigators as simply a stage in the oxidation of carotin, it is evident from the data herein presented that carotin is not converted into xanthophyll by the simple auto-oxidation process. The carotin spectrum never goes over into that of xanthophyll; on the other hand, both spectra pass through the same series of changes until oxidation is complete.

2. TEST FOR OXIDATION

The marked development of Band Group II during the early stage of the oxidation process, suggests the possibility that the original solutions, though freshly and carefully prepared, were nevertheless in a slightly oxidized condition, and that solutions of pure unoxidized carotin and xanthophyll might show no indication of the bands in question.

To test this hypothesis, fresh crystals of each pigment were prepared [23] by repeated crystallization. The crystals finally obtained were not dried and weighed, as in the previous preparations, but the possibility of oxidation during this operation was avoided by immediately dissolving the crystals in pure ethyl alcohol and diluting with alcohol to a concentration which was determined by rough trial to be suitable for the test.

The absorption measurements were made without delay, but no reduction in the relative intensity of Band Group II was observed for either pigment, beyond that shown in Figures 1 and 2. It appears, therefore, that this band group is characteristic of each pure unoxidized pigment, but develops rapidly in intensity during the earliest stage of oxidation. The extent to which this band group is developed thus provides a sensitive test for incipient oxidation.

VI. BEARING OF THE OXIDATION EXPERIMENTS ON THE WORK OF OTHER INVESTIGATORS

The oxidation experiments herein described have an important bearing on some previous work of Tswett,[24] who obtained by means of his chromatographic adsorption analysis a separation of different materials present in an extract from green leaves. The principle of the method lies in the phenomenon of surface adsorption, which is manifested to a marked degree when a solution containing the mixture of pigments is passed through a column of a suitable finely divided adsorbing material. The pigments are adsorbed on the surfaces of the particles, and may mutually displace each other in accordance with their adsorption "affinity" for the adsorber. Tswett used a column of finely divided calcium carbonate packed in a vertical glass tube. Upon passing a carbon disulphide solution of the pigments

[23] These preparations were made by Doctor Schertz, using the methods described in his papers, as previously cited. (See footnote 5, p. 172.)

[24] Ber. der Deut. Bot. Ges., 24, pp. 316, 384; 1906. See Also Palmer, Carotinoids and Related Pigments, p. 43.

slowly through this column from top to bottom, there appeared a stratification of the material into separate colored zones, each zone corresponding to a different pigment ingredient of the mixture. The zones could then be mechanically separated and the individual pigments extracted with suitable solvents.

By this method Tswett separated five yellow pigments (among other green chloroplast pigments) one of which he identified as carotin and the other four were distinguished as α, α', α'', and β xanthophylls. The order of increasing adsorption affinity for calcium carbonate was from xanthophyll β through the α'', α', and α forms to carotin, which is only slightly adsorbed. Xanthophyll α was orange-yellow in color and showed, by the spectrogram method, spectral absorption bands in alcoholic solution corresponding closely in position to the bands of pure xanthophyll, as herein exhibited in Figure 2. The α' and α'' xanthophylls were first formed in a single yellow zone which separated into a double zone when benzene was passed through the tube. They are only slightly different in their adsorption affinity for the carbonate. The positions of the absorption bands were the same for each material, but were reported by Tswett to be shifted slightly toward the ultra-violet as compared with the bands for xanthophyll α. Only the stronger components of Band Group I were recorded. Xanthophyll β showed more characteristic differences in its properties, as compared with the other xanthophylls. The two principal components of Group I were shifted very perceptibly toward the ultra-violet and located, respectively, in the frequency ranges 632 to 650 and 674 to 698.

An examination of the curves in Figure 5 provides a plausible and complete explanation of Tswett's observations and strongly suggests that the different xanthophylls described are but separate stages in the oxidation of this pigment, with xanthophyll α corresponding to the pure unoxidized material.

Thus, it may be noted that in the α-stage of oxidation there is a small but definite broadening of the components of Group I, particularly on the ultra-violet side. This change undoubtedly would be observed by the spectrogram method as a slight shift in the positions of the centers of the components. It may be presumed, therefore, that the α' and α'' modifications of xanthophyll both correspond to the α-stage of oxidation, as defined in the preceding section, but indicate however the existence of two definite substages in this process. Although the absorption curves herein presented do not show these two substages, they may well exist with nearly identical absorption spectra, but with definite differences in their adsorption affinity for calcium carbonate. It is unfortunate that the ultra-violet bands were not recorded, for the marked increase in the intensity of Group II in the mid-ultra-violet is a definite criterion for oxidation.

The marked change in the absorption spectrum during the β-stage of oxidation, undoubtedly corresponds to the formation of Tswett's xanthophyll β. As observed by the spectrogram method, the positions of the broadened and rapidly disappearing components of Group I, now centered at frequencies of 637 and 690 (fig. 5, curve *5D*), would appear more definitely shifted toward the higher frequencies than in the earlier stage of oxidation.

The α xanthophylls were found to predominate in the adsorption column whereas xanthophyll β formed only a relatively narrow zone.

It seems very probable indeed that Tswett was dealing, for the most part, with partially oxidized materials.

This conclusion is in accord with some more recent experiments of Schertz,[25] who found that when a carbon disulphide solution of carefully purified xanthophyll is passed through a column of calcium carbonate, the pigment is only slightly adsorbed. If the solution which has passed through the adsorption column is now exposed to air and light, a greater portion of the pigment will then be retained by the carbonate. Usually the longer the solution is exposed to the oxidizing agencies the greater the quantity of the pigment retained. Carotin behaved in approximately the same way. Solutions of pure carotin in carbon disulphide left only a trace of the yellow pigment in the adsorption column, whereas solutions of partially oxidized material left a definite colored zone. The effect was always greater with xanthophyll.

Although the data herein reported show the same oxidation stages for both pigments, the lower adsorption affinity of carotin for calcium carbonate may well account for the failure of previous investigators to detect the corresponding oxidation stages for this pigment.

The possibility that oxidation might account for the observations of Tswett was indeed suggested by Willstatter,[26] on the basis that the pigment, when in the adsorbed condition, would be particularly susceptible to oxidation. Furthermore, the possiblity was not excluded by Willstatter that xanthophyll, as abstracted from the other chloroplast pigments, might consist of several very similar isomeric bodies not easily detected or separated by the usual chemical methods.

In this connection some recent observations by Zechmeister and Tuzson [27] are of interest. These investigators found considerable divergence in the specific optical rotation of different preparations of xanthophyll and suggested as a possible explanation of these observations that the leaf extracts of xanthophyll might consist of very similar components with unequal specific rotation. These variations in the optical rotatory power of different preparations of presumably pure unoxidized xanthophyll recall somewhat analogous variations observed by the author in the relative intensity of Band Group II for some early preliminary preparations of these pigments. It would seem a pertinent question for further investigation whether different isomorphic forms of xanthophyll really exist, with slightly different optical properties, or whether the observed variations in specific rotation are again another manifestation of varying degrees of partial oxidation in the different preparations of the pigment. Considerable care is required in the preparation and handling of these pigments to avoid incipient oxidation.

The changes in the absorption spectrum, accompanying oxidation, also bear a direct relationship to the work of Zechmeister and his associates [28] on the progressive hydrogenation of carotin and xanthophyll. These investigators observed two definite stages in the hydrogenation of each pigment, each stage being attributed to the saturation of a different group of double bonds in the molecule. During the first stage of the process 18 atoms of hydrogen are taken up with the saturation of 9 double bonds and complete disappearance of the

[25] Plant Physiology, **4**, p. 337; 1929.
[26] Investigations on chlorophyll. English Translation, p. 212.
[27] Ber. der Deut. Chem. Ges., **62**, p. 2226; 1929.
[28] Ber. d. Deut. Chem. Gesell., **61**, pp. 566, 1534, 2003; 1928: **62**, pp. 2226, 2233; 1929.

color of the solution. The color fades continuously with increasing consumption of hydrogen. During the second and final stage of the hydrogenation process four additional atoms of hydrogen are taken up with the saturation of a different and more stable group of two double bonds. The first group of nine double bonds is assumed to form a conjugated system and is responsible for the strong absorptive properties of the molecule. Quantitative spectrophotometric measurements were not made of the progressive changes in the absorption spectrum during hydrogenation.

It has been shown that in the α-stage of the oxidation process the characteristic absorption spectrum of the molecule was not destroyed, there being moderate changes only in the relative intensities of the component bands. As the changes which occurred in the visible spectrum were small, the color of the solution remained nearly constant. It was during the β-stage that the color faded rapidly as a result of the sudden decrease in the intensity of the low-frequency components of Band Group I in the visible spectrum. In the hydrogenation process the opposite effect was observed, the color disappearing completely during the first stage of this process. In accordance with present chemical evidence it appears likely that during the oxidation process at least 11 atoms of oxygen are taken up by a molecule of carotin or xanthophyll. This quantity of oxygen is equivalent in primary valencies to the 22 atoms of hydrogen consumed in the hydrogenation process. In both chemical processes the changes in the absorption spectra are intimately related to the gradual saturation of the system of conjugated double bonds. In the oxidation process it appears that the α-stage corresponds to the saturation of the second group of noncolor producing bonds, this change being followed by the saturation of the first, or conjugated, group. In the hydrogenation process the saturation occurs in reverse order. On the basis of these observations it seems plausible to suggest that in the saturation of the 11 double bonds 2 atoms of oxygen are taken up during the α-stage and the remaining 9 atoms during the β-stage.

VII. CONCLUDING REMARKS

The present status of investigations on the molecular structure of carotin and xanthophyll is summarized in recent papers by Smith,[29] Gulland,[30] and by Karrer[31] and his associates. Carotin is conceived as an acyclic chain of four isoprene residues with two identical, or very similar, carbocyclic ring structures, one at each end of the chain. The entire atomic configuration is very symmetrical. The nine conjugated double bonds are in the isoprene chain and one (probably) nonconjugated double bond is located in each of the end rings. All investigators are not in complete agreement, however, on some details of this structure. The structure of xanthophyll is likewise not definitely determined. The position and function of the two oxygen atoms in the empirical formula for this molecule is not fixed, but chemical evidence points to their location in the end ring structures. In view of the similarity in physical and chemical properties of these

[29] Contributions to Marine Biology, Stanford University Press, p. 145; Sept. 1, 1930.
[30] J. Soc. Chem. Ind. (Transactions and Abstracts), **49**, p. 839; 1930.
[31] Helv. Chim. Acta., **13**, p. 1084; 1930.

pigments there can be little doubt that their molecules are constructed on essentially the same atomic pattern.

On the basis of this provisional picture of molecular structure we may explain the observation of two substages in the α-stage of oxidation as corresponding each to the saturation of one of the two double bonds in the end rings. It may be recalled that these two substages for xanthophyll were suggested by the interpretation herein applied to Tswett's chromatographic analysis. The β-stage of oxidation for each pigment may be ascribed to the progressive saturation of double bonds in the open chain structure of each molecule.

It is conceivable that the α-stage of oxidation may be reversible under proper conditions in the plant, so that these pigment molecules, whether existing independently as such in the plant cell or as part of a more complex atomic assemblage, may serve as an oxidation-reduction system concerned with the transference of oxygen. It has been shown that in the α-stage the strong absorptive properties of the molecule were practically unimpaired; so that the reversible changes in state of the molecule, accompanying the absorption and reemission of radiant energy, may be available to bring about, or assist in some unknown manner, the suggested oxidation-reduction reactions.

Further studies of the oxidation and reduction processes will undoubtedly contribute materially to our knowledge of the structure and possible functions of these pigments. The pigments in different stages of the processes should be isolated if possible, and their spectral absorptive properties determined quantitatively along with the quantity of oxygen or hydrogen taken up. The results obtained thus far are duly reflected in the suggested molecular structures of these pigments, and have, furthermore, yielded pertinent information on the carrier of the observed system of absorption bands. Thus it appears that the absorption mechanism is most closely allied with the system of conjugated double bonds.

The present status of our knowledge of the absorption process in these large and complex atomic systems is far too meager, of course, to warrant any definite conclusions therefrom concerning the origin of the spectra or the structure of the molecule. It is probable that the absorption process giving rise to the visible and ultra-violet spectrum can not be localized entirely within a pair or small group of atoms with their associated electronic binding system, or referred even to a spacial arrangement of identical or very similar small and independently acting absorption units; on the other hand, the absorption process more likely is concerned principally with the mutually interaction of the many valence electrons forming the binding system in the entire chain structure of the molecule. The manifold possibilities in the configurations or motions of this constellation of electrons may give rise to a very complex arrangement of energy states only the grossest features of which would be represented in Figure 3. The constraining and disturbing influence of the complex environmental conditions of the absorption mechanism probably hides a much finer basic arrangement of energy levels. We would expect that any structural changes in the end rings of the molecule, as accompanying the α stage of oxidation or the structural transition from carotin to xanthophyll, would exert a definite influence on the energy levels and thus bring about corresponding changes in the spectrum. The close simple relation which appears to exist between all the observed absorp-

tion bands indicates that they must all be referred to one absorption mechanism; and it would seem to be at least a plausible hypothesis that all essential parts of the molecular structure are more or less directly concerned in the absorption process.

In conclusion, it may not be amiss to point out certain experimental deficiencies in the various investigations as described in the preceding two sections. In the earlier work on the identification and classification of the chloroplast pigments, much labor and controversial discussion would undoubtedly have been avoided if the chemical investigations had been supplemented by thorough quantitative records of the absorption spectrum over a sufficiently wide range of spectral frequencies. In the present spectrophotometric study of the oxidation process no chemical determinations were made of the quantity of oxygen taken up. Furthermore, data on the optical rotatory power and its variations with oxidation would prove very valuable in connection with the observations of Zechmeister and Tuzson. In the hydrogenation experiments, on the other hand, quantitative spectrophotometric studies of the changes in the absorption spectra were not made and incomplete rotation data were obtained. In each case the additional physical or chemical data would be of great value in the interpretation of the results. These investigations, then, may collectively serve to illustrate the decided advantages which would certainly accrue from a greater organized effort on the part of both physicists and chemists to collaborate in applying the apparatus and methods of their respective sciences in the study of these biological problems.

WASHINGTON, *April 10, 1931.*

THEORY OF DESIGN AND CALIBRATION OF VIBRATING-REED INDICATORS FOR RADIO RANGE BEACONS

By G. L. Davies

ABSTRACT

This paper gives a general treatment of the theory of design of vibrating-reed indicators, which was developed in connection with measurement and design work on the tuned-reed course indicator for the aircraft radio range beacon. The equations and conclusions may be readily adapted to apply to any similar vibrating system.

By assuming that a reed may be replaced by an equivalent particle, vibrating in the plane of the driving poles, the differential equation of motion is simplified greatly and becomes readily solvable for small vibrations. Equations are given for determining the constants of the equivalent particle from the dimensions and constants of the reed. The expression for the frequency of a loaded uniform reed, computed by a method equivalent to one given by Rayleigh, checks very closely with that obtained by Drysdale and Jolley for a similar reed. This theory for small vibrations is applicable when the amplitude is small enough so that its square may be neglected in comparison with the square of the air gap.

From an analysis of large vibrations of tuning forks by Mallett, the behavior of the reed at relatively large amplitudes of vibration is inferred, although an exact quantitative verification of the theory is difficult.

Design equations are given for uniform reeds and for the type used in the reed indicator. From the results of both theory and experiment, the effect of the various factors of design and operation upon the reed frequency is discussed, and the calibration procedure necessary to take account of these factors is outlined.

CONTENTS

		Page
I.	Introduction	195
II.	Theory for small vibrations	196
	1. Equivalent particle constants	198
III.	Effect of large vibrations	199
IV.	Application of theory to reed design	201
V.	Calibration of reed indicators	208
VI.	Conclusion	213

I. INTRODUCTION

This theory of reed indicator design has been developed in connection with a program of measurement and design work on the tuned-reed visual course indicator for the aircraft radio range-beacon. The purpose of this work was to improve the sensitivity of the indicator, to standardize the design for production manufacture, and to develop apparatus and methods for laboratory and production calibration.

The theory of lateral vibrations of bars has been very completely developed by Lord Rayleigh.[1] However, his theory, while having

[1] Lord Rayleigh, Theory of Sound, 1, Ch. VIII, p. 255.

the advantage of great generality, is somewhat complicated for practical use, and is not applicable to damped, forced vibrations. Several investigators have developed simplifications of Rayleigh's theory, but these have not been found to be useful in connection with this problem. Mallett [2] has given a very thorough treatment of large vibrations of electrically driven tuning forks. With certain modifications, necessitated by differences in drives, his equations may be applied to vibrations of reeds and are used to explain some of the properties of reeds when vibrating at large amplitudes.

Rayleigh derived an equation for the frequency of free vibration of a uniform bar, but none of the investigations includes any equation for the frequency of a reed of nonuniform cross section, nor do they give any method for the calculation of the sensitivity of driven reeds. There is a definite need for these equations in indicator design, and they are developed in this work. The equation for frequency is obtained by Rayleigh's method, while an assumption that the reed is replaceable by an equivalent particle enables an expression for sensitivity to be derived.

The greatest problem encountered in production manufacture has been nonuniformity of indicators. This has necessitated the expenditure of an inordinately large amount of time in calibration, thus increasing costs of manufacture. In order to minimize this time, it is necessary to determine and eliminate the causes of nonuniformity. Also, careful and exact design results in a simplification of calibration procedure which is of great value to a manufacture.

It has also been necessary to develop apparatus and methods for calibration, which includes tuning the reed to the proper frequency and adjustment of its sensitivity and sharpness of resonance to the desired values.

II. THEORY FOR SMALL VIBRATIONS

A brief outline of the type of drive used in the reed indicator will give a clearer conception of what follows. Constructional details of the indicator are given in a publication by Dunmore,[3] and a diagrammatic sketch is shown in Figure 1. In this figure, A is the permanent magnet used to polarize the reed, B indicates the driving coils and pole pieces, and C is the reed. The magnetization of the permanent magnet is such that, with no current in the driving coils, both pole pieces have a polarity opposite to that of the reed and exert equal and opposite attractions upon the reed. The driving coils are connected in such a manner that when a direct current is passed through them, the ends of the coils nearest the reed have opposite magnetic polarities. Consequently, when a direct current flows in the coils, the attraction of one pole for the reed is increased while that of the other pole is decreased, and a force thus acts on the reed tending to displace it from its neutral position. If an alternating current flows in the coils, the attractions of the poles vary periodically with the current and the force on the reed varies correspondingly.

It is obvious that, as soon as the reed moves from the neutral position, a second force due to the permanent magnet comes into play,

[2] E. Mallett, Resonance Curves of Tuning Forks, Physical Society Proc., 39, p. 334; 1927.
[3] Design of Tuned-Reed Course Indicators for Aircraft Radio-Beacon, B. S. Jour. Research, 1 (RP23); November, 1928.

inasmuch as the reed is then nearer to one pole than to the other. This force also tends to pull the reed away from its neutral position.

Figure 2 shows a top view of the reed, with the damping vane attached at the narrow end.

For small vibrations, the square of the deflection from the neutral position may be neglected in comparison with the square of the gap.

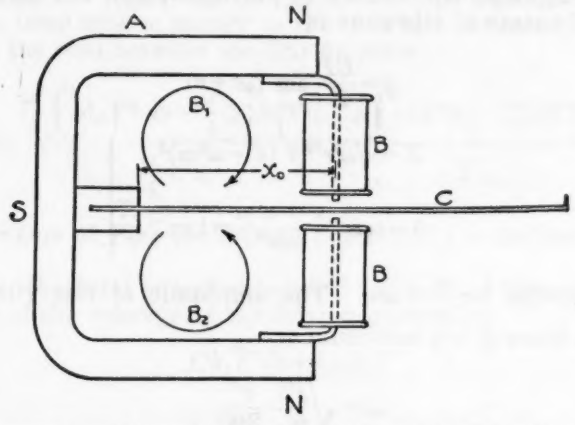

FIGURE 1.—*Schematic diagram of drive used in reed indicator (side view)*

If it is assumed that the entire reed may be replaced by an equivalent particle between the driving poles; that is, a particle of which the displacement at each instant is the same as that of a point on the reed between the driving poles, and which has the same kinetic energy, the same potential energy, and thus suffers the same loss of energy per unit of time as the reed, then the equation of motion may readily be written and solved. This assumption is the same as saying that the phase is the same at every point on the reed. There is little but

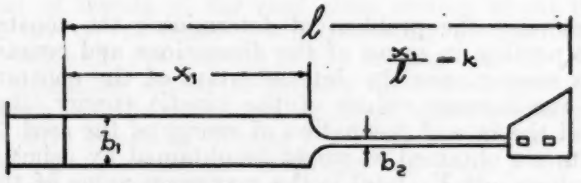

FIGURE 2.—*Top view of reed used in reed indicator*

pragmatic justification for this assumption, although its success in numerous similar cases warrants its adoption here. The final justification, of course, lies in the experimental verification of equations dependent upon the assumption. If the mass of this hypothetical particle is m, the damping force per unit velocity is r, and the restoring force per unit of displacement is s, the equation of motion is

$$my'' + (r + A_1)y' + (s - A_2)y = BI \cos \omega t \qquad (1)$$

where y is the displacement of that portion of the reed immediately between the magnet poles, B is the force per unit current, I is the

maximum instantaneous value, and ω the angular velocity of the current in the driving coils, and the primes over the y's indicate differentiation with respect to the time t. A_1 is a constant representing the increase in damping caused by magnetic and mechanical hysteresis, and A_2 is a constant denoting the decrease in stiffness caused by the permanent magnetic field. The quantities, $r+A_1$ and $s-A_2$, are replaced by r' and s' in the following. The solution of (1) for a steady state of vibration is

$$y=\frac{BI}{Z}\sin(\omega t+\theta) \tag{2}$$

where

$$Z=\sqrt{\omega^2 r'^2+(s'-\omega^2 m)^2}$$

and

$$\theta=\tan^{-1}\frac{s'-\omega^2 m}{\omega r'}=\tan^{-1}\frac{X}{r'} \tag{3}$$

X being written for $\frac{s'}{\omega}-\omega m$. The amplitude of this vibration is a maximum when Z is a minimum or

$$\omega=\sqrt{\frac{s'}{m}-\frac{r'^2}{2m^2}} \tag{4}$$

This equation shows that the reed vibrates with maximum amplitude when the frequency of the driving current is somewhat lower than the frequency of resonance of the damped reed outside a magnetic field because the quantity s' is less than the normal stiffness of the reed, and the quantity r' is greater than the normal damping force. The amount of this lowering of the frequency of resonance by the magnetic positional force is dependent upon the constants of the magnetic circuit and the position of the driving coils.

1. EQUIVALENT-PARTICLE CONSTANTS

There remains the problem of determining the constants of the equivalent particle in terms of the dimensions and constants of the reed. For convenience the determination of the constants will be based on the average values of the kinetic energy, the potential energy, and the rate of dissipation of energy of the reed. The same final results are obtained as would be obtained by using the instantaneous values. If $Y=f(x)$ is the maximum value of the displacement at any point x on the reed (x being measured from the base of the reed), the r. m. s. values of displacement, velocity, and acceleration at any point are $\frac{1}{\sqrt{2}}Y$, $\frac{1}{\sqrt{2}}\omega Y$, and $\frac{1}{2}\omega^2 Y$, respectively. The average kinetic energy of a small portion of the reed dx is

$$dT=\frac{1}{4}\omega^2 Y^2 A\rho dx \tag{5}$$

A being the cross-sectional area of the reed and ρ its density. The kinetic energy of a load of mass M on the reed is $\frac{1}{4}\omega^2 M Y_M^2$, Y_M being

the value of the displacement at the load. The total average kinetic energy is, then

$$T=\frac{\omega^2}{4}\int_o^l A\rho Y^2 dx+\frac{1}{4}\omega^2\Sigma MY_M^2 \tag{6}$$

If this is divided by one-half the square of the r. m. s. velocity at the driving point, the result will be the mass of the equivalent particle having the same kinetic energy as the reed and the same velocity as a point on the reed between the driving poles

$$\mathrm{m}=\frac{\frac{\omega^2}{4}\int_o^l A\rho Y^2\,dx+\frac{\omega^2}{4}\Sigma MY^2{}_M}{\frac{\omega^2}{4}Y^2{}_{x_0}}=\frac{\rho\int_o^l AY^2dx+\Sigma MY^2{}_M}{Y_{x_0}} \tag{7}$$

Y_{x_0} is the value of Y at the driving point, and l is the length of the reed.

Similarly, the total energy dissipated per unit of time divided by the square of the velocity at the driving point gives

$$r=\frac{\int_o^l k_1 Y^2 dx+k_2\,A_v Y^2{}_v}{Y^2{}_{x_0}} \tag{8}$$

and the potential energy of flexure divided by the square of the displacement at the driving point gives

$$s=\frac{E}{Y^2{}_{x_0}}\int_o^l I\left(\frac{d^2Y}{dx^2}\right)^2 dx \tag{9}$$

In these expressions k_1 and k_2 are constants depending upon the resistance of the air to the motions of the reed and the damping vane respectively, A_v the area of the damping vane, Y_v the value of Y at the center of area of the damping vane, Y_{x_0} the value of Y at the driving point, E Young's modulus for the material of the reed, and I the moment of inertia of the reed cross section about its neutral axis. This use of the letter I will be readily distinguishable from its use to designate the current in the driving coils of the reed, as these two quantities appear in entirely different expressions in the following work, and the context will indicate which quantity is meant. The letters A in equation (7) and I in equation (9) are kept under the integral signs because the reed may not have a uniform cross section. Of course, if the reed were not of the same material throughout, ρ and E would also have to be placed within the integrals. This would be a rare case, however.

The above equations define the motion of the reed, provided that the square of the amplitude in the air gap is negligible in comparison with the square of the gap itself.

III. EFFECT OF LARGE VIBRATIONS

When the vibration becomes so large that the square of the amplitude becomes comparable in magnitude with the square of the gap, these equations no longer hold. The frequency of resonance becomes

a function of the amplitude, and the resonance curve becomes unsymmetrical, tending to drop off more sharply on the low frequency side than on the high frequency side.

Mallett's treatment [4] of large vibrations of tuning forks may be applied to the reed indicator and admirably explains these effects. When properly transformed to conform to the conditions existing in the reed indicator and the notation used here, Mallett's solution becomes

$$\left.\begin{aligned}\left(\frac{s'-\omega^2 m}{\omega r'}\right) Y - CY^3 &= DI\cos\theta\\ Y + GY^3 &= DI\sin\theta\end{aligned}\right\} \tag{10}$$

Here, ω, I, m, r', and s' are the same as before, except that s' contains a small term depending upon the current in addition to the terms

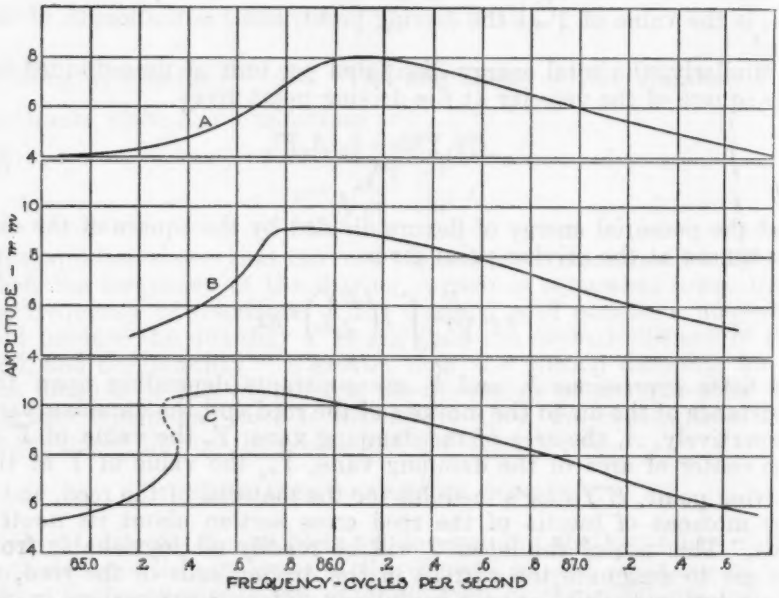

FIGURE 3.—*Resonance curves taken with constant current, showing increasing distortion as amplitude is increased*

A, 0.70 ma.; *B*, 0.83 ma.; *C*, 0.98 ma.

previously mentioned; Y is the amplitude of vibration of the equivalent particle; C, D, and G are constants depending upon the characteristics of the permanent magnet and coils and upon the dimensions of the magnetic circuits; and θ is the phase angle of the current, referred to the phase of the vibration as standard.

Resonance curves plotted from graphical solutions of these equations show an increasing dissymmetry as the amplitude is increased. The equations also show that the damping increases with amplitude. The fact that the current amplitude enters into the quantity s' also indicates that the frequency of resonance varies slightly with the driving current at constant amplitude of vibration, the frequency

[4] See footnote 2, p. 196.

decreasing as the current increases. Also, the damping should change slightly with current at constant amplitude, but this effect is too small to be detectable.

Experimental resonance curves show all of the above characteristics, the upper portions of curves taken at constant current being displaced toward the low-frequency side and becoming broader as the maximum amplitude is increased (fig. 3), while the upper portions of curves taken with variable current, the amplitude being held constant as the frequency is varied, are displaced toward the high-frequency side. (Fig. 4.) A sufficiently exact evaluation of the constants entering into equation (10) to permit a thorough quantitative check of these results has not yet been made.

It has been found desirable to sacrifice a certain amount of sensitivity in the indicator to eliminate the effects of large vibrations, since any change of the frequency of resonance with amplitude of either or

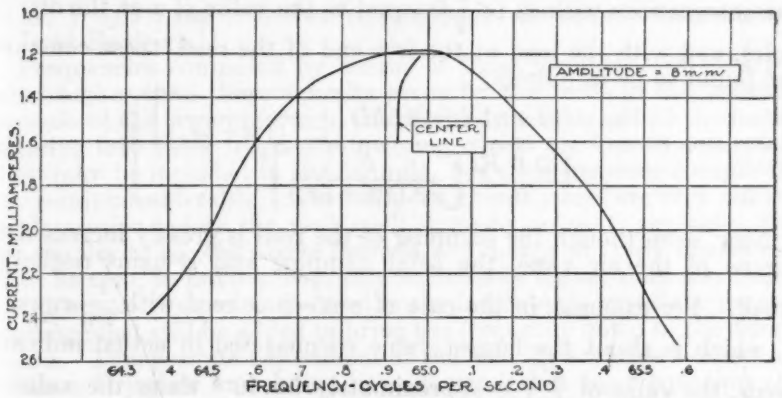

FIGURE 4.—*Resonance curve at constant amplitude, showing increase of frequency as current is decreased*

both reeds in an indicator (inasmuch as such a change is nearly always different for the two reeds), will almost certainly result in a shift of the course as the operating amplitude of the reeds varies. Such variation of operating amplitude is inevitable, since it is virtually impossible to maintain the output of an airplane radio receiving set constant under operating conditions. Therefore, the gaps between the reed and pole pieces are made so large that distortion of the resonance curve at normal operating amplitude is negligible. For the purposes of design, then, the vibration may be considered small, although an accurate calibration procedure must still take account of the large vibration effects.

IV. APPLICATION OF THEORY TO REED DESIGN

In order that equations (7), (8), and (9) may be used for the design of reeds, the form of the function Y, which defines the curve of deflections assumed by the reed during vibration, must be determined. If the cross section is uniform (provided the mass of the load is small in comparison with the mass of the reed, as is usually the case), Lord Rayleigh has shown theoretically that the curve assumed by a vibrat-

ing bar is very nearly the same as that which it would assume statically if deflected by a force acting at a distance from the base of three-fourths the total length. Later, however, Garrett[5] showed by experimental methods that the curve assumed during vibration is more accurately approximated if the force is considered to be applied four-fifths of the length of the reed from the base. By use of these data, the curve assumed by a uniform reed vibrating freely is found to be

$$Y=\frac{Px^2}{30EI}(12l-5x)\left(0<x<\frac{4}{5}l\right) \tag{11}$$

$$Y=\frac{8Pl^3}{375EI}(15x-4l)\left(\frac{4}{5}l<x<l\right) \tag{12}$$

where P is the force deflecting the reed statically. By substituting these expressions for Y in the formulas for m and s and carrying out the integrations with x_o ($<\frac{4}{5}l$) equal to the value of x at the driving poles, and with the load at the free end of the reed, these constants are found to be as follows:

$$\left.\begin{aligned} m&=(12.40A\rho l+49.5M)\left[\frac{l^3}{x_o^2(12l-5x_o)}\right]^2 \\ s&=\frac{153.6\ EI}{l^3}\left[\frac{l^3}{x_o^2(12l-5x_o)}\right]^2 \end{aligned}\right\} \tag{13}$$

Now, even though the damping of the reed is greatly increased by means of the air vane, the total damping still remains negligibly small. For example, in the case of a 65-cycle reed with $\frac{r'}{2m}$ equal to 3, which is about the largest value encountered in actual indicator reeds, the value of $\frac{r'^2}{4m^2}$ is approximately 5×10^{-5} times the value of $\frac{s'}{m}$, so that the effect of the damping upon the frequency of free vibration is less than 1 part in 20,000. Accordingly, the frequency of free vibration of a reed outside a magnetic field may be expressed

$$f=\frac{1}{2\pi}\sqrt{\frac{s}{m}} \tag{14}$$

Substituting for s and m the values given above,

$$f=\frac{0.1617\ cV}{(1+2R)\ l^2} \tag{15}$$

in which c is the thickness of the reed, $V=\sqrt{\frac{E}{\rho}}$ is the velocity of sound in the material of the reed, and R is the ratio of mass of load to mass of reed (this is assumed small). For a similar reed, Drysdale and Jolley[6] give

$$f=\frac{0.1637\ cV}{(1+2.05R)\ l^2} \tag{16}$$

[5] C. A. B. Garrett, On the Lateral Vibrations of Bars, Phil. Mag., 8 p. 581; 1904.
[6] Electrical Measuring Instruments, 2, p. 261. (A misprint has been corrected.)

The agreement between these two formulas affords excellent confirmation of the correctness of the assumptions made regarding the shape of the curve of deflections, since in the derivation of their formula Drysdale and Jolley used entirely different assumptions and a method different from that used here.

It should be pointed out, however, that the validity of equation (15) does not confirm the equivalent-particle assumption. The expression for the frequency may be obtained by equating the average kinetic and potential energies of the reed. Since the equivalent particle is assumed to have the same kinetic and potential energies as the reed, equating the average kinetic and potential energies of the particle necessarily gives the same frequency, as may be seen by substituting in equation (14) the values of s and m from equations (9) and (7). The method here given of computing the frequency, then, involves the determination of the form of the curve of deflections, $Y=f(x)$, and it is then equivalent to the approximate method of Lord Rayleigh.[7]

Frequencies computed by means of these formulas will be somewhat higher than those actually given by the reeds in the indicator because of the lowering due to the magnetic action. If all the factors entering into these frequency lowering effects are known accurately, they may be included in the formula, but their presence complicates the result considerably. Furthermore, these factors are very difficult to determine before the reed itself is made, so that, generally, it is far simpler to use the above formula and design the reed, considering R to be zero, to have a frequency sufficiently higher than the desired frequency so that, with the reed in the indicator, a certain amount of loading must still be added to bring the frequency down to the desired value. This permits adjustment of the load for accurate tuning.

Since Drysdale and Jolley have shown [8] that their equation (16) for the frequency of a reed checks very closely with experimental results, either equation (15) or (16) may be used to determine the velocity of sound in the alloy used for reeds in the indicator. This alloy, known as "Allegheny electric metal," is used because of its high magnetic permeability and low thermoelastic coefficient. The value of Young's modulus of this material, which is necessary for the calculation of the velocity of sound in it, is not available at present. From observations on a reed made from sheet stock 0.020 inch thick cold-rolled to a final thickness of 0.015 inch, the value of V was found to be 4×10^5 centimeters per second. This can be considered as an approximation only, since experience shows that V varies appreciably with the thickness to which the 0.020 inch stock is cold-rolled, the thinner material having somewhat lower values of V.

To obtain an expression for the sensitivity of a reed, equation (2) is used. This equation gives the value of the displacement of the reed at the driving poles. It is necessary to multiply this displacement by the ratio of the amplitude at the tip of the reed to the amplitude in the gap in order to determine the deflection of the free end of the reed. Thus, for the tip of the reed

$$y_l=\frac{Y_l}{Y_{x_0}}\cdot\frac{BI}{Z}\sin(\omega t+\theta) \tag{17}$$

[7] See footnote 1, p. 195.

[8] See footnote 6, p. 202.

For values of ω near resonance, Z may be considered as approximately equal to $\omega r'$. Consequently

$$y_1=\frac{Y_1}{Y_{z_0}}\cdot\frac{BI}{\omega r'}\sin(\omega t+\theta) \tag{18}$$

or

$$Y_1=\frac{BI}{\omega r'}\cdot\frac{Y_1}{Y_{z_0}} \tag{19}$$

Now, r' is different for reeds of different frequencies, but since it is necessary that all reeds in the indicator have resonance curves of the same shape, the sharpness of resonance S_R must be constant for all reeds. Sharpness of resonance is here defined by the equation

$$S_R=\frac{f_R}{f_1-f_2} \tag{20}$$

where f_1 and f_2 are the frequencies at which the amplitude on the resonance curve is 0.707 of the maximum amplitude, and f_R is the frequency at maximum amplitude. It may readily be shown that, defined in this manner

$$S_R=\frac{\omega_0 m}{r'} \tag{21}$$

where ω_0 is the angular velocity at resonance. On substitution of the value of r' obtained from equation (21), equation (19) becomes

$$Y_1=\frac{BIS_R}{\omega_0^2 m}\cdot\frac{Y_1}{Y_{z_0}} \tag{22}$$

or, since $\omega_0^2 m=s'$

$$Y_1=\frac{BIS_R}{s'}\cdot\frac{Y_1}{Y_{z_0}} \tag{23}$$

To a first approximation, s may be used in place of s', since A_2 is rarely greater than 5 per cent of s.

Now in the case of a forced vibration it is possible that even a uniform reed does not conform to the curve of deflections already given, unless the driving force is applied at a point four-fifths of the length from the base, which is not usually the case. Furthermore, reeds having other than uniform cross sections may be desirable in many instances, as in the reed indicator. In general, therefore, the curve of deflections must be determined experimentally and the corresponding equation developed. If it is possible to approximate to the curve of deflections by assuming the reed to be deflected by a single force at some point, the task of finding the equation of this curve may be simplified greatly. It should be pointed out here, however, that this method is useless in the case of a nonuniform reed unless the dimension (or dimensions) of the reed which varies with the distance from the base is expressible as a function of x which can be integrated. If this is not the case, it is necessary to fit a power series or other function of x to the observed curve. The equations for m, r, s, frequency, and sensitivity, will then have different forms from those given above. However, it may be shown, by suitable transformations of variables

and functions within the integrals, that the occurrence, in the equations for m, r, s, frequency, and sensitivity, of all quantities independent of x is not affected by the form of the function representing the curve of deflections. Thus, these equations may be of some value even though the exact form of the function representing the curve of deflections is not known. For a reed of the type that is used in the reed indicator (fig. 2), m and s may be written

$$m=\frac{\rho lc[f_1(b_1, b_2, k)+f_2(b_1, b_2, k)R]}{F_h^2} \tag{24}$$

$$s=\frac{c^3Ef_3(b_1, b_2, k)}{N_o l^3 F_h^2} \tag{25}$$

Here, b_1 and b_2 are the widths of the wide and narrow portions of the reed, k is the ratio of the length of the wide portion to the total length, and N_o is a numerical constant. F_h is a function derived from the equation of the curve of deflections and is equal to the value of F,

$$F=\frac{Y}{Y_l}=F\left(\frac{x}{l}\right) \tag{26}$$

for $x=x_o$, that is

$$F_h=\frac{Yx_o}{Y_l}=F\left(\frac{x_o}{l}\right)=F(h) \tag{27}$$

From these values for m and s

$$f=\frac{N_1 cV}{l^2}\sqrt{\frac{f_3\ (b_1, b_2, k)}{f_1\ (b_1, b_2, k)+f_2\ (b_1, b_2, k)\ R}} \tag{28}$$

$$Y=\frac{B'I\ S_R}{E}\frac{l^3\ F_h}{c^3\ f_3\ (b_1, b_2, k)} \tag{29}$$

where N_1 is a numerical constant and B' is the constant B of equation (4) multiplied by the numerical factors arising from the substitutions and transformations made to obtain equation (29). In these equations, the manner of occurrence of the quantities, c, l, ρ, E, and V is independent of the form of the function representing the curve of deflections. Therefore, if the values of b_1, b_2, and k are, or can be, fixed, and an approximate value for F_h obtained, either experimentally or mathematically, the equations have a certain field of usefulness as design equations. Thus, for the type of reed in use in the radiobeacon course indicator, F_h is found to be very nearly proportional to h^2, and the following relations are found useful, in connection with experimental data:

$$f\propto\frac{c}{l^2} \tag{30}$$

$$Y\propto\frac{l^3h^2}{c^3} \tag{31}$$

An exact equation for f may be derived by fitting to the experimentally observed curve of deflections an empirical equation and

using this equation to determine the values of N_1 and the functions of b_1, b_2, and k. This has been done in the present investigation as follows: The curve of deflections of the indicator reed was determined by measuring the double amplitude of the vibrating reed at a number of points along its length, by means of a traveling micrometer microscope. The distance from the base of the reed to the measuring point was determined in each case. The values for the double amplitude were then corrected for the thickness of the reed, divided by two, and plotted against the corresponding distances from the base of the reed. To fit this observed curve, it was found necessary to use three separate equations—the first, containing terms in x and x^2, applied from the base to the end of the wide portion; the second, also quadratic in x, applied from the end of the wide portion to a point three-fourths of the length from the base; and the third, which was linear, applied to the remaining portion of the reed. By calculation from these equations, taking $b_1=0.794$ cm, $b_2=0.127$ cm., and $k=0.465$ (which are the standard values for all indicator reeds), the values of f_1, f_2, and f_3 were found to be as follows:

$$f_1\ (b_1, b_2, k)=0.037.$$
$$f_2\ (b_1, b_2, k)=\ .172.$$
$$f_3\ (b_1, b_2, k)=\ .179.$$

Also

$$N_1=\frac{1}{2\pi}$$

Upon the introduction of these values, equation (28) becomes

$$f=\frac{0.35\ c\ V}{l^2\sqrt{1+4.65R}} \tag{32}$$

or, if R is small

$$f=\frac{0.35\ c\ V}{l^2(1+2.33R)} \tag{33}$$

This equation and the relations (30) and (31) have been found to check very well with experimental data taken on a large number of indicators. Figure 5 shows the current required to drive a reed at 8 mm. total tip amplitude plotted against h^2. Equation (32), of course, does not include the effect of magnetic action upon the reed frequency. As a consequence, frequencies calculated by this equation are consistently higher, by approximately 2 per cent, than the frequencies of the reeds in an indicator. In designing reeds, approximately five cycles per second allowance is made for the effect of magnetic action and load; that is, the dimensions for a 65-cycle reed are calculated from equation (32) by using $f=70$ cycles per second. In special cases, when an unusually large load must be attached to the reed, greater allowances must be made.

An interesting application of these results occurs in the 3-reed or 12-course indicator. Because of space limitations in this type of indicator, it is not possible to set the driving coils at the proper positions to give equal reed sensitivities for equal gaps. In this case, the distance from the driving pole to the free end of the reed is considered constant and the reed sensitivity varied by moving the base of the reed, thus varying the length and driving distance (x_0) simultaneously.

As the length of the reed is varied, the thickness must also be changed to keep the ratio $\frac{c}{l^3}$, and hence the frequency, constant. If d_1, d_2, and d_3 represent the distances from driving poles to reed tips, and l_1, l_2, and l_3 the lengths of the 65, 86⅔, and 108⅓ cycle reeds, respectively, the following equations are obtained from the given conditions:

$$\frac{\left(1-\frac{d_1}{l_1}\right)^2}{27l_1^3}=\frac{\left(1-\frac{d_2}{l_2}\right)^2}{64l_2^3}=\frac{\left(1-\frac{d_3}{l_3}\right)^2}{125l_3^3} \tag{34}$$

Each of these fractions is proportional to the sensitivity of the corresponding reed, so that a graph of the value of each fraction against

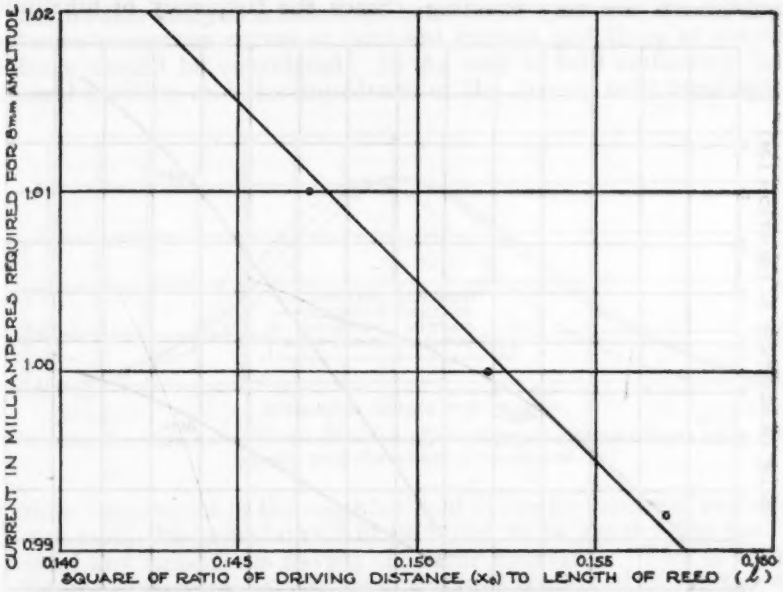

FIGURE 5.—*Relation between current necessary to drive reed at 8 mm tip double amplitude and square of ratio of driving distance* (x_o) *to length of reed* (l)

the corresponding length will show how the sensitivity of that reed changes as the length is varied under the prescribed conditions. Figure 6 shows the values of all three of the fractions plotted against a common scale of lengths for $d_1=d_2=4.70$ cm, and $d_3=3.64$ cm. The intersections of any horizontal line with these curves give the lengths required for equal sensitivities. For actual design, the horizontal line is taken as high as possible to give maximum sensitivity. After the lengths are determined from these curves, the corresponding thicknesses can readily be calculated.

The damping of the reed is not so easily obtained. The air-damping vane used on the reed introduces many factors the magnitudes of which have been difficult to control. Consequently, at the present time, no thorough experimental verification of theoretical

expressions for damping is available, and the design of the air dampers continues to be mainly empirical. Equation (8) indicates that the value of r', for a reed of fixed dimensions driven at a fixed point, should be a linear function of A_v, the area of the damping vane. The data available at present, however, when plotted against the area of the damping vane, give points that are too scattered definitely to determine the shape of the required curve. Further experimental work, perhaps, accompanied by a more detailed theoretical analysis, will be necessary for a final determination of equations for the design of damping vanes.

V. CALIBRATION OF REED INDICATORS

The tuning of the reed is of the utmost importance, as the operating requirements are very exacting. Since the frequency of maximum

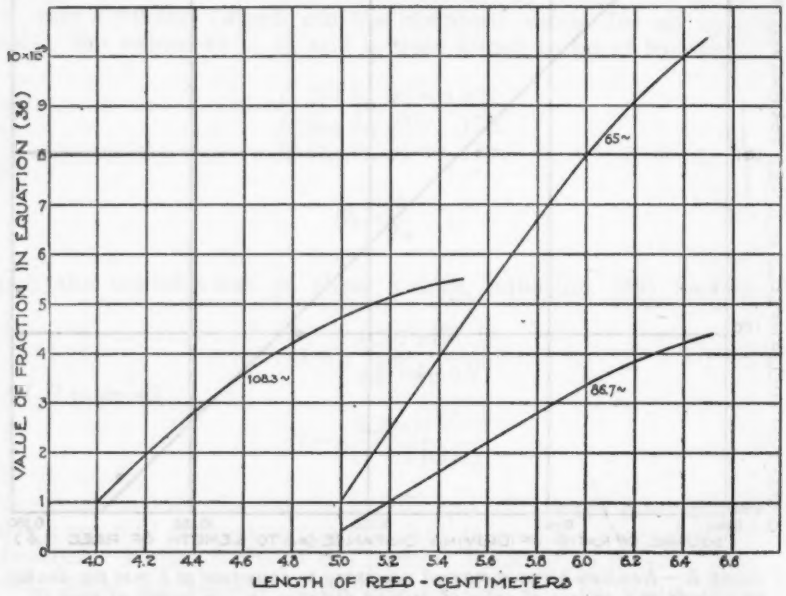

FIGURE 6.—*Curves for determining length of reeds in 12-course indicator*

response and the damping change with amplitude, a standard calibrating amplitude must be chosen and all measurements made at this amplitude. A very convenient method for determining the frequency and sharpness of resonance at a given amplitude Y consists in adjusting the driving source so that, as the frequency is varied, the maximum amplitude obtainable is equal to $\sqrt{2}Y$. If, then, the frequency alone is varied so that the reed vibrates with amplitude Y (which will occur at two frequencies), and the frequencies giving this amplitude measured, the frequency and sharpness of resonance may readily be computed. The measured frequencies are denoted by f_1 and f_2, and S_R is found by means of equation (20) while the frequency of resonance, f_R is given by

$$f_R = \frac{f_1 + f_2}{2} \tag{35}$$

As noted above, resonance curves taken with constant current show a marked dissymmetry, the upper portions being displaced toward the low-frequency side. If the voltage across the indicator instead of the current through it is held constant, this dissymmetry is even more pronounced. Curves taken at constant amplitude, with variable current, on the other hand, show only a slight dissymmetry, and here the displacement of the upper portions is toward the high-frequency side. The frequency and sharpness of resonance for the same reed will have different values when determined from these different resonance curves. Consequently, it is necessary to select as a standard, one of the three possible methods of tuning a reed—at constant voltage, at constant current, or at constant amplitude. The proper choice obviously will depend upon the conditions under which the indicator is to be used.

Before this analysis is taken up, however, the cause of the difference between resonance curves at constant current and those at constant voltage should be considered. If the reed is held stationary in its neutral position and the impedance of the driving coils measured at

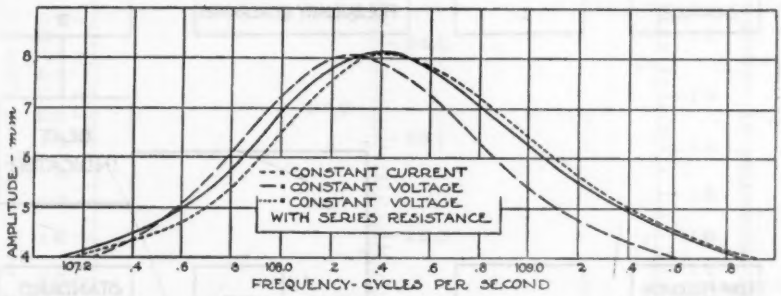

FIGURE 7.—*Resonance curves showing effect of impedance variations upon frequency and sharpness of resonance*

various frequencies in the neighborhood of the frequency of resonance of the reed, this impedance will be found to be exactly the same as that of any impedance having the same constants. This is termed the damped impedance. If, now, the reed is allowed to vibrate, and the impedance again measured, at frequencies near the frequency of resonance of the reed the impedance will have values considerably different from the damped impedance. At frequencies slightly below resonance, the impedance is greater than the damped impedance, while at frequencies above resonance the impedance is less than the damped impedance. Consequently, when the voltage is held constant for measurement of a resonance curve, the current through the driving coils will vary with the frequency, being lower for frequencies lower than resonance than it is for frequencies higher than resonance. This explains the greater dissymmetry evidenced by curves taken at constant voltage. These impedance variations must be considered in tuning the reed if the indicator is to be operated under conditions such that its impedance variations will cause variations of the current through it. (See fig. 7.)

Now, the reed indicator was developed for use in the output of a radio set as a visual course indicator for the radio range beacon. Furthermore, pilots are instructed to use it at a fixed amplitude

(8 mm). The volume control on the radio set may be either manual or automatic. If manual, the indicator may be considered to be operating in a series circuit comprising the indicator, a resistance equal to the output impedance of the set used, and a source of constant voltage but slightly varying frequency (because of slight variations in the modulating frequencies of the beacon transmitter). The conditions are the same if an automatic volume control operated by the received carrier wave is used. However, if an automatic volume control operated by the voltage across the indicator such as that recently developed by the National Bureau of Standards, is used, the fluctuations of the voltage across the indicator caused by variations in the modulation frequencies will be corrected by the volume control; and the voltage directly across the reed indicator, rather than that of the source in the series circuit mentioned above, will be maintained constant. Generally, the reed will be operated on a

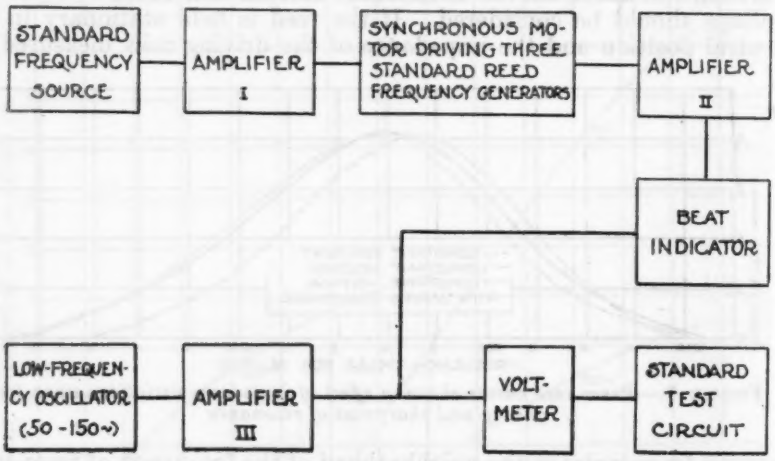

FIGURE 8.—*Schematic diagram of reed calibrating equipment*

resonance curve with a maximum amplitude of 8 mm. (This includes the width of the tab on the front of the reed, the actual amplitude of vibration being only 6 mm).

For use with a radio set having manual or carrier-operated automatic volume control, the indicator should be connected in series with a resistance equal to the output impedance of the radio set and a variable voltage of controllable frequency inserted in series with this circuit. This voltage is then adjusted so that the maximum amplitude obtainable, as the frequency is varied, is 8 mm, and, for determination of f_R and S, the frequencies f_1 and f_2 giving 6.2 mm amplitude are measured, the voltage in the circuit being held constant. This value of 6.2 mm is obtained by taking 70.7 per cent of the actual amplitude of vibration, 6 mm, and adding the 2 mm width of the tab on the tip of the reed. The sensitivities of all reeds in the indicator are adjusted so that their amplitudes are the same for a given voltage impressed in the circuit described above.

For use with a radio set equipped with an automatic volume control operated by the indicator voltage, sensitivity adjustments

are made as above, and tuning adjustments are made at the same amplitude. The voltage, during tuning adjustments, is maintained constant directly across the indicator terminals.

When tuned by either of these methods and operated under the corresponding conditions, the reeds show a minimum amount of variation due to the unavoidable causes pointed out in the above analysis of the operation of the reed.

In practical calibration work, the reed is driven by a vacuum-tube oscillator and when this oscillator is adjusted to one of the "test

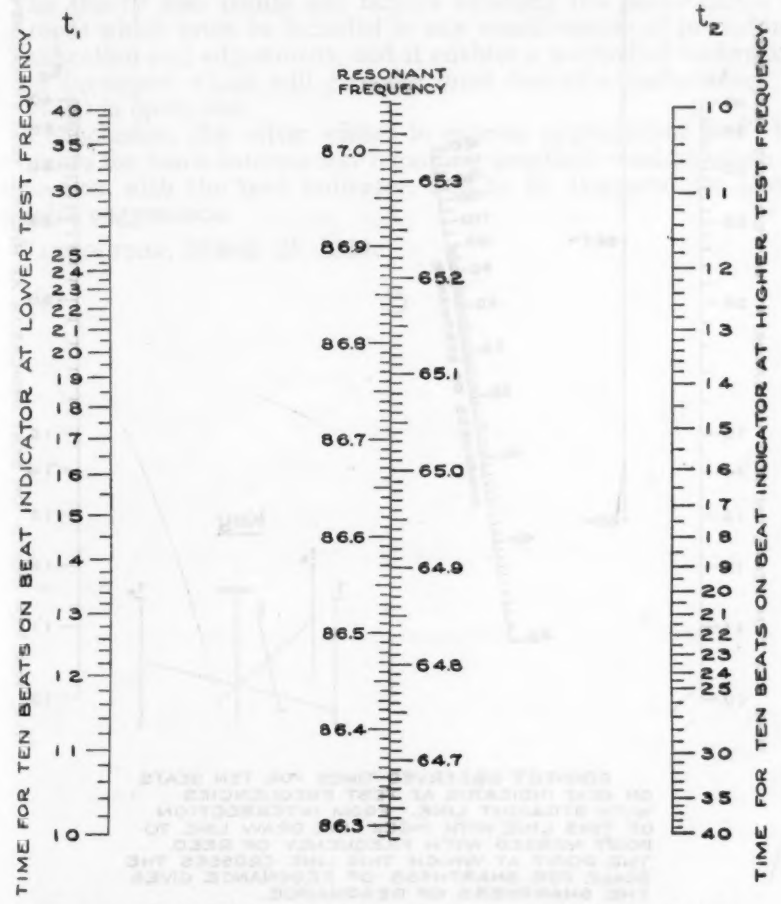

FIGURE 9.—*Chart for determining frequencies of resonance of reeds*

frequencies" (f_1 and f_2 of equation (20)) its frequency is determined by measuring with a stop watch the time required for 10 beats between the driving oscillator and a standard frequency source. The standard frequency source used at the National Bureau of Standards consists of three alternators, giving 65.000, 86.667, and 108.333 cycles per second, all mounted on the same shaft and driven by a 1,000-cycle synchronous motor. The current to drive this motor is obtained from the primary-standard frequency equipment. Beats between

the standard frequency and the driving oscillator are indicated by a vacuum-tube beat frequency indicator. A schematic diagram of the complete calibrating equipment is shown in Figure 8.

To eliminate the arithmetical work necessary to calculate the frequency and sharpness of resonance from the measured times for 10 beats at the test frequencies, two nomographic or alignment charts

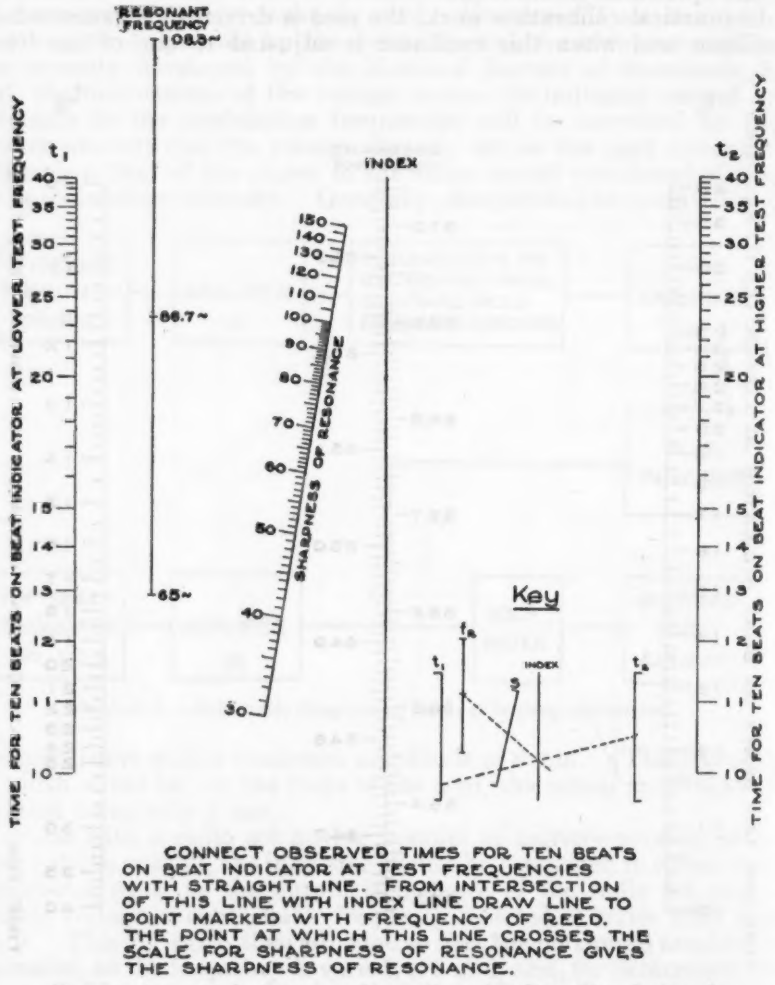
RESONANT FREQUENCY
108.3~
66.7~
65~
INDEX
SHARPNESS OF RESONANCE
TIME FOR TEN BEATS ON BEAT INDICATOR AT LOWER TEST FREQUENCY
TIME FOR TEN BEATS ON BEAT INDICATOR AT HIGHER TEST FREQUENCY
Key
INDEX
CONNECT OBSERVED TIMES FOR TEN BEATS ON BEAT INDICATOR AT TEST FREQUENCIES WITH STRAIGHT LINE. FROM INTERSECTION OF THIS LINE WITH INDEX LINE DRAW LINE TO POINT MARKED WITH FREQUENCY OF REED. THE POINT AT WHICH THIS LINE CROSSES THE SCALE FOR SHARPNESS OF RESONANCE GIVES THE SHARPNESS OF RESONANCE.

FIGURE 10.—*Chart for determining sharpness of resonance of reeds*

have been designed to facilitate the work. These charts are shown in Figures 9 and 10, the former being used to obtain the frequency and the latter for sharpness of resonance. In the first figure, the two measured times are located on the scales indicated for them, and the straight line connecting these two points crosses the central line at a point which determines the frequency of resonance. The second figure is self-explanatory.

VI. CONCLUSION

By means of Rayleigh's approximate method, equations are obtained for the frequency of free vibration of a uniform reed and for a particular type of nonuniform reed.

To obtain an expression for the sensitivity of a driven reed, the entire reed is assumed to be replacable by an equivalent particle located at the driving point. The equation thereby derived for the sensitivity of the reed checks very closely with results observed with the type of reed used in the reed indicator.

The theory also points out factors affecting the performance of the reeds which must be included in any consideration of procedures of calibration and adjustment, and it enables a method of calibration to be developed which will give the most desirable performance of the reeds in operation.

In conclusion, the writer wishes to express appreciation to F. W. Dunmore for much information regarding practical considerations in connection with the reed indicator, and to H. Diamond for many valuable suggestions.

WASHINGTON, March 25, 1931.

O